Impact of blue light on the ocular surface and nociception

Veronika Marek

Sorbonne Université

Ecole doctorale 394 Physiologie, Physiopathologie et Thérapeutique

Institut de la Vision

Equipe S12 « *Rôle des chimiokines dans la physiopathologie du segment antérieur de l'œil* »

Impact de la lumière bleue sur la surface oculaire et la nociception

Par **Véronika MAREK**

Thèse de doctorat de Sciences de la Vie

Co-dirigée par Alexandre Denoyer, Stéphane Mélik Parsadaniantz et Thierry Villette

Présentée et soutenue publiquement le 30/11/2018

Devant un jury composé de :

Pr Hélène Pouzet	Présidente
Dr Alicia Torriglia	Rapportrice
Pr Pierrick Poisbeau	Rapporteur
Pr Corinne Dot	Examinatrice
Dr Françoise Brignole-Baudouin	Examinatrice
Pr Alexandre Denoyer	Co-directeur
Dr Thierry Villette	Co-directeur

И они приняли рабочую гипотезу, что счастье в непрерывном познании неизвестного и смысл жизни в том же
(*Аркадий и Борис Стругацие* "*Понедельник начинается в субботу*")

Science is a way of thinking much more than it is a body of knowledge
(Carl Sagan)

Acknowledgments

I would first like to acknowledge my supervisors for their guidance, advices and help throughout the entire research process, as well as everyone at Essilor and the Vision Institute who played a role in the accomplishment of this work.

I would also like to thank my committee members for accepting to participate in my defense and for their critical reading of my manuscript.

Finally, I am grateful to all my friends without whom the fulfillment of this thesis would have never been possible.

Table of contents

Summary

Thesis title: Impact of blue light on the ocular surface and nociception

In our modern highly-illuminated world, symptoms of greater sensitivity to blue light increasingly appear. The impact of blue illumination on the ocular surface, the first barrier between the visual system and the external environment, is of particular interest. Since the crucial involvement of neurologic processes in ocular surface diseases such as dry eye is now widely recognized, the role of phototoxicity in neuro-ocular disorders is of great significance.

The aim of this work was to investigate the potential harmful role of blue light in the context of dry eye and in relation to ocular nociception and light aversion. We demonstrated in vitro the phototoxic impact of blue light in human epithelial cells of the cornea and conjunctiva, and in neural and neuroglial cells from mouse trigeminal ganglia. In vivo, we reported that the significant aversion to blue light in mouse was accompanied by inflammation in the ocular surface and trigeminal pathways. We gave some insights into the ocular nociceptive pathways involved in photophobic mechanisms, together with the role of specific non-visual photoreceptors, melanopsin and neuropsin.

This work sought to explain and corroborate frequent complaints about daily living increased photosensitivity in front of displays or under lightings rich in blue spectrum. Obtained results may therefore open new avenues for prevention and treatment of light-related ocular disorders and light aversion.

Key words (3): blue light, dry eye, trigeminal pathway

Résumé

Titre de la thèse : Impact de la lumière bleue sur la surface oculaire et la nociception

Dans le monde moderne fortement éclairé par la lumière artificielle, la sensibilité accrue à l'illumination bleue semble affecter de plus en plus de personnes. L'association de composantes à la fois inflammatoire et neurologique dans les pathologies de la surface oculaire, au premier rang desquelles figure la sécheresse, est désormais largement reconnue ; le rôle de la lumière bleue et les mécanismes impliqués dans la phototoxicité au niveau de la surface oculaire méritent ainsi aujourd'hui d'être mieux expliqués.

Le but de ce travail était d'étudier de potentiels effets nocifs de l'exposition à la lumière bleue dans le cadre de la sécheresse oculaire et en relation avec la nociception et la photophobie. Ainsi, nous rapportons in vitro l'effet toxique de la lumière bleue sur les cellules épithéliales de la cornée et de la conjonctive et sur les cellules neuronales et gliales du ganglion trijumeau. In vivo, l'aversion à la lumière bleue chez la souris était accompagnée par des processus inflammatoires spécifiques au niveau de la surface oculaire et le long des voies trigéminées. En outre, le rôle inédit des photorécepteurs non-visuels dans les voies nociceptives a été évoqué, plus spécifiquement via l'implication de la mélanopsine et de la neuropsine.

Ces résultats fondamentaux corroborent de fréquents symptômes rencontrés en pratique clinique et liés à l'augmentation de la photosensibilité face aux écrans et dans les salles illuminées par les éclairages dont le spectre a une riche composante bleue. Ainsi, ce travail pourrait ouvrir de nouvelles voies pour la prévention et le traitement de la phototoxicité au niveau de la surface oculaire et de la photophobie.

Mots clés (6) : lumière bleue, sécheresse oculaire, surface oculaire, nociception, voie trigéminée, photophobie

Introduction

Today, almost everybody is aware that ultraviolet (UV) light is highly dangerous for our eyes (1); now, the anxiety has shifted to another part of the electromagnetic spectrum, this time in the visible range. Currently, the topic of blue light hazard is highly in vogue (2), and this trend is not surprising. Indeed, in our daily life, we are permanently exposed to various types of light illuminating our surroundings. It comes from natural sun light as well as from different energy-saving artificial sources like light emitting diodes (LEDs) or compact fluorescent lamps replacing incandescent or halogen bulbs; our spectral exposure is mainly situated between the middle of the near ultraviolet (360 nm, UVA) and the end of the near infrared (1400 nm, IRA) (Figure 1). Light may provoke hazardous effects if it reaches a level capable of causing photochemical, photomechanical or photothermal damage. A dangerous level of irradiation may be attained either by an acute and intensive exposure to light or by a lower irradiance but chronic exposure. In specific situations, like looking at a sun eclipse or welding without protective goggles, everybody is well aware that light is a real danger (nevertheless, it seems that some persons still consider it as fake news…(3)). A typical example is working at higher altitudes or next to furnaces when respectively the invisible and intensive ultraviolet (UV) or infrared (IR) radiations rapidly trigger important damage (4,5). However, daily light conditions might be phototoxic as well, all the more for those who do not realize it and therefore do not protect our eyes or for those individuals being more at risk of long-term chronic damages by their family history of diseases, their weaker defense or higher light-related and disease-specific risk factors.

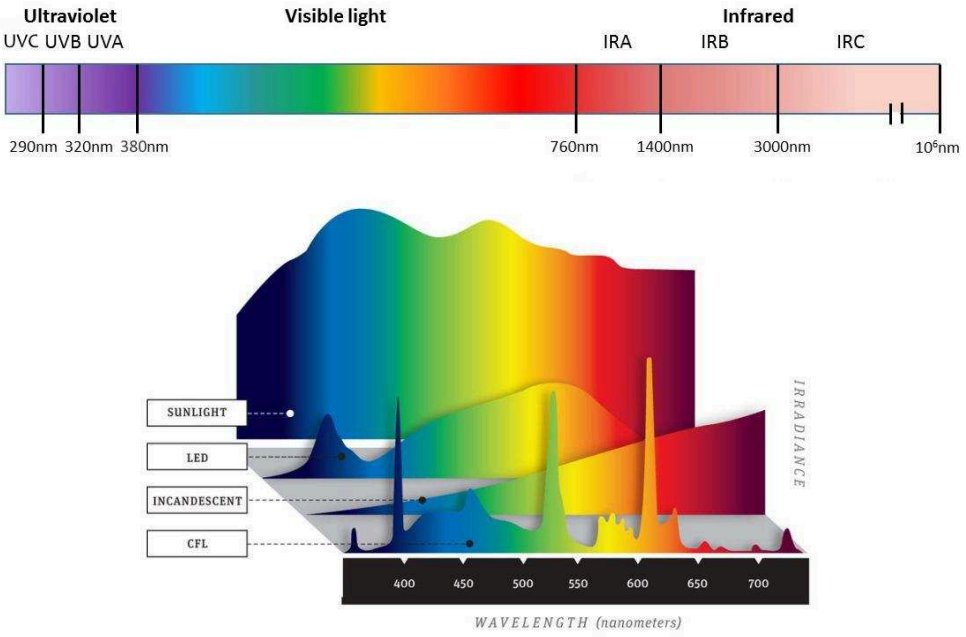

Figure 1. Light spectra in every-day life, from various sources

Top: Typical ranges of the sunlight electromagnetic spectrum including ultraviolet (UVC, UVB and UVA), visible (380-780 nm) and infrared (IRA, IRB and IRC) light. **Bottom:** typical spectra of daily light sources (LED – light emitting diodes, CFL – compact fluorescent lamps). These are open access images.

Since artificial light sources and particularly digital screens highly emit in the blue spectrum, the problem of blue light noxiousness has been intensively debated (6,7). It has been discussed that the spectrum of artificial lighting in which we now spend much of our lives may have unintended and harmful impact on alertness, sleep, and wakefulness (8). Today, almost every optical shop offers lenses, corrective or not, that filter out one or another part of blue spectrum. The number of smartphone applications that continuously adapt the screen blue-cut level increases as well (9). This blue spectrum filtering-out is supposed to be amazingly beneficial, soothing, protecting, and improving all the aspects of your eyes' state… "*What's wrong with it if this stuff can really help*?" perhaps you will ask. The key word is "really".

To date, different light-induced ocular diseases have been really identified, including photokeratitis, pterygium and cataract (10–14). Thanks to numerous studies dedicated to blue light phototoxicity in the pathologies of retinal diseases, now we know that blue light does really damage the retina; it has been proven by various in vitro (15–20) and in vivo (21–29) studies. Special attention should be paid to the work of Krigel et al. since, to the best of our knowledge, it is the first in vivo study that investigated the noxious effects not only of various light wavebands but also of various light sources (LED vs. fluorescent lamps) as well as of various protocols (acute vs. chronic exposure) (28). Moreover, in contrast to the majority of published protocols of strong illumination, here, the authors used the moderate values of irradiance that were quite comparable to the exposures in real life.

In addition to retinal diseases, ocular problems caused by visual displays have been also much reported (30–41). However, many anti-blue-light advertisements propose to alleviate/prevent/treat various other disorders or at least symptoms, from dry eye to ocular pain. Nevertheless, only few studies can scientifically confirm their effect. Moreover, besides the proof of the effect itself, it is also important (or at least interesting) to understand its nature and mechanisms.

Our interest in blue-light-induced non-retinal ocular disorders started with an observation made in the Clinical Investigation Center of Quinze-Vingts National Ophthalmology Hospital (Paris) in which patients suffering from the dry eye disease (DED) consult: these patients frequently complain about the increased sensitivity to light. Corroborated by notions in the literature, this observation urged us to suspect a potential harmful influence of the blue light illumination on the etiology and pathophysiology of DED. We hypothesized that filtering out some spectral parts of visible light that reaches our eyes from everyday-life illumination might alleviate dry eye symptoms and ameliorate the quality of vision and of life of the patients. To test the idea, an exploratory clinical study was performed in 2015. We proposed to the DED patients to wear the specially designed filtering spectacles, for 2-3 weeks and in all daily life situations as far as possible. Violet-blue (400-450 nm) and turquoise blue (460-510 nm) wavebands were chosen to be filtered out. To assess the impact, we clinically evaluated patients' eyes in the beginning and at the end of the trial. We observed that the participants wearing the blue turquoise filtering spectacles demonstrated amelioration in tear break-up time, clinical state of conjunctiva and eyelids, hyperemia level, blinking rate and tear meniscus height; moreover, in self-evaluation questionnaires, patients themselves declared a beneficial effect. However, the sample population has not been sufficient to

statistically confirm the efficacy of such filtering eyewear on reducing certain DED symptoms.

We were then wondering what the mechanism of this effect could be? Since the ocular surface has a highly important role in the pathology of dry eye, we suspected that phototoxicity in cells of this structure might be a clue. Then, we focused on the fact that in ophthalmology, increased photosensitivity is related to ocular discomfort that frequently transforms into ocular pain. Ocular surface is extremely innervated by nerve fibers from neurons of the trigeminal ganglia (TG). If the ocular surface suffers from an exposure to blue light, it seems logical that a phototoxic message might be further transmitted to the trigeminal pathway thus increasing nociception and provoking pain. Therefore, the next step was to understand whether the trigeminal neurons themselves might be directly impacted by illumination. Finally, we considered the extreme photosensitivity condition and corresponding ocular pain – the photophobia. Within the frame of this syndrome, quite frequent today, we were looking to answer the following questions: is this symptom wavelength-dependent, how is it triggered and what mechanism is it operated by?

Phototoxic role of blue light in relation to these three ophthalmic disorders – dry eye, ocular pain and photophobia – became the topic of the current work. Thus, in this introduction, I will first remind briefly the structure and functions of the ocular surface, in particular of the cornea and conjunctiva as well as will describe the system of corneal innervation and of nociceptive messages propagation. Then I will present the dry eye disease and pathologies related to ocular pain and photophobia. Next, I will give a state-of-the-art of the current findings concerning the interaction of light with tissues of the ocular surface. I did my best to provide with all the important details of light protocols (irradiance, spectrum, time of exposure) that are frequently unclear in the papers and are therefore difficult to compare. To understand how the luminous flux can be received outside the image-forming system, I will review the probable locations and roles of non-visual photoreceptors. With this in mind, I will further discuss the pathways of increased photosensitivity and its relation to nociception and ocular pain. Finally, I will conclude by highlighting the related questions that remain unanswered.

Ocular surface

Ocular surface is the very first “screen” that protects the entire visual system from the external environment. In a limited sense, this structure consists of cornea and conjunctiva (42). In a broad sense, ocular surface comprises also the eyelids, eyelashes, tear film, main and accessory lacrimal glands, and the meibomian glands (43). In the healthy ocular surface, its center is occupied by the cornea followed by corneal limbus that then comes into conjunctiva (Figure 2). These structures are protected by tear film that provides with lubrication and maintains a smooth refractive surface for optimal visual performance. Together with secretory appendages and connecting innervation, ocular surface composes the integrated lacrimal functional unit (LFU) that maintains the homeostasis of tears and of ocular surface itself (44).

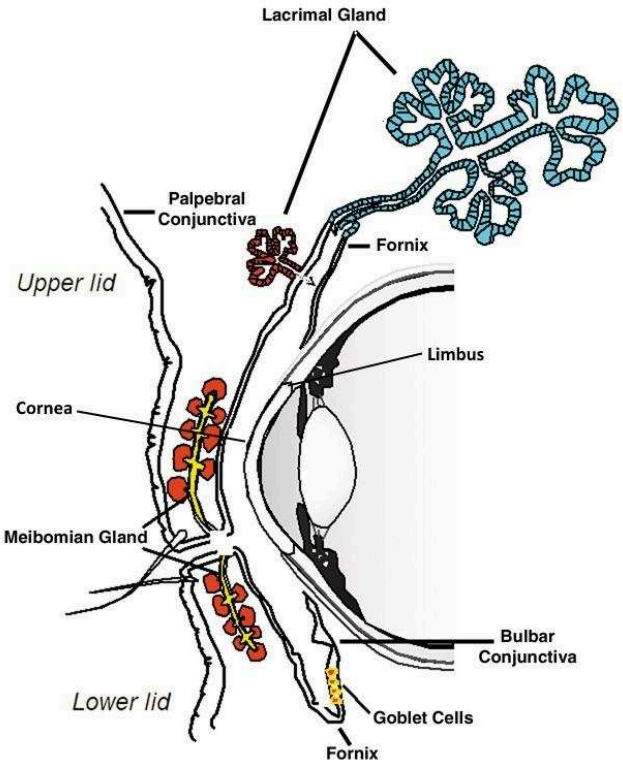

Figure 2. Structures comprised in the ocular surface

(open-access image)

Among all the structures of LFU, cornea is the one the mostly exposed to the ambient environment and its potential harmful triggers like pollution and light. Corneal main role is to transmit light till the retina; therefore, it must be transparent and avascular. To keep this transparency, the cornea benefits from the immune privilege (few immune cells) and from the inhibition of the inflammatory reactions (45). Nutrition of the cornea occurs via diffusion from the tear film at the outside and from the aqueous humour at the inside surface as well as by means of numerous nerve fibers. The human cornea is about 11 mm in diameter and 0.5 mm in thickness (46); it has 5 main layers (Figure 3a). The very first one, in direct contact with the tear film, is the superficial epithelium that represents 10% of corneal thickness; it has about 5-6 levels of easily-regenerating cells. Superficial epithelium is followed by acellular highly-fibrous Bowman layer (Figure 3b). The next layer is the thickest one: the corneal stroma takes 90% of entire corneal thickness. This layer consists of regularly-arranged collagen fibers and provides the cornea with its transparency. It contains keratocytes – the special fibroblasts that are used for repair and maintenance (Figure 3c). In addition, it is this layer that suffers from infiltration of dendritic cells and macrophages in case of inflammation. Finally, there is a thin Descemet's membrane serving as a basement membrane for the last endothelium unicellular layer. Unlike the epithelial cells, the endothelial ones cannot regenerate. They are in direct contact with the aqueous humour and maintain corneal hydratation.

a.

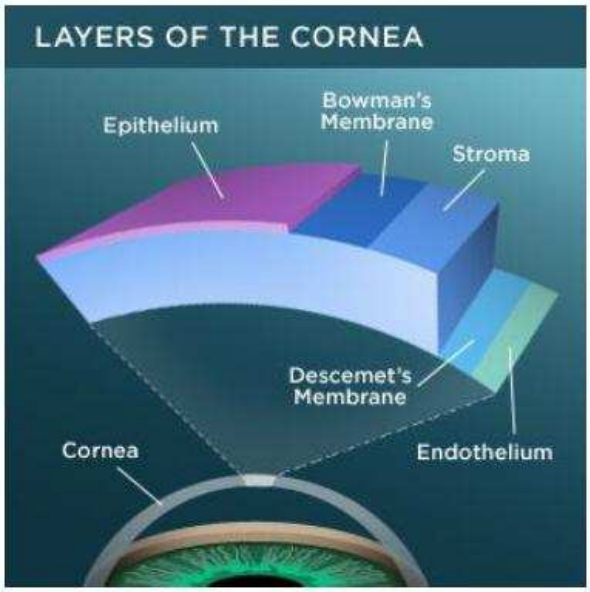

b.

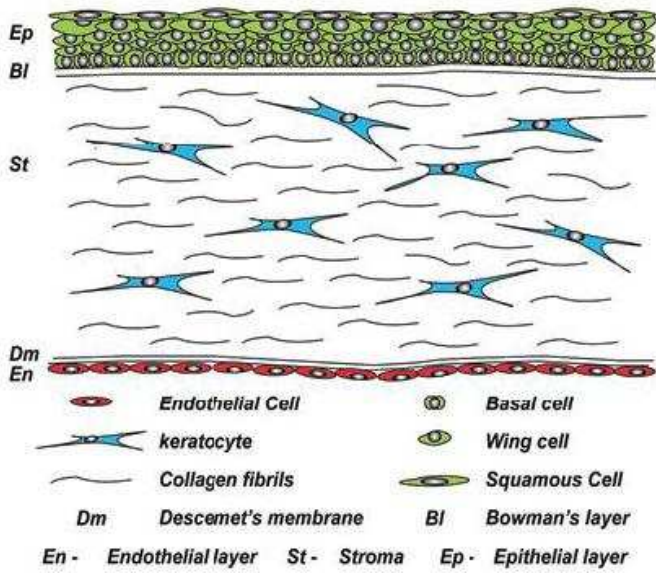

c.

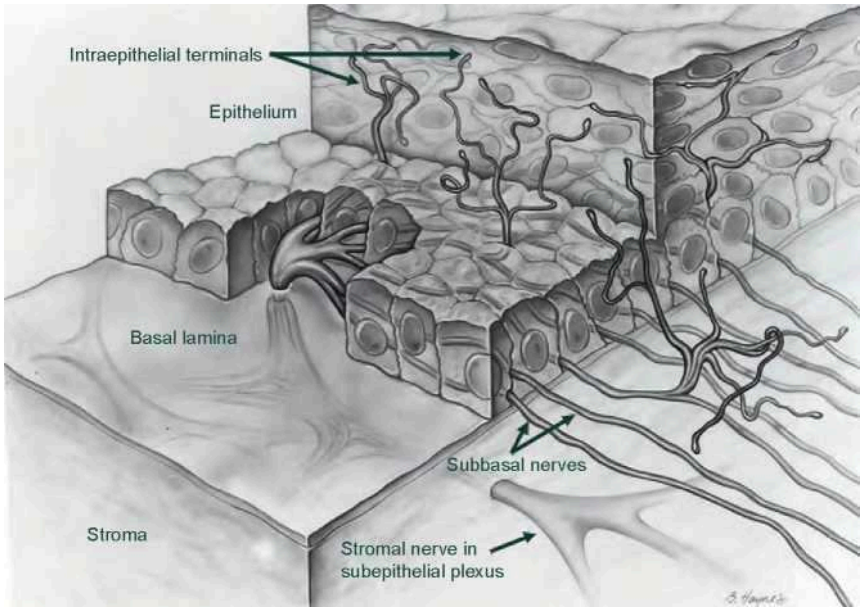

Figure 3. Internal corneal structure

a, b. Corneal layers. **c.** Innervation of the cornea. These are open access images.

The conjunctiva is a mucous membrane lying on the lamina propria of loose connective tissue; it covers the anterior segment of the eye and the internal side of eyelids (44,45). The conjunctiva has three parts: palpebral conjunctiva that lines the eyelids, bulbar conjunctiva that covers the eyeball and fornix conjunctiva that is the junction between the first two ones

(Figure 2). The thickness of conjunctiva varies from 2 to 10 cellular layers, in dependence on its location. Its stratified non-keratinized epithelium is interspersed by goblet cells. Epithelial and goblet cells secrete proteins and gel-forming mucins that are essential for tear film. Since the cornea is privileged from immune reactions, it is the conjunctiva who mediates inflammation. Its main role is to protect the eye against outer environment. It has a dense network of immune cells whose number significantly increases in case of inflammation. Furthermore, to better ensure the inflammatory reaction, conjunctiva has numerous vessels and is highly innervated.

Cell lines of human ocular surface are an important tool to model various ocular surface diseases and to evaluate ocular drugs and cosmetics. In the laboratory, use of cell culture has a number of advantages like homogeneity and increased reproducibility permitting for high throughput reproducible experiments (47). Although 3D corneal tissue model has been developed (48), the human corneal epithelial (HCE) cell line still remains one of the most widely used models for the in vitro studies of cornea-related disorders and especially of DED (e.g. (49,50)). A review of current human corneal cell culture models might be found in (51). As compared to the cornea, the number of works dedicated to conjunctiva is less important (the one performed in our team might be found in (52)). Two conjunctival epithelial cell lines are mainly used today, the Wong-Kilbourne derivative of the Chang cells (ChWK) (53) and the more recent University Institute of Applied Ophthalmobiology - Normal Human Conjunctiva (IOBA-NHC) cells (54). They have some differences in the gene profile expression and might be more or less suitable for modeling of selected biological functions. The comparison of these two cell lines to each other as well as to the primary culture of conjunctival epithelial cell was reported in (47).

Innervation of ocular surface

Cornea is the most sensitive part of the human body: per 1 mm^2 it contains about 7000 nociceptors – the sensory nerve endings that respond to external stimuli (55). In rabbit, the density of corneal nerve fibers is known to be 20 to 40 times higher than in the tooth pulp and extremely greater as compared to the skin (300 to 600 times) (56).

Electrophysiological recordings of single sensory corneal nerve fibers revealed the existence of different functional types of ocular nociceptors. They can be broadly classified as polymodal nociceptors, cold thermoreceptors and selective mechano-nociceptors (57) (Figure 4). Most of nociceptors are polymodal; they are activated by various stimuli including near-noxious or noxious mechanical energy, heat, and chemical irritants as well as by endogenous chemical mediators. The cold thermoreceptors represent 10-15% of the total population of corneal sensory nerve endings; their activity is increased and decreased by moderate cooling and heating, respectively. Mechano-nociceptors cover about 20-30% of the peripheral axons innervating the cornea and respond only to mechanical stimuli that are strong enough to damage corneal epithelial cells.

a. **b.**

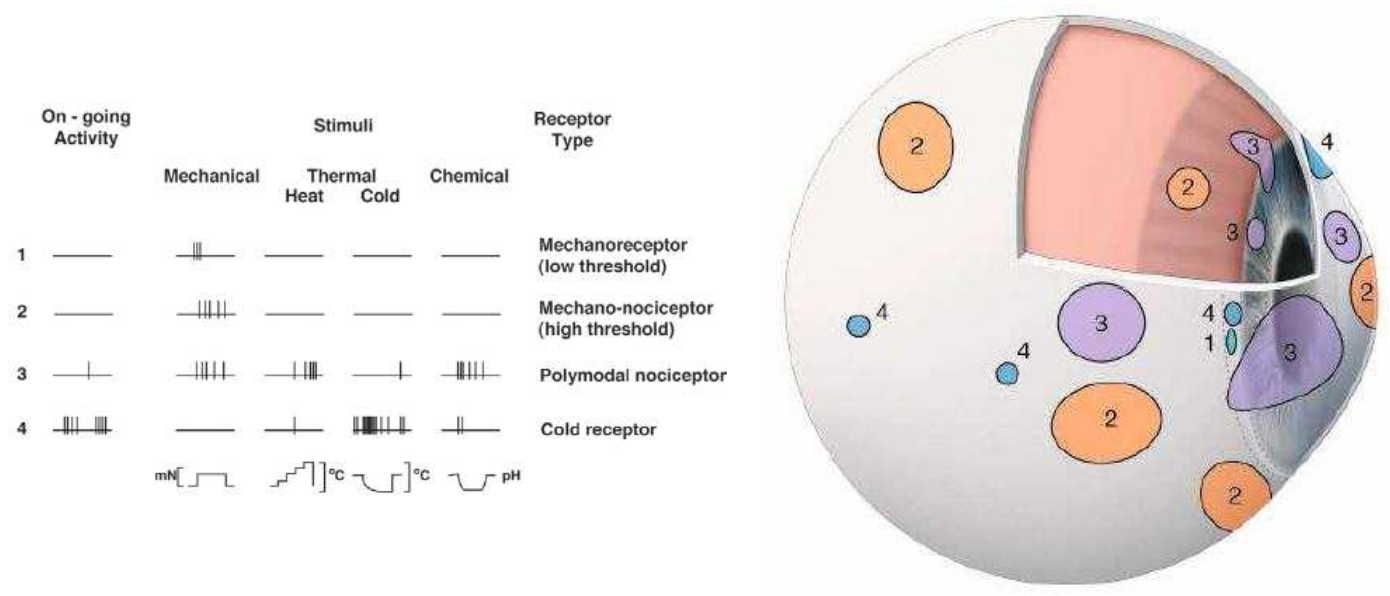

Figure 4. Functional types of sensory nerve endings on the ocular surface

a. Nerve impulse activity of various populations of nociceptors at rest and after application of different stimuli (from (57)). **b.** Schematic diagram of the location and receptive field size of various ocular sensory fibers of the anterior segment of the eye (from (45)).

Sensory neurons that supply the ocular surface originate from the trigeminal ganglion (TG) and forms an important part of LFU (Figure 5) (58).

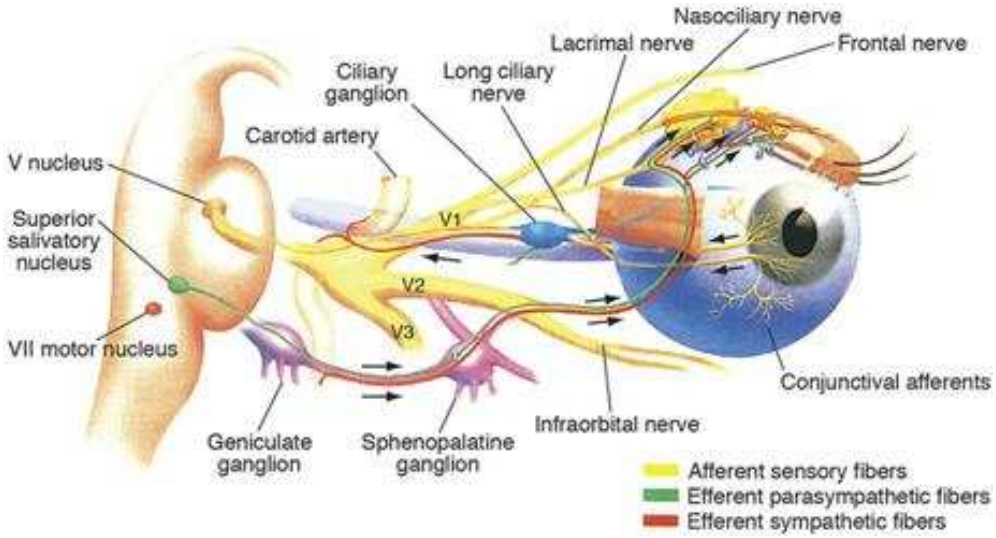

Figure 5. Representation of the integrated LFU

V1, V2 and V3 represent the ophthalmic, maxillary and mandibular branches of the TG, respectively (from (44)).

TG is a sensory ganglion of the trigeminal nerve that ensures the sensation and motor functions of the face. It has three branches: mandibular, maxillary and ophthalmic; the last two ones contain the cell bodies of ocular surface sensory nerve endings. They account for only 1-5% of total number of TG neurons; in mouse and rat, that represents about 100-200 neuron cells (59). These nerves travel to the cornea and the anterior bulbar conjunctiva via the nasociliary branch of the ophthalmic nerve and via the communicating branch to the ciliary ganglion. They give rise to long and short ciliary nerves, respectively, that pierce the sclera at the back of the eye and run forward to the anterior segment. Further, the ciliary nerves divide to multiple branches and form a plexus that in turn supply the innervation of the entire ocular surface as well as the skin covering the eyelid margins.

TG neurons synapse in multiple rostrocaudal levels of the trigeminal brainstem nuclear complex (TBNC) (Figure 6). They mainly terminate in the transition region between Vi (interpolaris nucleus) and Vc (caudalis nucleus) (Vi/Vc transition) and at the Vc/upper cervical cord junction (Vc/C1 region) (Figure 7). Some nerve endings were also found in Vp (principal trigeminal nucleus) and Vo (subnucleus oralis). Ocular neurons in the Vi/Vc transition encode the intensity of mechanical, thermal and chemical stimulation of the entire ocular surface; they are sensitive to bright light and to changes in the moisture status of the ocular surface. Neurons in the Vc/C1 region also respond to mechanical, thermal, light and chemical stimuli, at the same threshold as Vi/Vc neurons. However, unlike the latter, the receptive field for most Vc/C1 ocular neurons includes only a portion of the ocular surface and all neurons are activated by noxious stimulation of periorbital skin (58,60).

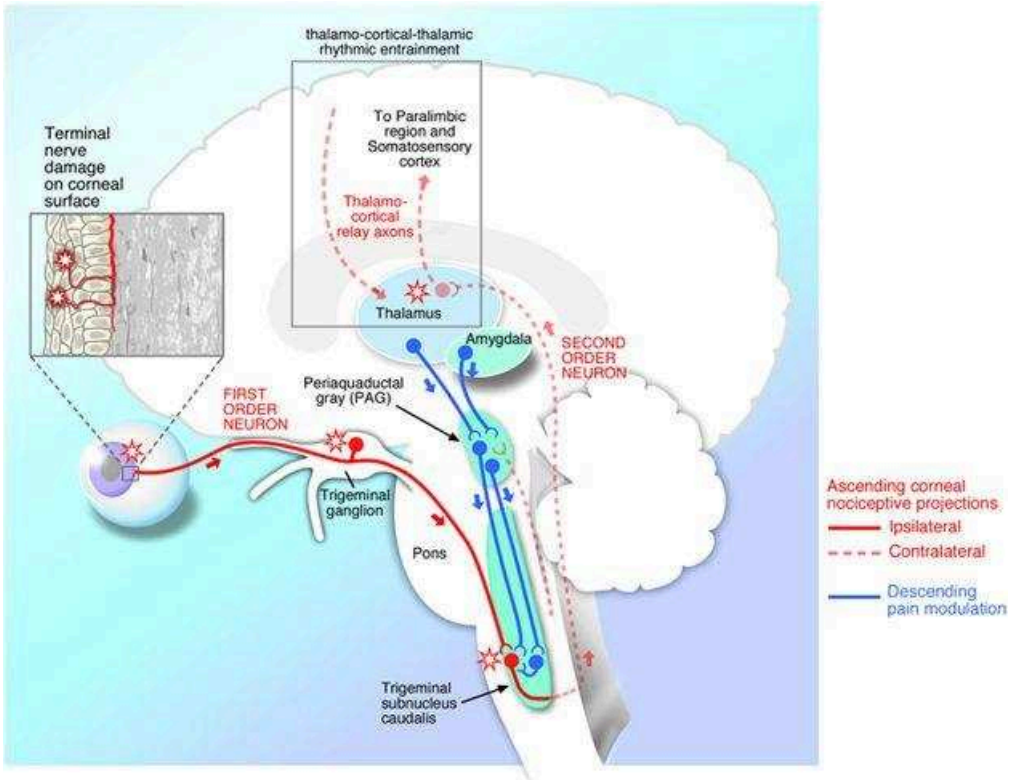

Figure 6. Propagation of nociceptive messages from cornea-innervating trigeminal system (from (60)).

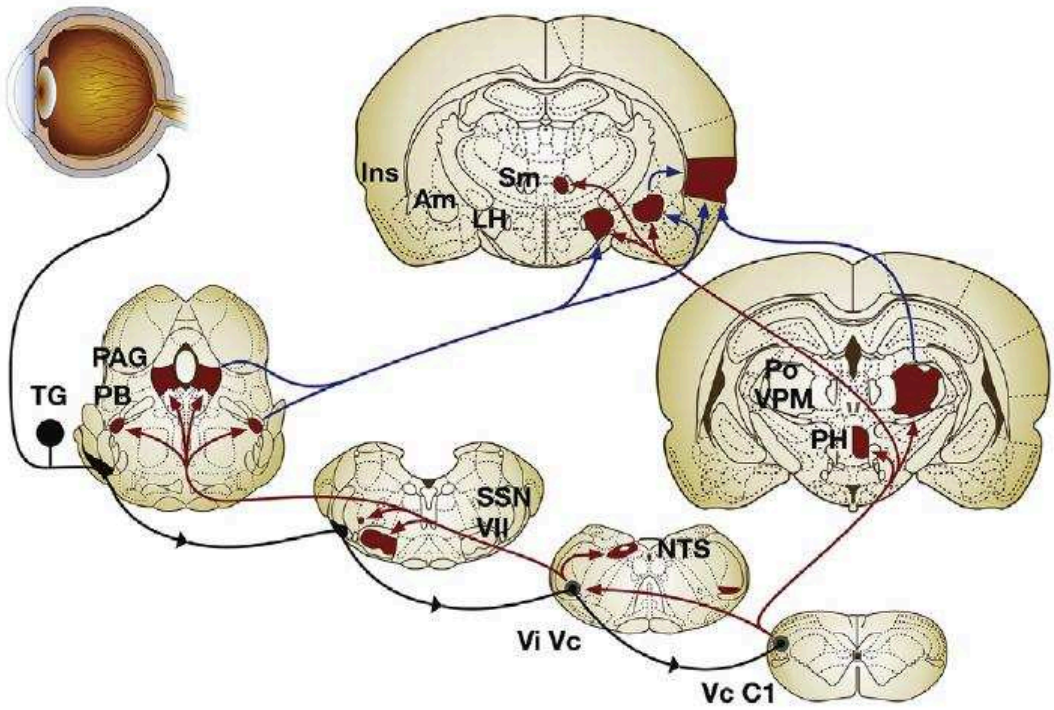

Figure 7. Main ascending pathways for trigeminal sensory fibers supplying the eye

Primary afferent fibers are drawn in black, second-order projections in red and third-order projections in blue. The abbreviations are explained in the text below (from (57)).

From TBNC, second-order ocular neurons in Vi/Vc and Vc/C1 project to brain regions that mediate various functions: facial motor nucleus (VII) for eyeblink, superior salivatory nucleus (SSN) for lacrimation, nucleus tractus solitariu (NTS) for cardiovascular reflexes. Higher projections contribute to ocular pain (periaqueductal gray (PAG), lateral hypothalamus (LH), posterior hypothalamus (PH), and amygdala (Am)) and to sensory-discriminative aspects (posterior nuclear group (Po), ventral posteromedial nucleus (VPM) and insular cortex (Ins)) (58,60).

Dry eye disease

Today, dry eye disease or keratoconjunctivitis sicca is the leading reason for ophthalmological consultations (59); in dependence on the operational dry eye definition used and the characteristics of the population studied, its prevalence varies from 5 up to 50 % (61). A limited number of studies have discussed the incidence of DED. It has been reported that in a Caucasian population (48-91 years old), the incidence was 13.3% over 5 years and 21.6% over 10 years, being higher in women (25%) than men (17.3%) for the latter period.

Since the original recognition of DED in 1995, numerous dry-eye-related in vitro, in vivo and clinical studies have been performed; much has been learned about the basis and the impact of the disease. Initially, the discomfort was identified as the principal symptom of dry

eye; then, in 2007, the definition expanded to include visual disturbance (62). The actual definition was proposed in 2017 in TFOS DEWS II report: dry eye is a multifactorial disease of the ocular surface characterized by a loss of homeostasis of the tear film, and accompanied by ocular symptoms, in which tear film instability and hyperosmolarity, ocular surface inflammation and damage, and neurosensory abnormalities play etiological roles (43).

Dry eye cannot be characterized by a single process, sign or symptom since it has a number of different interacting causes or impacts. This is all the more important given that many other ocular surface diseases can be co-morbid with dry eye. Tear hyperosmolarity and tear instability are considered as the core drivers of DED. This allowed for definition of two major types of DED: evaporative dry eye (EDE) and aqueous-deficient dry eye (ADDE).The first one is the result of an excessive evaporation from the tear film in the presence of normal lacrimal function (e.g. in case of tear lipid layer deficiency that accompanies meibomian gland dysfunction (MGD)) whereas in the second one, hyperosmolarity results from a reduced lacrimal secretion in the presence of a normal rate of tear evaporation (e.g. in case of lacrimal gland damage in aged people). Hybrid DED also exists; moreover, in a sense, all forms of DED are evaporative, since without evaporation, tear hyperosmolarity cannot occur.

A large number of studies have been performed to evaluate the risk factors of DED. However, its comprehensive understanding is complicated due to methodological differences between studies, differences in population groups and diagnostic criteria (61). Widely accepted DED risk factors are the following: female sex, older age, MGD, digital devices use, Asian race, contact lens wear, eye surgery, Sjögren syndrome (affects the body's moisture-producing glands) and Grave's disease as well as other autoimmune diseases, environmental hazardous conditions like pollution and low humidity, systemic connective diseases, and certain classes of medications including antihistamines and antidepressants. Ocular symptoms are the main problem that drives patients to seek for eye care. Among the numerous DED symptoms, the most frequent ones are itching and burning, soreness and pain, light sensitivity, foreign body sensation, ocular irritation, blurred/poor vision, eye redness, and intolerance to environment conditions (wind, air conditioning) as well as to contact lenses (63).

However, dry eye may also be asymptomatic and present only the clinical signs; the reverse situation is also possible. Furthermore, signs and symptoms might be completely decorrelated. This fact highly complicates the establishment of clear classification of DED. The current one is based on a clinical decision algorithm, beginning with the assessment of symptoms, and followed by review for signs of ocular surface disease (43) (Figure 8). Clinical assessment of DED includes but is not limited to studying of patient's case history, various questionnaires (to decipher symptoms), examinations via the slit-lamp and in vivo confocal microscope (IVCM) (to assess the ocular surface), various evaluations of tears (tear quantity by means of Schirmer's test and phenol red thread test, tear stability by tear break-up time (TBUT) measurement, tear osmolarity). A report about DED diagnostic methodology might be found in (64).

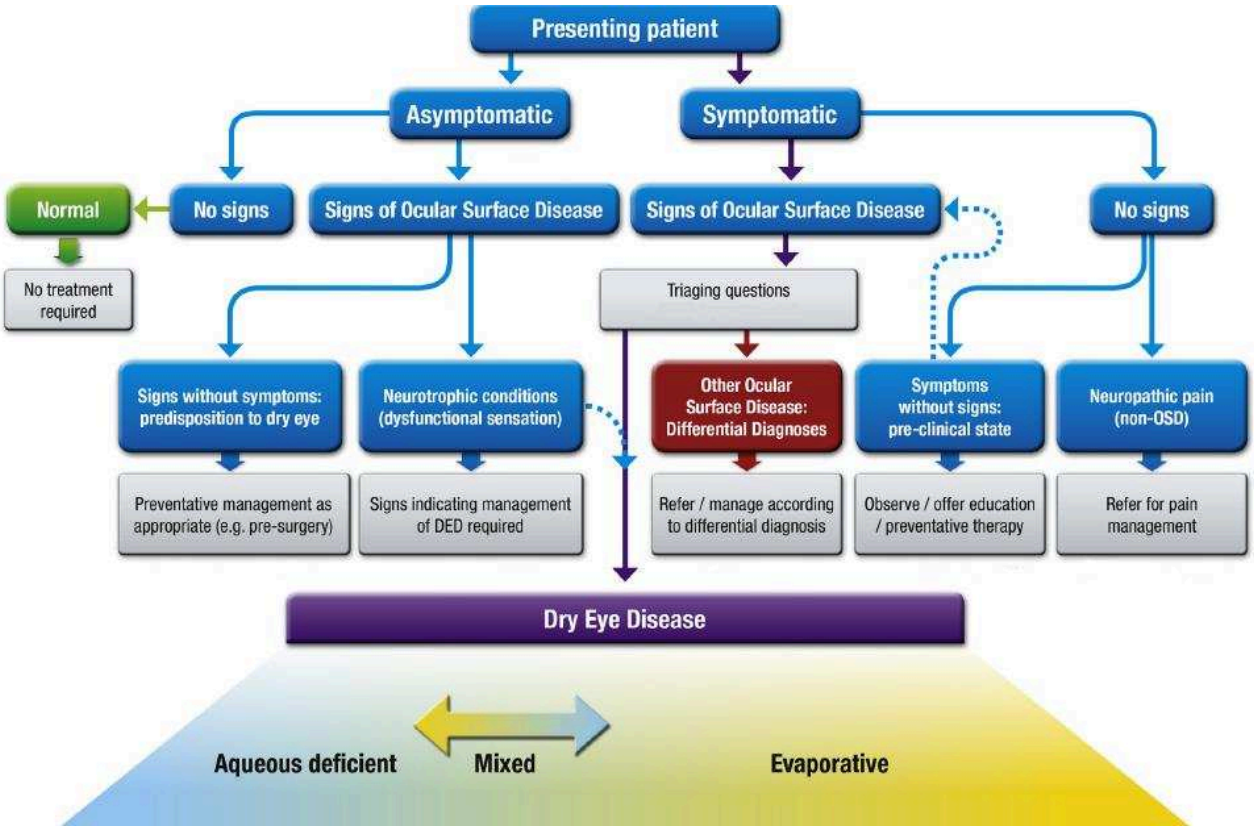

Figure 8. DED classification

The upper portion of the figure describes a clinical decision algorithm whereas the lower one represents the etiological classification of DED (from (43)).

Classification is not the only complex issue of DED; another one is the definition of the precise process underlying its pathology. In the simplest model, tear hyperosmolarity is the starting point that initiates the chain of events leading to ocular surface damage (44). It gives rise to symptoms, generates inflammatory responses and leads to chronic ocular surface damage and self-perpetuated disease. Briefly, tear hyperosmolarity stimulates a cascade of events in the epithelial cells of the ocular surface, involving alteration of MAP kinases and NFkB signaling pathways, generation of inflammatory cytokines and induction of oxidative stress. These lead to a reduced expression of mucins, a death of surface epithelial cells and a loss of goblet cells that in turn compromises ocular surface wetting. Finally, ocular surface hyperosmolarity is amplified, which completes the vicious circle of dry eye and establishes the mechanism that perpetuates the disease (Figure 9). Tear hyperosmolarity is not necessarily the starting point of DED (65). This vicious circle offers entry points for any cause of disease like ocular surface inflammation or altered mucin expression, due to various disorders. DED pathological mechanisms are intensively studied by means of various animal models (like desiccating stress or lacrimal gland ablation) or of ocular surface cell cultures (like corneal or meibomian gland epithelial cells). The details about DED investigation can be found in (44).

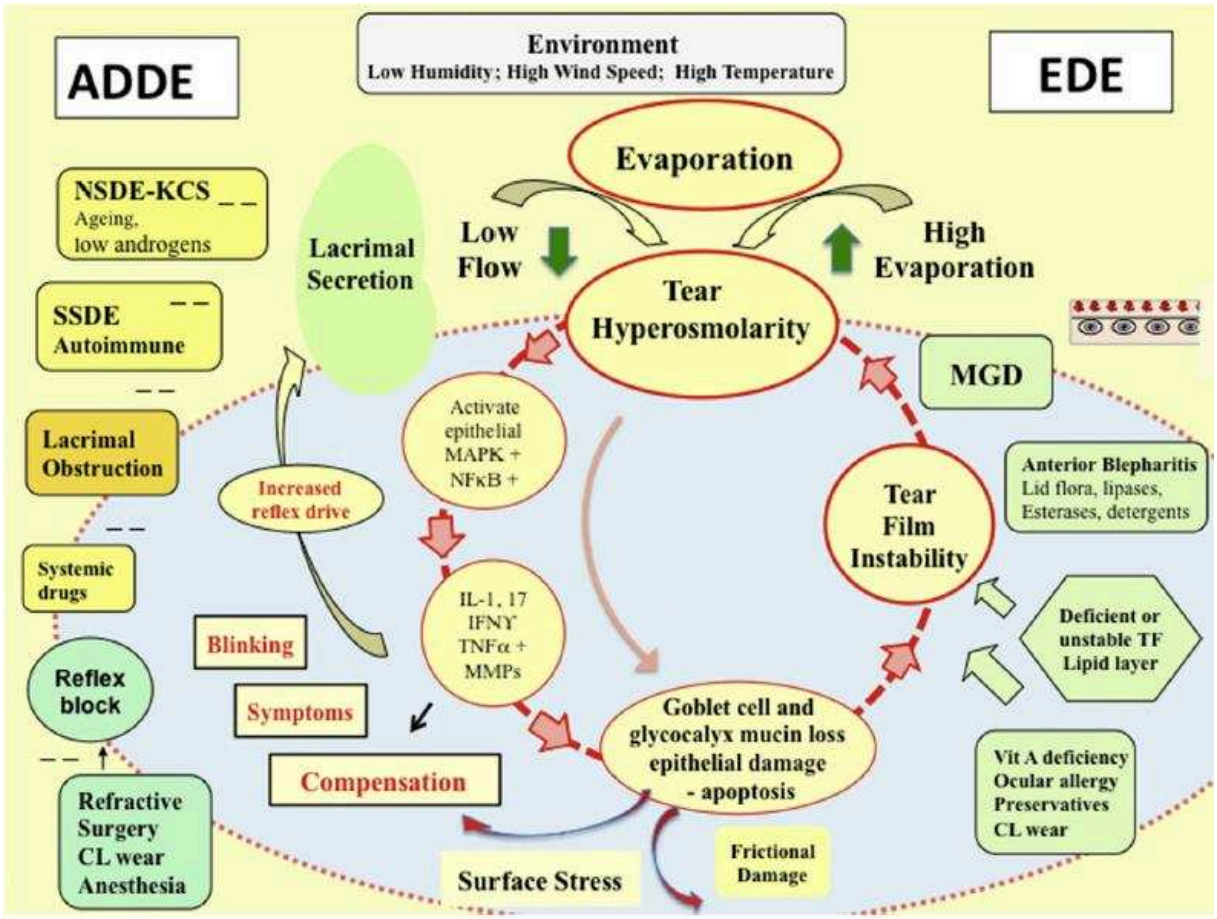

Figure 9. The vicious circle of dry eye

EDE – evaporative dry eye, ADDE – aqueous-deficient dry eye, NSDE-KCS – non-Sjögren Syndrome Dry Eye - keratoconjunctivitis sicca, SSDE – Sjögren Syndrome Dry Eye, CL – contact lenses (from (44)).

Dry eye management is complicated due to its multifactorial etiology. Current therapies include treatments for tear insufficiency and lid abnormalities, anti-inflammatory medications, surgical approaches, some dietary modifications and environmental considerations. Nevertheless, "the management of DED remains something of an art", and highly depends on a specific case of every patient. More information about current anti-DED solutions might be found in (66).

Light and ocular surface

Patients consulting for ophthalmology and especially those suffering from ocular surface diseases like DED frequently complain about exacerbated photosensitivity and increased symptoms of discomfort in various luminous conditions (61,67–69) and when being in front of monitors (32,33,39,41). Numerous studies investigated the impact of near UV on the structures of ocular surface and some works are dedicated to IR exposure (70–74); however, so far, quite few works paid attention to the phototoxicity due to the visible light.

Two groups of researchers investigated the phototoxicity of wide-spectral white light. It is widely accepted that dry eye symptoms occur and persist in some patients after the cataract surgery (75). Thus, Hwang et al. hypothesized that exposure to white light from an operating microscope might induce an injury to the ocular surface and damage the tear film (76). They exposed rabbits to light of $4*10^4$ and $10*10^4$ lux for 30 minutes (one should note that their white spectrum also comprised a UVB light of 280-320 nm) and reported a light-induced deterioration of clinical results (Shirmer's test and corneal fluorescein staining), morphological changes in cells of ocular surface and a decrease in number of goblet cells. They also found a decrease in mucin MUC5AC expression and, in tears, an increase in the pro-inflammatory cytokine IL-1β rate. On the basis of the same hypothesis, Ipek et al. studied in vitro whether light would have an effect on wound healing closure (77). They illuminated the post-scratched primary culture of fibroblasts from porcine eyes by laboratory light microscope of 10^4 lux irradiance for 10 minutes. 24 hours after exposure, illuminated cells exhibited a significant decrease in viability and a slower wound closure rate. Recently, this group reported the same phototoxicity in the primary culture of porcine conjunctival fibroblasts in an hyperosmolar dry eye model (78). Thus, both teams concluded that dry eye symptoms manifested by many patients after ophthalmic surgeries may be explained by the phototoxic effect of the operating microscope.

Several works were dedicated to spectrum-dependent phototoxicity in ocular surface. Lee et al. investigated which visible wavelengths emitted by LEDs within the range of 410-850 nm (i.e., it also included a part of IRA) would be the most dangerous for human corneal epithelial (HCE) cells (50). They found that various radiant exposures (1–100 J/cm^2) of 410 and 480 nm significantly decreased cell viability and induced reactive oxygen species (ROS) formation, commonly observed in dry eye. They therefore argued that exposure to blue light might have a role in the pathology of DED. Niwano et al. studied the influence of 405 nm violet light on rabbit corneal epithelial cells (79). After 1–3 minutes of various exposures (53.8–167.4 J/cm^2), the sub-confluent (10–30%) cells exhibited a significant decrease in viability as well as some morphological changes. No such reduction was observed for the confluent cells (90–100%). Later, the same group found these effects in the primary culture of cells of human ocular surface (80) and concluded that blue light in the near-UV region might be hazardous to corneal epithelial cells undergoing mitosis. In addition, the authors reported that UV and blue light filters were effective in protecting cells from the phototoxic damage.

To our knowledge, within the frame of ocular surface phototoxicity, there was the only one in vivo study. Lee et al. exposed mice to the LED-derived light of three narrow wavebands centered at 630 (red), 525 (green) and 410 (blue) nm of 48.8, 59.5 and 29.2 mW/cm^2 irradiances, respectively; the animals were illuminated twice daily for 10 days (10). For the blue-illuminated group, they observed a significant decrease in tear break-up time and important corneal fluorescein staining. In the cornea, they reported an important number of apoptotic cells, ROS production and increased rates of IL-1β and IL-6. In both cornea and conjunctiva, malondialdehyde (MDA, product of lipid peroxidation process) rate and CD4+CCR5+ T cells number were up-regulated. Since all these signs are the ones usually observed in patients suffering from DED (44,81,82), the authors concluded that 410 nm blue light might aggravate clinical dry eye parameters in murine model when compared to visible light of other wavelengths.

Taken together, these works established that exposure to light, particularly to its blue-spectral part, does harm the ocular surface and does provoke the DED-related photodamage.

DED-related ocular pain

One of the important novelties in the last definition of dry eye is the fact that neurosensory pathways have been recognized as playing an etiological role. The aim of the entire TFOS DEWSII Pain and Sensation Report was to "highlight the neurobiological mechanisms underlying the discomfort that accompany DED" (58). Even if until a few decades ago, the term "pain" within the frame of eye pathology was generally reserved for the sensations accompanying traumatic or infectious diseases (like keratitis or angle closure glaucoma), today, ocular pain is recognized as one of the most consistent clinical features of chronic dry eye (83,84). In clinics, ocular pain can be evaluated by means of surveys and questionnaires, by measurement of corneal sensitivity (e.g. via the Cochet-Bonnet esthesiometer) and by IVCM examinations of corneal nerves and immune cells. Biomarkers in tears and in conjunctival cytological imprints (a cellulose acetate filter is applied to the ocular surface to remove the superficial layers of the ocular surface epithelium) can also be used as an indicators of the status of ocular surface innervation and inflammation (58,59).

According to International Association for the Study of Pain (IASP), pain is "an unpleasant sensory and emotional experience associated with actual or potential tissue damage or described in terms of such damage" (58). On the basis of etiology, duration and clinical features, various types of pain can be distinguished. However, one should take into account that the use of pain-related terms, defined in the following paragraph, is frequently confusing in the literature.

Since nociception includes all forms of information processing triggered by noxious (i.e., damaging to normal tissues) stimuli (85), nociceptive pain is defined as the one provoked by actual or threatened damage to tissues (58). Nociceptive pain is due to activation of nociceptors that however function normally; it usually persists as long as the stimulus is applied. In contrast, neuropathic pain is caused by a lesion or a disease of the somatosensory nervous system. At least two subtypes of neuropathic pain can be distinguished: allodynia describes pain from a normally non-painful stimulus whereas hyperalgesia is an exacerbated painful response to a stimulus that is initially considered as provoking pain (67,85). The sensitization of nociceptive nerve endings will, however, usually induce both hyperalgesia and allodynia by shifting stimulus-response curve to lower intensities. Neuropathic pain can be categorized not only etiologically (like degenerative or traumatic or toxic) but also anatomically (into peripheral vs. central) since it is generated by functional disturbances at different levels of the neuroaxis. When pain persists longer than the normal time of healing, it becomes chronic pain (58).

Currently, the number of ocular pain treatments is quite restricted. Artificial tears as well as anti-inflammatory, immuno-modulatory and analgesic medication are frequently used. However, not only their efficiency remains limited but also, when long-term used, they may provide with additional ocular disorders (59).

Differentiating DED-related nociceptive pain from peripheral and central neuropathic ocular pain is important for further successful treatment of patients (58). DED-related pain is a unique type of corneal pain that is associated with excessive tear film evaporation modulated by environmental factors; it is exacerbated by circumstances that promote tear film evaporation and alleviated by those that suppress it (83). Excessive evaporation causes increased tear osmolarity as well as rapid cooling of the ocular surface. Both events in turn cause stress to the ocular epithelium and may lead to local inflammation and to peripheral nerve damage. These may then provoke genetic and molecular changes that modify the electrophysiological characteristics of sensory neurons. In the longer term, these changes may result in deregulated transmission and processing of pain signals and therefore in chronic pain (58). This common impact of dryness and inflammation on the activity of various ocular surface nociceptors provides with important changes in sensation, blinking and tearing (Figure 10).

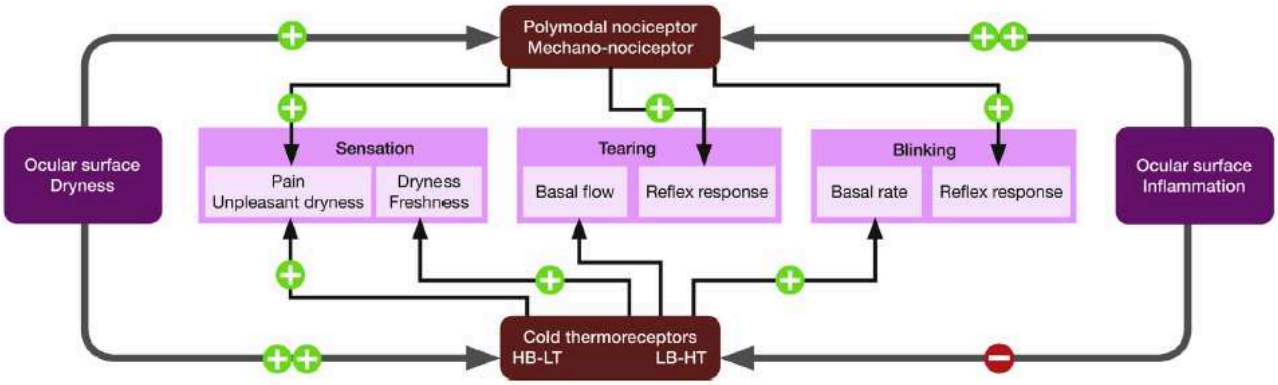

Figure 10. Inflammation and dryness in DED

The scheme summarizes how ocular inflammation and ocular surface dryness provoke variable increases (+) or decreases (-) in nerve impulse activity of polymodal- and mechano-nociceptors and in cold thermoreceptors. The latter are divided into 2 subtypes dependent on their characteristics: high background activity + low cooling threshold (HB-LT) or low background activity + high cooling threshold (LB-HT) (from (58)).

Photophobia

Photophobia or increased photosensitivity or light aversion – all these terms relate to highly debilitating sensory disturbance provoked by visible light. Since the eye is the most highly innervated structure of the body, this discomfort, also referred to as photoallodynia or neuropathic photosensitivity, frequently provides with the corneal nociceptive or neuropathic pain (59,60,83). Similar to the different terms used to describe various types of pain, the system of definitions related to photophobia is even more confusing.

In photophobic patients, exposure to normally non-painful illumination causes discomfort in the eye. Photoallodynia was reported as unexplained painful photophobia typically characterized by increased sensitivity to illumination from computer screens and from

fluorescent and metal halide lamps (the symptom concerns less the incandescent lights) (83). Like dry eye, photophobia may be hardly detectable in clinics: many patients with a chief complaint of photophobia will have a normal eye exam (68). Moreover, it may be comorbid to various neurologic disorders. For example, 80% of migraineurs heavily suffer from increased light sensitivity (86). However, dry eye is still one the most common ocular cause for photophobia (68). Nonetheless, DED-related photophobia only starts to be widely recognized. For example, in the last TFOS DEWS II report concerning pain and sensation, increased sensitivity to light has been only mentioned (58).

Non-visual photoreception

Since the ocular pain and photophobia are the symptoms of dry eye, the pathology of ocular surface, the next question is how the cells of ocular surface can receive the phototoxic message? The one well-known photoreception pathway passes through the molecules of mitochondrial respiratory chain, such as flavins and cytochrome oxidases, that can directly absorb blue–violet light (18,19). However, is it the single possibility of light reception? In other words, can the parts of ocular system outside the retina be also photosensitive? Sure, they do not have retinal receptors for vision like rods and cones (87); nonetheless, they still might receive the luminous message by means of non-visual photoreceptors.

IpRGC and melanopsin

The best known photosensitive cells providing with non-visual functions are atypical retinal photoreceptors called intrinsically photosensitive retinal ganglion cells (ipRGC). Their discovery at the bound of the 19th – 20th centuries allowed for explanation of circadian photoentrainment in blind patients and in mice lacking visual photoreceptors. The ipRGCs project in both non-image and image-forming brain areas, including the suprachiasmatic nucleus (SCN) for circadian photoentrainment, the olivary pretectal nucleus (OPN) for the pupillary light reflex (PLR) and the dorsal lateral geniculate nucleus (dLGN) for image formation. ipRGCs projections were also found in some additional brain regions, suggesting other yet unidentified light-related functions (88). A great number of papers has been dedicated to various roles of ipRGC known to date (e.g. (89–93)).

IpRGCs combine the input from visual photoreceptors with their own intrinsic response. It was shown that the photopigment melanopsin or opn4 is necessary and sufficient for inner retinal photoreception and that the ipRGC population and melanopsin-expressing cell population were identical (94). Initially considered as a single cell type, it was later revealed that ipRGCs possessed a far more complex classification. In nocturnal rodents, five different types of ipRGCs with different morphological and physiological properties were identified (M1-M5), with additional two sub-types for the first of them (expressing or not the special marker Brn3b) (Figure 11). In primates and humans, two subtypes (M1 and M2) of ipRGCs have been reported so far; the diversity of ipRGCs may continue to expand. For more details, see (88,94).

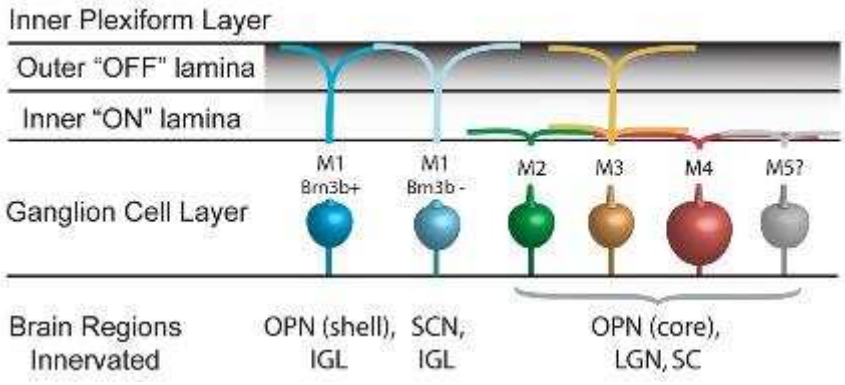

Figure 11. Various subtypes of ipRGCs

Illustration of currently known subtypes of ipRGCs in nocturnal rodents (M1–M5 plus two sub-types of M1 cells, Brn3b transcription factor-positive and -negative) with their correspondent neural projections to the brain. SCN – suprachiasmatic nucleus, OPN – olivary pretectal nucleus, LGN – lateral geniculate nucleus, IGL – intergeniculate leaflet, SC – superior colliculus.

IpRGCs exhibit the three main differences with the classical visual photoreceptors. The first one is related to the kinetics of photoreception (88). When compared to highly-sensitive and fast rods and cones, melanopsin-mediated response is rather sluggish. Less sensitivity of ipRGCs is explained by the fact that the density of melanopsin on the cell membrane is about 3 molecules per μm^2 while for rods and cones it is about $25*10^3$ molecules per μm^2. However, the unitary response of ipRGC is larger than that known for any vertebrate sensory neuron; it lasts about 10 seconds, i.e., about 20-fold and 100-fold longer than for rods and cones, respectively. Moreover, ipRGCs present a high degree of temporal signal integration observed in no other sensory cell: their persistent response may last till ~ 5 minutes (95).

The second difference is in the transduction cascade. In ciliary photoreceptors like vertebrate rods and cones, light decreases the level of cyclic guanosine monophosphate (cGMP) which closes cGMP-gated cation channels and causes the cell membrane to hyperpolarize. In contrast to this graded hyperpolarization, in ipRGCs, photon reception leads to depolarization and to production of action potentials (94). However, the correspondent mechanism of light into an electrical signal conversion still remains elusive. Since melanopsin is more similar to invertebrate than vertebrate visual pigments and by analogy to the phototransduction cascade in most invertebrates, the prevailing view is that light-activated visual pigment excites a G_q type G protein causing in turn the opening of transient receptor potential (TRP) ion channels via a signaling pathway that involves phospholipase C. Nonetheless, none of the steps in this sequence of events are understood extensively; for more detail see (95).

The third difference is in the process of chromophore regeneration. In the ciliary opsins, it requires the transport of the correspondent chromophore – retinal – to another cell type. The main retinal recycling mechanism is located in the retinal pigment epithelium (RPE) where numerous enzymes convert all-trans-retinal back to 11-cis-retinal and return it to photoreceptors. However, for ipRGCs operation, the RPE photocycle is not necessary: here, the all-trans-retinal is not released from the opsin. Instead, after having been activated by blue

light (~ 480 nm), the melanopsin then absorbs a second photon of a reversing yellow-red wavelength (~ 540 nm) that re-isomerizes all-trans- back to 11-cis-retinal. However, other mechanisms of chromophore recycling were also proposed (94).

Thus, melanopsin was initially supposed to exist either in a resting dark (11-cis-retinal-bound or just melanopsin) or in an active meta- (all-trans-retinal-bound or metamelanopsin) state and was therefore called bistable. A defining feature of bistable pigment is that it activates from a single conformational state. However, according to two recent studies, it is not the case for melanopsin. Matsuyama et al. expressed mouse melanopsin in human embryonic kidney cells and characterized the photochemical properties of the pigment, for the first time (96). According to them, melanopsin in dark state and in meta-state presented absorption maxima at 467 nm and at 476 nm, respectively. Moreover, they discovered that when exposed to long-wavelength orange or red light, melanopsin exhibited another peak of absorption at 446 nm. They found that it was a new state containing 7-cis-retinal and called it extramelanopsin. Extramelanopsin is most probably formed from metamelanopsin and is photoconverted back to the meta-state via short-wavelength irradiation (Figure 12). However, it was unclear whether 7-cis-retinal related to this new state had any physiological role.

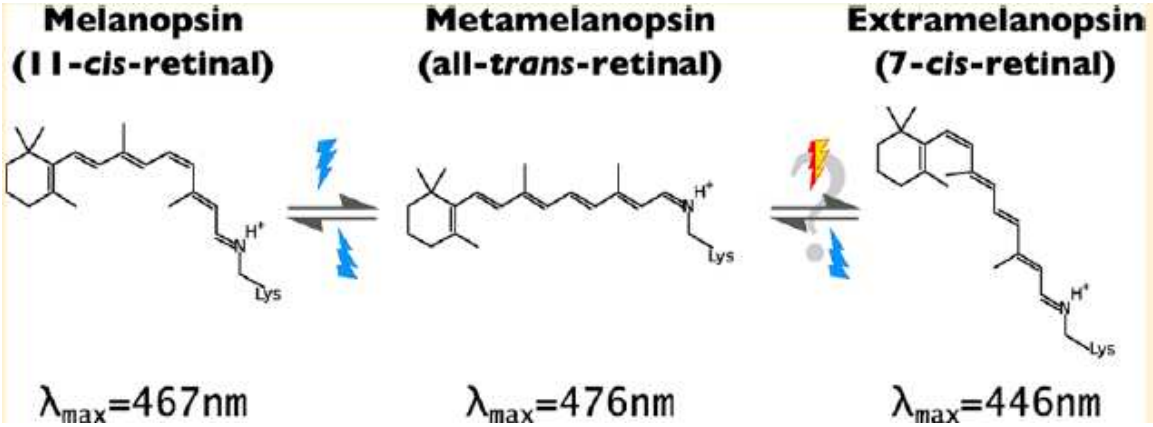

Figure 12. Photochemical properties of three states of melanopsin (proposed by Matsuyama et al. (96))

Later, Emanuel and Do confirmed on mouse retina that melanopsin indeed exhibited tristability since it possessed two silent and one signalling state (97). According to them, the dark-adapted melanopsin had an absorption maximum at 471 nm (that they referred to as cyan). With the 600-nm (red-orange) background light, the maximum was blue-shifted to 453 nm (violet state) thus confirming that melanopsin activated from more than one state and was therefore not bistable. By applying the background light of various spectra, they observed that ipRGCs exhibited an action spectrum that might be described as the weighted sum of cyan and violet states. Thus, light produced an equilibrium of cyan, violet, and signaling meta- (476 nm) states in dependence on wavelength of illumination; moreover, photon absorption by one state caused it to isomerize to another. The authors therefore concluded that melanopsin may be activated by a wider range of wavelengths and therefore features, in addition to previously discussed temporal integration, the chromatic integration.

To sum up, according to these two studies (96,97) that reported very close results, melanopsin appears to be tristable in its native environment as well as when purified (Figure 13). It is currently unknown whether this tristability is unique to mammalian melanopsin or is also a property of other visual pigments.

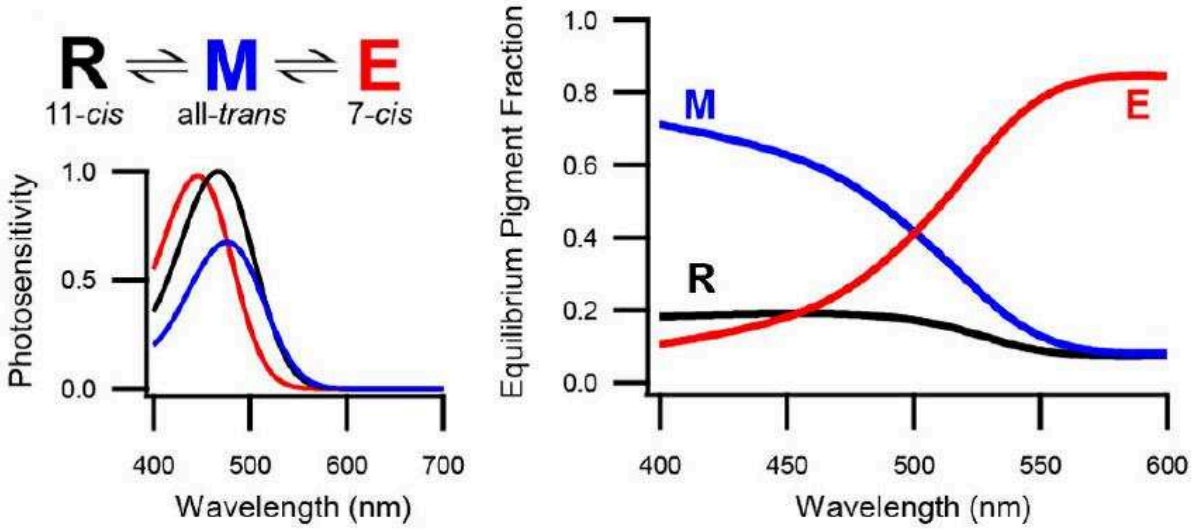

Figure 13. Three states of melanopsin

Resting dark (R, black) or 'cyan state', metamelanopsin (M, blue) and extramelanopsin or 'violet state' (E, red). **Left:** the relative photosensitivities as a function of wavelength. **Right:** numerical simulation of equilibrium fraction of each pigment state as a function of wavelength (from (97)).

Out-retinal melanopsin

The presence of melanopsin was discovered in mammalian tissues outside the retina. Very recently, Delwig et al. reported the previously unrecognized localization of melanopsin in nerve fibers within the mouse cornea (98). Genetically (the opn4 gene drove the expression of fluorescent protein) and by immunolabeling, they found melanopsin mainly at the expansions of nerve fibers that invaded the extracellular spaces in corneal epithelial layer. The RT-qPCR on isolated corneal tissue did not reveal any melanopsin mRNA suggesting that the presence of this protein in the cornea was provided by nerve endings of sensory neurons from the ophthalmic branch of the trigeminal ganglia that innervate the ocular surface (60). This group also confirmed the previously reported findings of Matynia et al. who discovered the genetic signature of melanopsin in the ophthalmic branch of TGs (99). Moreover, Delwig et al. reported melanopsin presence in primary neuronal TG culture. However, they failed to see the evidence for correspondent protein expression. Matynia et al. did show melanopsin immunoreactivity in human TGs but did not describe it in mouse TGs. Interestingly, in addition to neurons of human TGs, this group also reported numerous melanopsin-positive satellite glial cells. In the study of Delwig et al., calcium imaging and electrophysiological recordings failed to reveal any response to 3 minutes of 20 mW/cm^2 white light either in cells

and fibers in the cornea or in TG neurons. This result is in discrepancy with Matynia et al. who reported the intrinsic photosensitivity of trigeminal melanopsin-expressing cells in response to 5 seconds of 480 nm light of 28 mW/cm^2 irradiance. The work of Lei et al. implicitly confirmed the results of Delwig et al. In their clinical study, topical ocular anesthesia did not alter the psychophysical photophobia thresholds for either blue (460 and 480 nm) or red (540, 580 and 630 nm) light of various irradiances (0.4–3.8 mW/cm^2) (54, personal communication). It was therefore suggested that probable photoactivity of TG neurons made little contribution to photophobia under physiological conditions, if any.

Besides the retina and trigeminal system, melanopsin was also found in the iris and ciliary body. Xue et al. detected opn4 mRNA and protein expression in the mouse iris (101). They then showed that iris provided with intrinsic PLR (iPLR, i.e., non-dependent on retinal input) that was driven by melanopsin. They also observed the light-induced tension responses in iris sphincter muscles. Vugler et al. reported the existence of a distinctive plexus of melanopsin-positive fibers at the edge of the rat retina (102). Later, by means of immunochemistry in mice, the same group identified the melanopsin-rich ciliary marginal zone (CMZ) plexus and observed melanopsin-positive fibres projecting from ipRGCs at the CMZ directly into the ciliary body (103). They also reported that melanopsin was expressed at low levels in the ciliary body itself. Taken together, the findings of these 3 works revealed that melanopsin-dependent iPLR might be composed of at least 2 components, one involving constriction of iris sphincter muscle and another involving intrinsic signalling in the ciliary body / CMZ (for the pupillometry, 480 nm light of 0.06–60.0 mW/cm^2 irradiance was used). These results disagree with the study of Rupp et al. who reported that direct PLR at “physiological light intensities” was driven by input from ipRGCs that projected to the iris, and was not an intrinsic property of iris itself. Near the iris muscle and in the cornea, they observed the axonal fibers that originated from the melanopsin-expressing retinal cells (104).

Thus, the function of out-retinal melanopsin in trigeminal neurons and in their corneal afferents as well as in the iris and ciliary body still remains elusive and need more investigations.

Neuropsin

Another non-visual photoreceptor which is gaining today an increasing attention is neuropsin or opn5. This photopigment was first identified in 2003 by Tartellin et al. who showed, by means of RT-PCR, the expression of neuropsin in mouse eye, brain and testis, in human retina, brain and testis, and in human cell lines derived from neural retina and RPE (105). Later, Kojima et al. reported that mammalian (mouse and human) neuropsin had an absorption maximum at 380 nm (106). After exposure to UV light, neuropsin was converted to a blue-light-absorbing photoproduct with an absorption maximum at 470 nm; it was stable in the dark and could be reverted to the initial UV-absorbing state by the subsequent exposure to orange light. By means of Western blot on mouse tissue extracts, they identified the brain, the retina and surprisingly the outer ears as major sites for opn5 protein expression. They also reported that in the retina, neuropsin immuno-reactivities were detected in a large number of RGCs as well as in a subset of horizontal and amacrine cells. By means of RT-PCR and

immunochemistry, Nieto et al. demonstrated the presence of neuropsin in RGC-5 cells (rat retinal cell line) (107). They observed that, in response to white light stimulation, these cells exhibited intrinsic photosensitivity capable to regulate the levels of intracellular Ca^{2+} (1-2 $*10^4$ lux for 30-60 s) and Fos expression (800-1000 lux for 30-180 min), akin to features commonly associated with inner retinal cells. In rat retina, they detected neuropsin immunostaining in the ganglion cell layer (GCL), inner plexiform layer (IPL) and inner nuclear layer (INL).

The potential role of neuropsin in retinal photodamage was reported by Benedetto et al. (24). In rats, after 4 days of constant white 200 lux illumination, they found increasing levels of opn5-immunolabeling in some cells of GCL and INL. Neuropsin-related light entrainment was extensively investigated by the group of Van Gelder. They demonstrated that mouse retinas exposed to 370 and 417 nm light/dark cycles had stable entrainment phases. The photoentrainment was significantly weaker for 475 nm and was absent for 530 and 628 nm light (108). By means of opn5 knock-out mice, these researchers proved that retinal ex vivo photoentrainment required the presence of neuropsin. They confirmed the localization of opn5 in RGC layer and also detected its transcripts in both fresh and cultured corneas. Moreover, they found that corneal circadian rhythm was also light-entrainable ex vivo and neuropsin-dependent. This was the first evidence for photosensory function in the mammalian cornea. Later, by means of RT-PCR, this group reported the presence of melanopsin and neuropsin in mouse iris – ciliary body complex (109). Nevertheless, the complex showed no photic entrainment after 4-days-exposure to the light/dark cycle, either sole or when co-cultured with wild-type retina or cornea. Moreover, they found that when using the $Opn4^{-/-}$;rd1/rd1 mice (i.e., mice lacking functional melanopsin, rods and cones) in which the circadian phase of behavior was desynchronized from the light-dark cycle, the intraocular pressure (IOP) rhythm remained synchronized to behavior and not to the local light signals. The authors therefore concluded that, unlike in retina and cornea, iris – ciliary body complex and IOP associated to it were not entrained locally within the eye. Instead, they relied on synchronization with behavior rhythms defined by signals from central nervous system.

To sum up, the number of studies related to neuropsin remains limited to date. Further investigations are highly necessary to determine the function of neuropsin in iris and ciliary body as well as to better understood its operation in cornea and retina.

Pathways of increased photosensitivity

Now let me go back from the process of photoreception to the symptom it causes – to the photophobia. Light aversion may arise from various causes and frequently accompany numerous ocular diseases. Indeed, photophobia symptoms are common for many ophthalmological (dry eye, blepharitis, retinal dystrophy), neurological (blepharospasm, traumatic brain injury) and even psychiatric (depression, anxiety) disorders (67). As it has been already mentioned, increased photosensitivity provoked by light from visual displays was frequently reported (32,33,39,41). Photophobia was first described in 1934 and was related to as “exposure of the eye to light definitely induces or exacerbates pain” (69); since that, our knowledge about this sensory disorder highly advanced. Nevertheless, the current

understanding of photophobia process is still quite elusive; much of its neurochemistry as well as a pathway for light as a stress-related nociceptive stimulus are still unclear. Consequently, at present there is no pharmacotherapeutic treatment: cure for photophobia remains a challenge for ophthalmologists and relies primarily on optical devices such as wearing filtering glasses (68,110). So far, there have been no major randomized control trials for photophobia management (86).

Today, 3 pathways that might represent photophobia circuits are usually proposed. It is admitted that these 3 circuits could interact and that more circuits could be found. Briefly, in the first of these pathways, light passes by intrinsically photosensitive retinal ganglion cells (ipRGC) and causes, through several neural cascades, ocular vasodilation and activation of pain-sensing neurons near blood vessels. The second one involves a direct connection between ipRGCs and pain centers in the thalamus. The third pathway does not involve the optic nerve and implies the existence of phototransducers within the eye that can directly stimulate trigeminal afferents even after cutting the optic nerve. These 3 pathways are schematically represented in Figure 14. Further, I will present them in more detail as well as will discuss other circuits potentially underlying photophobia.

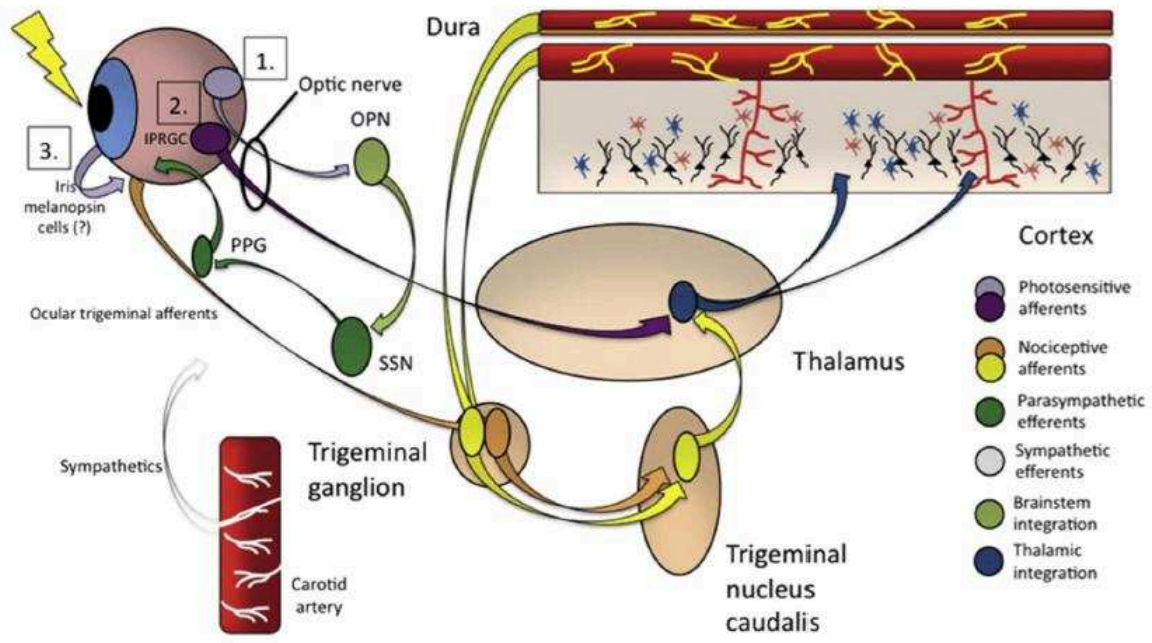

Figure 14. Photophobia circuits proposed to date

1. ipRGCs receive light signal and project it to the olivary pretectal nucleus (OPN) (light green). OPN projections activate superior salivatory nucleus (SSN) (dark green) and further, via pterygopalatine ganglion (PPG), causes ocular vasodilation and activation of ocular trigeminal afferents (orange). These afferents then project to trigeminal nucleus caudalis, thalamus, and cortex. **2.** ipRGCs project directly to thalamic neurons (blue) that also receive intracranial nociceptive afferent signal (yellow neurons in TG and trigeminal nucleus caudalis). The output of thalamic neurons then projects to sensory and association cortices. **3.** Melanopsin containing, intrinsically photosensitive ganglion-like cells (for example, in the iris) may directly activate the trigeminal pathway (from (69)).

Counterintuitively, blind patients may still experience photophobia (111) suggesting that this syndrome is not necessarily related to vision or at least to the high-resolution vision. Blind people might still retain a residual perception of light that would not allow for normal image-forming vision but would be capable to transmit a photophobic message. Indeed, Hughes et al. reported the residual light response in triple knock-out (TKO) mice lacking melanopsin as well as essential components of phototransduction signaling pathways present in rods and cones (25). In TKO mice, by means of electroretinogram (ERG) test, they detected a responses following 1-30 second stimulation with 500 nm light, and to a less extent with 360 nm light (these responses were highly attenuated as compared to wild type retinae). Since the ipRGCs were considered as non-functional in absence of melanopsin, such wavelength selectivity would support a role for rods (and not cones). Then, by means of immunochemistry in TKO retinae, they found at least two distinct cell types that showed robust light-induced cFos expression. The majority of responsive cells was located in INL and GCL and was identified as "a rare and atypical subset of amacrine cells". The authors therefore proposed a novel light sensing pathway that originated in rods and propagated to this small subset of amacrine cells.

Nonetheless, this weak residual rod function does not seem to have the main role in photophobia pathway: one would appeal more to the importance of non-visual photoreceptors. Indeed, the group of Matynia reported that ipRGCs were the primary circuit for light aversion (112). In pupil-dilated (by atropine) mice with ablated opn4-cells ($Opn4^{-/-}$), aversion to white light of 2000 lux significantly decreased as compared to wild type; however, when functional rod and cone receptors were ablated, light aversion was still present. Interestingly, the similar level of aversion for 500 or 2000 lux exposure was observed suggesting that ipRGC-dependent light aversion saturated around 500 lux. Later, these researchers investigated photo- and corneal mechanical sensitivity in a mouse model of corneal surface damage (113). They reported that benzalkonium chloride (BAC)-induced light aversion required functional melanopsin-expressing cells. Strikingly, they also observed a small reduction in corneal mechanosensitivity in mice lacking melanopsin-expressing cells; this effect was more apparent after corneal surface damage. This finding means that even without light stimulation, opn4-expressing cells did have a role in corneal sensitivity and nociception raising the possibility of a direct interaction between melanopsin and trigeminal innervation. Then several explanations may exist. The first one would appeal to the intrinsic sensitivity of the cornea and trigeminal afferents since melanopsin was found in corneal nerve fibers and in trigeminal neurons (98,99), as discussed above.

Another explanation was proposed by group of Okamoto who supposed the indirect activation of the trigeminal system. First, they demonstrated in rats that 30 minutes (30s on, 30s off) white light (1-2 * 10^4 lux) stimulation provoked cFos expression in the caudal brainstem (Vi/Vc, Vc/C1, dPa5, NTS) (114). This result was in line with Moulton et al. who reported the fMRI-detected activation of trigeminal pathways in humans suffering from photophobia (115). Interestingly, in the study of Okamoto, the caudal Vc/C1 junction region was unique among all trigeminal brainstem regions in which cFos labeling depended on light intensity. The authors therefore proposed that Vc/C1 neurons mediated sensory-discriminative aspects of ocular pain, while Vi/Vc neurons were responsible for ocular homeostasis and intraocular functions. Topical lidocaine application had almost no effect on cFos immuno-

activity. This finding means that neurons supplying the ocular surface played only a minor role in neuronal activation of the trigeminal brainstem complex. Intraocular injection of noripinephrine, a vasoconstrictor, prevented cFos expression in most trigeminal brainstem regions, but not in Vc/C1. Thus, the authors proposed that intraocular autonomic outflow played an important role in response to light. Further, by means of electrophysiology and orbicularis oculis electromyographic measurements, they analyzed the activity of nociceptive neurons in the Vi/Vc and Vc/C1 regions (116–118). They reported that lidocaine injection into the TG or into the eye blocked completely or at least significantly reduced the evoked neural response while lidocaine application on the ocular surface had little effect. Thus, this group argued that the input through the TG was necessary and the origin of light-evoked brainstem activity was in sensory neurons within the eye and not on the ocular surface. Intraocular injection of vasoconstrictor agents inhibited light-evoked activity as well. In addition, they proved that these agents did not have a direct action on sensory neurons since the correspondent intra-TG microinjection or application on the ocular surface provided with no effect. Topical atropine instillation did not alter the light response either. The authors concluded that "intraocular adrenergic mechanisms such as altered vasomotor function contributed to light-evoked activation of neurons in the trigeminal system whereas cholinergic activity <...> had no influence". This group proposed that TG neurons could be activated by transmitters released from parasympathetic postganglionic neurons; moreover; the fibers situated next to ocular blood vessels could be activated by mechanical deformation of these vessels due to changes in blood flow. Interestingly, the authors also demonstrated that light-induced tear reflex was mediated by neurons at the Vi/Vc, but not the Vc/C1 region.

Several others light-aversive pathways are possible. Dolgonos et al. were wondering whether an intraretinal mechanism might produce photophobia (119). In rats, they characterized the effects of bright light (1.28, 9.1 and 15.1 mW/cm^2, for 3-4 minutes) on reflex and spontaneous blinking before and after lesioning the optic nerve. They observed that exposure to light enhanced the air-puff-induced trigeminal blink, even after optic nerve lesion, corroborating the fact that blind persons might experience photophobia independently on central visual pathways. The authors proposed that so-called associational ganglion cells were a candidate for activating trigeminal pathways. Instead of entering the optic nerve, the axons of associational ganglion cells would travel to the retinal periphery, near the pars plana of the ciliary body (near the junction of the iris and sclera), where rich trigeminal innervation was found. Thus, associational ganglion cells might directly activate trigeminal nociceptors and sensitize the neurons of spinal trigeminal nucleus. Moreover, in view of melanopsin presence in iris and ciliary body (101–103) (discussed above), a direct transmission of light signal from these structures to the TG pathway would be possible.

Finally, Matynia et al. proposed an alternative pathway for light avoidance behavior, μ opioid receptors (μOR)-dependent but ipRGC-independent, that was revealed by application of morphine (112). μOR are localized in the brain and in RGCs although the precise RGC localization is unknown. Morphine affects the PLR and circadian rhythms that are both known to be regulated by ipRGCs. In their study, morphine subcutaneous injection induced light aversion that was fully reversed by the μOR antagonist naloxone. Opn4$^{-/-}$ mice treated with morphine showed the same level of light aversion as the wild type mice; here again, the effect was reversed by injection of naloxone. Strikingly, these researches reported later that

morphine did induce light aversion even in Opn4$^{-/-}$ mice with optic nerve crush as well as in Opn4$^{-/-}$;rd1/rd1 mice lacking all known photoreceptors (120). This finding means that other mechanisms for light-dependent behavior exist, in the absence of optic nerve and trigeminal innervation. With these results in mind, one may appeal to the potential role of neuropsin in photophobic message transmission. However, according to Hughes et al., there was a minimal, if any, role for opn5 in mediation of excitatory light responses in the TKO retina. They did not detect changes in spike firing rate after stimulation with either 500 nm or 360 nm light, as one would expect from the activation of neuropsin in RGCs (25). Nonetheless, as proposed by Buhr et al., the nature of light signal drived by neuropsin might be absolutely different from the conventional electrical signals: for example, "opn5-triggered signal transduction could lead to an electrically silent biochemical reaction rather than to a change in membrane potential" (108).

Concluding remarks

To sum up, in this introduction I briefly presented the anatomy of ocular surface and its innervation as well as described the disorders of dry eye, ocular pain and photophobia. Today, in view of great number of complaints about blue-light-exacerbated ocular-surface-related disorders, the topic concerning the interaction of light with the ocular surface starts to be extensively investigated. However, more research is necessary to better understand the exact mechanisms of wavelength- and time-dependent blue-toxicity and its consequences.

I also discussed the characteristics of non-visual photoreceptors, melanopsin and neuropsin, and reviewed the potential mechanisms of light aversion that have been proposed to date. One should note that here, we were interested in photophobia that was not initially co-morbid with any other syndrome. For example, the tangled photophobia-migraine pathways were out of the scope of this review. Numerous studies that have already explored the probable mechanisms underlying the light-induced exacerbation of migraine might be found in (120–125).

Since the discovery of melanopsin-comprising ipRGCs in 2002 and neuropsin in 2003, the research about these photopigments has advanced considerably. Our understanding of photophobia pathways has made a great progress as well. However, numerous questions remain open and many controversies still persist. What is the role of melanopsin in the iris and ciliary body, anyway? Are the trigeminal neurons and correspondent corneal fibers that contain melanopsin intrinsically photosensitive? If yes, do they participate in photophobia mediation? If not, what is the role of melanopsin in these tissues? Does light provide with any phototoxicity when applied directly to trigeminal neurons? Can all the proposed mechanisms of trigeminal ipRGC-dependent and -independent activation be complementary? Can the retina be directly innervated by the TG neurons as it has been recently suggested (126)? Are there different types of opn4-expressing cells outside the retina like there are five ones for the mouse ipRGCs? May neuropsin be important for light-aversive behavior? Do the neurons of trigeminal ganglia express opn5? All these issues required to be extensively studied.

Article 1: role of blue light in the dry eye disease

V. Marek, S. Mélik Parsadaniantz, T. Villette, F. Montoya, C. Baudouin, F. Brignole-Baudouin, A. Denoyer, **Blue light phototoxicity toward human corneal and conjunctival epithelial cells in basal and hyperosmolar conditions**, Free Radical Biology and Medicine 126 (2018) 27–40

As the bibliographic search demonstrated, the question "What is the impact of blue light on the dry eye disease?" has not been answered in detail yet. Thus, the first part of the current work was dedicated to this subject.

Due to the significant implication of the ocular surface in the pathophysiology of DED, here, we investigated the cytotoxicity of blue light exposure on this part of the eye. We worked in vitro on human epithelial corneal and conjunctival cell lines since the cornea and conjunctiva represent the most important parts of the ocular surface. If some studies have already communicated several blue-light-related effects in the cornea, to date, no work reported the phototoxicity in the conjunctiva. We were also wondering whether the photosensitivity of these two cell types would be the same.

In addition, we were interested whether the ocular surface cells placed in dry-eye-mimicking conditions would suffer more from the induced phototoxicity when compared to healthy cells. We therefore worked both in normal and hyperosmolar conditions of culturing where the latter ones represented the dry eye model. Moreover, we were seeking to demonstrate the spectral specificity of phototoxic effect as well as to investigate its wavelength-dependency within the blue spectra. Both issues were explored by means of specifically designed illumination protocols.

Greater conjunctival phototoxicity, correlation between hyperosmolarity and photosensitivity and spectral dependence of the cytotoxic effects are the main innovative points of this part of thesis. The proposed pathway of blue-light phototoxicity on the ocular surface is represented in the Figure 15.

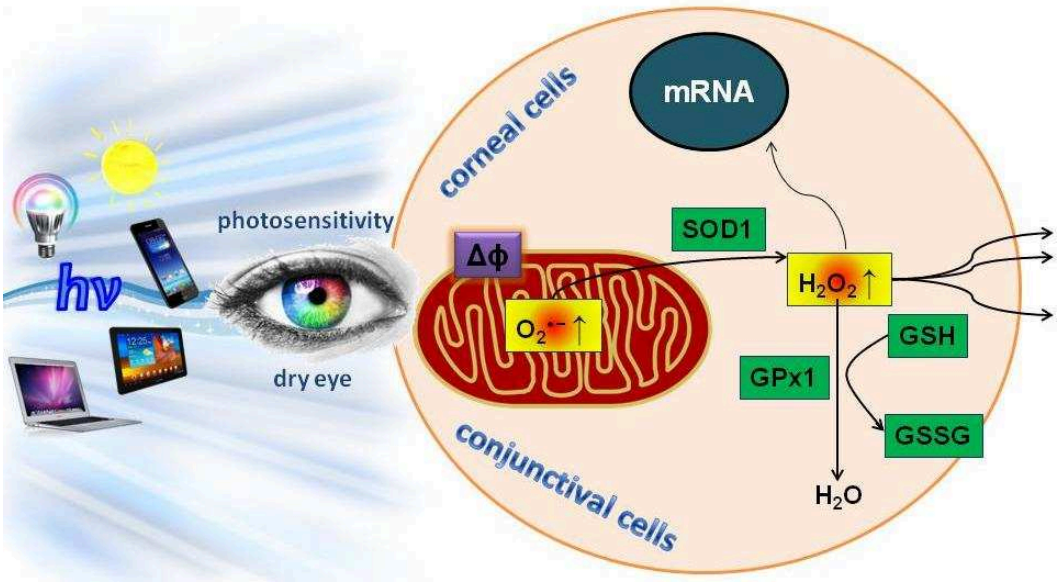

Figure 15. Scheme of blue light phototoxicity in the ocular surface

Free Radical Biology and Medicine 126 (2018) 27–40

Contents lists available at ScienceDirect

Free Radical Biology and Medicine

journal homepage: www.elsevier.com/locate/freeradbiomed

Original article

Blue light phototoxicity toward human corneal and conjunctival epithelial cells in basal and hyperosmolar conditions

Veronika Marek[a,b,*], Stéphane Mélik-Parsadaniantz[b], Thierry Villette[a], Fanny Montoya[a], Christophe Baudouin[b,c,d], Françoise Brignole-Baudouin[b,c,e], Alexandre Denoyer[b,c,f]

[a] Essilor International, R&D Department, Paris, France
[b] Sorbonne Université, INSERM, CNRS, Institut de la Vision, Paris, France
[c] Centre Hospitalier National d'Ophtalmologie des Quinze-Vingts, Paris, France
[d] Versailles-Saint-Quentin-en-Yvelines Université, Versailles, France
[e] Sorbonne Paris Cité – Paris Descartes Université, Faculté de Pharmacie de Paris, Département de Toxicologie, Paris, France
[f] CHU Robert Debré, Université Reims Champagne-Ardenne, Reims, France

ARTICLE INFO

Keywords:
Blue light
Cornea
Conjunctiva
Dry eye
Hyperosmolarity
Ocular surface
Oxidative stress

ABSTRACT

Aims: The ocular surface is the very first barrier between the visual system and external environment. It protects the eye from the exposure to various light sources that significantly emit in blue spectrum. However, the impact of blue light on the ocular surface has been poorly explored so far. In this study, we investigated in vitro the phototoxicity of blue light illumination in human epithelial cells of the ocular surface. We worked either in basal conditions or under hyperosmolar stress, in order to mimic dry eye disease (DED) that is the most common disease involving the ocular surface.

Results: Corneal and conjunctival epithelial cells suffered the most from violet-blue light but also from longer-wave blue light. Exposure to blue wavebands significantly decreased cellular viability, impacted on cellular morphology and provoked reactive oxygen species (ROS) over-production. Conjunctival epithelial cell line had a greater photosensitivity than the corneal epithelial one. Hyperosmolar stress potentiated the blue light phototoxicity, increasing inflammation, altering mitochondrial membrane potential, and triggering the glutathione-based antioxidant system.

Innovation: In human epithelial corneal and conjunctival cells of the ocular surface, we demonstrated the harmful impact of blue light on viability, redox state and inflammation processes, which was modified by hyperosmolarity.

Conclusion: Blue light induced cell death and significant ROS production, and altered the expression of inflammatory genes and operation of the cellular defensive system. We established for the first time that hyperosmolar stress impacted phototoxicity, further suggesting that DED patients might be more sensitive to blue light ocular toxicity.

1. Introduction

Today it is widely discussed that blue light may provoke an important ocular phototoxicity [1]. Various blue and UV light-induced and/or -aggravated ocular pathologies have been recognized, including photokeratitis, pterygium, cataract, and corneal and retinal degeneration [2–6]. In particular, patients suffering from dry eye disease (DED) frequently complain about the exacerbated photosensitivity and increased symptoms of discomfort when exposed to various visible light sources [7,8]. According to the TFOS DEWS II report [9], dry eye is *a multifactorial disease of the ocular surface characterized by a loss of homeostasis of the tear film, and accompanied by ocular symptoms, in which tear film instability and hyperosmolarity, ocular surface inflammation and damage, and neurosensory abnormalities play etiological roles* [10]. Today, DED is the current leading reason for ophthalmological consultations [11]; in dependence on the operational dry eye definition used and the

Abbreviations and sign: DED, Dry Eye Disease; HCE cell line, Human Corneal Epithelial cell line; HO, HyperOsmolar; HYP, Hoeschst/YO-PRO/PI; IOBA-NHC or IOBA cell line, cell line from Normal Human Conjunctiva; IR, InfraRed; MMP, Mitochondrial Membrane Potential; PI, Propidium Iodide; RT, Room Temperature; UVt, UltraViole; λ↑, excitation wavelength (for fluorescence readings); λ↓, emission wavelength (for fluorescence readings)

* Corresponding author at: Essilor International R&D, F-75012 Paris, France.
E-mail address: marekv@essilor.fr (V. Marek).

https://doi.org/10.1016/j.freeradbiomed.2018.07.012
Received 13 April 2018; Received in revised form 12 June 2018; Accepted 19 July 2018
Available online 21 July 2018
0891-5849/

characteristics of the population studied, its prevalence varies from 5 up to 45% [7].. DED was initially recognized as a disease of aging people, however, the dry eye patients are currently getting younger [12]. Since younger generations spend a significant part of their day looking at various screens highly emitting in the blue spectrum [13,14], this "rejuvenation" is not surprising. Indeed, there are numerous studies describing the appearance and/or worsening of DED signs and symptoms in visual display users [15–18].

The global pathogenesis of DED as well as the relationship between DED and exposure to visible light specifically are still not clear [19]. So far many works were dedicated to the dangerous role of light in retinal diseases; in particular, the detrimental effect of blue light on the retina has been extensively investigated [20–22]. However, little attention has been paid to the impact of blue light on the ocular surface, even though the cornea, the conjunctiva and the tear film represent the very first barrier between light and the entire visual system and are deeply involved in the pathophysiology of dry eye [19]. Among various tissues comprised in the ocular surface, cornea and conjunctiva are the structures the mostly exposed to the ambient environment and are probably the most susceptible to blue light [23]. In our daily life, our eyes are constantly illuminated by various types of artificial and natural sources, mainly ranging from UVA (360 nm) to IRA (1400 nm) and providing with an important blue irradiance. Several studies investigated the impact of near UV and IR light on the ocular surface [24–28] but only several ones analyzed the impact of blue light exposure [2,29–33]. Given our specialized practice in the clinical management of DED and previous basic studies on ocular surface inflammation and toxicity [34–37], we hypothesized about a potential harmful influence of blue light on the triggering and evolution of DED. Thus, the aim of this in vitro study was to investigate the impact of blue-light exposure on human epithelial cells of ocular surface, cultured either in basal conditions or additionally stressed by hyperosmolar conditions (HO) frequently used as an in vitro model of dry eye [38]. In particular, we studied the impact of various blue wavebands on cellular viability and health, oxidative stress, mitochondrial function and inflammatory cytokines expression.

2. Results

2.1. Wide blue wavebands induced oxidative stress but did not affect the cellular viability

First, we investigated the phototoxicity of wide spectral illumination directly after the end of light exposure. For both HCE and IOBA cell lines, neither blue (380–525 nm) nor yellow (538–662 nm) wavebands did not alter the cellular viability, either in basal or in HO conditions, as compared to the dark (Fig. 1). No morphological changes were observed either (Supplementary Fig. S1). Accordingly, we did not find any significant changes in fluorescent signals of markers of cellular proliferation (Hoechst), apoptosis (YO-PRO) and necrosis (Propidium Iodide [PI]) (Supplementary Fig. S2). However, the level of hydrogen peroxide (H_2O_2) was significantly increased under blue light exposure while it was not observed under yellow light one (Fig. 1). Level of H_2O_2 in HCE was statistically higher than in IOBA. Moreover, HO pre-stimulation further enhanced the production of H_2O_2 in HCE cells compared to normal culture condition.

2.2. Narrow wavebands of blue light provoked an important cellular death

To determine which wavelengths are more phototoxic, we further exposed cells to specific narrow-waveband (10 nm) illuminations of the same irradiance as for the previously used wide spectra. HCE viability significantly decreased at 420 nm (Fig. 2A), to greater extent in HO than in basal conditions. The near-UV 390 nm, used more like a positive control, drastically killed cells, as expected. Similarly, IOBA viability significantly decreased at 420 and 390 nm, with a more important decrease in HO conditions at 390 nm (Fig. 2B). Interestingly, IOBA cells demonstrated two other significant changes: i) the viability modestly increased at 480 nm under HO stress, ii) at 630 nm, viability in HO conditions was lower than in normal ones (while not significantly differing from the HO dark control). Additionally measured HYP (Hoechst, YO-PRO and PI) fluorescent signals were significantly increased at 390 nm but not at 420 nm; HO conditions amplified this increase for HCE but inhibited it for IOBA (data not shown). Measured variations in viability were in accordance with the observed morphological changes appeared after exposure to various blue wavebands (Fig. S3).

2.3. HCE succeeded to recover after the exposure to 420 nm illumination while IOBA did not

To assess the ability of cells to recover, we monitored the cellular viability, cellular proliferation, and death rates 4 and 24 h in the dark after the end of exposure. In HCE, the deleterious impact of 420 nm exposure recovered with time after 4 h in the dark; however, it remained more severe under HO stress (Fig. 2A). IOBA cells retained the important impact of 420 nm illumination for both culturing conditions whatever the observation time (Fig. 2B). Interestingly, IOBA viability was significantly deteriorated by HO stress at 4 h, but not after 24 h of recovery.

For both cell lines, the viability remained significantly decreased at 390 nm and demonstrated no difference between culturing conditions. Because the deleterious effect under 390 nm was too important, for both cell lines in a time-course analysis, it was not possible to restore viability with time (Fig. 2A, B). HCE recovered after the exposure to 420 nm in normal conditions but not in HO conditions (Fig. 2C). Surprisingly, HCE under HO stress demonstrated a small increase in viability in 24 h after the recovery from 430 nm illumination. On the contrary, in both conditions, IOBA viability significantly decreased in time after the 420 nm illumination (Fig. 2D). There were also small decreases for 430 nm in normal and for 480 nm in HO conditions.

Accordingly to viability rate, for both cell lines, rates of HYP fluorescent staining remained highly elevated after the 390 nm illumination (data not shown); the values significantly varied over time only for this wavelength (Fig. 3). During the recovery time, under normal conditions, HCE proliferation (Hoechst staining) monotonically increased in time while under HO conditions, the proliferation rate at + 24 h decreased as compared to + 4 h (Fig. 3A1, B1). Accordingly, their apoptosis level (YO-PRO) decreased over time in basal but not in HO conditions (Fig. 3A2, B2). On the contrary, apoptosis rate continued to increase in IOBA cells (Fig. 3C2, D2); cell proliferation dropped either in basal or in HO culturing (Fig. 3C1, D1). For both cell lines, the necrosis rate (PI) increased after 4 h of recovery then went down (Fig. 3A3, B3, C3, D3).

2.4. Exposure to blue light induced oxidative stress and compromised the mitochondria

Illuminations of 420 nm produced a significant increase in H_2O_2 level that was modulated by HO stress (Fig. 4A, B)·H_2O_2 rate after exposure to 430 nm turned out to be mainly non-significant. In full compliance with the measured values of cellular viability and death, both cell lines displayed an important increase in the production of H_2O_2 under positive-control 390 nm illumination. HO stress weakened this production in HCE and strengthened it in IOBA. Follow-up of the hydrogen peroxide rate showed that for both cell lines in both conditions, H_2O_2 level significantly varied in time only after harmful 430, 420 and 390 nm illuminations (Fig. 4C, D; the values that did not vary in time are not shown). In HCE and in IOBA in normal conditions, ROS rate at 430 nm significantly decreased in time. Under HO stress, that was 420 nm exposure that provoked time alterations of H_2O_2. In HCE, recovery time allowed for its significant elimination while in IOBA, its rate only went up. After the exposure to 390 nm, hydrogen peroxide

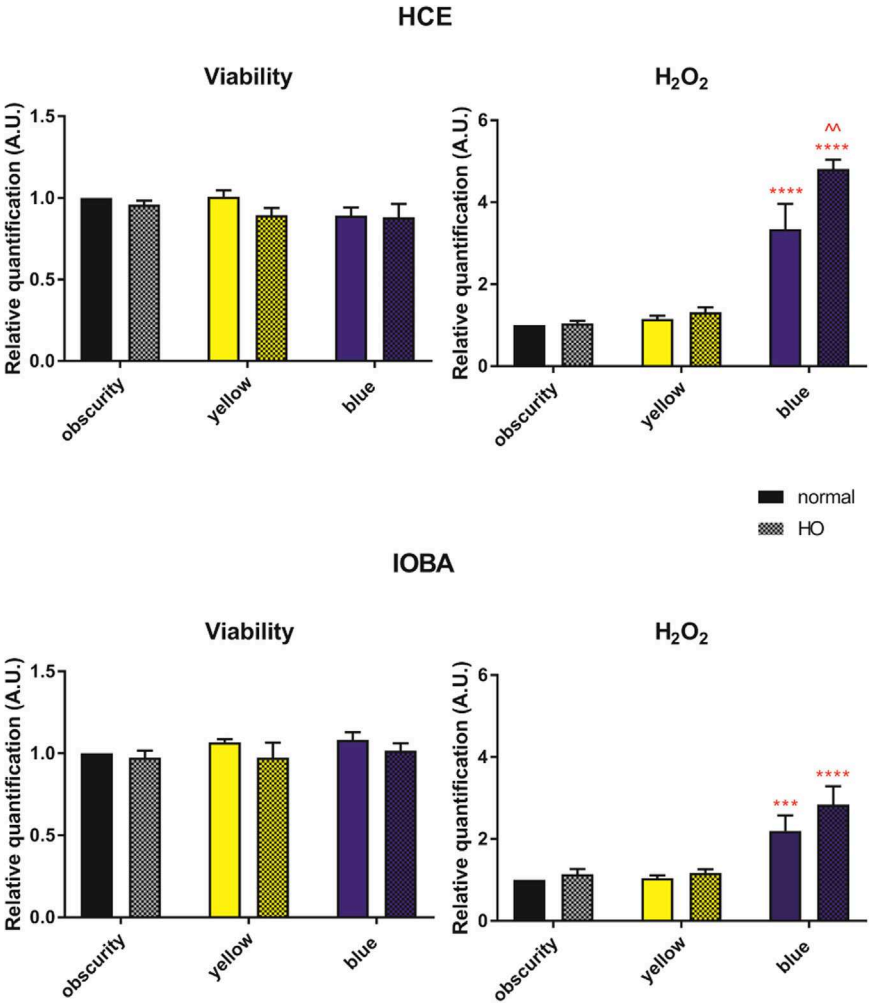

Fig. 1. Impact of wide-spectral illumination assessed directly after the end of exposure. Cellular viability and level of hydrogen peroxide generation (H_2O_2) measured directly after 17 h of wide-spectral illumination. Control or illumination conditions are denoted by *obscurity* (cells kept in the dark), *yellow* (538–662 nm) and *blue* (380–525 nm). Clear bars correspond to normal and hatched bars to hyperosmolar (*HO*) conditions of culturing. Results shown represent the mean ± SEM. Stars (*) refer to differences with the correspondent dark control within the same culturing condition and carets (^) refer to differences between culturing conditions (normal *vs.* HO) within the same light condition. Red signs correspond to an increase in values. Statistical significance: $p < 0.01$ (**/^^), $p < 0.001$ (***/^^^), $p < 0.0001$ (****/^^^^).

level remained highly elevated after either 4 or 24 h of recovery. For both cell lines, it increased in 4 h of recovery and then decreased again in 24 h. These variations were more important in IOBA than in HCE.

Directly after the end of light exposure, we then explored the level of another important ROS, the mitochondrial superoxide anion ($O_2^{\bullet -}$). The $O_2^{\bullet -}$ rate was significantly increased after exposure to 430, 420 and 390 nm (Fig. 5A, B). We observed an important fluorescent staining of oxidation products for the same wavelengths (Fig. 5C). For 390 nm, under HO stress, the effect was weaker for HCE and stronger for IOBA.

Since we found a significant increase in mitochondrial oxidative stress level, we then studied another marker of cellular health that is the mitochondrial membrane potential (MMP). In IOBA in HO conditions, we observed a significant decrease in MMP under 420 nm illumination. Surprisingly, IOBA cell line demonstrated an unexpected increase of MMP after 430 nm exposure that was even more pronounced under HO stress. In basal conditions, IOBA also had a MMP increase at 480 nm (Fig. 6B). In HCE, MMP significantly decreased in cells illuminated by 390 nm, with no difference between culturing conditions (Fig. 6A). The same decrease took place in IOBA cells. The measured values were in accordance with the observed fluorescent staining (Fig. 6C).

2.5. Blue light phototoxicity impaired the antioxidant defensive system

The highly important oxidative stress induced by light phototoxicity may trigger off the antioxidant system scavenging for ROS species. HCE demonstrated a modest significant increase in total glutathione (GSH) in HO conditions at 420 nm. For both cell types at 390 nm, we observed a significant increase in levels of both GSH and GSSG (oxidized glutathione). Under HO stress, this increase was less pronounced in HCE and more pronounced in IOBA cells (Fig. 5D1,2, E1,2). Interestingly, in HCE, further calculated GSH/GSSG ratio did not demonstrate any significant differences either between wavebands or between culturing conditions (Fig. 5A3), but one should notice important dispersion of the results for the 390 nm. In IOBA, the ratio between total and oxidized glutathione was significantly increased at 390 nm with no difference between culturing conditions (Fig. 5B3).

2.6. Blue light induced changes in mRNA expression of cytokines and antioxidants

Because of the important cellular death, we were not able to process cells exposed to 390 nm light for the RT-qPCR (their number was not sufficient).

In HCE in basal conditions, mRNA expression of IL-6 was significantly up-regulated directly after exposure to 420 and 430 nm. Under HO stress, the wavelength dependence of IL-6 seemed to be qualitatively the same as in normal conditions. However, due to important fluctuations induced by HO medium, it appeared to be statistically non-significant (Fig. 7A1). In both culturing conditions, CXCL8 was up-regulated at 420 nm exposure, to a greater extent under HO stress (Fig. 7A2). Both TGFβ2 and CCL2 were down-regulated in normal conditions under 420, 430 and 480 nm illuminations. In HO conditions, the expression of both cytokines was significantly increased but with no spectral dependence (Fig. 7A3, A4). One should notice that the variations of TGFβ2 expression were quite low.

In IOBA cells, IL-6 expression did not vary, either in normal or in HO

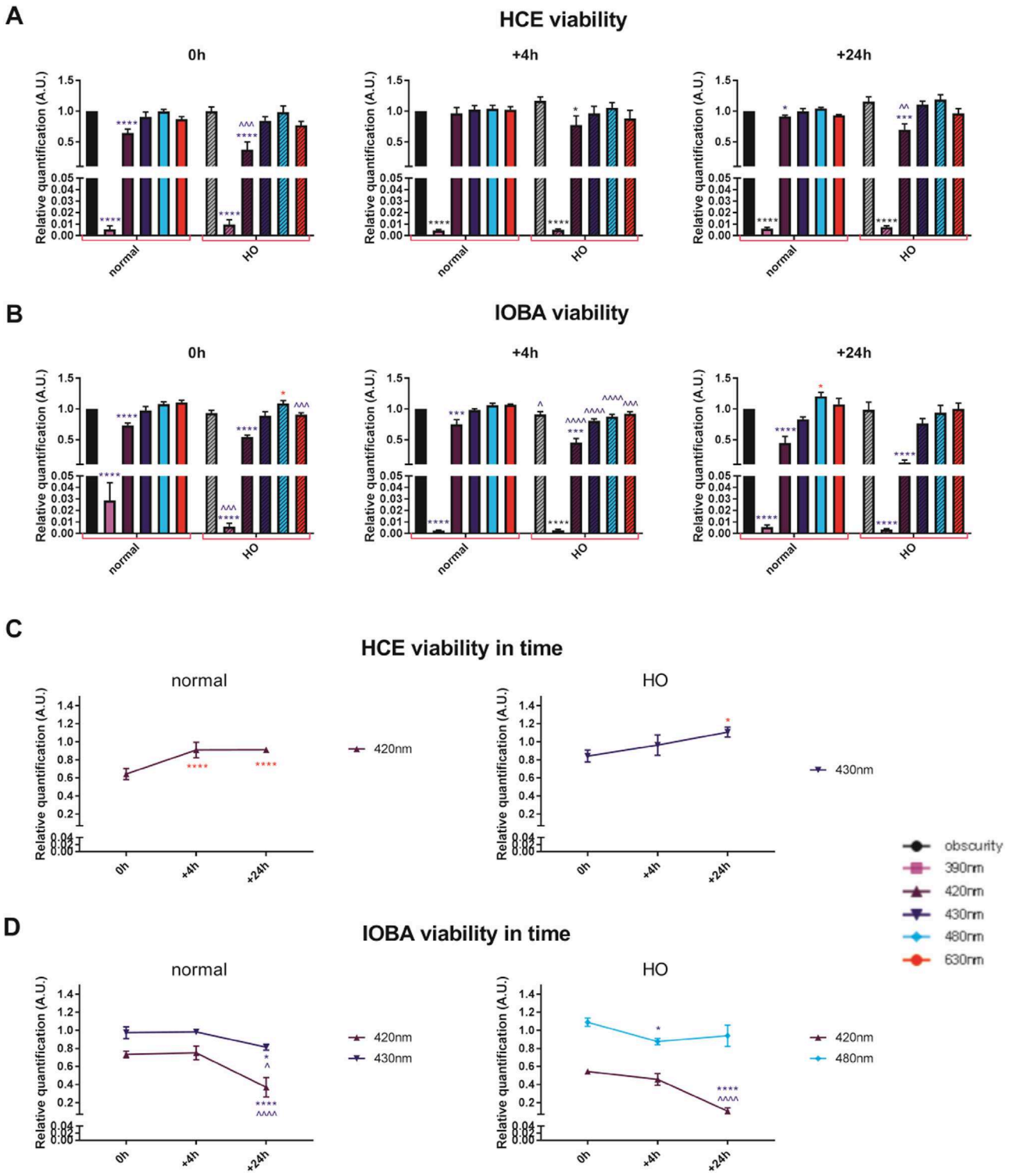

Fig. 2. Impact of narrow-spectral illumination on cellular viability and its further recovery. (**A**, **B**) Cellular viability measured directly after 17 h of narrow-spectral illumination (*0 h*), then in 4 (+*4 h*) or in 24 (+*24 h*) hours of recovery in the dark. Clear bars correspond to normal and hatched bars to hyperosmolar (*HO*) conditions of culturing. Wavebands are represented by the correspondent colors; they are denoted on the color code scheme where each 10 nm spectral band is designated by its central wavelength. Results shown represent the mean ± SEM. Stars (*) refer to differences with the correspondent dark control within the same culturing condition and carets (^) refer to differences between culturing conditions (normal vs. HO) within the same light condition. Red signs correspond to an increase and blue signs to a decrease in values. Statistical significance: $p < 0.05$ (*/^), $p < 0.01$ (**/^^), $p < 0.001$ (***/^^^), $p < 0.0001$ (****/^^^^). (**C**, **D**) Time course of viability recovery in normal or hyperosmolar conditions. Viability rates were measured directly after the end of exposure to light (*0 h*), then in 4 (+*4 h*) and in 24 (+*24 h*) hours of recovery in the dark. Only the wavebands for which significant changes in time were observed are shown. Each 10 nm spectral band is designated by its central wavelength. Results shown represent the mean ± SEM. For points for which the error bars are shorter than the height of the symbol, error bars are not drawn. Stars (*) refer to differences with values at 0 h time point and carets (^) refer to differences with values at + 4 h time point. Significances of change are denoted near the plot of the correspondent waveband at the correspondent time point. Red signs correspond to an increase and blue signs to a decrease in values. Statistical significance: $p < 0.05$ (*/^), $p < 0.0001$ (****/^^^^).

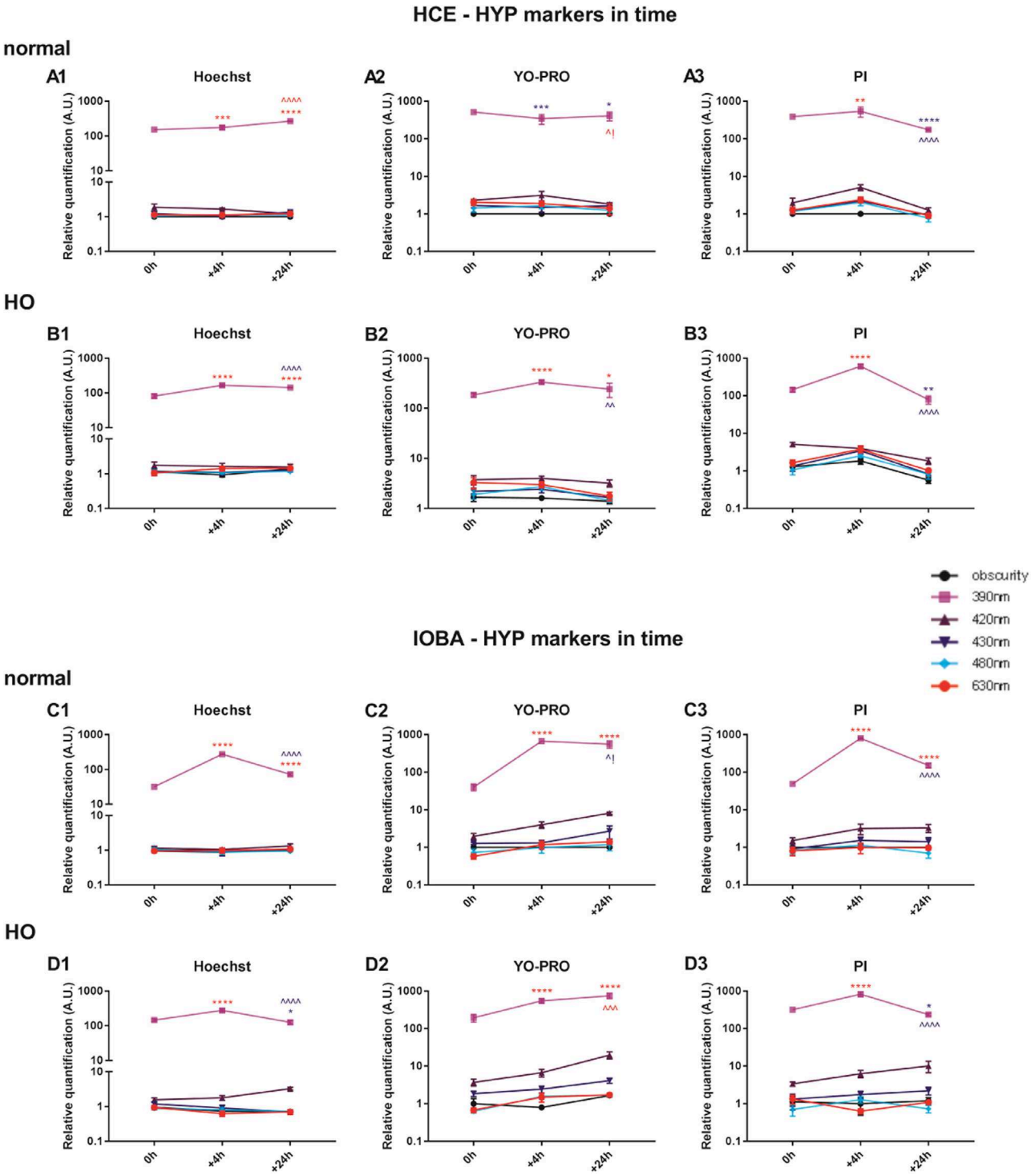

Fig. 3. Time changes in rates of cellular death after a narrow-spectral illumination. Time course of rates of cellular apoptosis (Hoechst – A1-D1, YO-PRO – A2-D2) and necrosis (PI – A3-D3), in normal (**A**, **C**) and hyperosmolar (**B**, **D**) conditions. Measurements were done directly after the end of exposure to light (*0 h*), then in 4 (*+4 h*) and in 24 (*+24 h*) hours of recovery in the dark. Each 10 nm spectral band is designated by its central wavelength. Results shown represent the mean ± SEM. For points for which the error bars are shorter than the height of the symbol, error bars are not drawn. Stars (*) refer to differences with values at 0 h time point and carets (^) refer to differences with values at + 4 h time point. Significances of change are denoted near the plot of the correspondent waveband at the correspondent time point. Red signs correspond to an increase and blue signs to a decrease in values. Statistical significance: $p < 0.05$ (*/^), $p < 0.01$ (**/^^), $p < 0.001$ (***/^^^), $p < 0.0001$ (****/^^^^). *! or ^! mean that, according to the GraphPad notes, the individual p-value is greater than 0.05 in the third digit following the point, the observed difference remaining still statistically significant.

conditions (Fig. 7C1). CXCL8 was significantly down-regulated at 420 and 430 nm, with no difference between culturing conditions (Fig. 7C2). TGFβ2 expression decreased for 420 and 430 nm exposure in normal conditions. No statistically significant wavelength dependence was observed under HO stress; however, the value for 420 nm was greater than the one in the basal conditions (Fig. 7C3). The CCL2 values of cycle threshold (Ct) being too high (~36–37), we did not consider them as reliable and therefore did not present.

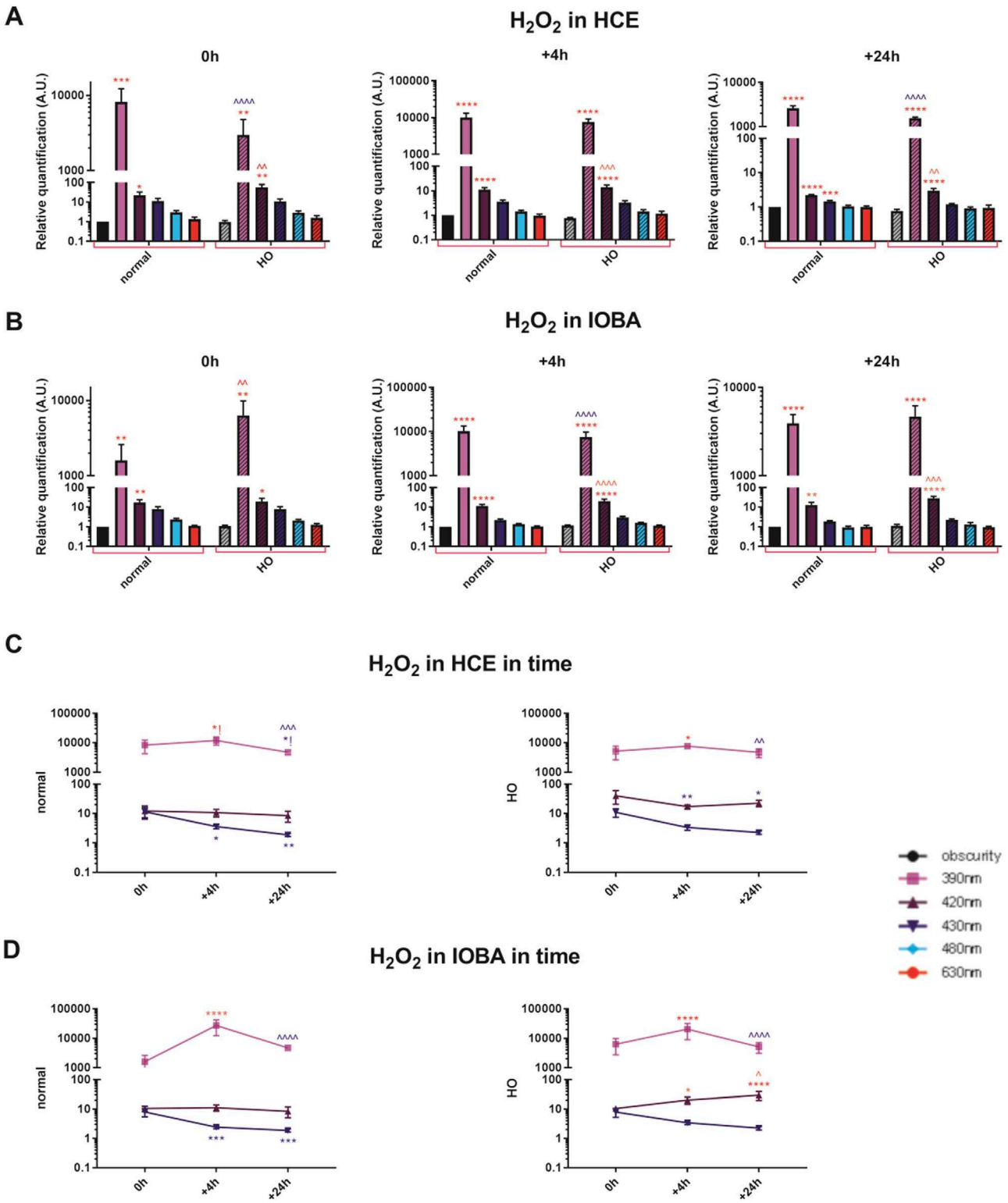

Fig. 4. Time changes in H_2O_2 (hydrogen peroxide) production after a narrow-spectral illumination. (**A**, **B**) Rates of hydrogen peroxide (H_2O_2) were measured directly after 17 h of narrow-spectral illumination (*0 h*), then in 4 (*+4 h*) or in 24 (*+24 h*) hours of recovery in the dark. Clear bars correspond to normal and hatched bars to hyperosmolar (*HO*) conditions of culturing. Wavebands are represented by the correspondent colors; they are denoted on the color code scheme where each 10 nm spectral band is designated by its central wavelength. Results shown represent the mean ± SEM. Stars (*) refer to differences with the correspondent dark control within the same culturing condition and carets (^) refer to differences between culturing conditions (normal vs. HO) within the same illumination condition. (**C**, **D**) Time course of hydrogen peroxide (H_2O_2) production in normal or hyperosmolar conditions. ROS levels were measured directly after the exposure to light (*0 h*), then in 4 (*+4 h*) and in 24 (*+24 h*) hours of recovery in the dark. Only the wavebands for which significant changes in time were observed are shown. Each 10 nm spectral band is designated by its central wavelength. Results shown represent the mean ± SEM. For points for which the error bars are shorter than the height of the symbol, error bars are not drawn. Stars (*) refer to differences with values at 0 h time point and carets (^) refer to differences with values at + 4 h time point. Significances of change are denoted near the plot of the correspondent waveband at the correspondent time point. Red signs correspond to an increase and blue signs to a decrease in values. Statistical significance: $p < 0.05$ (*/^), $p < 0.01$ (**/^^), $p < 0.001$ (***/^^^), $p < 0.0001$ (****/^^^^). * ! or ^! mean that according to the GraphPad calculations, the observed difference is still statistically significant, however, the correspondent $p > 0.05$.

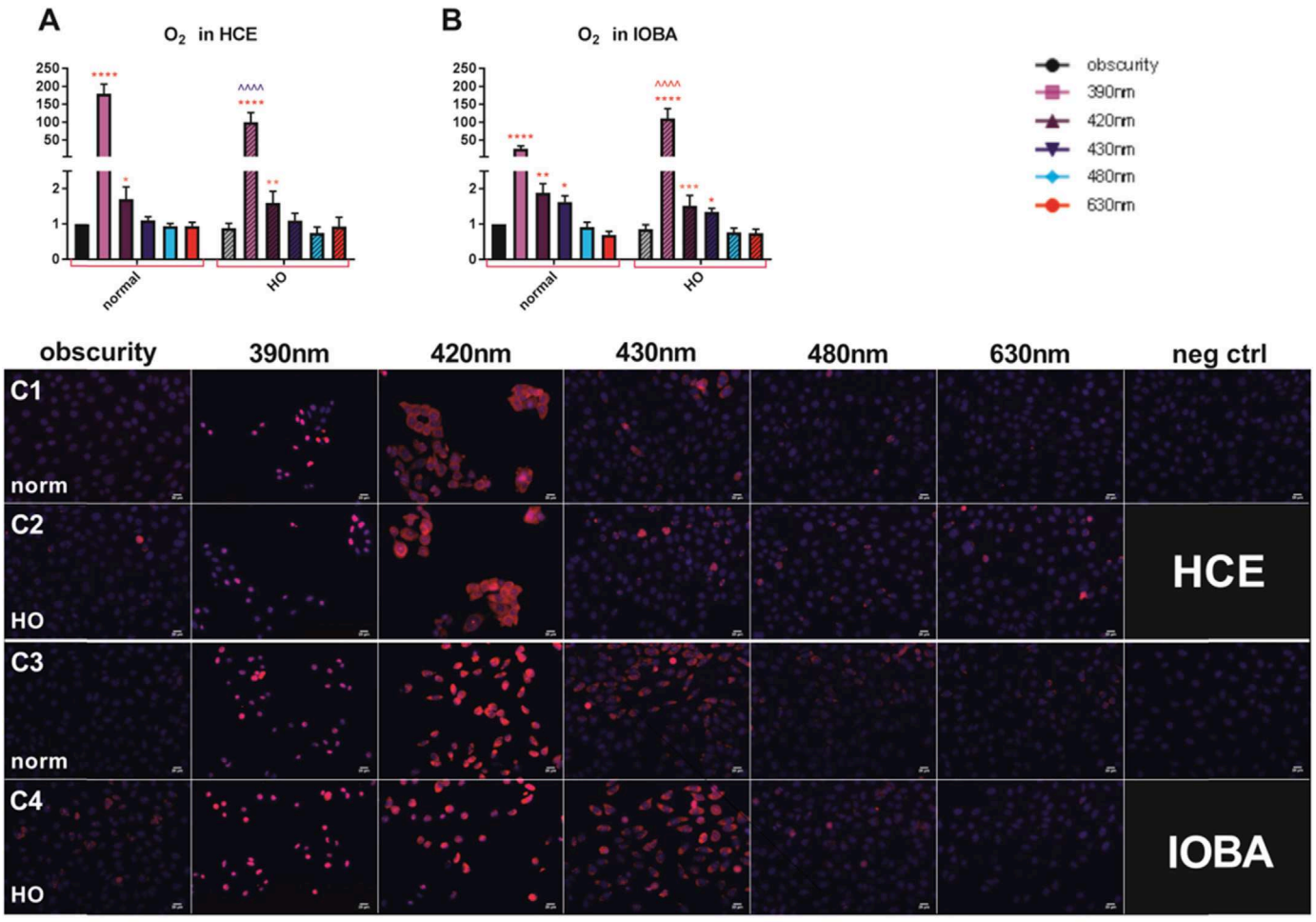

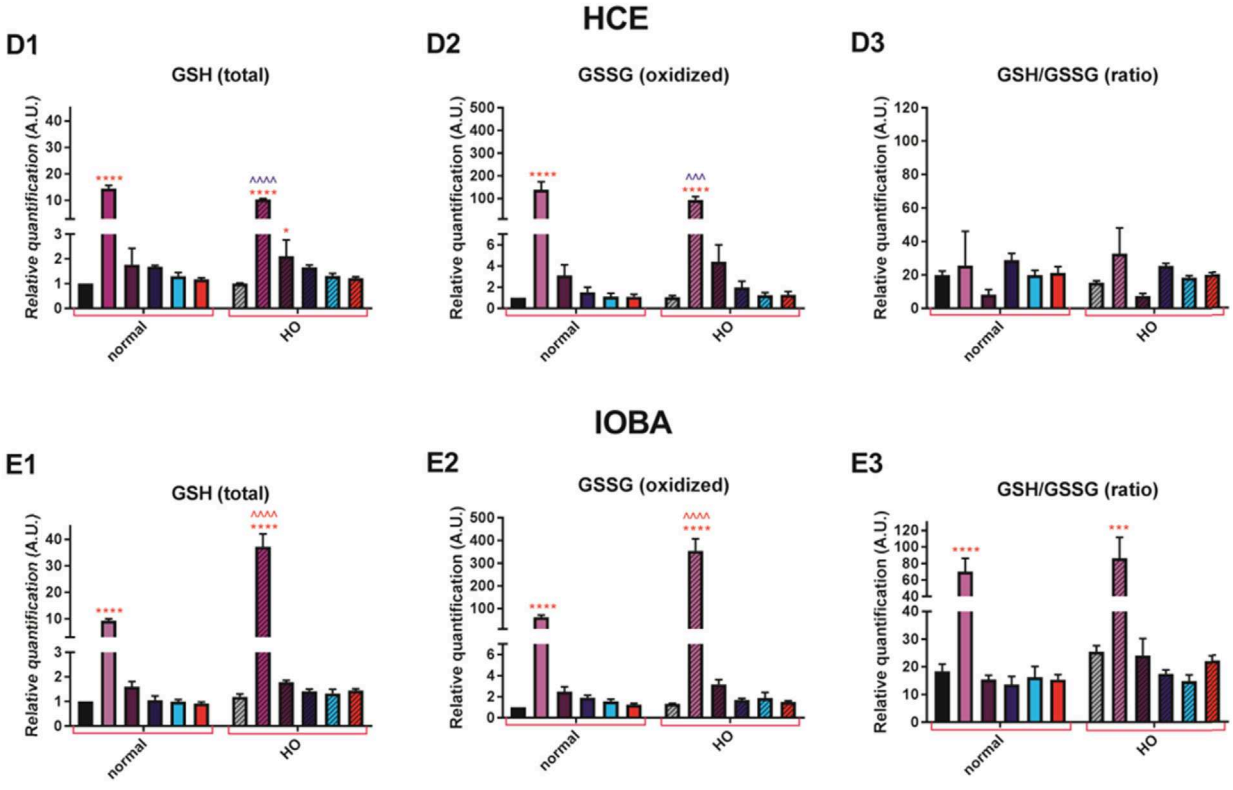

(caption on next page)

Fig. 5. Rates of mitochondrial superoxide anion ($O_2^{\bullet -}$) and implication of glutathione-based antioxidant system immediately after the end of a narrow-spectral illumination. (**A**, **B**) Level of mitochondrial superoxide anion ($O_2^{\bullet -}$) production. (**C**) Fluorescent images of $O_2^{\bullet -}$ accumulation in HCE (C1,2) and IOBA (C3,4) either in normal (*norm* – C1,3) or in hyperosmolar (*HO* – C2,4) conditions. Magnification: x20. Scale bar represents 20 µm. $O_2^{\bullet -}$ aggregates stained with the MitoSOX dye fluoresced in red and cell nuclei were counter-stained with DAPI (blue). No super-oxide reactive dye was added to the negative control (*neg ctrl*). (**D**, **E**) Rates of total (GSH – D1, E1) and oxidized (GSSG – D2, E2) glutathione and their ratios (D3, E3). Clear bars correspond to normal and hatched bars to hyperosmolar (*HO*) conditions of culturing. Wavebands are represented by the correspondent colors; they are denoted on the color code scheme where each 10 nm spectral band is designated by its central wavelength. Results shown represent the mean ± SEM. Stars (*) refer to differences with the correspondent dark control within the same culturing condition and carets (^) refer to differences between culturing conditions (normal vs. HO) within the same illumination condition. Red signs correspond to an increase and blue signs to a decrease in values. Statistical significance: $p < 0.05$ (*/^), $p < 0.01$ (**/^^), $p < 0.001$ (***/^^^), $p < 0.0001$ (****/^^^^).

For both cell types, mRNA expression of NFκB did not demonstrate any spectral dependence. Nevertheless, under HO stress, it was significantly up-regulated at 420 nm for HCE and at 480 nm for IOBA as compared with basal conditions (Fig. 7B1, D1).

In HCE in normal conditions, GPx1 expression slightly decreased at 420 nm. This value was significantly smaller than the one under HO stress (Fig. 7B2). In both culturing conditions, SOD1 was up-regulated at 420 and 430 nm, to a more extent in HO conditions at 420 nm (Fig. 7B3). In IOBA, GPx1 was down-regulated at 420 and 430 nm in both culturing conditions with no difference between them; SOD1 did not vary (Fig. 7B2,D2).

3. Discussion

In clinical practice, environmental triggers such as light are known to potentially damage the ocular surface and aggravate dry eye signs, symptoms and the corresponding social impact [39]. This issue is even more important since today, in addition to sunlight, our life is highly illuminated by various light artificial sources. Here, we demonstrated in vitro the noxious and specific effects of visible violet-blue light on human epithelial cells of the ocular surface, and the influence of media osmolarity on this phototoxicity.

The originality of our work was to investigate and compare the phototoxicity on epithelial cells from the cornea and conjunctiva. These two main tissues of the ocular surface are the most exposed to the ambient environment and have fundamental roles in health and protection of the eye. In addition to the human corneal epithelial (HCE) cell line, the most widely used one for the in vitro studies of dry eye [40], we worked on a spontaneously immortalized epithelial cell line from normal human conjunctiva (IOBA-NHC) [41] which retains most of morphological and functional characteristics of human conjunctival epithelium [42,43]. Moreover, it was reported that IOBA line had a highly similar profile of biomarkers concerning cellular defense, communication and development when compared to primary culture of human conjunctival epithelial cells [42]. In order to mimic in vitro dry eye conditions, HO stress was applied to these cells [38]. To make HO media, we added 69 mM of NaCl since greater values were reported to induce an important cell death [38,44] and would probably bias the impact of light phototoxicity. The measured osmolarity values were within the range of the hyperosmolarity commonly used in experimental settings (e.g. [38,45],). For both cell types, we decided to keep the same composition of culture media, in order not to induce an additional stress and to be able to assess the specific phototoxic effect. We used the irradiance range of wide-spectral illuminations that well

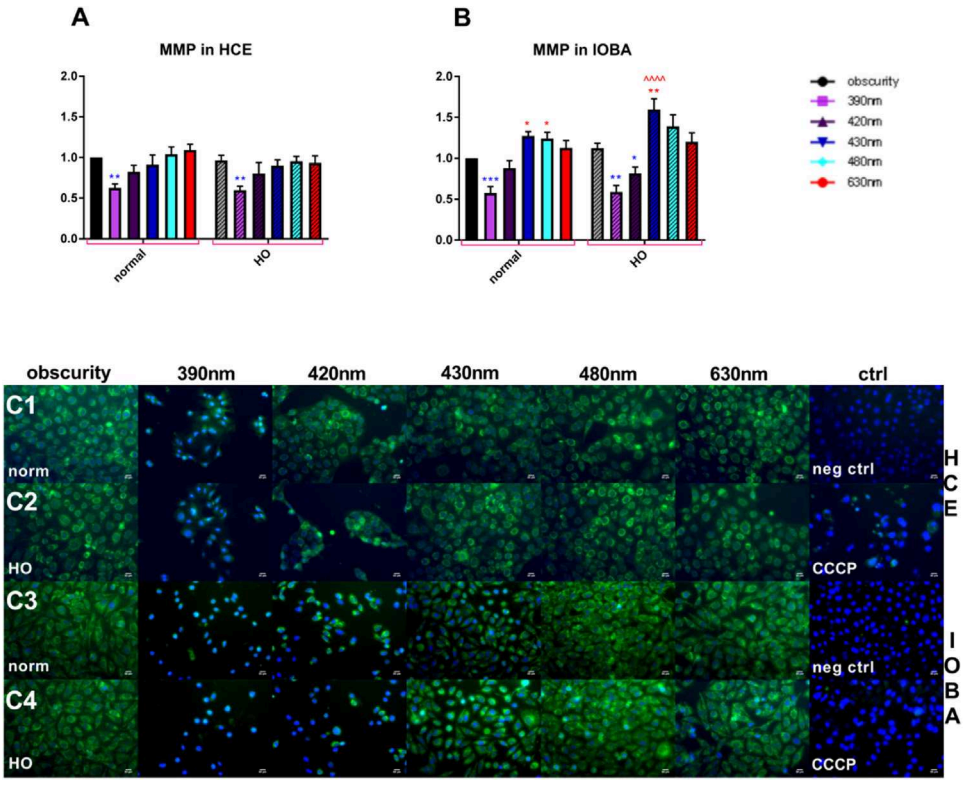

Fig. 6. Mitochondrial membrane potential status immediately after the end of a narrow-spectral illumination. (**A**, **B**) Values of measured mitochondrial membrane potential. Clear bars correspond to normal and hatched bars to hyperosmolar (*HO*) conditions of culturing. Wavebands are represented by the correspondent colors; they are denoted on the color code scheme where each 10 nm spectral band is designated by its central wavelength. Results shown represent the mean ± SEM. Stars (*) refer to differences with the correspondent dark control within the same culturing condition and carets (^) refer to differences between culturing conditions (normal vs. HO) within the same illumination condition. Red signs correspond to an increase and blue signs to a decrease in values. Statistical significance: $p < 0.05$ (*/^), $p < 0.01$ (**/^^), $p < 0.0001$ (****/^^^^). (**C**) Fluorescent microscope images representing MMP status in HCE (C1,2) and IOBA (C3,4) either in normal (*norm* – C1,3) or in hyperosmolar (*HO* – C2,4) conditions. MITO-ID® membrane potential dye fluoresced in green and cell nuclei were counter-stained with DAPI (blue). Magnification: x20. Scale bar represents 20 µm. No MITO-ID® dye was added to the negative control (*neg ctrl*). *CCCP* corresponds to cells with added carbonyl cyanide 3-chlorophenylhydrazone, to abolish MMP.

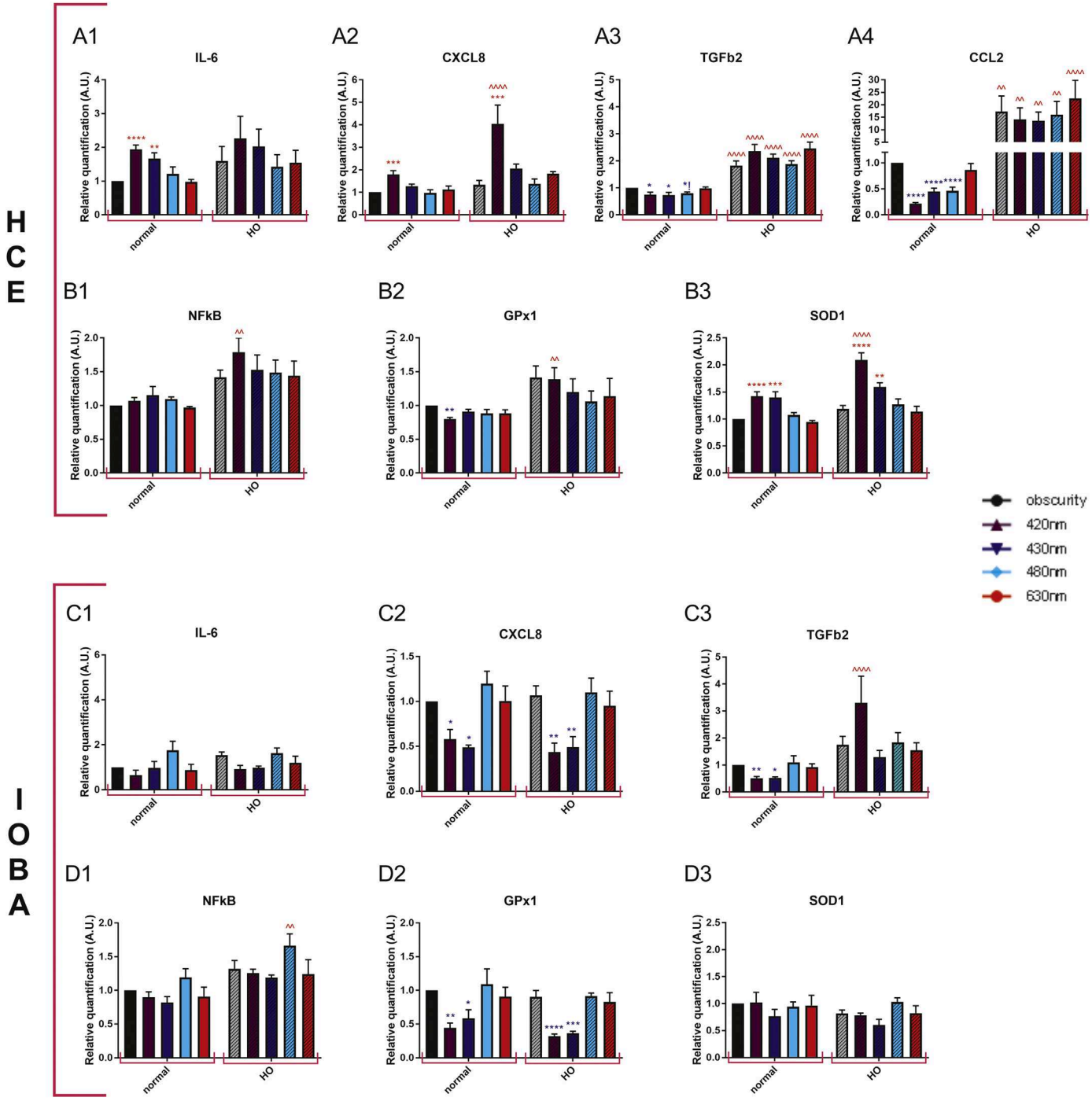

Fig. 7. Changes in mRNA expression levels measured immediately after the end of a narrow-spectral illumination. (**A**) IL-6, IL-8, TGFβ2, CCL2, (**B**) NFκB, GPx1, SOD1 in HCE; (**C**) IL-6, IL-8, TGFβ2 (**D**) NFκB, GPx1, SOD1 in IOBA. Clear bars correspond to normal and hatched bars to hyperosmolar (*HO*) conditions of culturing. Wavebands are represented by the correspondent colors; they are denoted on the color code scheme where each 10 nm spectral band is designated by its central wavelength. Results shown represent the mean ± SEM. Stars (*) refer to differences with the correspondent dark control within the same culturing condition and carets (^) refer to differences between culturing conditions (normal vs. HO) within the same illumination condition. Red signs correspond to an increase and blue signs to a decrease in values. Statistical significance: $p < 0.05$ (*/^), $p < 0.01$ (**/^^), $p < 0.001$ (***/^^^), $p < 0.0001$ (****/^^^^).

approximate the real-life conditions (Supplementary Fig. S4B1, B2). Indeed, according to recent measurements performed in the R&D department of Essilor (publication currently in preparation), we can easily be exposed to 4.89 mW/cm^2 of a 380–780 nm ambient light when being outside on a sunny slightly cloudy day. This measurement corresponds to the entire visible solar spectrum (380–780 nm) while the irradiances

of its blue (380–500 nm) and yellow (500–600 nm) spectral parts are 1.28 mW/cm^2 and 1.4 mW/cm^2 respectively.[1] We set the time of illumination at 17 h since it is the average duration of wakefulness per day. This study demonstrated the phototoxicity of such wide-spectral blue illumination on the ocular surface in terms of increased ROS generation level.

Next, we explored the impact of narrow 10 nm wavebands situated within the large blue spectrum to better understand the specific wavelength dependency of phototoxicity. As we were limited to 5 various wavelengths that could be used simultaneously (illumination system constraint), we chose the most violet blue one that was also supposed to serve as a positive control (390 nm), the blue light whose toxicity is currently widely discussed (420 and 430 nm), the turquoise blue implicated in circadian rhythms (480 nm), and also the red light (630 nm). The part of the plate was always kept in the dark for the control condition.

We demonstrated the significant decrease in viability for blue-illuminated cells. Morphologically, both cell lines noticeably collapsed at 390 nm and presented alterations at 420 and sometimes at 430 nm, even if the viability rate for the latter did not show a significant quantitative decline. These results are in line with those of Niwano *et al.*, Ayaki *et al.* and Lee *et al.* who found a significant decrease in the viability of rabbit corneal epithelial cell lines [31], primary cultures of human ocular cells [30] and HCE cell line [29] respectively illuminated by 410 ± 10 nm waveband (in average). As opposed to HCE line, no recovery after exposure was observed in 420 nm-illuminated IOBA cells; moreover, their morphological alterations appeared to be more important than in HCE. Together these results may suggest that conjunctival cells are more prone to blue light phototoxicity than the corneal ones. This higher photosensitivity of IOBA cell line would be logical taking into account the ocular immunology. Indeed, the conjunctival epithelium is very rich in highly interconnected immunocompetent cells, which makes the conjunctiva the first location of the ocular inflammatory response. One of the main roles of the conjunctiva is to protect the “noble” corneal structure and to preserve its integrity and transparency that are essential for the correct visual function. On the contrary, the cornea benefits from the immune privilege (few immune cells, no blood vessels) and from the inhibition of inflammatory reactions. Thus, the conjunctiva naturally participates in the inflammation process to a much greater extent than the cornea and is therefore more responsive to phototoxic stress [46–48]. To better understand the pathways of occurring cellular death, we calculated the ratios between YO-PRO (apoptosis) and PI (necrosis) signals at various times after the end of illumination (Supplementary Fig. S6). For both cell types at 390 nm, this ratio significantly increased at least at the end of the 24 h recovery. Thus, we concluded about the prevailing role of apoptosis in the post-illumination phototoxic processes. Additional HO stress did not allow HCE line to restore viability as it was possible in normal conditions; it also impacted the proliferation and apoptosis rate. In IOBA after 4 h of recovery, we observed the amplification of phototoxicity by concomitant HO stress suggesting that light exposure could enhance ocular surface damage observed in DED, further emphasizing the commonly observed susceptibility of dry eye patients to blue light exposure.

Oxidative stress and excessive ROS generation are widely considered as key factors in the pathogenesis of ocular surface diseases, and notably in DED [39,49–52]. Indeed, in our model we observed an important increase in $O_2^{\bullet -}$ rate in mitochondria, the main source of electrons for reduction of molecular oxygen to $O_2^{\bullet -}$ [53]. We than showed that H_2O_2, a specie that is poorly reactive but critical for signaling systems [53,54], followed exactly the same trend but to a greater extent (the smaller rates of superoxide anion were probably due to the fact that $O_2^{\bullet -}$ was transformed into other ROS species). Since H_2O_2 production demonstrated very important values, we than followed its rate in time. The peak observed for 390 nm in 4 h after exposure correlated with the previously detected peak of necrosis at that time point. At 420 nm, H_2O_2 rate remained steady while it significantly decreased at 430 nm, highlighting the greater toxicity of 420 nm illumination as compared to the 430 nm one. Our results concerning the ROS production are in agreement with those of Lee [29] and Ayaki [30]. Interestingly, in some experiments (cellular death rates and ROS production) in normal culturing conditions, the rates of immediate HCE cells' responses were stronger than IOBA cells' ones while there was no such a difference after recovery time. We therefore propose that in IOBA cells, the phototoxic process takes more time to activate the response of the same order than in HCE. Thus, the IOBA cell defense system cannot be switched on enough quickly making the conjunctival cells more sensitive to the impact of light. Indeed, the conjunctival tissues are more protected by eyelids than the corneal ones; that means that naturally the conjunctiva is supposed to be less illuminated by light than the cornea and may therefore posses a less adapted defense system.

Since oxidative stress is a result of an imbalance between free radical generation and scavenging, we further explored the functioning of ROS-eliminating system. In order to increase their antioxidant capacity [55], both cell lines triggered off their glutathione-based antioxidant system by increasing the levels of GSH and GSSG. As opposed to HCE, IOBA cells illuminated by blue-violet light demonstrated a significant increase in GSH/GSSG ratio, which is considered to determine the oxidant/anti-oxidant balance [56,57]. It suggests that in IOBA, the conjunctival anti-oxidant system was impaired, in agreement with already discussed greater photosensitivity of IOBA cells. Also, because ROS accumulation is known to be produced in mitochondria, we then checked the state of the mitochondrial membrane potential. In keeping with the previous results, for more violet exposures, we detected the loss of MMP that is considered to be a sensitive indicator of mitochondrial damage [58,59]. Surprisingly, IOBA cells demonstrated a significantly increased MMP after the 430 nm illumination. Even if the disruption of MMP is frequently considered as an important landmark in apoptotic signaling [60], numerous studies reported an increase in MMP as the very first response to stress. They suggest that mitochondrial hyperpolarization and ROS production precedes the decrease in MMP and represents an early event in apoptosis; the underlying cellular mechanism is though still incompletely understood (reviewed in [61,62]). Thus, the literature led us to suppose that 430 nm illumination may provoke early signs of cytotoxicity. MMP elevation was observed in various cell types (e.g., in T cells, HeLa cells, fibroblasts and astroglial cells, for more detail see [63–66]); however, no data are available concerning mitochondrial hyperpolarization in cells of the ocular surface. Together, our results suggest that 430 nm light, while being definitely less dangerous than its more short-wavelength visible counterparts, is still phototoxic to the ocular surface.

Combination of light exposure with HO stress is one of the main innovative points of our study. While being enough harmful for IOBA, in HCE, additional hyperosmolarity provides with a priming effect stimulating the HCE defense system and allowing cells for better struggle against phototoxicity. This effect may be explained by the hormesis theory [67] according to which, exposure to low continuous or higher intermittent doses of a stress agent, that would otherwise be harmful at larger or chronic doses, promotes favorable biological adaptations which protect against greater subsequent stress [68]. This concept is particularly extended to the mitochondria (mitohormesis) supposing that mild perturbations in mitochondrial homeostasis coordinate nuclear and cytosolic responses that make the whole cell less susceptible to future perturbations [68] (reviewed in [69,70]). Thus, we suggest that preexisting hyperosmolar stress provoked a mild oxidative stress

[1] Measurements were done at 10 a.m. in the center Paris at the end of May; the measurement setup was installed on the 5th floor, the detector orientation corresponded to the −15° of the head lowering; given values represent the average of irradiances measured in the four main directions (North, Est, South, West).

which further played a role of perturbation necessary for mitohormesis. As a result, this process made HCE cells more adapted for struggling against phototoxicity. Nevertheless, this trigger factor turned out to be outside the hormetic zone for more sensitive conjunctival cells, thus providing IOBA with more important cytotoxicity.

Last, we investigated the mRNA expression for genes whose regulation is widely implicated in DED. Chemokine CXCL8, one of the major mediators of the inflammatory response, and proinflammatory cytokine IL-6 are important biomarkers of ocular surface inflammation and DED [71]. While being expectedly up-regulated in blue-illuminated HCE, in IOBA, CXCL8 expression went down. We ascribed this fact to a possible negative loop regulation that turned on when highly stressed IOBA cells produced CXCL8 in excess amount. Two other cytokines implicated in the ocular surface homeostasis and inflammation are CCL2 and TGFβ2. The former is produced by a variety of cell types, either constitutively or after induction by oxidative stress [72,73]. Our team has previously studied the induced expression of chemokines in the inflamed ocular surface; more particularly, in case of ocular surface toxicity induced by benzalkonium chloride, the deregulation of CX3CL1 and CCL2 in the conjunctival epithelium was demonstrated [37]. Together with TGFβ2, one of the most important ligands involved in modulation of cell behavior in ocular tissues [74], these markers were down-regulated in normal conditions. However, additional HO stress probably broke down the negative loop regulation leading to a significant increase in their expression. HO also slightly increased the expression NFκB, a protein complex that controls transcription of DNA, cytokine production, and cell survival, in accordance with previous studies where NFκB was reported to have a role in HO-induced cellular signaling [38,75]. In HCE, the observed mRNA up-regulation of SOD1, one of the main antioxidant enzymes [57,76], meaning a setting-up of cellular defense system, even better adjusted under HO hormetic effect. On the opposite, in IOBA, no changes for SOD1 together with down-regulation of GPx1 led again to a greater phototoxicity in this cell line. Together, these experiments allowed to observe the blue-light-induced alterations in mRNA expression of biomarkers implicated in the inflammatory response and antioxidant defense of ocular surface cells.

To sum up, we hypothesize that when blue light reaches the cell, it primarily impacts the mitochondria, increasing the rate of superoxide anion and changing its membrane potential. $O_2^{\bullet -}$ is then transformed into hydrogen peroxide by means of superoxide dismutase·H_2O_2 is further partially expulsed from the cell thus increasing the level of extracellular ROS. In cytosol, hydrogen peroxide is eliminated by means of glutathione-based defensive system. In addition, induced oxidative stress affects the regulation of inflammatory cytokines and of genes responsible for the functioning of the antioxidant system. One should note that the majority of harmful effects observed in this work were not detected after exposure to the control red light, thus confirming the blue wavelength specificity of the presented phototoxic effects. Moreover, it is worth to note that our findings are in line with recent in vivo results of Lee *et al.* who reported that overexposure to blue light induced oxidative damage and apoptosis to the cornea, probably resulting in increased ocular surface inflammation and dry eye [2].

Our work demonstrates the deleterious effects of blue light on the eye, not only on the retina but on the ocular surface. *In vivo* studies may confirm the present in vitro results including the role of various cell types such as goblet cells [77,78] or potentially beneficial treatments like contrived tear products currently available on the market. Our findings corroborate the daily photosensitivity observed in DED patients in clinical practice, and show that they might be more prone to blue light phototoxicity. Wearing glasses that would filter out the blue wavebands the most toxic for the ocular surface and highly present in the given illumination conditions (like sunlight, office illumination, light from screens etc.) might provide DED patients with an important relief. In parallel, precisely adjusting the color spectrum in computer/smartphone displays could also improve the symptoms and quality of life in patients with dry eye. Thus, a clinical study that would investigate such benefits is worth to be done.

4. Materials & methods

4.1. Cell lines

The human corneal epithelial cell line (HCE, RCB-1384; Riken Cell Bank, Tsukuba, Japan) was cultured in DMEM/F12 no phenol red buffer (i.e., without photosensitizer), supplemented with 10% fetal bovine serum (FBS), 1% penicillin (10,000 units/mL) and streptomycin (10,000 µg/mL) as described previously [40]. The IOBA-NHC cell line derived from normal human conjunctival epithelium [41] was cultured in DMEM/F12 no phenol red buffer supplemented with 1 g/mL bovine pancreas insulin, 2 ng/mL mouse epidermal growth factor (EGF), 0.1 g/mL cholera toxin from vibrio cholerae, 5 g/mL hydrocortisone suitable for cell culture, 10% fetal bovine serum (FBS), 1% penicillin (10,000 units/mL) and streptomycin (10,000 µg/mL) as described previously [37]. DMEM/F12 no phenol red (i.e., without photosensitizer), FBS, penicillin and streptomycin were purchased from Gibco (Life technologies, Carlsbad, CA, USA); insulin, EGF, cholera toxin and hydrocortisone were purchased form Sigma Aldrich (St. Louis, MO, USA). Both cell lines were cultured under classic conditions (moist atmosphere, 5% CO_2, 37 °C); cells from passages 2–15 were used. Cells were seeded in black 96-well plates (Greiner Bio-One GmbH, Kremsmünster, Austria) 24 h before the beginning of light exposure, to achieve 60–70% confluence. We choose this confluence since it was reported that confluent cells (90–100%) may demonstrate no reduction in viability after the light exposure [31]. Moreover, if the cells have already reached the full confluence by the beginning of illuminatoin, they would undergo certain cell death independently on light impact, thus making it complicated to discern the purely phototoxic effect.

4.2. Hyperosmolar conditions

Hyperosmolar media were prepared by adding 69 mM of sodium chloride (Sigma-Aldrich, St. Louis, MO, USA) to supplemented media. Osmolarity values of normal (basal) and hyperosmolar (HO) media were measured with an osmometer (Roebling 13DR, Berlin, Germany):

$$\mathrm{HCE(basal)} = 315\mathrm{mOsm},\quad \mathrm{HCE(HO)} = 442\mathrm{mOsm} \Rightarrow \triangle(\mathrm{HCE_{HOstress}}) = 127\mathrm{mOsm}$$
$$\mathrm{IOBA(basal)} = 324\mathrm{mOsm},\quad \mathrm{IOBA(HO)} = 455\mathrm{mOsm} \Rightarrow \triangle(\mathrm{IOBA_{HOstress}}) = 131\mathrm{mOsm}$$

4.3. Light emitting devices and protocol

4.3.1. Wide-spectral illuminations – WL-Box device

Cells were exposed to either blue (380–525 nm) or yellow (538–662 nm) light provided by a custom-made xenon-based device; the average irradiance was 1.15 mW/cm^2 (Supplementary Fig. S3A1,2, B1,2).

4.3.2. Narrow-spectral illuminations – BL-Box device

Cells were exposed to 5 various 10 nm-wide light wavebands provided by a custom-made LED-based fibered device as described previously [20]. The central wavelengths of these wavebands were 390, 420, 430, 480 and 630 nm; their irradiances were 1.05, 1.13, 1.16, 1.11 and 1.53 mW/cm^2 respectively (Supplementary Fig. S3A3, B3).

Cells in black 96 well-plate were exposed to either wide (WL-Box) or narrow (BL-Box) wavebands of light for 17 h; for each experiment, one subdivision of a well plate was maintained in darkness. Seven hours before the exposure beginning, cell basal media were either changed to the hyperosmolar ones, or just renewed (Fig. S3C). Except for the follow-up time experiments, all the assessments of light phototoxicity were performed immediately after the end of illumination. When time

changes were monitored (for cell viability, proliferation and death rates and for hydrogen peroxide production), after the end of light exposure, cells were kept in dark under standard conditions (moist atmosphere, 5% CO_2, 37 °C) for either 4 or 24 h.

4.4. Quantification of cell viability and H_2O_2 generation

The CellTiter-Glo® Assay and the ROS-Glo™ H_2O_2 Assay (Promega, Madison, WI, USA) were multiplexed according to the manufacturer's protocol. Briefly, cells were incubated with H_2O_2 Substrate Solution for 3 h before the end of exposure. Then, half of the supernatant of the illuminated well plate (plate N1) was carefully transferred to another well plate (plate N2), without touching the adherent cells. Then, the CellTiterGlo Detection Solution was added to the plate N1 and the ROS-Glo Detection Solution was added to the plate N2. Both plates were incubated at room temperature (RT) in the dark for 20 min before luminescence reading on an Infinite M1000 microplate reader (Tecan, Männedorf, Switzerland). Luminiscence values were normalized with respect to control cells considered as 100% viable. For ROS quantification, the values were also normalized with respect to viability.

4.5. Cell death assays - HYP (Hoechst/YO-PRO/PI) test

The apoptotic cells are permeable for YO-PRO®-1 (Invitrogen, Eugene, Oregon, USA) while remaining non-permeable to Propidium Iodide (Interchim, Montluçon, France) which only stains necrotic cells [79,80]. Hoechst 33342 (Invitrogen, Eugene, Oregon, USA) is a DNA-intercalating agent that may therefore represent the cellular proliferation. Unlike propidium iodide, it is not excluded by live or apoptotic cells. It has been observed that short exposure of cells to low concentrations of Hoechst leads to strong rapid labeling of apoptotic cells while live cells require much longer incubation time to obtain comparable fluorescence intensity. Thus, Hoechst labeling has been also proposed as an assay of apoptosis [81]. The reagents were mixed together in the PBS (Gibco, Life technologies, Carlsbad, CA, USA) at the following concentrations: Hoechst – 1/1000, YO-PRO – 1/150, PI – 1/15000. Such a mixing was possible since the tree dyes have different excitation/emission spectra (Fig. S5). At the end of light exposure, the well plate was centrifuged at 1500 rpm during 5 min. Media were carefully replaced with100 µl of prepared solution; the well plate was then incubated for 30 min at RT in the dark. Further, 100 µl of PBS were added to wells; the well plate was centrifuged again (1500 rpm, 5 min) and supernatants were replaced with 100 µl of fresh PBS. Finally, the fluorescent signals were read on an Infinite M1000 microplate reader (Tecan, Männedorf, Switzerland) in the following order, to avoid cross-excitations if there were any (hardly probable): Hoechst - $\lambda\uparrow$ = 350 nm, $\lambda\downarrow$ = 461 nm; YO-PRO - $\lambda\uparrow$ = 491 nm, $\lambda\downarrow$ = 509 nm; PI - $\lambda\uparrow$ = 535 nm, $\lambda\downarrow$ = 617 nm. Measured values were normalized with respect to control cells considered as 1 and also to viability.

4.6. Quantification of $O_2^{\bullet -}$ generation

Superoxide anion levels were quantified using the MitoSOX™ Red Mitochondrial Superoxide Indicator kit (Life Technologies, Carlsbad, CA, USA). MitoSOX reagent working solution (5 µM) was prepared by diluting MitoSOX reagent stock solution (5 mM in DMSO (Sigma Aldrich, St. Louis, MO, USA)) in DMEM/F12 no phenol red buffer. At the end of light exposure, media were replaced with 100 µl of MitoSOX reagent working solution; the well-plate was then incubated for 10 min at 37 °C in the dark. Cells were further carefully washed 3 times with warm PBS; finally 100 µl of PBS was added to wells. The fluorescent signal was read on an Infinite M1000 microplate reader (Tecan, Männedorf, Switzerland): $\lambda\uparrow$ = 510 nm, $\lambda\downarrow$ = 580 nm. Measured values were normalized according to control cells considered as 1 and also according to viability.

4.7. Mitochondrial membrane potential assessment

Mitochondrial membrane potential was measured using the Mito-ID membrane potential cytotoxicity kit (Enzo Life Sciences, Farmingdale, NY, USA). Carbonyl cyanide 3-chlorophenylhydrazone (CCCP, working solution was prepared in DMEM/F12 no phenol red buffer) was added 30 min before the end of light exposure to a few wells to abolish the mitochondrial membrane potential as a positive control (final concentration in wells was 8 µM). At the end of light exposure, the MitoID dye solution prepared according to the manufacturer's protocol was directly dispensed into each well; the well-plate was then incubated for 30 min at RT in the dark. The fluorescent signal was read on an Infinite M1000 microplate reader (Tecan, Männedorf, Switzerland): $\lambda\uparrow$ = 490 nm, $\lambda\downarrow$ = 590 nm. Measured values were normalized with respect to control cells considered as 1.

4.8. Measurement of glutathione

The rate of reduced and oxidized forms of glutathione was measured with the GSH/GSSG-Glo™ Assay kit (Promega, Madison, WI, USA). At the end of light exposure, cells were treated either with Total or Oxidized Glutathione Reagent for 5 min under shaking at RT. Luciferin Generation Reagent was then added to all the wells; the well-plate was incubated for 30 min at RT before adding the Luciferin Detection Reagent. Luminescence was read on a microplate reader Infinite M1000 microplate reader (Tecan, Männedorf, Switzerland). Measured values were normalized with respect to control cells considered as 1 and also with respect to viability. The ratio GSH/GSSG was calculated according to the manufacturer's protocol.

4.9. Imaging

Cells were fixed with 4% paraformaldehyde-PBS (Sigma-Aldrich) for 10 min, then washed twice with PBS and imaged with the inverted Nikon TiE microscope (image recording via Metamorph 7.7). Images were then processed with the Fiji software (ImageJ version).

4.10. RT-qPCR

After the end of illumination, cells were washed and lysed; total RNA was extracted using a NucleoSpin RNA XS extraction kit (Macherey-Nagel, Düren, Germany). RNA quality and quantity were assessed using a ND-1000 spectrophotometer (Thermo Scientific, Waltham, Massachusetts, USA). cDNA was further synthesized from equal amounts of RNA using Multiscribe reverse transcriptase (TaqMan Reverse Transcription Reagents, Applied Biosystems, Life Technologies, Carlsbad, CA, USA) according to the manufacturer's protocol. Finally, cDNA were diluted in DNAse/RNAse free water (Gibco) to a final concentration of 5 ng/µl. Real-time quantitative PCR was performed with 25 ng of cDNA added to a 15 µl solution of Applied Biosystems Mastermix (TaqMan Universal PCR Master Mix) and primers to a final volume of 20 µl. All primers and reagents were purchased from Applied Biosystems: GAPDH (Hs02786624_g1), HPRT1 (Hs02800695_m1), IL-6 (Hs00174131_m1), CXCL8 (Hs00174103_m1), TGFβ2 (Hs00234244_m1), CCL2 (Hs00234140_m1), NFκB1 (Hs00765730_m1), GPx1 (Hs00829989_gH), SOD1 (Hs00533490_m1). Target cDNA was amplified using the 7300 Real-Time PCR system (Applied Biosystems). Changes in mRNA expression were calculated as $\Delta\Delta Ct = \Delta Ct_{illuminated} - \Delta Ct_{control}$ with $\Delta Ct = Ct_{target\_gene} - Ct_{HK\_gene}$. Ct means *cycle threshold* and HK_gene means *housekeeping gene* (HPRT for HCE and GAPDH for IOBA). Non-illuminated cells cultured in basal conditions were taken as controls.

4.11. Statistical analysis

All experiments were repeated at least three times in technical

replicate. Statistical analyzes were performed using GraphPad (GraphPad Software, La Jolla, CA, USA). One- or two-way ANOVA analysis with repeated (time follow-up experiments) or non-repeated measures followed by False Discovery Rate multiple correction (two-stage step-up method of Benjamini, Krieger and Yekutieli, false discovery rate Q = 0.05) were used. All data are presented as mean ± SEM. Differences were considered significant when $p < 0.05$ (*/^), $p < 0.01$ (**/^^), $p < 0.001$ (***/^^^) or $p < 0.0001$ (****/^^^^).

Acknowledgements

We thank Coralie Barrau and William Rostène for insightful comments, Camille Ehrismann for technical support of the illumination systems and Karima Kessal for technical assistance and advices.

Sources of funding

This work was funded by Essilor International, within the frame of research collaboration with Sorbonne Université / Institut de la Vision.

Conflicts of interest

The authors report no conflicts of interest

Appendix A. Supporting information

Supplementary data associated with this article can be found in the online version at doi:10.1016/j.freeradbiomed.2018.07.012.

References

[1] J. Marshall, Understanding risks of phototoxicity on the eye, Point Vue, International Rev. Ophthalmic Opt. 〈http://www.pointsdevue.com/article/understanding-risks-phototoxicity-eye〉 (Accessed 7 November 2017).
[2] H.S. Lee, L. Cui, Y. Li, J.S. Choi, J. Choi, Z. Li, G.E. Kim, W. Choi, K.C. Yoon, Influence of light emitting diode-derived blue light overexposure on mouse ocular surface, PLoS One (2016), https://doi.org/10.1371/journal.pone.0161041.
[3] A.P. Cullen, Photokeratitis and other phototoxic effects on the cornea and conjunctiva, Int. J. Toxicol. (2002) 455–464, https://doi.org/10.1080/1091581029016988.
[4] J. Voke, Radiation effects on the eye. Part 3a - ocular effects of ultraviolet radiation, Optom. Today (1999) 27–32 (http://www.optometry.co.uk/pages/articles/articles1999.php%5Cn C:%5CLibrary%5CVoke1999.pdf).
[5] P.L. Turner, E.J.W. Van Someren, M.A. Mainster, The role of environmental light in sleep and health: Effects of ocular aging and cataract surgery, Sleep. Med. Rev. 14 (2010) 269–280, https://doi.org/10.1016/j.smrv.2009.11.002.
[6] J. Voke, Radiation effects on the eye. Part 3b - ocular effects of ultraviolet radiation, Optom. Today (1999) 37–41 (http://www.optometry.co.uk/pages/articles/articles1999.php%5Cn C:%5CLibrary%5CVoke1999b.pdf).
[7] F. Stapleton, M. Alves, V.Y. Bunya, I. Jalbert, K. Lekhanont, F. Malet, K. Na, D. Schaumberg, M. Uchino, J. Vehof, E. Viso, S. Vitale, The ocular surface TFOS DEWS II epidemiology report, Ocul. Surf. 15 (2017) 334–365, https://doi.org/10.1016/j.jtos.2017.05.003.
[8] M. Wade, Symptoms of dry eye disease, Discov. Eye Found. (2015), 〈http://discoveryeye.org/symptoms-of-dry-eye-disease/〉 (Accessed 6 November 2015).
[9] Tear Film & Ocular Surface Society, DRY EYE REDEFINED: TFOS DEWS II REPORT, TFOS. 〈http://www.tfosdewsreport.org/〉 (Accessed 10 November 2017).
[10] J.P. Craig, K.K. Nichols, J.J. Nichols, B. Caffery, H.S. Dua, E.K. Akpek, K. Tsubota, C.-K. Joo, Z. Liu, J. Daniel Nelson, F. Stapleton, TFOS DEWS II definition and classification report, Ocul. Surf. 15 (2017) 276–283, https://doi.org/10.1016/j.jtos.2017.05.008.
[11] A. Réaux-le-Goazigo, A. Labbé, C. Baudouin, Melik-Parsadaniantz, Stéphane, La douleur oculaire chronique: mieux la comprendre pour mieux la traiter, Med./Sci. 33 (2017) 749–757.
[12] W. Hauser, Dry eye: a young Person's disease? Rev. Optom. (2017), 〈https://www.reviewofoptometry.com/article/dry-eye-a-young-persons-disease〉 (Accessed 6 November 2017).
[13] Text Request, How Much Time Do People Spend on Their Mobile Phones in2017?, Hackernoon. (n.d.). 〈https://hackernoon.com/how-much-time-do-people-spend-on-their-mobile-phones-in-2017-e5f90a0b10a6〉 (Accessed 7 November 2017).
[14] J. Lupis, The State of Traditional TV: Updated With Q1 2017 Data, Mareketing Charts. (n.d.). 〈http://www.marketingcharts.com/featured-24817〉 (Accessed 7 November 2017).
[15] A. Yazici, E.S. Sari, G. Sahin, A. Kilic, H. Cakmak, O. Ayar, S.S. Ermis, Change in tear film characteristics in visual display terminal users, EJO 25 (2015) 85–89, https://doi.org/10.5301/ejo.5000525.
[16] M. Kaido, I. Toda, T. Oobayashi, M. Kawashima, Reducing short-wavelength blue light in dry eye patients with unstable tear film improves performance on tests of visual acuity, PLoS One 11 (2016) 1–10, https://doi.org/10.1371/journal.pone.0152936.
[17] R. Courtin, B. Pereira, G. Naughton, A. Chamoux, F. Chiambaretta, C. Lanhers, F. Dutheil, Prevalence of dry eye disease in visual display terminal workers: a systematic review and meta-analysis, BMJ (2016), https://doi.org/10.1136/bmjopen-2015-009675.
[18] M. Uchino, N. Yokoi, Y. Uchino, M. Dogru, M. Kawashima, A. Komuro, Y. Sonomura, H. Kato, S. Kinoshita, D. a. Schaumberg, K. Tsubota, Prevalence of dry eye disease and its risk factors in visual display terminal users: the Osaka study (e1), Am. J. Ophthalmol. 156 (2013) 759–766, https://doi.org/10.1016/j.ajo.2013.05.040.
[19] A.J. Bron, C.S. de Paiva, S.K. Chauhan, S. Bonini, S. Jain, E. Knop, M. Markoulli, Y. Ogawa, V. Perez, Y. Uchino, N. Yokoi, D. Zoukhri, D.A. Sullivan, TFOS DEWS II pathophysiology report, Ocul. Surf. 15 (2017) 511–538, https://doi.org/10.1016/j.jtos.2017.05.004.
[20] E. Arnault, C. Barrau, P. Gondouin, K. Bigot, T. Villette, S. Picaud, D. Cohen-Tannoudji, Phototoxic action spectrum on a retinal pigment epithelium model of age-related macular degeneration exposed to sunlight normalized conditions, PLoS One 8 (2013), https://doi.org/10.1371/journal.pone.0071398.
[21] K. Ogawa, Y. Kuse, K. Tsuruma, S. Kobayashi, M. Shimazawa, H. Hara, Protective effects of bilberry and lingonberry extracts against blue light-emitting diode light-induced retinal photoreceptor cell damage in vitro, BMC Complement. Altern. Med. 14 (2014) 1–11.
[22] C. Roehlecke, U. Schumann, M. Ader, C. Brunssen, S. Bramke, H. Morawietz, R.H.W. Funk, Stress reaction in outer segments of photoreceptors after blue light irradiation, PLoS One 8 (2013) e71570, https://doi.org/10.1371/journal.pone.0071570.
[23] I.K. Gipson, The ocular surface: the challenge to enable and protect vision, Ocul. Surf. 48 (2010) 4390–4398, https://doi.org/10.1167/iovs.07-0770.The.
[24] C. Zinflou, P.J. Rochette, Free radical biology and medicine ultraviolet A-induced oxidation in cornea: characterization of the early oxidation-related events, Free Radic. Biol. Med. 108 (2017) 118–128, https://doi.org/10.1016/j.freeradbiomed.2017.03.022.
[25] C. Cejka, J. Platenik, R. Buchard, V. Guryca, J. Sirc, M. Vejerazka, J. Crkovska, T. ARdan, J. Michalek, B. Brunova, J. Cejkova, Effect of two different UVA doses on the rabbit cornea and lens, Photochem. Photobiol. (2009) 794–800, https://doi.org/10.1111/j.1751-1097.2008.00478.x.
[26] A. Golu, I. Gheorghisor, A.T. Balasoiu, F. Balta, E. Osiac, L. Mogoanta, A. Bold, The effect of ultraviolet radiation on the cornea – experimental study, RJME 54 (2013) 1115–1120.
[27] S.P. Gendron, P.J. Rochette, Modifications in stromal extracellular matrix of aged corneas can be induced by ultraviolet A irradiation, Aging Cell. (2015) 433–442, https://doi.org/10.1111/acel.12324.
[28] P. Dadoukis, I. Klagas, E. Papakonstantinou, Infrared irradiation alters the expression of matrix metalloproteinases and glycosaminoglycans in the cornea and crystalline lens, Graefes Arch. Clin. Exp. Ophthalmol. (2013) 1929–1936, https://doi.org/10.1007/s00417-013-2349-9.
[29] J. Lee, S. Kim, S. Lee, H. Kim, H. Ahn, Z. Li, Blue light – induced oxidative stress in human corneal epithelial cells: protective effects of ethanol extracts of various medicinal plant mixtures, Cornea 55 (2014) 4119–4127, https://doi.org/10.1167/iovs.13-13441.
[30] M. Ayaki, Y. Niwano, T. Kanno, K. Tsubota, Blue light induces oxidative damage in human ocular surface cells in culture, ARVO 2015 Annu. Meet. Abstr. (2015).
[31] Y. Niwano, T. Kanno, A. Iwasawa, M. Ayaki, K. Tsubota, Blue light injures corneal epithelial cells in the mitotic phase in vitro, Br. J. Ophthalmol. 98 (2014) 990–992, https://doi.org/10.1136/bjophthalmol-2014-305205.
[32] H. Bin Hwang, H.S. Kim, Phototoxic effects of an operating microscope on the ocular surface and tear film, Cornea 33 (2014) 82–90, https://doi.org/10.1097/ICO.0000000000000001.
[33] T. Ipek, M.P. Hanga, A. Hartwig, J. Wolffsohn, C. O'Donnell, Dry eye following cataract surgery: the effect of light exposure using an in-vitro model, Cont. Lens Anterior Eye (2017) 3–6, https://doi.org/10.1016/j.clae.2017.11.003.
[34] A. Denoyer, G. Rabut, C. Baudouin, Tear film aberration dynamics and vision-related quality of life in patients with dry eye disease, Ophthalmology 119 (2012) 1811–1818, https://doi.org/10.1016/j.ophtha.2012.03.004.
[35] A. Pauly, E. Brasnu, L. Riancho, F. Brignole-Baudouin, C. Baudouin, Multiple endpoint analysis of BAC-preserved and unpreserved antiallergic eye drops on a 3D-reconstituted corneal epithelial model, Mol. Vis. 17 (2011) 745–755 〈https://www.ncbi.nlm.nih.gov/pmc/articles/PMC3062522/pdf/mv-v17-745.pdf〉.
[36] C. Baudouin, P. Aragona, G. Van Setten, M. Rolando, M. Irkeç, J.B. Del Castillo, G. Geerling, M. Labetoulle, S. Bonini, Diagnosing the severity of dry eye: a clear and practical algorithm, Br. J. Ophthalmol. 98 (2014) 1168–1176, https://doi.org/10.1136/bjophthalmol-2013-304619.
[37] A. Denoyer, D. Godefroy, I. Celerier, J. Frugier, L. Riancho, F. Baudouin, W. Rostene, C. Baudouin, CX3CL1 expression in the conjunctiva is involved in immune cell trafficking during toxic ocular surface inflammation, Mucosa Immunol. 5 (2012) 703–711, https://doi.org/10.1038/mi.2012.43.
[38] E. Warcoin, C. Baudouin, C. Gard, F. Brignole-Baudouin, In vitro inhibition of NFAT5-mediated induction of CCL2 in hyperosmotic conditions by cyclosporine and dexamethasone on human HeLa-modified, PLoS One (2016) 1–19, https://doi.org/10.1371/journal.pone.0159983.
[39] S. Seen, L. Tong, Dry eye disease and oxidative stress, Acta Ophtalmol. (2017) 1–9, https://doi.org/10.1111/aos.13526.
[40] H. Liang, C. Baudouin, P. Daull, J.-S. Garrigue, F. Brignole-Baudouin, Ocular safety

of cationic emulsion of cyclosporine in an in vitro corneal wound-healing model and an acute in vivo rabbit model, Mol. Vis. 18 (2012) 2195–2204 〈http://www.pubmedcentral.nih.gov/articlerender.fcgi?artid=3425577&tool=pmcentrez&rendertype=abstract〉.
[41] Y. Diebold, M. Calonge, A. Enrı, S. Callejo, R.M. Corrales, V. Sa, K.F. Siemasko, M.E. Stern, Characterization of a spontaneously immortalized cell line (IOBA-NHC) from normal human conjunctiva, IOVS 44 (2003), https://doi.org/10.1167/iovs.03-0560.
[42] L. Tong, Y. Diebold, M. Calonge, J. Gao, M.E. Stern, R.W. Beuerman, Comparison of gene expression profiles of conjunctival cell lines with primary cultured conjunctival epithelial cells and human conjunctival tissue, Gene Expr. 14 (2009) 265–278.
[43] A. Enríquez-De-Salamanca, V. Calder, J. Gao, G. Galatowicz, C. García-vázquez, I. Fernández, M.E. Stern, Y. Diebold, M. Calonge, Cytokine cytokine responses by conjunctival epithelial cells: an in vitro model of ocular inflammation, Cytokine 44 (2008) 160–167, https://doi.org/10.1016/j.cyto.2008.07.007.
[44] A. Guzman-Aranguez, M.J. Pérez de Lara, J. Pintor, Hyperosmotic stress induces ATP release and changes in P2×7 receptor levels in human corneal and conjunctival epithelial cells, Purinergic Signal. 13 (2017) 249–258.
[45] Y. Ren, H. Lu, P.S. Reinach, Q. Zheng, J. Li, Q. Tan, H. Zhu, W. Chen, Hyperosmolarity-induced AQP5 upregulation promotes inflammation and cell death via JNK1/2 Activation in human corneal epithelial cells, Sci. Rep. 7 (2017) 1–11, https://doi.org/10.1038/s41598-017-05145-y.
[46] H. Zhan, H. Towler, V.L. Calder, The immunomodulatory role of human conjunctival epithelial cells, IOVS 44 (2003) 3906–3910, https://doi.org/10.1167/iovs.02-0665.
[47] C. Baudouin, P.-J. Pisella, H.-X. Thanh, Surface Oculaire Rapport 2015, Elsevier, Masson, 2015.
[48] S. Pflugfelder, C. de Paiva, The pathophysiology of dry eye disease: what we know and future directions for research, Am. Acad. Ophtalmol. 124 (2017) 4–13, https://doi.org/10.1016/j.ophtha.2017.07.010.
[49] A. Macri, C. Scanarotti, A.M. Bassi, S. Giuffrida, G. Sangalli, C.E. Traverso, Evaluation of oxidative stress levels in the conjunctival epithelium of patients with or without dry eye, and dry eye patients treated with preservative-free hyaluronic acid 0. 15% and vitamin B12 eye drops, Cornea (2015) 425–430, https://doi.org/10.1007/s00417-014-2853-6.
[50] Y. Uchino, T. Kawakita, T. Ishii, N. Ishii, New mouse model of dry eye disease: oxidative stress affects functional decline in the lacrimal gland, Cornea 31 (2012) 63–67.
[51] T.H. Wakamatsu, M. Dogru, K. Tsubota, Tearful relations: oxidative stress, inflammation and eye diseases, Arq. Bras. Oftalmol. 2 (2008) 72–79.
[52] S.K. Ward, T.H. Wakamatsu, M. Dogru, O.M. a. Ibrahim, M. Kaido, Y. Ogawa, Y. Matsumoto, A. Igarashi, R. Ishida, J. Shimazaki, C. Schnider, K. Negishi, C. Katakami, K. Tsubota, The role of oxidative stress and inflammation in dry eye disease, Cornea 28 (2009) 70–74, https://doi.org/10.1167/iovs.09-4130.
[53] P. Newsholme, E. Rebelato, F. Abdulkader, M. Krause, A. Carpinelli, R. Curi, Reactive oxygen and nitrogen species generation, antioxidant defenses, and b-cell function: a critical role for amino acids, J. Endocrinol. 214 (2012) 11–20, https://doi.org/10.1530/JOE-12-0072.
[54] G.P. Bienert, J.K. Schjoerring, T.P. Jahn, Membrane transport of hydrogen peroxide, Biochim. Biophys. Acta - Biomembr. 1758 (2006) 994–1003, https://doi.org/10.1016/j.bbamem.2006.02.015.
[55] N. Ballatori, S.M. Krance, S. Notenboom, S. Shi, K. Tieu, C.L. Hammond, Glutathione dysregulation and the etiology and progression of human diseases, Biol. Chem. 390 (2009) 191–214, https://doi.org/10.1515/BC.2009.033.Glutathione.
[56] I. Rebrin, R.S. Sohal, Pro-oxidant shift in glutathione redox state during aging Igor, Adv. Drug Deliv. Rev. 60 (2008) 1545–1552, https://doi.org/10.1016/j.addr.2008.06.001.Pro-oxidant.
[57] Y. Chen, G. Menta, V. Vasiliou, Antioxidant defenses in the ocular surface, Ocul. Surf. 7 (2009) 176–185, https://doi.org/10.1002/nbm.3066.Non-invasive.
[58] G. Gupta, R.K. Chaitanya, M. Golla, R. Karnati, Allethrin toxicity on human corneal epithelial cells involves mitochondrial pathway mediated apoptosis, Toxicol. Vitr. 27 (2013) 2242–2248, https://doi.org/10.1016/j.tiv.2013.09.011.
[59] J. Gao, R. Sana, V. Calder, M. Calonge, W. Lee, L.A. Wheeler, M.E. Stern, Mitochondrial permeability transition pore in inflammatory apoptosis of human conjunctival epithelial cells and T cells: effect of cyclosporin A, Cornea 54 (2013) 4717–4733, https://doi.org/10.1167/iovs.13-11681.
[60] D.D. Newmeyer, S. Ferguson-Miller, Mitochondria: releasing power for life and unleashing the machineries of death, Cell 112 (2003) 481–490, https://doi.org/10.1016/S0092-8674(03)00116-8.
[61] B. Kadenbach, S. Arnold, I. Lee, M. Hüttemann, The possible role of cytochrome c oxidase in stress-induced apoptosis and degenerative diseases, Biochim. Biophys. Acta - Bioenergy 1655 (2004) 400–408, https://doi.org/10.1016/j.bbabio.2003.06.005.
[62] M. Forkink, G.R. Manjeri, D.C. Liemburg-Apers, E. Nibbeling, M. Blanchard, A. Wojtala, J.A.M. Smeitink, M.R. Wieckowski, P.H.G.M. Willems, W.J.H. Koopman, Mitochondrial hyperpolarization during chronic complex i inhibition is sustained by low activity of complex II, III, IV and v, Biochim. Biophys. Acta - Bioenerg. 1837 (2014) 1247–1256, https://doi.org/10.1016/j.bbabio.2014.04.008.
[63] A. Perl, P.J. Gergely, G. Nagy, A. Koncz, K. Banki, Mitochondrial hyperpolarization: a checkpoint of T-cell life, death and autoimmunity, Trends Immunol. 25 (2004) 360–367, https://doi.org/10.1016/j.it.2004.05.001.Mitochondrial.
[64] K. Banki, E. Hutter, N. Gonchoroff, A. Perl, Elevation of mitochondrial transmembrane potential and reactive oxygen intermediate levels are early events and occur independently from activation of caspases in Fas signaling, J. Immunil. 162 (1999) 1466–1479.
[65] A.M. De Sousa Leal, Violacein induces cell death by triggering mitochondrial membrane hyperpolarization in vitro, BMC Microbiol. 15 (2015) 4–11, https://doi.org/10.1186/s12866-015-0452-2.
[66] A. Bajić, M. Spasić, P.R. Andjus, D. Savić, A. Parabucki, A. Nikolić-Kokić, I. Spasojević, Fluctuating vs. continuous exposure to H2O2: the effects on mitochondrial membrane potential, intracellular calcium, and NF-κB in Astroglia, PLoS One 8 (2013) 1–10, https://doi.org/10.1371/journal.pone.0076383.
[67] H. Selye, C. Fortier, Adaptive reactions to stress, Assoc. Res. Nerv. Ment. Diseas. 29 (1949) 3–18.
[68] T.L. Merry, M. Ristow, Mitohormesis in exercise training, Free Radic. Biol. Med. (2015), https://doi.org/10.1016/j.freeradbiomed.2015.11.032.
[69] M. Ristow, K. Zarse, How increased oxidative stress promotes longevity and metabolic health: the concept of mitochondrial hormesis (mitohormesis), Exp. Gerontol. 45 (2010) 410–418, https://doi.org/10.1016/j.exger.2010.03.014.
[70] M. Ristow, K. Schmeisser, Mitohormesis: promoting health and lifespan by increased levels of reactive oxygen species (ROS), Dose-Response 12 (2014) 288–341, https://doi.org/10.2203/dose-response.13-035.Ristow.
[71] N. Deschamps, C. Baudouin, Dry eye and biomarkers : present and future, Curr. Ophthalmol. Rep. (2013) 65–74, https://doi.org/10.1007/s40135-013-0008-2.
[72] U. Spandau, A. Toksoy, S. Verhaart, R. Gillitzer, F.E. Kruse, High expression of chemokines Gro-a (CXCL-1), IL-8 (CXCL-8), and MCP-1 (CCL-2) in inflamed human corneas in vivo, Lab. Sci. 121 (2003) 2–8.
[73] S.L. Deshmane, S. Kremlev, S. Amini, B.E. Sawaya, Monocyte chemoattractant protein-1 (MCP-1): an overview, J. Interf. Cytokine Res. 29 (2009) 313–326, https://doi.org/10.1089/jir.2008.0027.
[74] S. Saika, TGFβ pathobiology in the eye, Lab. Investig. 86 (2006) 106–115, https://doi.org/10.1038/labinvest.3700375.
[75] E.-J. Chang, Y. Sun, Im, E.P. Kay, J.Y. Kim, J.E. Lee, H.K. Lee, The role of nerve growth factor in hyperosmolar stress induced apoptosis, J. Cell. Physiol. 216 (2008) 69–77, https://doi.org/10.1002/jcp.21377.
[76] M.P. Cabrera, R.H. Chihuailaf, Antioxidants and the integrity of ocular tissues, Vet. Med. Int. 2011 (2011) 1–8, https://doi.org/10.4061/2011/905153.
[77] M.A. Shatos, J.D. Ríos, Y. Horikawa, R.R. Hodges, E.L. Chang, C.R. Bernardino, P.A.D. Rubin, D.A. Dartt, Isolation and characterization of cultured human conjunctival goblet cells, Investig. Ophthalmol. Vis. Sci. 44 (2003) 2477–2486, https://doi.org/10.1167/iovs.02-0550.
[78] D.A. Dartt, R.R. Hodges, D. Li, M.A. Shatos, K. Lashkari, C.N. Serhan, Conjunctival goblet cell secretion stimulated by leukotrienes is reduced by resolvins D1 and E1 to promote resolution of inflammation, J. Immunol. 186 (2011) 4455–4466, https://doi.org/10.4049/jimmunol.1000833.
[79] M. Dutot, H. Liang, T. Pauloin, F. Brignole-Baudouin, C. Baudouin, J.-M. Warnet, P. Rat, Effects of toxic cellular stresses and divalent cations on the human P2×7 cell death receptor, Mol. Vis. 14 (2008) 889–897 〈http://www.ncbi.nlm.nih.gov/pubmed/18490962%5Cnhttp://www.pubmedcentral.nih.gov/articlerender.fcgi?artid=PMC2386509〉.
[80] C. Mehanna, C. Baudouin, F. Brignole-Baudouin, Spectrofluorometry assays for oxidative stress and apoptosis, with cell viability on the same microplates: a multiparametric analysis and quality control, Toxicol. Vitr. 25 (2011) 1089–1096, https://doi.org/10.1016/j.tiv.2011.03.007.
[81] A. Pauly, F. Brignole-Baudouin, J.M. Guenoun, L. Riancho, P. Rat, J.M. Warnet, C. Baudouin, Comparative study of topical anti-allergic eye drops on human conjunctiva-derived cells: responses to histamine and IFNγ and toxicological profiles, Graefe'S. Arch. Clin. Exp. Ophthalmol. 245 (2007) 534–546, https://doi.org/10.1007/s00417-006-0353-z.

Article 2: blue-phototoxicity in cells of trigeminal ganglia

V. Marek, A. Potey, A. Réaux-Le-Goazigo, E. Reboussin, A. Charbonnier, T. Villette, C. Baudouin, W. Rostène, A. Denoyer, S. Mélik-Parsadaniantz, **Neurotoxicity of blue light: in vitro evidence on trigeminal neurons and glial cells**, submitted to the Free Radical Biology and Medicine Journal on the 23th October 2018

As I have discussed in the introduction, trigeminal neural pathways are of extreme significance for the dry eye disease pathophysiology. Importantly, ocular surface innervation and nociception have a significant role in both photophobic mechanisms and pain propagation.

We were therefore wondering whether the blue light exposure might also impact the neural cells of trigeminal ganglia. Thus, we expanded our previous in vitro study about blue-light phototoxicity in cells of the ocular surface to the primary culture of neurons and glial cells from mouse TG. Here again, we were seeking to demonstrate spectral specificity of the observed phototoxic effect. Given the greater sensitivity of neurons as compared to cells of the ocular surface, we decided not to challenge them with the additional dry eye stress. However, instead of hyperosmolarity, we applied supplementary antimitotic treatment, since we were looking to differentiate between neuronal and neuroglial phototoxically induced responses.

In addition to the paradigm of the previous study and on the basis of the very recent works, we were also searching for alternative ways of neural light-induced cytotoxicity triggering and propagation. Thus, we investigated the implication of melanopsin and neuropsin in the trigeminal phototoxicity. To the best of our knowledge, this is the first declaration of direct phototoxic impact of blue light on TG neurons and neuroglial cells as well as the first report of the role of non-visual photoreceptors in the correspondent cytotoxic processes. Taken together, our results may be integrated in the scheme presented in Figure 16.

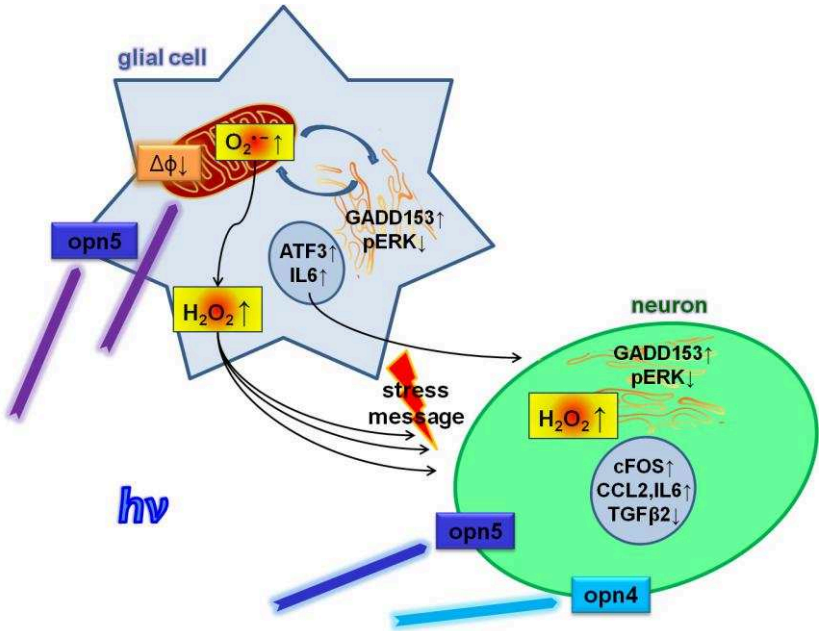

Figure 16. Scheme of blue light phototoxicity in the trigeminal pathway

Manuscript Details

Manuscript number	FRBM_2018_699
Title	Neurotoxicity of blue light: in vitro evidence on trigeminal neurons and glial cells
Article type	Original article

Abstract

Today the noxiousness of blue light from natural and particularly artificial (fluorescent tubes, LED panels, visual displays) sources is actively discussed in the context of various ocular diseases. Many of them have an important neurologic component and are associated with ocular pain. This neuropathic signal is provided by nociceptive neurons from trigeminal ganglia. However, the phototoxicity of blue light on trigeminal neurons has not been explored so far. The aim of the present in vitro study was to investigate the cytotoxic impact of various wavebands of visible light (410-630 nm) on primary cell culture of mouse trigeminal neural and glial cells. Three-hour exposure to narrow wavebands of blue light centered at 410, 440 and 480 nm of average 1.1 mW/cm2 irradiance provoked cell death, altered cell morphology and induced oxidative stress and inflammation. These effects were not observed for other tested visible wavebands. We observed that neurons and glial cells processed the light signal in different manner, in terms of resulting ROS species generation, inflammatory biomarkers expression and phototoxic mitochondrial damage. We analyzed the pathways of photic signal reception, and we proposed that, in trigeminal cells, in addition to widely known mitochondria-mediated light absorption, light could be received by means of non-visual opsins, melanopsin (opn4) and neuropsin (opn5). We also investigated the mechanisms underlying the observed phototoxicity, further suggesting an important role of the endoplasmic reticulum in neuronal transmission of blue-light-toxic message. Taken together, our results give some insight into circuit of tangled pain and photosensitivity frequently observed in patients consulting for these ocular symptoms.

Keywords	blue light; trigeminal neural cells; glial cells; non-visual opsins; neurophototoxicity
Taxonomy	Animal Cell Culture, Cytotoxicity Assay, Cell Death, Neurotoxicology

Corresponding Author	Veronika Marek
Order of Authors	Veronika Marek, Anaïs Potey, Annabelle REAUX LE GOAZIGO, Elodie Reboussin, Angéline Charbonnier, Thierry Villette, Christophe Baudouin, William Rostène, Alexandre Denoyer, Stephane Melik Parsadaniantz
Suggested reviewers	Pierrick Poisbeau, Kazuo Tsubota, Anna Matynia, David Copenhagen, Samer Hattar

Submission Files Included in this PDF

File Name [File Type]

Marek _ cover letter.docx [Cover Letter]

Marek _ highlights.docx [Highlights]

graphical abstract.tif [Graphical Abstract]

Marek _ Blue light sensitivity of trigeminal cells.docx [Manuscript File]

Figure 1.tif [Figure]

Figure 2.tif [Figure]

Figure 3.tif [Figure]

Figure 4.tif [Figure]

Figure 5.tif [Figure]

Figure 6.tif [Figure]

Figure S1.tif [Supplementary Material]

Figure S2.tif [Supplementary Material]

Figure S3.tif [Supplementary Material]

Figure S4.tif [Supplementary Material]

Marek _ earlier submission _ response.docx [Supplementary Material]

To view all the submission files, including those not included in the PDF, click on the manuscript title on your EVISE Homepage, then click 'Download zip file'.

From:
Veronika Marek
Essilor International, R&D
13 rue Moreau 75012 Paris, France
marekv@essilor.fr

To:
Kelvin J. A. Davies
Editor-in-Chief
Journal *Free Radical Biology & Medicine*

Dear Dr. Davies,

I am pleased to submit an original research article entitled ***Neurotoxicity of blue light:* in vitro *evidence on trigeminal neurons and glial cells*** for consideration for publication in the *Free Radical Biology & Medicine* journal. We recently uncovered the impact of blue light on the ocular surface (Marek *et al.*, *Blue light phototoxicity toward human corneal and conjunctival epithelial cells in basal and hyperosmolar conditions*, Free Radical Biology and Medicine 126 (2018) 27–40), and the current manuscript expands our exploration of the influence of daily light on the ocular surface and nociception.

Given the important number of complaints about increased photosensitivity in front of visual displays and in rooms highly illuminated by artificial lighting (rich in blue wavebands), here for the 1st time, we investigated the potential direct impact of blue light on neurons innervating the ocular surface. The role of nociceptive trigeminal neurons is all the more important in phototoxicity since greater photosensitivity is frequently accompanied by ocular pain. We found that cytotoxic effect was spectrally dependent (410, 440 and 480 nm) and provoked important cell death, oxidative stress and inflammation. Furthermore, we substantiated the significance of endoplasmic reticulum and of non-visual photoreceptors (melanopsin and neuropsin) in transmission of blue-toxic message in trigeminal cells.

We believe that this manuscript is appropriate for publication by *Free Radical Biology & Medicine* because it gives an insight into phototoxic signalling underlying death and oxidative stress in nociceptive neurons and glial cells. The importance of this subject is corroborated by recent confusing reports about potential intrinsic photosensitivity of trigeminal neurons. Moreover, our work may further have an important medical implication suggesting new treatments of increased sensitivity to daily light accompanied by ocular pain.

This manuscript has not been published and is not under consideration for publication elsewhere. We have no conflicts of interest to disclose, but we do declare that Veronika Marek and Thierry Villette are the employees of Essilor International. This work has been funded by Essilor within the frame of research collaboration with Sorbonne Université / Institut de la Vision (Paris).

Should you select our manuscript for peer review, we would like to suggest the following potential referees because they would have the requisite background to evaluate our findings:

Kazuo Tsubota; Keio University, Tokyo, Japan; tsubota@sc.itc.keio.ac.jp
Pierrick Poisbeau; Institut des Neurosciences Cellulaires et Intégratives (INCI), Strasbourg, France; poisbeau@inci-cnrs.unistra.fr
Anna Matynia; University of California, Los Angeles, USA; matynia@jsei.ucla.edu
Samer Hattar; National Institute of Mental Health, Bethesda, MD, USA; samer.hattar@nih.gov
David Copenhagen; University of California, San Francisco, USA; cope@phy.ucsf.ed

To the best of our knowledge, none of the above-suggested persons have any conflict of interest, financial or otherwise.

Thank you for your consideration.

Sincerely,
Veronika Marek.
Research engineer (Essilor International R&D, Paris)

Highlights:

- blue light provokes a cytotoxic response in cells from mouse trigeminal ganglia
- neural and glial cells process the blue-toxic message in different ways
- melanopsin and neuropsin may be implied in trigeminal photic signal reception
- neural blue-toxicity gives an insight into circuit of tangled pain and photosensitivity

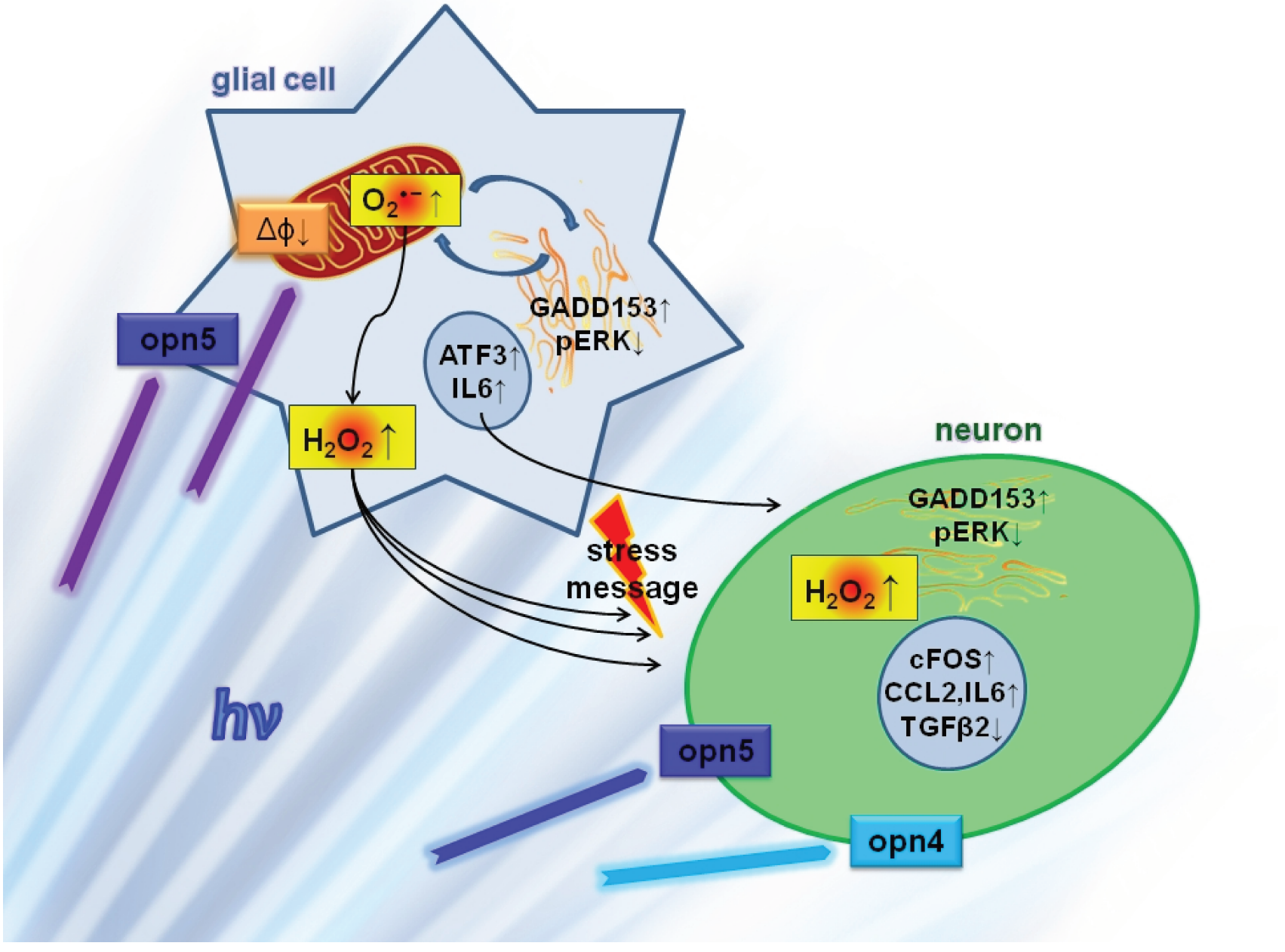
glial cell
$O_2^{\bullet-}\uparrow$
$\Delta\phi\downarrow$
opn5
GADD153↑
pERK↓
ATF3↑
IL6↑
$H_2O_2\uparrow$
neuron
GADD153↑
pERK↓
$H_2O_2\uparrow$
stress
message
cFOS↑
CCL2,IL6↑
TGFβ2↓
hv
opn5
opn4

Neurotoxicity of blue light: *in vitro* evidence on trigeminal neurons and glial cells

Running title: Blue light sensitivity of trigeminal cells

V. Marek[*,1,2], A. Potey[2], A. Réaux-Le-Goazigo[2], E. Reboussin[2], A. Charbonnier[2], T. Villette[1], C. Baudouin[2,3,5], W. Rostène[2], A. Denoyer[2,3,4], S. Mélik Parsadaniantz[2]

[*]*corresponding author:*
Essilor International R&D, 13 rue Moreau, 75012 Paris, France
nika.marek@gmail.com
+33 6 19 56 97 24

[1]*R&D, Essilor International, Paris, France*
[2]*Sorbonne Université, INSERM, CNRS, Institut de la Vision, Paris, France*
[3]*Centre Hospitalier Nationale d'Ophtalmologie des Quinze-Vingts, Paris, France*
[4]*CHU Robert Debré, Université Reims Champagne-Ardenne, Reims, France*
[5]*Versailles-Saint-Quentin-en-Yvelines Université, Versailles, France*

Abstract

Today the noxiousness of blue light from natural and particularly artificial (fluorescent tubes, LED panels, visual displays) sources is actively discussed in the context of various ocular diseases. Many of them have an important neurologic component and are associated with ocular pain. This neuropathic signal is provided by nociceptive neurons from trigeminal ganglia. However, the phototoxicity of blue light on trigeminal neurons has not been explored so far. The aim of the present *in vitro* study was to investigate the cytotoxic impact of various wavebands of visible light (410-630 nm) on primary cell culture of mouse trigeminal neural and glial cells.

Three-hour exposure to narrow wavebands of blue light centered at 410, 440 and 480 nm of average 1.1 mW/cm^2 irradiance provoked cell death, altered cell morphology and induced oxidative stress and inflammation. These effects were not observed for other tested visible wavebands. We observed that neurons and glial cells processed the light signal in different manner, in terms of resulting ROS species generation, inflammatory biomarkers expression and phototoxic mitochondrial damage. We analyzed the pathways of photic signal reception, and we proposed that, in trigeminal cells, in addition to widely known mitochondria-mediated light absorption, light could be received by means of non-visual opsins, melanopsin (opn4) and neuropsin (opn5). We also investigated the mechanisms underlying the observed phototoxicity, further suggesting an important role of the endoplasmic reticulum in neuronal transmission of blue-light-toxic message. Taken together, our results give some insight into circuit of tangled pain and photosensitivity frequently observed in patients consulting for these ocular symptoms.

Key words: blue light, trigeminal neural cells, glial cells, non-visual opsins, neurophototoxicity

Highlights:

- blue light provokes a cytotoxic response in cells from mouse trigeminal ganglia
- neural and glial cells process the blue-toxic message in different ways
- melanopsin and neuropsin may be implied in trigeminal photic signal reception
- neural blue-toxicity gives an insight into circuit of tangled pain and photosensitivity

Abbreviations and conventional signs

AraC – antimitotic treatment (Cytosine-1-β-D-arabinofuranoside)
DED – dry eye disease
ER – endoplasmic reticulum
λ↑ – excitation wavelength
λ↓ – emission wavelength
LED – light emission diode
mixed culture – TG culture without antimitotic treatment
ROS – reactive oxygen species
TG – trigeminal ganglion

Introduction

Ambient light from natural (sun) and artificial (fluorescent tubes, LED panels, visual displays) luminous sources is recognized as an aggravating factor for various ocular diseases (1). Since artificial sources and particularly digital screens highly emit in the blue spectrum, the issue of blue light noxiousness has been much discussed (2,3). In western countries, one of the main reason for visiting an ophthalmologist is exacerbated photosensitivity and ocular symptoms of discomfort in various luminous conditions (4–7) like being in front of monitors (8–11). So far a lot of studies have already investigated the UV and blue-light photodamage related to ocular diseases such as keratitis, cataract, and retinal degeneration (12–16). Similarly, the interest in dry-eye-related phototoxicity on the ocular surface is constantly growing (17–22).

Many eye diseases that are discussed in relation to light damage have a neurologic component, and are mostly associated with ocular pain (6,23,24). In higher vertebrates, this neuropathic signal arises from a particular set of nociceptive neurons located in the trigeminal ganglion (TG) whose axons travel to the eye through the trigeminal ophthalmic nerve and its distal branches (25). Thus, it could be supposed that blue light might have a direct impact on these nociceptive cells that are not originally related to vision though. This issue is even more relevant since a recent study reported the intrinsic photosensitivity of trigeminal ganglia (26). However, to the best of our knowledge, no thorough study about the phototoxicity in trigeminal neural cells has been published so far.

We previously reported the blue light phototoxicity onto the ocular surface in an *in vitro* model of dry eye disease (DED) (17) and *in vivo*, the implication of trigeminal pain-related pathways in ocular inflammation (27). In the present work, we demonstrate *in vitro* the major cell death and oxidative stress related cytotoxic impact of blue light on primary cultured neural cells from mouse trigeminal ganglia. On both neurons and glial cells, we detail the ways of light signal reception and the subsequent pathways of phototoxic message transmission. On the basis of our experimental data, we hypothesize about potential implication of melanopsin and neuropsin in trigeminal phototoxicity.

Results

Blue light decreases neural cell viability and modifies neuronal morphology

The shortest-wavelength 410 nm blue light significantly decreased trigeminal neural cell viability (0.43 ± 0.06, $q < 0.0001$, $p < 0.0001$). Antimitotic treatment (AraC) amplified the observed impact (0.15 ± 0.07, $q < 0.0001$, $p < 0.0001$) revealing it also for 440 nm exposure (0.78 ± 0.12, $q = 0.0110$, $p = 0.0052$ when compared to the non-AraC dark control) (Fig. 1A). Accordingly, for blue wavebands, the rate of fluorescent signals generated by cell death markers significantly increased (YO-PRO for apoptosis: normal conditions – 10.48 ± 0.88, $q < 0.0001$, $p < 0.0001$ for 410 nm, antimitotic treatment – 28.25 ± 4.01, $q < 0.0001$, $p < 0.0001$; 1.83 ± 0.20, $q < 0.0001$, $p < 0.0001$ and 1.53 ± 0.19, $q = 0.0037$, $p = 0.0035$ for 410, 440 and 480 nm, respectively; PI for necrosis: 8.64 ± 2.80, $q = 0.0065$, $p = 0.0015$ and 17.82

± 4.60, $q < 0.0001$, $p < 0.0001$ for 410 nm in normal and antimitotic conditions, respectively) (Fig. 1C,D). In addition, the rate of DAPI, a DNA intercalant that can therefore be considered as another marker of apoptosis, increased for 410 nm illumination as well (1.37 ± 0.17, $q = 0.0036$, $p = 0.0008$ and 1.29 ± 0.13, $q = 0.0079$, $p = 0.0019$ for 410 nm in normal and antimitotic conditions, respectively) (Fig. 1B).These results were confirmed by microscopic observations for YO-PRO and PI (Fig. 1E,F). Interestingly, the ratio between apoptotic and necrotic signals did not show a significant prevalence of any of them (Fig. 1G). Indeed, for 410 nm illumination in merge representation, most of detected dying cells exhibited white fluorescent signal, i.e. the sum of red (PI), green (YO-PRO) and blue (DAPI) stainings, meaning that these cells exhibited both necrotic and apoptotic processes (Fig. 1H).

These data were corroborated by immunocytological studies. First, blue-light-induced cell death was confirmed by GADD153 antibody staining that revealed both growth arrest and DNA damage. Corresponding fluorescent signal was detected after illumination by 410 nm in mixed cell culture and by 410, 440 and 480 nm under antimitotic treatment (Fig. 2A). Further, staining with neuronal PAN antibody revealed the decreased number of neuron cell bodies exposed to 410 nm light as compared to dark control condition (Fig. 2B,C). Moreover, the cell neurites showed more dotted structures, which is also related to neuronal damage (27) (Fig. 2B, S1A). Last, high-content quantitative analysis of acquired images identified that blue light-induced morphological changes were mostly neuronal and not glial ones. Indeed, we found a significant decrease in neuron cell number (0.38 ± 0.08, $q < 0.0001$, $p < 0.0001$ and 0.19 ± 0.03, $q = 0.0023$, $p = 0.0005$ for 410 nm in normal and antimitotic conditions, respectively) (without modifications in cell body area) as well as in total neurite length (0.67 ± 0.19, $q = 0.0352$, $p = 0.0084$ and 0.37 ± 0.08, $q = 0.0042$, $p = 0.0010$ for 410 nm in normal and antimitotic conditions, respectively) while the impact on the number of glial cells turned out to be non-significant when compared to the appropriate dark control (Fig. 2C-F).

Phototoxicity provokes oxidative stress and inflammation

We measured the rates of generated H_2O_2 and $O_2^{\bullet -}$, the two major reactive oxygen species (ROS). In conformity with cell viability and death, oxidative stress level significantly increased after exposure to 410 nm light (66.48 ± 22.64, $q = 0.0008$, $p = 0.0002$ and 7.56 ± 1.70, $q = 0.0027$, $p = 0.0006$ for H_2O_2 and $O_2^{\bullet -}$, respectively); the effect was amplified in the presence of AraC (150.61 ± 48.81, $q < 0.0001$, $p < 0.0001$ and 37.77 ± 10.28, $q < 0.0001$, $p < 0.0001$ for H_2O_2 and $O_2^{\bullet -}$, respectively) (Fig. 3A,B). Moreover, the antimitotic treatment induced an important photosensitivity to 440 and 480 nm light that did not take place in mixed culture. Cells exposed to these wavebands demonstrated a significant increase in hydrogen peroxidase level (by 25.04 ± 11.20, $q = 0.0021$, $p = 0.0020$ and 27.51 ± 8.82, $q = 0.0016$, $p = 0.0008$ for 440 and 480 nm, respectively) (Fig. 3A). Quantitative measurements of mitochondrial $O_2^{\bullet -}$ rate were corroborated by microscopic observations (Fig. 3C, S1B). Interestingly, the correspondent fluorescent signal was provided by glial and not by neuronal cells. This observation was confirmed by high-content quantitative analysis (Fig. 3D): most of the cells exhibiting the red staining from superoxide anion were also labeled by anti-glial cell antibody (anti-GFAP) (Fig. 3E).

In addition, we analyzed the mRNA expression of biomarkers implicated in neuronal activation and cellular inflammation. Exposure to 410 nm provoked a significant increase in

ATF3 rate in mixed culture (1.52 ± 0.14, q = 0.0257, p = 0.0061); cFOS and IL-6 expression increased in both conditions (1.90 ± 0.28, q = 0.0232, p = 0.0055 and 2.34 ± 0.20, q = 0.0023, p = 0.0005 for cFOS and 2.66 ± 0.40, q < 0.0001, p < 0.0001 and 1.99 ± 0.33, q = 0.0010, p = 0.0002 for IL-6, in normal and antimitotic conditions, respectively). Under antimitotic treatment using AraC, CCL2 level significantly increased for 410 (2.10 ± 0.65, q = 0.0284, p = 0.0180) and also for 480 (2.30 ± 0.62, q = 0.0184, p = 0.0058) nm illumination while TGFβ2 rate not-significantly went down as a nondecreasing function of wavelength (Fig. 4).

Pathways of blue light phototoxicity

To better understand the mechanisms underlying the observed phototoxicity, we investigated the implication of kinase cascade that is known to have an important role in integrating and processing of external signals. In both neurons and glial cells exposed to all the blue wavebands, staining with pERK1/2 antibody revealed an important decrease or even an absence of the correspondent fluorescent signal (Fig.5A). This result (independent on AraC) revealed that blue light did induce an important deregulation of internal cell signaling processes.

Since we observed an important light-induced ROS rate, we then examined the status of mitochondria, the main cellular generator of oxidative stress. In neurons, we did not detect any illumination-related differences in mitochondrial staining (data not shown). In glial cells, however, we observed a qualitative increase of fluorescent signal after exposure to 410 nm light (Fig.5B,C).

Photoreception

To investigate whether the culture of cells from trigeminal ganglia possessed any other photoreceptive targets in addition to blue-violet sensitive molecules of the respiratory chain, we looked for the putative role of other pigments by performing immunocytological staining with anti-melanopsin (opn4) and anti-neuropsin (opn5) antibodies. We detected melanopsin immuno-reactivity in some sensory neurons for all the light conditions as well as for the dark control (Fig. 6A, S4). As for neuropsin, we observed the correspondent staining in several glial cells after illumination whatever the wavelength. In neurons, we detected the opn5-staining only after exposure to 410, 480 and 630 nm light (Fig. 6C). These results were similar for both mixed and antimitotically-treated cultures.

Discussion

Here, we demonstrated *in vitro* the cytotoxic impact of blue light on primary cell culture of mouse trigeminal cells, further specifying the implication of each cell population through the use of supplementary antimitotic treatment (AraC).

To investigate the wavelength specificity of trigeminal phototoxicity, we explored the impact of narrow 10 nm wavebands situated within the large blue-green spectrum. We chose the violet (410 nm) and the blue (440 nm) wavelengths known to be harmful for the retina (28,29), the turquoise blue (480 nm) implicated in circadian rhythms (30), the green light (510 nm) reported to be soothing for photophobic migraineurs (31,32) and also the red light (630

nm). The part of the plate was kept in the dark for the control condition; the red-illuminated part served as a second control since, to our knowledge, there are no data about any damage from red-light exposure. We used the irradiance range that would approximate the real-life conditions. Indeed, according to recent measurements performed in the R&D department of Essilor (personal communication), on a sunny slightly cloudy day, we can easily be exposed to 4.89 mW/cm^2 of 380-780 nm light (entire solar visible spectrum) and to 1.28 and 1.4 mW/cm^2 of its blue (380-500 nm) and yellow (500-600 nm) spectral parts respectively (at 10 a.m. in the center Paris at the end of May). We set the illumination time at 3 hours since longer exposures to violet light were too harmful for cells and the shorter ones did not induce any cell death (Fig. S3).

Blue light has a harmful impact on entire TG cell population

All our experiments demonstrated that 410 nm blue light significantly impacted the primary culture of neural cells, decreasing their viability and increasing cell death. The blue-toxic effects were more important when AraC was applied. Since antimitotic treatment significantly decreased the number of glial cells (Fig. 2F), it reduced neuronal protection and support, thus making neurons more vulnerable to induced stress (33). Application of AraC allowed to reveal the harmful impacts of two longer blue wavelengths, 440 and 480 nm. Interestingly, 480 nm light induced an alteration in the rate of apoptosis as assessed by YO-PRO but not in viability. This can be explained by the fact that YO-PRO is an early apoptosis marker implying that cells expressing it might still be alive. Transcription factor GADD153 has been reported as a mediator of apoptosis, of particular potential relevance to neural death (34,35). In our experiments, results of staining with anti-GADD153 antibody followed the wavelength-pattern of YO-PRO induction. Interestingly, the majority of dead cells were stained with both apoptotic and necrotic markers meaning that both mechanisms were involved in the effect of blue light-induced cell death.

Oxidative stress and excessive ROS generation are the key factors in the pathogenesis of various ocular surface diseases (36,37). In the retina and cornea, the phototoxicity of blue light is mostly reported as inducing an oxidative stress (17,18,28,38). As expected, in our experiments, exposure to 410 nm light increased the rates of hydrogen peroxidase and of mitochondrial superoxide anion. The smaller rate of the latter as compared to the former is probably due to the fact that initially generated $O_2^{\bullet -}$ was then transformed into other ROS species (39). In line with the apoptotic rate, antimitotic treatment amplified the photo-oxidative stress significantly increasing the level of H_2O_2 after exposure to 440 and 480 nm light.

We showed that kinase pathways were implicated in neural phototoxicity. It is well recognized that ERK1/2 plays opposing roles, acting to promote cell survival while also participating in cell death and neurodegeneration (40). In our experiments, anti-pERK1/2 staining, already reported to be down-regulated by oxidative stress (41), was noticeably decreased after exposure to blue light, in line with ROS rates measurements. Thus, the phototoxic breakdown of pERK1/2 pro-survival and regulating functions impaired the cellular signaling pathways and defense of neural cells against induced stress. These results are in agreement with those of Kuse *et al*. who also detected a down-regulation of pERK1/2 in photoreceptor-derived cells exposed to blue LEDs (42).

Oxidative stress is also known to provoke inflammatory response; therefore, the next step was to investigate the mRNA expression of inflammation-related biomarkers. We had previously studied the induced expression of chemokines in the inflamed ocular surface (43) and in trigeminal neurons (27). Here, we demonstrated that blue-light induced an up-regulation of IL-6 and CCL2, both widely considered as pro-inflammatory cytokines when present at high concentrations (44). Furthermore, CCL2 is highly implicated in trigeminal nociception (45,46). TGFβ2, one of the major ligands involved in the modulation of cell behavior in ocular tissues (47) and in neural inflammatory responses (48), showed a trend for down-regulation at 410 and 440 nm exposures. We may ascribe this fact to a probable negative loop regulation that turned on when highly stressed cells produced TGFβ2 in excess amount as we have previously proposed for the phototoxically-stressed cells of ocular surface (17). Moreover, TGFβ2 was reported to have an anti-inflammatory role (49), meaning that TGFβ2 underproduction may be partially responsible for an enhanced phototoxicity. We also investigated the mRNA expression of cFOS and ATF3, markers of neural activation and stress. Normally low, they are rapidly up-regulated in response to neural stimulation (50,51). Indeed, we detected a significant increase in level of both markers in response to 410 nm light exposure.

Besides the mitochondrial respiratory chain, opsins are also involved in TG cells photosensitivity

The next question was how the luminous signal was received by neural cell cultures. It is known that photoreception may be linked to molecules of the mitochondrial respiratory chain, such as flavins and cytochrome oxidases, that can directly absorb blue–violet light (52,53). However, it is not the unique possibility of light reception.

Even if visual photoreceptor cells like rods and cones are absent in trigeminal neural culture, we cannot exclude the possible role of non-visual receptors. It has been recently reported that small number of neurons in the ophthalmic branch of trigeminal ganglia express melanopsin (opn4) and are intrinsically photosensitive (26). Moreover, another recent study discovered the previously unrecognized localization of this photopigment in nerve fibers within the cornea (54). Another non-visual photoreceptor, gaining today an increasing attention, is neuropsin (opn5). Its presence and importance for photoentrainment have been observed in the retina and cornea; however, its precise functions are still unclear (55,56). Thus, we checked for the presence of these non-visual opsins in neural trigeminal culture.

By means of immunochemistry, we observed the presence of melanopsin in neuronal cell bodies, in line with Delwig *et al*. (54). Only some neurons exhibited melanopsin immunoreactivity, in agreement with Matynia *et al*., according to whom melanopsin is expressed overall in approximately 3% of TG neurons (26). It is also in compliance with the fact that neurons innervating the ocular surface represent only 1-5% of the total number of trigeminal neural cells (24,57). As for neuropsin, we observed its expression only after illumination. It was present in some glial cells, independently on wavelength, and also in neurons, after exposure to 410, 480 and 630 nm light. According to Buhr *et al*. (55), neuropsin is sensitive to 370, 417 and 475 nm light. While the last two wavelengths are close to our 410 and 480 nm, they though did not detect any photoentrainment for 630 nm

exposure. However, one should take into account that their study was done on the retina and not on the TG.

Taken together, these results imply that in addition to mitochondria-mediated photoreception system, neural cells may possess another and specific one based on non-visual opsins.

Blue light impacts neurons and glial cells in different ways

ATF3 increased only in mixed cultures, whereas TGBβ2 (a trend) and CCL2 (significant) levels were altered only under antimitotic treatment, therefore attributing deregulation of the latter two to neurons only.

Immunostaining with anti-neuronal and anti-glial antibodies, corroborated by correspondent quantitative analysis, showed that blue light decreased the number of neuron cell bodies and modified the structure of their neurites while the morphology of glial cells did not significantly change. However, surprisingly, microscopic observations of mitochondrial oxidative stress and correspondent quantitative analysis revealed that $O_2^{\bullet -}$ was mainly generated by glial cells and not by neurons. To check the mitochondrial status of all the neural cells, we tracked them with a specific fluorescent dye that enters the mitochondria dependently on the proton flux between the outside and inside of the cell. Increased depolarization results in additional dye influx and an increase in fluorescence, while hyperpolarization provides with a decrease in fluorescence (58). Here again, exposure to 410 nm light provoked an accumulation of fluorescent signal in mitochondria of glial cells but not of neurons. Thus, neuronal mitochondria did not seem to be affected while there was a blue light induced loss in mitochondrial membrane potential in glial cells. We might ascribe the observed difference in blue light absorption at mitochondrial level to a difference in cytochrome oxidase activity. Indeed, it has been reported that this enzyme demonstrated different properties in neural and non-neural cells; however, the results were somehow contradictory (59,60).

Last, since we observed an increase in H_2O_2 rate after exposure to 440 and 480 nm only in antimitotically-treated cultures, we could hypothesize that neurons were able to be light-sensitive through non-visual opsins' pathway. Indeed, Matsuyama *et al*. reported the maxima of melanopsin absorption at 446, 467 and 476 nm exposure (61) thus making it a potential candidate for 440- and 480-nm-phototoxicity transmitter. According to generally accepted statement, the ROS species are generated by mitochondria (62) that turned to be non-impacted in neurons though. However, there might be another possibility to produce H_2O_2. Recently, Konno *et al*. reported that H_2O_2 can be generated within the endoplasmic reticulum (ER) but the corresponding mechanisms are still not clear (63). This possibility is corroborated by our experiments concerning pERK1/2 and GADD153 stainings. Indeed, when protein folding in the ER is impaired due to various physiological and pathological conditions, the organelle has several specific pathways to overcome the stress. The apoptotic one occurs when functions of the ER are severely damaged and may use the pERK1/2 signaling followed by transcriptional activation of GADD153 gene (64).

A new proposal of a model for the phototoxic pathway in TG culture

To sum up, we demonstrated for the first time the blue light phototoxicity in primary culture of trigeminal cells, both in neurons and neuroglial cells. We proposed that non-visual opsins and endoplasmic reticulum have important roles in the cytotoxic process. Taken together, our results might be integrated in the following scheme of blue-light-toxicity trigeminal pathway. Luminous flux is mainly absorbed by glial cells by means of respiratory chain and neuropsin (opn5). Thus induced phototoxicity provokes glial cells death (apoptosis and necrosis) and stress (ATF3) as well as ROS over-production ($O_2^{\bullet -}$, H_2O_2) and inflammation (IL6). This stress messages then reaches neurons and damages them via the ER pathways with additional oxidative stress and nociceptive message generation (CCL2).

Our findings shed some light on mechanisms underlying the common symptoms of increased sensitivity to daily light frequently accompanied by ocular pain. Thus, this study may open new avenues for the treatment of this disorder, e.g. by using optical devices that would filter out the most toxic blue wavebands for ocular nociception in the given illumination conditions, or by controlling the emission spectra of smartphones and visual displays.

Materials & Methods

Cell culture

Adult male C57BL/6 mice (30 g; Janvier Labs, Le Genest Saint Isle, France) were maintained under controlled conditions (22 ± 1 °C, 60 ± 10% relative humidity, 12/12 h light/dark cycle, food and water ad libitum). All experiments were approved by the Charles Darwin Ethics Committee for Animal Experimentation (Ce5/2011/05) and carried out in accordance with Directive 2010/63/EU of the European Parliament and the Council of 22 September, 2010 and French law (2013/118). Trigeminal ganglia (TGs) were removed from 10 mice and placed in Neurobasal-A without phenol red (i.e., without photosensitizer) buffer. TGs were pooled in 1 ml of fresh Neurobasal-A without phenol red buffer containing 10 mg/ml of collagenase A and incubated at 37 °C for 1 hour. Then TGs were placed in 1 ml of Trypsine 0.05% mixed with 50 µl of DNAse 50µg/ml and incubated at 37 °C for 10 minutes. TGs were transferred in 'STOP' solution (800 µl of FBS and 1.2 ml of PBS) and mechanically dissociated using a pipette. Dissociated TGs were pelleted by centrifugation (800 rpm, 10 minutes), the collagenase-containing supernatant was discarded, and cells were resuspended in Neurobasal-A without phenol red supplemented with 2% B-27 minus AO (i.e., without antioxidants), 200 mM L-glutamine, 45% glucose, 1% penicillin and 1% streptomycin. Another mechanical dissociation was performed. Cells were then filtered on a Falcon 70 µm cell strainer and centrifuged (800 rpm, 10 minutes). Supernatant was discarded, cells were resuspended in supplemented Neurobasal-A without phenol red and distributed into 24-well culture plates (CellVis, Mountain View, CA, USA), coated beforehand with poly-D-lysine/laminin (400 µl/well).

Cells were incubated in a 37 °C incubator (5% CO2, 95% humidity) (day 0 – D0). The medium was changed at D3. In order to understand, whether the phototoxicity would depend on cell population, the medium was completed or not with AraC (Cytosine-1-β-D-

arabinofuranoside) at 5 µM to prevent glial cell proliferation (27,33,65), to give *mixed* or *AraC-treated* culture, respectively. The medium was changed again at D7. Cells were illuminated at D10; the medium was replaced by fresh non-supplemented Neurobasal A without phenol red just before illumination.
Neurobasal-A without phenol red, FBS, B-27 minus AO, L-glutamine, penicillin and streptomycin were purchased from Gibco (Life technologies, Carlsbad, CA, USA); trypsin, collagenase A, DNAse, poly-D-lysine, laminin and AraC were purchased form Sigma Aldrich (St. Louis, MO, USA).

Light emitting devices and protocol
Cells were exposed to 5 various 10-nm-wide light wavebands provided by a custom-made LED-based fibered device as described previously (28,29). The central wavelengths of these wavebands were 410, 440, 480, 510 and 630 nm; the irradiance was 1.1 mW/cm^2 except for the 630 nm waveband for which it was 1.53 mW/cm^2 (due to the illumination system limit) (Fig. S3). Irradiance level, spectral, and uniformity measurements were assessed using the calibrated spectroradiometer JAZ (Ocean Optics, Dunedin, USA). Cells in black 24 well-plate were illuminated for 3 hours; for each experiment, one subdivision of a well plate was maintained in dark (control cells). All the experiments to assess the light impact on cells were performed immediately after the end of light exposure.

Quantification of cell viability and H_2O_2 rate
The CellTiter-Glo® Assay and the ROS-Glo™ H_2O_2 Assay (Promega, Madison, WI, USA) were performed according to the manufacturer's protocol. Briefly, H_2O_2 Substrate Solution was added to cells before the light exposure. At the end of exposure, half of the supernatant of the illuminated well plate (plate N1) was carefully transferred to another well plate (plate N2), without touching the adherent cells. Then, the CellTiterGlo Detection Solution was added to the plate N1 and the ROS-Glo Detection Solution was added to the plate N2. Both plates were incubated at room temperature (RT) in the dark for 20 min before luminescence reading on an Infinite M1000 microplate reader (Tecan, Männedorf, Switzerland). Luminescence values were normalized with respect to control cells (in the dark) in normal conditions considered as 100% viable. For ROS quantification (plate N2), the values were also normalized with respect to viability.

Cell death assay - YO-PRO/PI staining
The apoptotic cells are permeable to YO-PRO®-1 (Invitrogen, Eugene, Oregon, USA) while remaining non-permeable to Propidium Iodide (Interchim, Montluçon, France) which only stains necrotic cells (66,67). The two reagents were mixed together in PBS (Gibco, Life technologies, Carlsbad, CA, USA) at the following concentrations: YO-PRO – 1/150, PI – 1/15000. Such a mix was possible since the two dyes have different excitation/emission spectra. At the end of light exposure, the well plate was centrifuged at 1500 rpm during 5 minutes. Media were carefully replaced with 350 µl of prepared solution; the well plate was then incubated for 30 minutes at RT in the dark. Further, 350 µl of PBS were added to wells; the well plate was centrifuged again (1500 rpm, 5 minutes) and supernatants were replaced with 350 µl of fresh PBS. The fluorescent signals were read on an Infinite M1000 microplate

reader (Tecan, Männedorf, Switzerland) in the following order, to avoid cross-excitations if there were any (hardly probable): YO-PRO - λ↑ = 491 nm, λ↓ = 509 nm; PI - λ↑ = 535 nm, λ↓ = 617 nm. Measured values were normalized with respect to control cells (in the dark) in normal conditions considered as 1 and also to viability. Cells were then fixed with 4% paraformaldehyde-PBS (Sigma-Aldrich) and counterstained with DAPI, for further microscopic imaging.

Quantification of $O_2^{\bullet -}$ rate

Superoxide anion levels were quantified using the MitoSOX™ Red Mitochondrial Superoxide Indicator dye (Life Technologies). MitoSOX reagent working solution (5 µM) was prepared by diluting MitoSOX reagent stock solution (5 mM in DMSO (Sigma Aldrich)) in Neurobasal A without phenol red buffer. At the end of light exposure, medium was replaced with 350 µl of MitoSOX reagent working solution; the well-plate was then incubated for 10 minutes at 37 ºC in the dark. Cells were further carefully washed 3 times with warm PBS; 350 µl of fresh PBS was added to wells. The fluorescent signal was read on an Infinite M1000 microplate reader (Tecan, Männedorf, Switzerland): λ↑ = 510 nm, λ↓ = 580 nm. Measured values were normalized according to control cells (in the dark) in normal conditions considered as 1 and also according to viability. Cells were then fixed with 4% paraformaldehyde-PBS (Sigma-Aldrich) for further immunostaining and microscopic imaging.

Immunostaining

Fixed cells were incubated with blocking buffer (3% NDS, 0.3% Triton) for 1 hour and then stained with the following primary antibodies: mouse anti-PAN (EMD Millipore Corp., MAB2300, 1/1000), chicken anti-GFAP (Thermofisher, PA1-10004, 1/2000), mouse anti-GADD153 (Santa Cruz Biotechnology, sc-7351, 1/400), goat anti-p-ERK½ (the phosphorylated-ERK, the active form of the kinase) (Santa Cruz Biotechnology, sc-16982, 1/400), rabbit anti-opn4 (ATS, AB-N39, 1/500), rabbit anti-opn5 (Biorbyt, orb223499, 1/500). For anti-opn4 and -opn5 stainings, cells were incubated with antibodies diluted in PBS for 2 nights at 4 °C. Otherwise, antibodies were diluted in blocking buffer; incubation was done at RT for 1 hour. For revelation, cells were incubated with Alexa Fluor secondary antibodies (1:500 in PBS, Invitrogen) for 1 hour at RT.

For all the immunostainings, negative control experiments (without incubation with a primary antibody) were performed, in order to ensure the absence of non-specific fluorescent signal.

Mitochondrial status assessment

Mitochondria status was assessed with MitoTracker™ Deep Red FM dye (Life Technologies, Carlsbad, CA, USA). MitoTracker reagent working solution (25 µM) was prepared by diluting MitoSOX reagent stock solution (1 mM in DMSO (Sigma Aldrich, St. Louis, MO, USA)) in Neurobasal w/o phenol red buffer. At the end of light exposure, medium was replaced with 350 µl of MitoTracker reagent working solution; the well-plate was then incubated for 30 minutes at RT in the dark. Cells were then fixed with 4% paraformaldehyde-PBS (Sigma-Aldrich) and counterstained with DAPI, for further microscopic imaging.

Imaging

Cells were imaged with the inverted Nikon TiE microscope (image recording via Metamorph 7.7); images were then processed with the Fiji software (ImageJ version).

For high-content quantitative analysis based on immunostainings with anti-PAN and anti-GFAP antibodies as well as with MitoSOX™ Red Mitochondrial Superoxide Indicator dye, cells were imaged with an automated microscope Thermo-Cellomics Arrayscan (Thermofisher, Waltham, MA, USA). Images were then analyzed by system-provided algorithms (Neuronal Profiling and Target Activation bioapplications of Visual Studio software) to evaluate cell number, cell area, neurite length and DAPI-staining intensity. For each well (of 1.9 cm^2 total surface), a central part of 0.81 cm^2 surface was analyzed (this corresponded to 81 scanned fields of 1002 μm side each).

Imaging of anti-melanopsin and anti-neurosin immunostainings were performed on an Olympus FV1200 laser-scanning confocal microscope (Olympus, Rungis, France). DAPI, AlexaFluor-594, AlexaFluor-647 and AlexaFluor-488 were excited by using 405, 559 and 635 nm laser diodes lines and 488-515 nm argon ion laser lines, respectively. The objective used was an UPLSAPO 20X NA 0.85-WD 0.20.

Identical exposure settings, that minimized oversaturated pixels in the final images, were used for each illumination condition.

RT-qPCR

After the end of illumination, cells were washed and lysed; total RNA was extracted using a NucleoSpin RNA XS extraction kit (Macherey-Nagel, Düren, Germany) according to the provided protocol. RNA quality and quantity were assessed using a ND-1000 spectrophotometer (Thermo Scientific, Waltham, Massachusetts, USA). cDNA was further synthesized from equal amounts of RNA using Multiscribe reverse transcriptase (TaqMan Reverse Transcription Reagents, Applied Biosystems, Life Technologies, Carlsbad, CA, USA) according to the manufacturer's protocol. Finally, cDNA were diluted in DNAse/RNAse free water (Gibco) to a final concentration of 2 ng/μL. Real-time quantitative PCR was performed with 10 ng of cDNA added to a 15 μL solution of Applied Biosystems Mastermix (TaqMan Universal PCR Master Mix) and primers to a final volume of 20 μL. All primers and reagents were purchased from Applied Biosystems: GAPDH (Mm99999915_m1), ATF3 (Mm00476033_m1), cFOS (Mm00487425_m1), IL6 (Mm00446190_m1), CCL2 (Mm00441242_m1), TGFβ2 (Mm00436955_m1). Target cDNA was amplified using the 7300 Real-Time PCR system (Applied Biosystems). Changes in mRNA expression were calculated as $\Delta\Delta Ct = \Delta Ct_{illuminated} - \Delta Ct_{control}$ with $\Delta Ct = Ct_{target\_gene} - Ct_{HK\_gene}$. Ct means *cycle threshold* and HK_gene means *housekeeping gene* (GAPDH). Since the application of antimitotic treatment changed the cell population and therefore the expression of house-keeping genes, we did not compare the mRNA levels between mixed culture and the one with AraC. The calculation was done for each group (mixed culture or AraC-treated culture) separately; non-illuminated cells within every group were taken as controls.

Statistical analysis

All experiments were repeated at least three times in technical replicate (the exact number of performed experiments is specified in the legends of the corresponding figures). Statistical analyzes were performed using GraphPad (GraphPad Software, La Jolla, CA, USA). Two-way ANOVA analysis with non-repeated measures followed by False Discovery Rate multiple correction (two-stage step-up method of Benjamini, Krieger and Yekutieli, false discovery rate q = 0.05) were used. All data are presented as mean ± SEM. Values given in the *Results* section were rounded to the second decimal digit to facilitate the reading. When not specified, the corresponding p and q values were given for the comparison with the respective dark control (within the same AraC or non-AraC group). Differences were considered significant when $p < 0.05$ (*/^), $p < 0.01$ (**/^^), $p < 0.001$ (***/^^^) or $p < 0.0001$ (****/^^^^).

Acknowledgements
We are grateful to Fanny Montoya for implementation of some preliminary experiments. We thank Coralie Barrau and Camille Ehrismann for technical support of the illumination systems and Stéphane Fouquet for the support of imaging facility. We also thank the cell culture, imaging and HTS platforms at the Institut de la Vision (Paris).

Sources of funding
This work was funded by Essilor International, within the frame of research collaboration with Sorbonne Université / Institut de la Vision (Paris).

Conflict of interest
VM and TV are Essilor employees. AP, AR, ER, AC, CB, WR, AD, and SM declare no competing interests.

Bibliography

1. Marshall J. Understanding risks of phototoxicity on the eye [Internet]. Point de Vue, International Review of Ophthalmic Optics. 2014 [cited 2017 Nov 7]. Available from: http://www.pointsdevue.com/article/understanding-risks-phototoxicity-eye
2. Text Request. How Much Time Do People Spend on Their Mobile Phones in 2017? [Internet]. Hackernoon. [cited 2017 Nov 7]. Available from: https://hackernoon.com/how-much-time-do-people-spend-on-their-mobile-phones-in-2017-e5f90a0b10a6
3. Lupis J. The State of Traditional TV: Updated With Q1 2017 Data [Internet]. Mareketing charts. [cited 2017 Nov 7]. Available from: http://www.marketingcharts.com/featured-24817
4. K. Digre, K.C. Brennan. Shedding Light on Photophobia. J Neuroophthalmol. 2012;32(1):68–81.
5. Katz BJ, Digre KB. Diagnosis, pathophysiology, and treatment of photophobia. Surv Ophthalmol [Internet]. Elsevier Inc; 2016;61(4):466–77. Available from: http://dx.doi.org/10.1016/j.survophthal.2016.02.001
6. Wu Y, Hallett M. Photophobia in neurologic disorders. Transl Neurodegener [Internet]. Translational Neurodegeneration; 2017;6(1):26. Available from:

http://translationalneurodegeneration.biomedcentral.com/articles/10.1186/s40035-017-0095-3
7. Stapleton F, Alves M, Bunya VY, Jalbert I, Lekhanont K, Malet F, et al. The Ocular Surface TFOS DEWS II Epidemiology Report. Ocul Surf [Internet]. Elsevier Ltd; 2017;15(3):334–65. Available from: http://dx.doi.org/10.1016/j.jtos.2017.05.003
8. Yazici A, Sari ES, Sahin G, Kilic A, Cakmak H, Ayar O, et al. Change in tear film characteristics in visual display terminal users. EJO. 2015;25(2):85–9.
9. Kaido M, Toda I, Oobayashi T, Kawashima M. Reducing Short-Wavelength Blue Light in Dry Eye Patients with Unstable Tear Film Improves Performance on Tests of Visual Acuity. PLoS One [Internet]. 2016;11(4):1–10. Available from: http://dx.doi.org/10.1371/journal.pone.0152936
10. Courtin R, Pereira B, Naughton G, Chamoux A, Chiambaretta F, Lanhers C, et al. Prevalence of dry eye disease in visual display terminal workers : a systematic review and meta-analysis. BMJ. 2016;
11. Uchino M, Yokoi N, Uchino Y, Dogru M, Kawashima M, Komuro A, et al. Prevalence of dry eye disease and its risk factors in visual display terminal users: The Osaka study. Am J Ophthalmol [Internet]. Elsevier Inc.; 2013;156(4):759–766.e1. Available from: http://dx.doi.org/10.1016/j.ajo.2013.05.040
12. A.P. Cullen. Photokeratitis and Other Phototoxic Effects on the Cornea and Conjunctiva. Int J Toxicol. 2002;(Spring / Primavera):455–64.
13. Voke J. Radiation effects on the eye. Part 3a - Ocular effects of ultraviolet radiation. Optom Today [Internet]. 1999;27–32. Available from: http://www.optometry.co.uk/pages/articles/articles1999.php %5Cn C:%5CLibrary%5CVoke1999.pdf
14. Turner PL, Someren EJW Van, Mainster MA. The role of environmental light in sleep and health : Effects of ocular aging and cataract surgery. Sleep Med Rev [Internet]. Elsevier Ltd; 2010;14(4):269–80. Available from: http://dx.doi.org/10.1016/j.smrv.2009.11.002
15. Voke J. Radiation effects on the eye. Part 3b - Ocular effects of ultraviolet radiation. Optom Today. 1999;37–41.
16. Krigel A, Berdugo M, Picard E, Levy-Boukris R, Jaadane I, Jonet L, et al. Light-induced retinal damage using different light sources, protocols and rat strains reveals LED phototoxicity. Neuroscience [Internet]. IBRO; 2016;339:296–307. Available from: http://dx.doi.org/10.1016/j.neuroscience.2016.10.015
17. Marek V, Mélik-parsadaniantz S, Villette T, Montoya F, Baudouin C, Brignole-Baudouin F, et al. Blue light phototoxicity toward human corneal and conjunctival epithelial cells in basal and hyperosmolar conditions. Free Radic Biol Med [Internet]. Elsevier B.V.; 2018; Available from: https://doi.org/10.1016/j.freeradbiomed.2018.07.012
18. Lee J, Kim S, Lee S, Kim H, Ahn H, Li Z. Blue Light – Induced Oxidative Stress in Human Corneal Epithelial Cells : Protective Effects of Ethanol Extracts of Various Medicinal Plant Mixtures. Cornea. 2014;55(7):4119–4127.
19. Ayaki M, Niwano Y, Kanno T, Tsubota K. Blue light induces oxidative damage in human ocular surface cells in culture. ARVO 2015 Annu Meet Abstr. 2015;
20. Niwano Y, Kanno T, Iwasawa A, Ayaki M, Tsubota K. Blue light injures corneal epithelial cells in the mitotic phase in vitro. Br J Ophthalmol [Internet]. 2014;98(7):990–2. Available from: http://www.ncbi.nlm.nih.gov/pubmed/24682182
21. Hwang H Bin, Kim HS. Phototoxic effects of an operating microscope on the ocular surface and tear film. Cornea [Internet]. 2014;33(1):82–90. Available from: http://www.ncbi.nlm.nih.gov/pubmed/24310622

22. Ipek T, Hanga MP, Hartwig A, Wolffsohn J, O'Donnell C. Dry eye following cataract surgery: The effect of light exposure using an in-vitro model. Contact Lens Anterior Eye [Internet]. 2017;(July):3–6. Available from: http://linkinghub.elsevier.com/retrieve/pii/S1367048417302370
23. Albilali A, Dilli E. Photophobia : When Light Hurts, a Review. Curr Neurol Neurosci Rep. Current Neurology and Neuroscience Reports; 2018;18(62):4–9.
24. Réaux-le-Goazigo A, Labbé A, Baudouin C, Melik-Parsadaniantz, Stéphane. La douleur oculaire chronique : mieux la comprendre pour mieux la traiter. Medecine/Science. 2017;33:749–57.
25. Belmonte C, Aracil A, Acosta C, Luna C, Gallar J. Nerves and Sensations from the Eye Surface. Ocul Surf. 2004;2(4):248–53.
26. Matynia A, Nguyen E, Sun X, Blixt FW, Parikh S, Kessler J, et al. Peripheral Sensory Neurons Expressing Melanopsin Respond to. Front Neurql Circuits. 2016;10(August):1–15.
27. Launay P, Reboussin E, Liang H, Kessal K, Godefroy D, Rostène W, et al. Neurobiology of Disease Ocular in fl ammation induces trigeminal pain , peripheral and central neuroin fl ammatory mechanisms. Neurobiol Dis. 2016;88:16–28.
28. Marie M, Bigot K, Angebault C, Barrau C, Gondouin P, Pagan D, et al. Light action spectrum on oxidative stress and mitochondrial damage in A2E-loaded retinal pigment epithelium cells. Cell Death Dis [Internet]. Springer US; 2018;9(3). Available from: http://dx.doi.org/10.1038/s41419-018-0331-5
29. Arnault E, Barrau C, Gondouin P, Bigot K, Villette T, Picaud S, et al. Phototoxic Action Spectrum on a Retinal Pigment Epithelium Model of Age-Related Macular Degeneration Exposed to Sunlight Normalized Conditions. PLoS One. 2013;8(8).
30. Legates TA, Fernandez DC, Hattar S. Light as a central modulator of circadian rhythms, sleep and affect. Nat Rev Neurosci. 2014;15(7):443–54.
31. Nir R-R, Noseda R, Bernstein C, Buettner C, Fulton AB, Bertisch SM, et al. Color-Selective Photophobia in Ictal vs . Interictal Migraineurs and in Healthy Controls. Pain. 2018;(May).
32. Noseda R, Bernstein CA, Nir RR, Lee AJ, Fulton AB, Bertisch SM, et al. Migraine photophobia originating in cone-driven retinal pathways. Brain. 2016;139(7):1971–86.
33. Godefroy D, Gosselin RD, Yasutake A, Fujimura M, Combadie're C, Maury-Brachet R, et al. The chemokine CCL2 protects against methylmercury neurotoxicity. Toxicol Sci. 2012;125(1):209–18.
34. Kim S, Cheon H-S, Kim S-Y, Juhnn Y-S, Kim Y-Y. Cadmium induces neuronal cell death through reactive oxygen species activated by GADD153. BMC Cell Biol [Internet]. 2013;14(1):4. Available from: http://bmccellbiol.biomedcentral.com/articles/10.1186/1471-2121-14-4
35. Silva RM, Ries V, Oo TF, Yarygina O, Jackson-Lewis V, Ryu EJ, et al. CHOP/GADD153 is a mediator of apoptotic death in substantia nigra dopamine neurons in an in vivo neurotoxin model of parkinsonism. J Neurochem. 2005;95(4):974–86.
36. Ward SK, Wakamatsu TH, Dogru M, Ibrahim OM a, Kaido M, Ogawa Y, et al. The role of oxidative stress and inflammation in Dry Eye Disease. Cornea. 2009;28(9):70–4.
37. Wakamatsu TH, Dogru M, Tsubota K. Tearful relations : oxidative stress , inflammation and eye diseases. Arq Bras Oftalmol. 2008;2(7):72–9.
38. Jaadane I, Boulenguez P, Chahory S, Carré S, Savoldelli M, Jonet L, et al. Retinal damage induced by commercial Light Emitting Diodes (LED). Free Radic Biol Med. 2015;

39. Bienert GP, Schjoerring JK, Jahn TP. Membrane transport of hydrogen peroxide. Biochim Biophys Acta - Biomembr [Internet]. 2006;1758(8):994–1003. Available from: http://linkinghub.elsevier.com/retrieve/pii/S0005273606000472
40. Luo Y, DeFranco DB. Opposing roles for ERK1/2 in neuronal oxidative toxicity: Distinct mechanisms of ERK1/2 action at early versus late phases of oxidative stress. J Biol Chem. 2006;281(24):16436–42.
41. Li GY, Li T, Fan B, Zheng YC, Ma TH. The D1 dopamine receptor agonist, SKF83959, attenuates hydrogen peroxide-induced injury in RGC-5 cells involving the extracellular signal-regulated kinase/p38 pathways. Mol Vis [Internet]. 2012;18(December):2882–95. Available from: http://www.ncbi.nlm.nih.gov/pubmed/23233790%5Cnhttp://www.ncbi.nlm.nih.gov/pmc/articles/PMC3519376/pdf/mv-v18-2882.pdf
42. Kuse Y, Ogawa K, Tsuruma K, Shimazawa M, Hara H. Damage of photoreceptor-derived cells in culture induced by light emitting diode-derived blue light. Sci Rep. 2014;4(5223):1–12.
43. Denoyer A, Godefroy D, Celerier I, Frugier J, Riancho L, Baudouin F, et al. CX3CL1 expression in the conjunctiva is involved in immune cell trafficking during toxic ocular surface inflammation. Mucosa Immunol. 2012;5(6):703–11.
44. Deschamps N, Baudouin C. Dry Eye and Biomarkers : Present and Future. Curr Ophthalmol Rep. 2013;65–74.
45. Dauvergne C, Molet J, Goazigo AR, Mauborgne A, Boucher Y. Implication of the chemokine CCL2 in trigeminal nociception and traumatic neuropathic orofacial pain. Eur J Pain. 2014;18:360–75.
46. Van Steenwinckel J, Auvynet C, Sapienza A, Reaux-Le Goazigo A, Combadière C, Melik Parsadaniantz S. Stromal cell-derived CCL2 drives neuropathic pain states through myeloid cell infiltration in injured nerve. Brain Behav Immun [Internet]. Elsevier Inc.; 2015;45:198–210. Available from: http://dx.doi.org/10.1016/j.bbi.2014.10.016
47. Saika S. TGFβ pathobiology in the eye. Lab Investig. 2006;86(2):106–15.
48. Meyers EA, Kessler JA. TGF-b Family Signaling in Neural and Neuronal Differentiation, Development, and Function. Cold Spring Harb Perspect Biol. 2017;9(8):1–26.
49. Sanjabi S, Zenewicz LA, Kamanaka M, Flavell RA. Anti- and Pro-inflammatory Roles of TGF-β, IL-10, and IL-22 In Immunity and Autoimmunity. Curr Opin Pharmacol. 2009;9(4):447–53.
50. Bullitt E. Expression ofC-fos-like protein as a marker for neuronal activity following noxious stimulation in the rat. J Comp Neurol [Internet]. 1990;296(4):517–30. Available from: http://www.ncbi.nlm.nih.gov/pubmed/2113539%5Cnhttp://doi.wiley.com/10.1002/cne.902960402
51. Hunt D, Raivich G, Anderson PN. Activating Transcription Factor 3 and the Nervous System. Front Mol Neurosci [Internet]. 2012;5(February):1–17. Available from: http://journal.frontiersin.org/article/10.3389/fnmol.2012.00007/abstract
52. Godley BF, Shamsi FA, Liang F-Q, Jarrett SG, Davies S, Boulton M. Blue Light Induces Mitochondrial DNA Damage and Free Radical Production in Epithelial Cells. J Biol Chem [Internet]. 2005;280(22):21061–6. Available from: http://www.jbc.org/lookup/doi/10.1074/jbc.M502194200
53. Lascaratos G, Ji D, Wood JPM, Osborne NN. Visible light affects mitochondrial function and induces neuronal death in retinal cell cultures. Vision Res. 2007;47(9):1191–201.

54. Delwig A, Chaney SY, Bertke AS, Verweij J, Quirce S, Larsen DD, et al. Melanopsin expression in the cornea. Vis Neurosci. 2018;35.
55. Buhr ED, Yue WWS, Ren X, Jiang Z, Liao HR, Mei X, et al. Circadian oscillators in mammalian retina and cornea. PNAS. 2015;(7):1–6.
56. Guido ME, Nieto PS, Valdez DJ, Acosta-rodrı VA. Expression of Novel Opsins and Intrinsic Light Responses in the Mammalian Retinal Ganglion Cell Line RGC-5 . Presence of OPN5 in the Rat Retina. PLoS One. 2011;6(10).
57. Launay PS, Godefroy D, Khabou H, Rostene W, Sahel JA, Baudouin C, et al. Combined 3DISCO clearing method, retrograde tracer and ultramicroscopy to map corneal neurons in a whole adult mouse trigeminal ganglion. Exp Eye Res. 2015;139:136–43.
58. ThermoFisher Scientific. Membrane Potential Indicators [Internet]. [cited 2018 Jul 19]. Available from: https://www.thermofisher.com/fr/en/home/life-science/cell-analysis/cell-viability-and-regulation/ion-indicators/membrane-potential-indicators.html
59. Hamberger A, Blomstrand C, Lehninger AL. Comparative studies on mitochondria isolated from neuron-enriched and glia-enriched fractions of rabbit and beef brains. J Cell Biol. 1970;45:221–34.
60. Tolani AJ, Talwar GP. Differential Metabolism of Various Brain Regions. Biochem J. 1962;88(1960):357–62.
61. Matsuyama T, Yamashita T, Imamoto Y, Shichida Y. Photochemical properties of mammalian melanopsin. Biochemistry. 2012;51(27):5454–62.
62. Newsholme P, Rebelato E, Abdulkader F, Krause M, Carpinelli A, Curi R. Reactive oxygen and nitrogen species generation , antioxidant defenses , and b-cell function : a critical role for amino acids. J Endocrinol. 2012;214:11–20.
63. Konno T, Melo EP, Lopes C, Mehmeti I, Lenzen S, Ron D, et al. ERO1-independent production of H2O within the endoplasmic reticulum fuels Prdx4-mediated oxidative protein folding. J Cell Biol. 2015;211(2):253–9.
64. Liu Z, Lv Y, Zhao N, Guan G, Wang J. Protein kinase R-like ER kinase and its role in endoplasmic reticulum stress-decided cell fate. Cell Death Dis. 2015;6(7):1–10.
65. Djogo T, Robins SC, Schneider S, Kryzskaya D, Liu X, Mingay A, et al. Adult NG2-Glia Are Required for Median Eminence-Mediated Leptin Sensing and Body Weight Control. Cell Metab [Internet]. Elsevier Inc.; 2016;23(5):797–810. Available from: http://dx.doi.org/10.1016/j.cmet.2016.04.013
66. Dutot M, Liang H, Pauloin T, Brignole-Baudouin F, Baudouin C, Warnet J-M, et al. Effects of toxic cellular stresses and divalent cations on the human P2X7 cell death receptor. Mol Vis [Internet]. 2008;14(March):889–97. Available from: http://www.ncbi.nlm.nih.gov/pubmed/18490962%5Cnhttp://www.pubmedcentral.nih.gov/articlerender.fcgi?artid=PMC2386509
67. Mehanna C, Baudouin C, Brignole-Baudouin F. Spectrofluorometry assays for oxidative stress and apoptosis, with cell viability on the same microplates: A multiparametric analysis and quality control. Toxicol Vitr [Internet]. Elsevier Ltd; 2011;25(5):1089–96. Available from: http://dx.doi.org/10.1016/j.tiv.2011.03.007

Captions to main figures

Figure 1.
Impact of blue light illumination on cell viability and death.
A-D. Rates of cell viability (n=5), apoptosis (DAPI and YO-PRO, n=4) and necrosis (PI, n=4) after light exposure.
E, F. Cells were immunostained with Hoechst (blue), YO-PRO (green) and PI (red) dyes. Wells where the observed fluorescent signal was the most important are outlined in the color of the correspondent waveband. Scale bars represent 100 μm. Numbers on wells indicate the correspondent light conditions (dark control or central wavelength).
G. Ratio between rates of apoptotic and necrotic fluorescent signals.
H. Merge of all the three immunostainings (Hoechst, YO-PRO, PI; n=4) in cells exposed to 410 nm light. Scale bar represents 50 μm.
Clear bars correspond to mixed and hatched bars to AraC-treated culture. Wavebands are represented by the correspondent colors; each 10 nm spectral band is designated by its central wavelength. Results shown represent the mean ± SEM. Stars (*) refer to differences with the correspondent dark control within the same culture condition and carets (^) refer to differences between culturing conditions (mixed *vs.* AraC) within the same light condition. Red signs correspond to an increase and blue signs to a decrease in values. Statistical significance: $p < 0.05$ (*/^), $p < 0.01$ (**/^^), $p < 0.001$ (***/^^^), $p < 0.0001$ (****/^^^^).

Figure 2.
Blue light provoked expression of cell damage marker and altered cell morphology.
A. Immunostaining with DAPI (blue) and anti-GADD153 antibody (red). Arrows indicate GADD153-positive cells.
B. Immunostaining with anti-PAN antibody. Examples of dotted structure of axons after exposure to 410 nm are shown by arrows. Presented images correspond to mixed culture.
Scale bars represent 100 μm. Wells where the observed fluorescent signal was the most important are outlined in the color of the correspondent waveband. Numbers on wells indicate the correspondent light conditions (dark control or central wavelength).
C-F. Quantification of neural (cell number, neurites length and cell area) and glial (cell number) morphology (n=4). Clear bars correspond to mixed and hatched bars to AraC-treated culture. Wavebands are represented by the correspondent colors; each 10 nm spectral band is designated by its central wavelength. Results shown represent the mean ± SEM. Stars (*) refer to differences with the correspondent dark control within the same culture condition and carets (^) refer to differences between culturing conditions (mixed *vs.* AraC) within the same light condition. Red signs correspond to an increase and blue signs to a decrease in values. Statistical significance: $p < 0.05$ (*/^), $p < 0.01$ (**/^^), $p < 0.001$ (***/^^^), $p < 0.0001$ (****/^^^^).

Figure 3.
Exposure to blue light induced oxidative stress.
A,B. Measured rates of hydrogen peroxidase (n=5) and superoxide anion (n=3).

C. Fluorescent images of $O_2^{\bullet -}$ accumulation (red); cells were counterstained anti-PAN (green) and anti-GFAP (blue) antibody. Presented images correspond to AraC-treated culture. Scale bar represents 100 μm. Wells where the observed fluorescent signal was the most important is outlined in the color of the correspondent waveband. Numbers on wells indicate the correspondent light conditions (dark control or central wavelength).
D. Zoom on a well exposed to 410 nm light ($O_2^{\bullet -}$ - red, PAN – green, GFAP - blue) antibody. Scale bar represents 50 μm.
E. Ratio between the number of cells presented red and blue fluorescent signals simultaneously (i.e., the number $O_2^{\bullet -}$ - generating glial cells) and the number of all the red cells (i.e., the number of all the $O_2^{\bullet -}$ - generating cells) (n=4).
Clear bars correspond to mixed and hatched bars to AraC-treated culture. Wavebands are represented by the correspondent colors; each 10 nm spectral band is designated by its central wavelength. Results shown represent the mean ± SEM. Stars (*) refer to differences with the correspondent dark control within the same culture condition and carets (^) refer to differences between culturing conditions (mixed *vs.* AraC) within the same light condition. Red signs correspond to an increase and blue signs to a decrease in values. Statistical significance: $p < 0.05$ (*/^), $p < 0.01$ (**/^^), $p < 0.001$ (***/^^^), $p < 0.0001$ (****/^^^^).

Figure 4.
Relative mRNA expression of inflammation- and neuronal activation-related biomarkers.
n=4-5. Clear bars correspond to mixed and hatched bars to AraC-treated culture. Wavebands are represented by the correspondent colors; each 10 nm spectral band is designated by its central wavelength. Results shown represent the mean ± SEM. Stars (*) refer to differences with the correspondent dark control within the same culture condition. Red signs correspond to an increase and blue signs to a decrease in values. Statistical significance: $p < 0.05$ (*), $p < 0.01$ (**), $p < 0.001$ (***), $p < 0.0001$ (****).

Figure 5.
Processing of blue-light phototoxic message.
A. Immunostaining with anti-pERK (red) and anti-PAN (green) antibodies. Wells where the pERK fluorescent signal importantly decreased (as compared to dark control) or disappeared are outlined in blue. Numbers on wells indicate the correspondent light conditions (dark control or central wavelength). Scale bar represents 100 μm.
B,C. Immunostaining with mitochondria-tracking dye (red) and with DAPI (blue), in dark control or in 410-nm-illuminated wells (mixed culture). Arrows indicate accumulation of signal from compromised mitochondria. B corresponds to 10x and C corresponds to 20x magnification. Scale bars represent 50 μm.

Figure 6.
Non-visual photoreception in trigeminal cells.
A. Confocal images of immunostaining with anti-opn4 (red), anti-PAN (green) and DAPI (blue) antibodies (mixed culture). Arrows indicate melanospin-positive neurons.

B. Confocal images of immunostaining with anti-opn5 (red), anti-PAN (green) and anti-GFAP (blue) antibodies (mixed culture). Neuropsin-positive cells are indicated by arrows, pink for glial cells and yellow for neurons.
Numbers on wells indicate the correspondent light conditions (dark control or central wavelength). Scale bars represent 100 μm.

Captions to supplementary figures

Figure S1.
A. Immunostaining with anti-PAN antibody. Examples of dotted structure of axons after exposure to 410 nm are shown by arrows. Presented images correspond to AraC-treated culture.
B. Fluorescent images of $O_2^{\bullet -}$ accumulation (red); cells were counterstained anti-PAN (green) and anti-GFAP (blue) antibodies. Presented images correspond to mixed culture.
Scale bars represent 100 μm. Wells where the observed fluorescent signal was the most important are outlined in the color of the correspondent waveband. Numbers on wells indicate the correspondent light conditions (dark control or central wavelength).

Figure S2.
Representative 24-well plate illumination by various narrow 10 nm wavebands. For every experiment, one subdivision of a well-plate was maintained in darkness.

Figure S3.
Preliminary experiments in mixed culture - levels of cell viability (n=3) after weaker or longer light exposures. Wavebands are represented by the correspondent colors; each 10 nm spectral band is designated by its central wavelength. Results shown represent the mean ± SEM. Stars (*) refer to differences with the correspondent dark. Statistical significance: $p < 0.05$ (*/^), $p < 0.01$ (**/^^), $p < 0.001$ (***/^^^), $p < 0.0001$ (****/^^^^).

Figure S4.
Confocal images of immunostaining with anti-melanopsin antibody (mixed culture). The image is the same as in the Fig. 6, however, green and blue colors of anti-PAN and DAPI immunostainings were removed to highlight the red melanopsin immuno-reactivity. Very bright red spots were considered as non specific since they matched with neither neuronal nor glial immunostainings (Fig. 6). Scale bars represent 100 μm.

Main figures

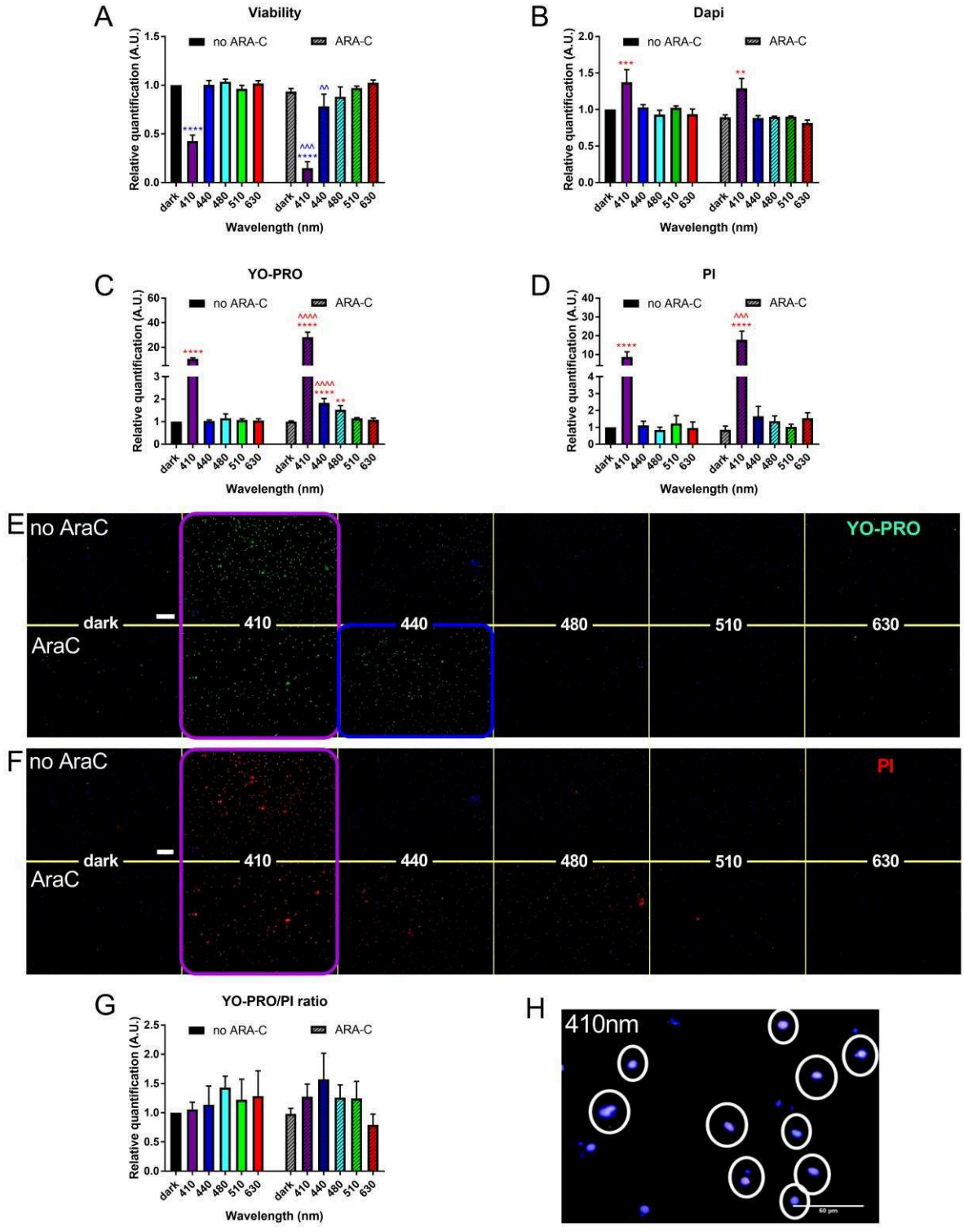

Figure 1. Impact of blue light illumination on cell viability and death.

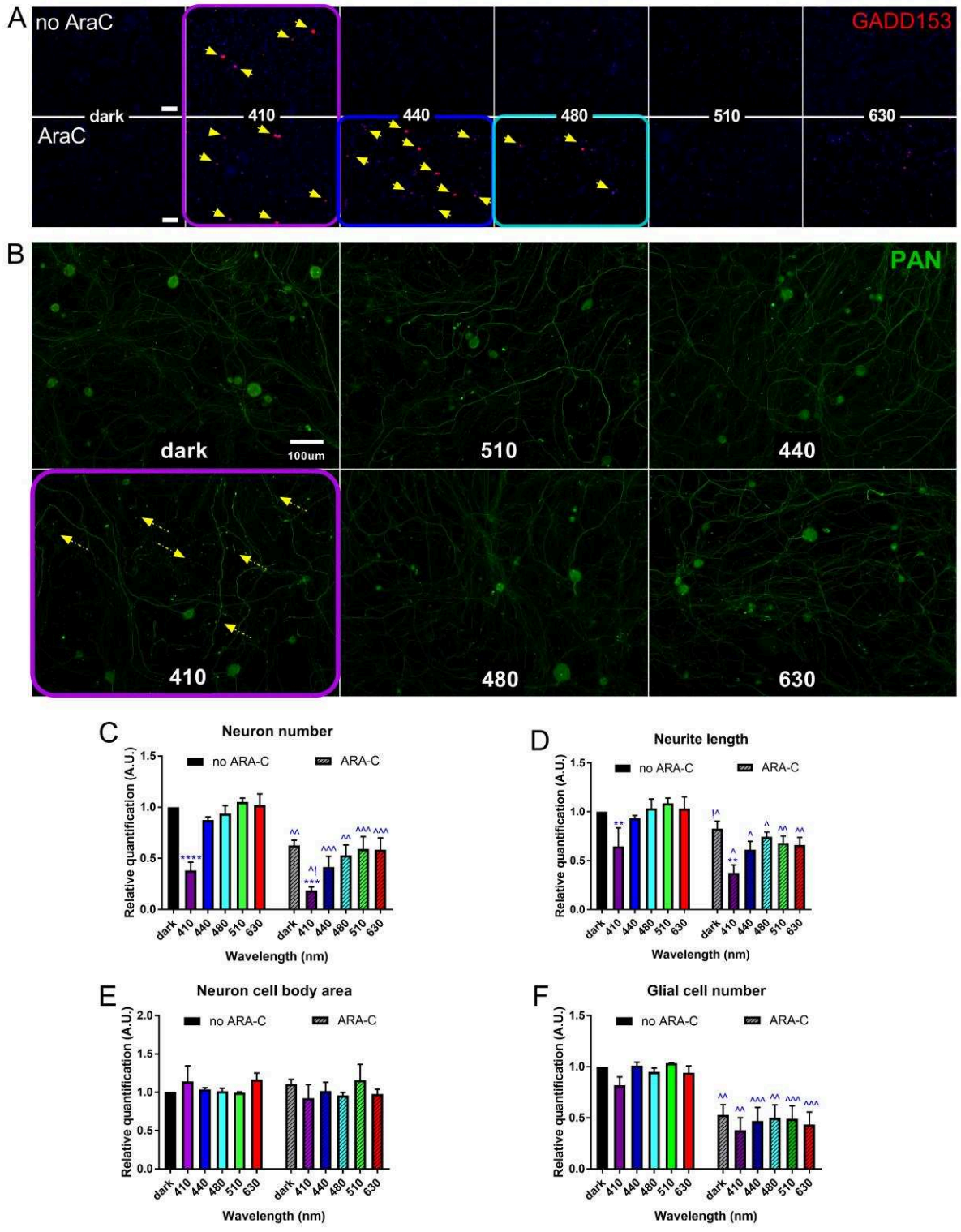

Figure 2. Blue light provoked expression of cell damage marker and altered cell morphology.

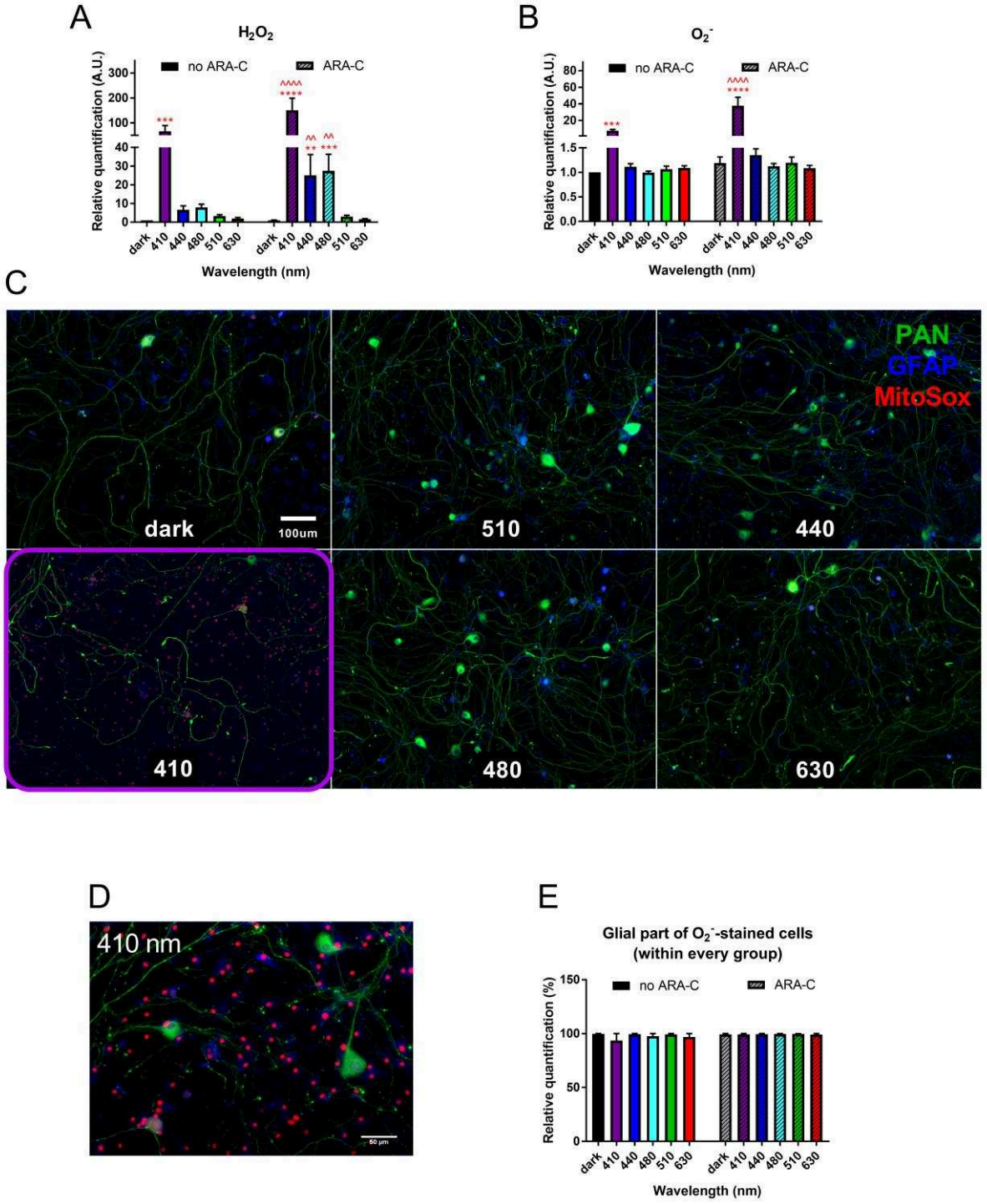

Figure 3. Exposure to blue light induced oxidative stress.

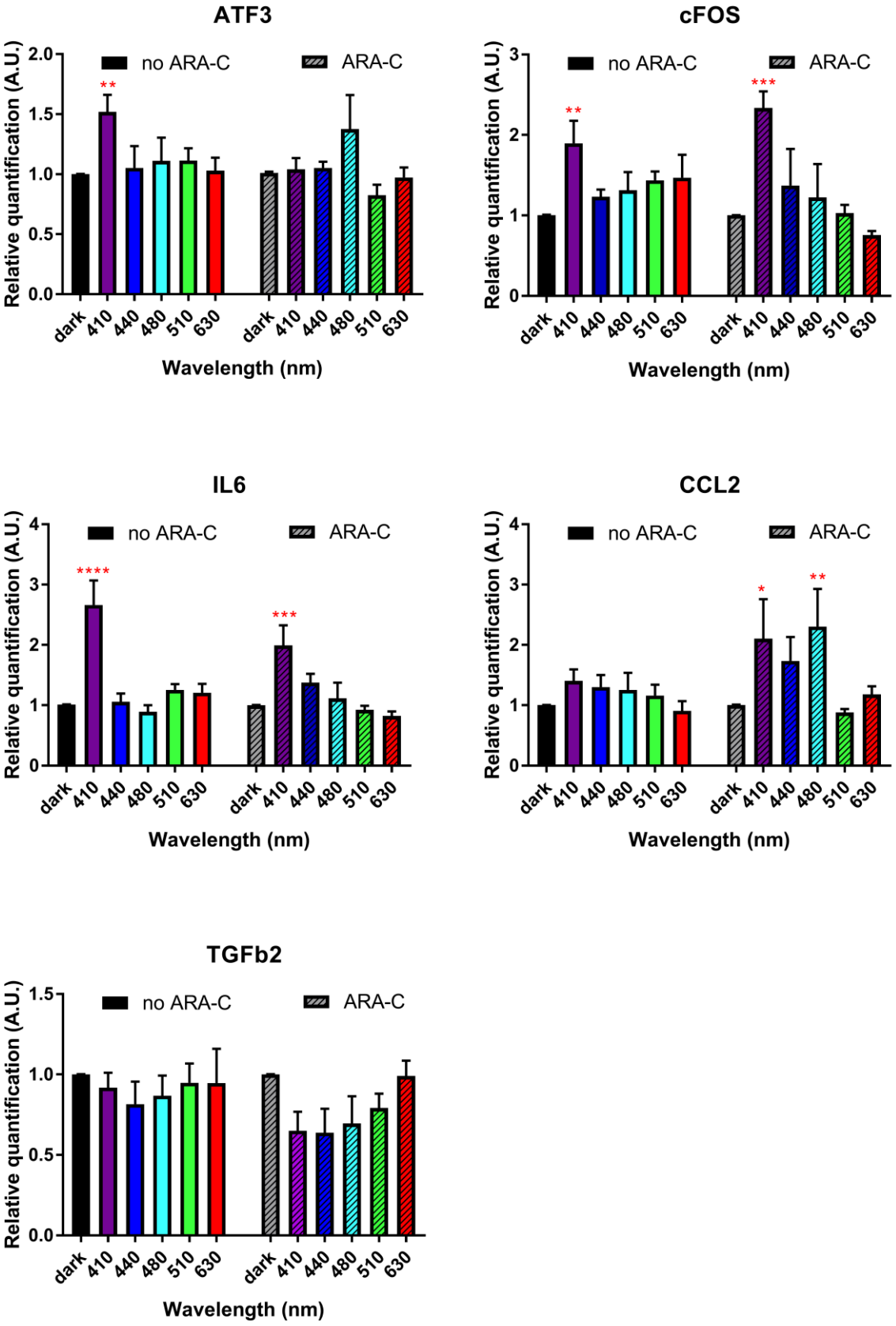

Figure 4. Relative mRNA expression of inflammation- and neuronal activation-related biomarkers.

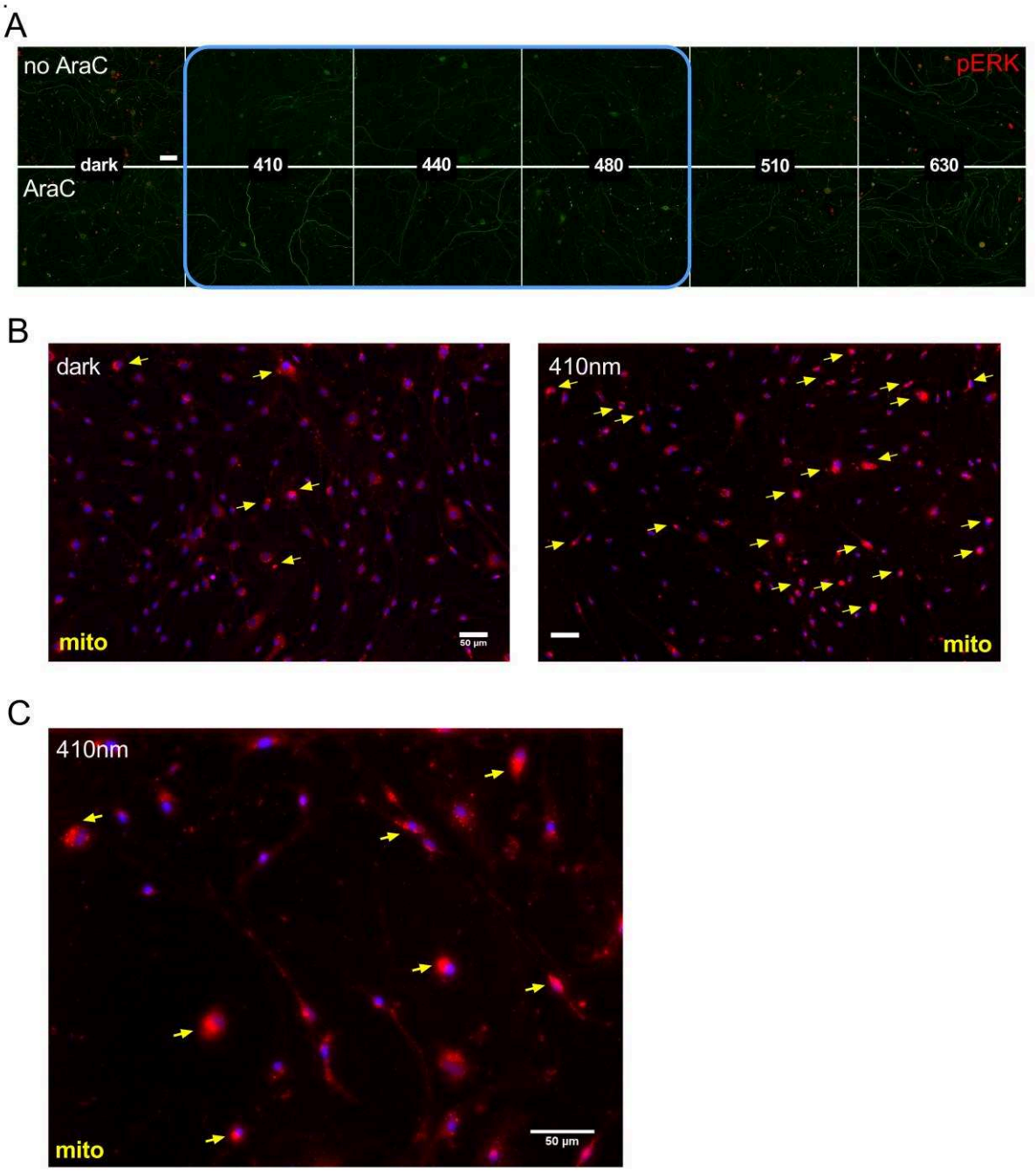

Figure 5. Processing of blue-light phototoxic message.

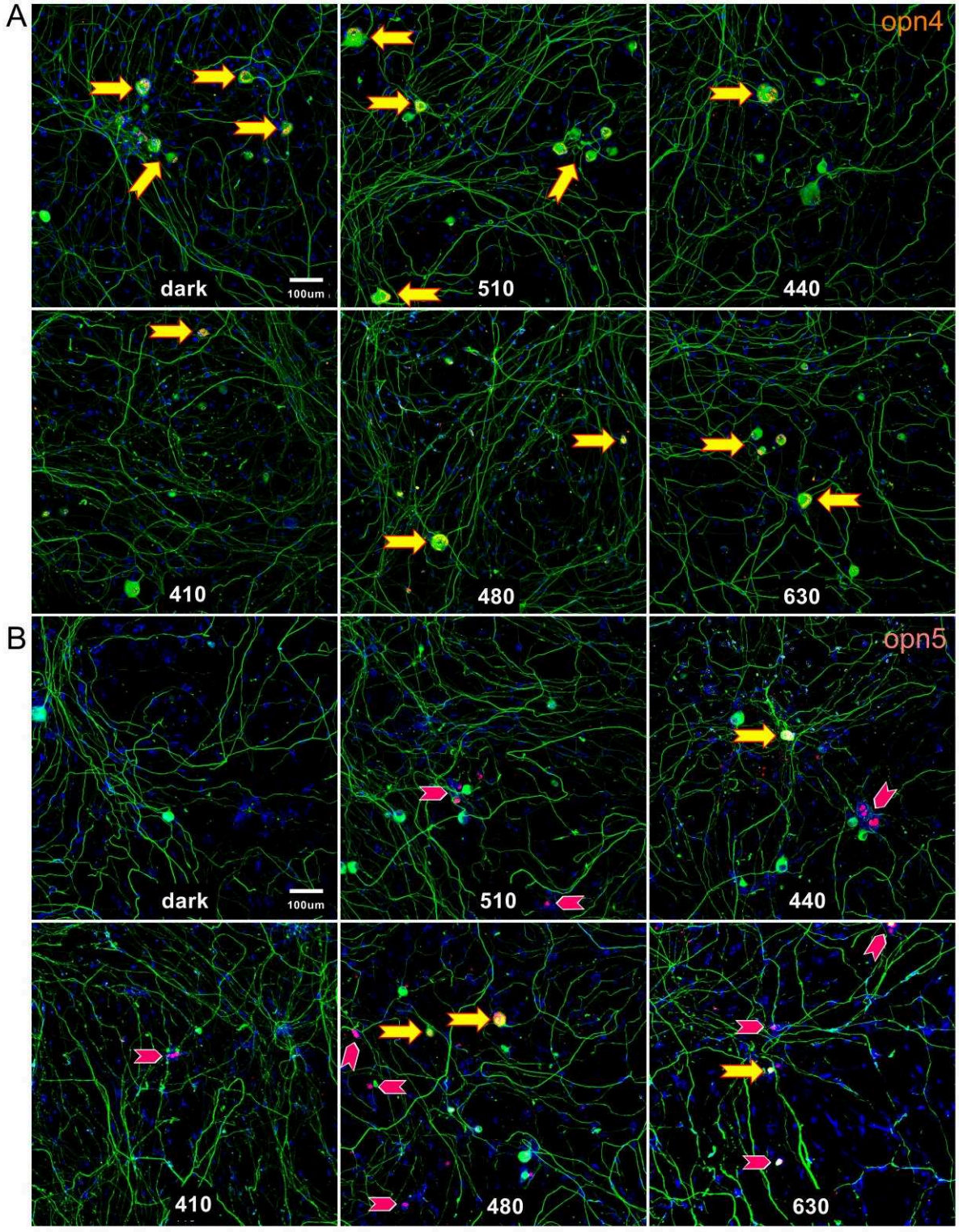

Figure 6. Non-visual photoreception in neural cells.

Supplementary figures

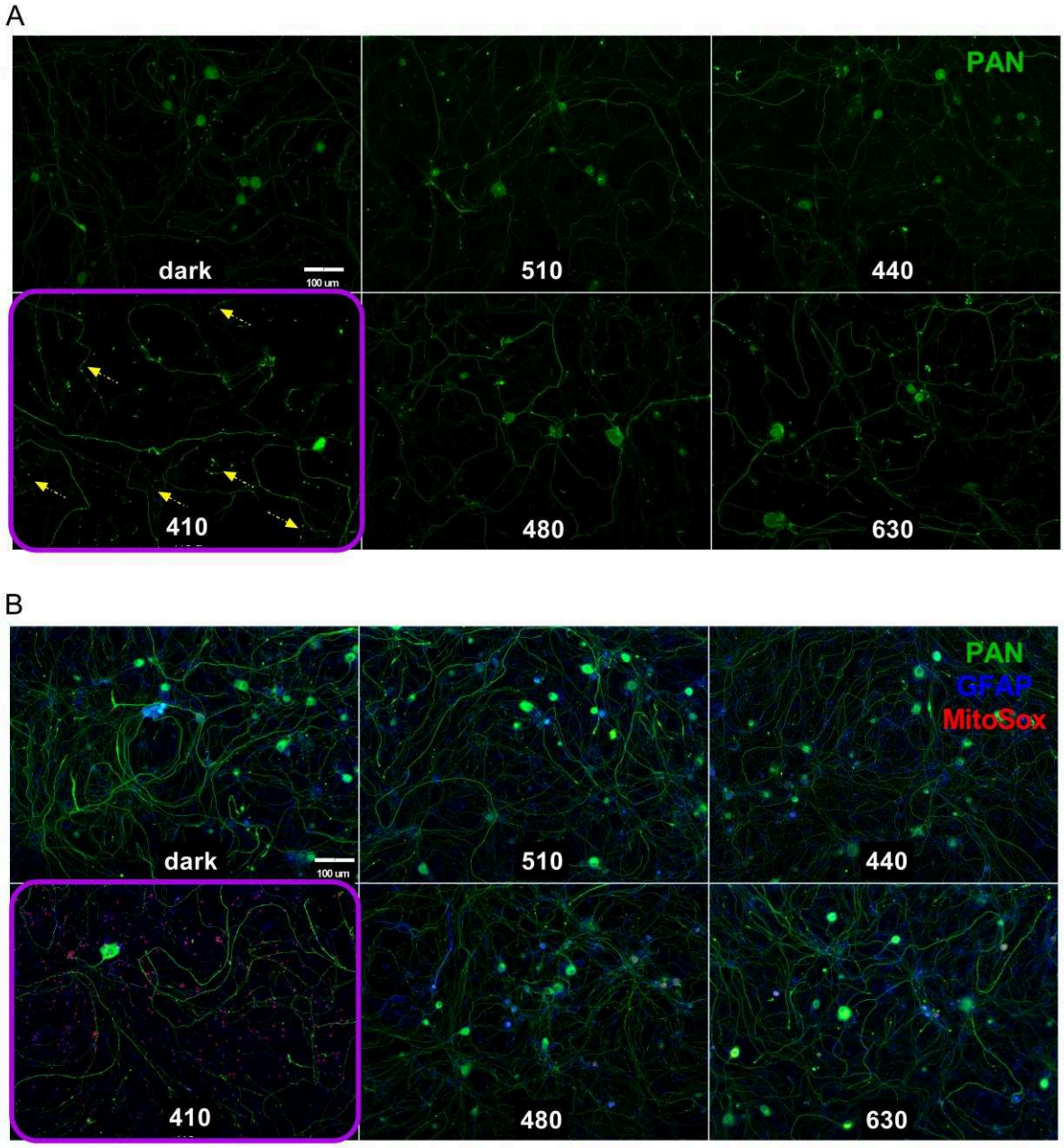

Figure S1.

dark	510nm	440nm
410nm	480nm	630nm

Figure S2.

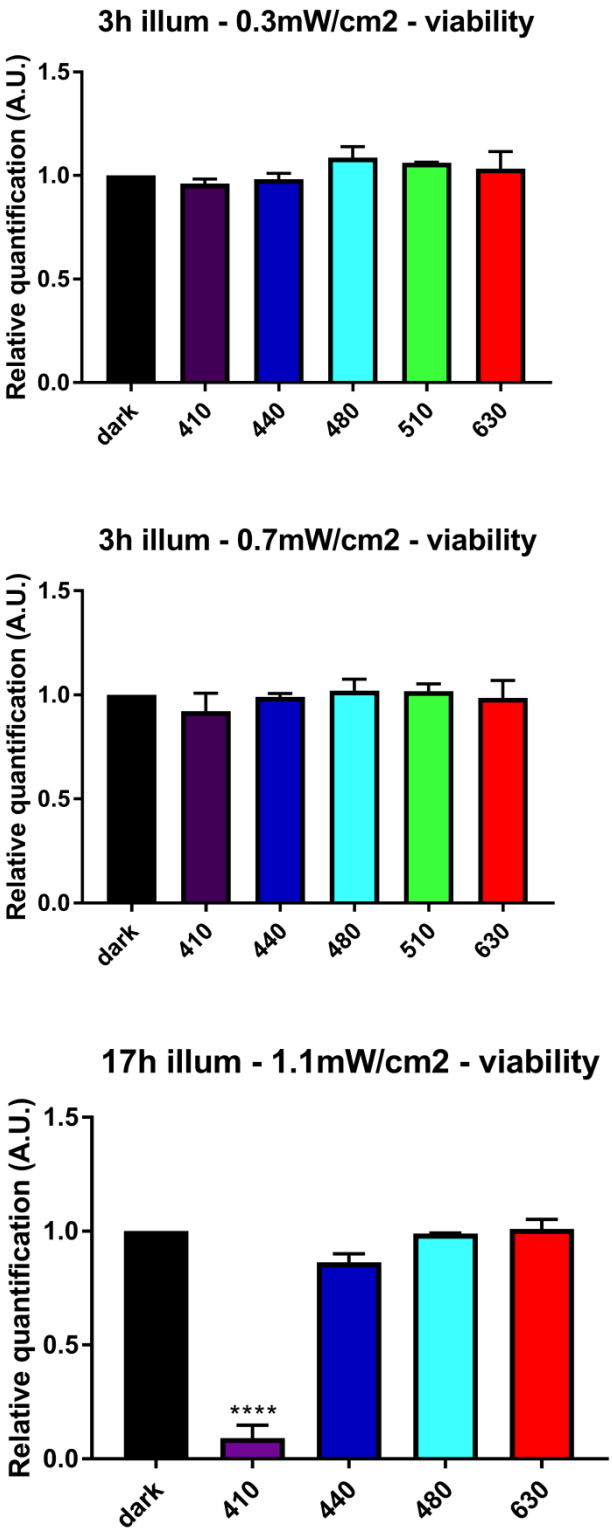
3h illum - 0.3mW/cm2 - viability
Relative quantification (A.U.)
1.5
1.0
0.5
0.0
dark
410
440
480
510
630
3h illum - 0.7mW/cm2 - viability
Relative quantification (A.U.)
1.5
1.0
0.5
0.0
dark
410
440
480
510
630
17h illum - 1.1mW/cm2 - viability
Relative quantification (A.U.)
1.5
1.0
0.5
0.0
****
dark
410
440
480
630

Figure S3.

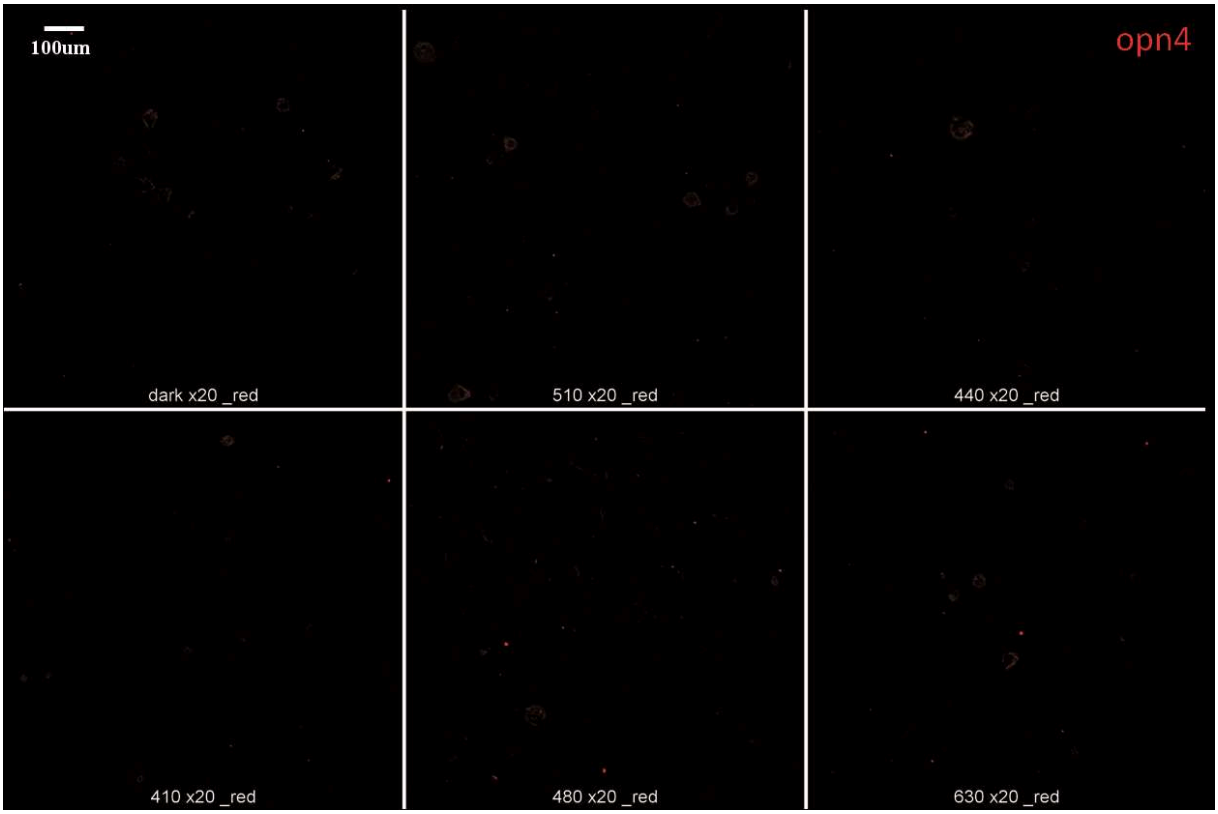
100um
opn4
dark x20 _red
510 x20 _red
440 x20 _red
410 x20 _red
480 x20 _red
630 x20 _red

Figure S4.

Earlier submission

We previously submitted our work to Cell Death Discovery journal. This choice was made following the suggestion of Gerry Melino, the receiving Editor of Cell Death and Differentiation journal, who proposed it because "*of the translational and clinical involvement of our results*"**:**

I, therefore, strongly suggest you to transfer this manuscript to Cell Death Discovery, where I have personally discussed and agreed your paper with the Receiving Editor. This is more adequate, as we both have already seen the manuscript, and I am the one who suggested the transfer.

However, we received the following answer from a reviewer:

While the trigeminal nerve innervates the face, including regions around the eye I am not aware that it innervates the retina. This makes me question what the relevance is of exposing primary cultured trigeminal neurones to light of 410 nM and examining the effects on cell toxicity. While this cranial nerve conveys ocular pain signals associated with blue light, exposing those cells to 410 nM light, which they are not exposed to in situ, in vivo seems of little relevance.
AraC, is given as - antimitotic treatment, which is a correct description of what it is used for but ought to be given as - Cytosine-1-β-D-arabinofuranoside, which is what it is an abbreviation of. More importantly no mention in the text is given as to why AraC is used. AraC is cytotoxic, and the effects of blue light at 410 nm are more pronounced in the presence of AraC, but what that shows is again not clear, nor it is discussed in any detail.
I do not feel this report is suitable for publication.

We felt truly disappointed with such an answer since we found it absolutely inadequate. Please, find below our responses:
1. *While the trigeminal nerve innervates the face, including regions around the eye I am not aware that it innervates the retina.*
In this paper, we say nowhere that trigeminal nerves innervate the retina.
By the way, even if it is not in the scope of the current work, some reports discuss the probable connections between the retina and trigeminal afferents. Although it was initially believed that the retina lacked trigeminal sensory innervation (1), recently Warfvinge *et al*. reported that nerves originating from the TGs did innervate the retina (2). Moreover, this group has already detected the presence of CGRP neuropeptide in the rat retina (3).
2. *While this cranial nerve conveys ocular pain signals associated with blue light, exposing those cells to 410 nM light, which they are not exposed to in situ, in vivo seems of little relevance.*
First, this is not an *in vivo* study: it is an *in vitro* one since we worked on the primary culture of cells from mouse trigeminal ganglia. Second, the trigeminal cells are exposed to light since the cornea, the tissue the mostly illuminated by ambient light, is innervated by the trigeminal nerves.

3.

Cytosine-1-β-D-arabinofuranoside

We added this full correct name in the abbreviations and in Materials and Methods section.

More importantly no mention in the text is given as to why AraC is used.

It is, on the page 5: *Here, we demonstrated* in vitro *the cytotoxic impact of blue light on primary cell culture of mouse trigeminal cells, further specifying the implication of each cell population through the use of supplementary antimitotic treatment (AraC).*

as well as in Materials and Methods section (page 10):

In order to understand, whether the phototoxicity would depend on cell population, the medium was completed or not with AraC at 5 µM to prevent glial cell proliferation, to give *mixed* or *AraC-treated* culture, respectively. Reference on the previous using of AraC were also given (4–6).

<…> *but what that shows is again not clear, nor it is discussed in any detail.*

It is, on the page 6: The blue-toxic effects were more important when AraC was applied. Since antimitotic treatment significantly decreased the number of glial cells, it reduced neuronal protection and support, thus making neurons more vulnerable to induced stress. Further, it is this antimitotic treatment that allowed us to discuss the difference between neural and glial processing of the phototoxic message (page 8).

We hope that our explanations make clear the absolute lack of correspondence between our work and the response we received.

Bibliography:

1. Albilali A, Dilli E. Photophobia : When Light Hurts, a Review. Curr Neurol Neurosci Rep. Current Neurology and Neuroscience Reports; 2018;18(62):4–9.
2. Warfvinge K, Sörensen, Karin D Edvinsson L, Fedulov V, Haanes KA, Blixt FW. Expression of the CGRP family peptides and their receptors in the rat retina. In: nvest Ophthalmol Vis Sci [Internet]. 2018. p. 59(9):5504. Available from: https://iovs.arvojournals.org/article.aspx?articleid=2692859&resultClick=1
3. Blixt FW, Radziwon-balicka A, Edvinsson L, Warfvinge K. Distribution of CGRP and its receptor components CLR and RAMP1 in the rat retina. Exp Eye Res [Internet]. Elsevier Ltd; 2017;161:124–31. Available from: http://dx.doi.org/10.1016/j.exer.2017.06.002
4. Launay P, Reboussin E, Liang H, Kessal K, Godefroy D, Rostène W, et al. Neurobiology of Disease Ocular in fl ammation induces trigeminal pain , peripheral and central neuroin fl ammatory mechanisms. Neurobiol Dis. 2016;88:16–28.
5. Djogo T, Robins SC, Schneider S, Kryzskaya D, Liu X, Mingay A, et al. Adult NG2-Glia Are Required for Median Eminence-Mediated Leptin Sensing and Body Weight Control. Cell Metab [Internet]. Elsevier Inc.; 2016;23(5):797–810. Available from: http://dx.doi.org/10.1016/j.cmet.2016.04.013
6. Godefroy D, Gosselin RD, Yasutake A, Fujimura M, Combadie're C, Maury-Brachet R, et al. The chemokine CCL2 protects against methylmercury neurotoxicity. Toxicol Sci. 2012;125(1):209–18.

Article 3: causes and consequences of blue photophobia

V. Marek, E. Reboussin, A. Charbonnier, J. Dégardin-Chicaud, T. Villette, A. Denoyer, C. Baudouin, A. Réaux-Le-Goazigo, S. Mélik Parsadaniantz, **Implication of melanopsin and trigeminal neural pathways in blue light photosensitivity in vivo**, submitted to the Frontiers in Neuroscience Journal on the 17th October 2018

On the basis of the state-of-the-art presented in the introduction to this thesis, we identified numerous non-answered questions related to light aversion. The goal of this part of the work was to shed some (not phototoxic) light on potential answers to the following three:

- Can the blue light exposure trigger off the photophobia in healthy subjects without any precedent ocular disorder?
- What chain of inflammatory events might be activated by exposure to blue light?
- What is the main mediator of the photophobic signal?

Indeed, not only the patients already suffering from the ocular pathologies present with photophobic symptoms: healthy persons may complain about increased photosensitivity as well. Thus, we were wondering whether in naïve mice exposed to blue light the signs of light aversion may appear. Since we have already reported the dry-eye-related phototoxic effects in the epithelial cells of cornea and conjunctiva, here, we investigated clinically the state of the ocular surface and the function of lacrimation. Since we previously demonstrated the phototoxic effects in the TG neurons and neuroglial cells, we were also interested in probable alterations of ocular surface sensitivity as well as in neuro-inflammation in trigeminal pathways. Furthermore, to approach the issues concerning the photophobia circuits, we analyzed how light aversion might be reversed pharmacologically. All the conclusions about applied drug treatments were done on the basis of the behavioral tests meaning that the probable bias potentially introduced by a human factor was minimized.

To our knowledge, it is the first in vivo study revealing the blue wavelength specificity of photophobia that was inferred from behavior assessment supplemented by various pharmacological treatments. Taken together, our results demonstrated that blue-light photophobia was mainly mediated by melanopsin-containing cells and did not rely on visual photoreceptors. Although the ocular surface exhibited phototoxically-induced dry eye signs of inflammation and melanopsin-dependent mechanical sensitivity, the intra-corneal trigeminal fibers appeared to have a minimal role in intrinsic photosensitivity, if any. Nevertheless, the phototoxic process necessarily implicated the trigeminal nerves since light induced inflammation in the TGs and brainstems. According to our results, the photic signal was received by the ipRGCs and then somehow transmitted to the trigeminal pathways, simultaneously inducing the phototoxic stress in the retina.

Implication of melanopsin and trigeminal neural pathways in blue light photosensitivity in vivo

V. Marek*[,1,2], E. Reboussin[2], J. Dégardin-Chicaud[2], A. Charbonnier[2], T. Villette[1], A. Denoyer[2,3,4], C. Baudouin[2,3,5], A. Réaux-Le-Goazigo[2] and S. Mélik Parsadaniantz[2]

[1]R&D, Essilor International, Paris, France

[2]Sorbonne Université, INSERM, CNRS, Institut de la Vision, Paris, France

[3]*Centre Hospitalier Nationale d'Ophtalmologie des Quinze*-Vingts, Paris, France

[4]CHU Robert Debré, Université Reims Champagne-Ardenne, Reims, France

[5]Versailles-Saint-Quentin-en-Yvelines Université, Versailles, France

*** Correspondence:**
Veronika Marek
nika.marek@gmail.com

Keywords: blue light, photophobia, trigeminal pathway, melanopsin, ocular nociception, dry eye, neurotoxicity

Abstract

Photophobia may arise from various causes and frequently accompanies numerous ocular diseases. In modern highly-illuminated world, complaints about greater photosensitivity to blue light increasingly appear. However, the pathophysiology of photophobia is still debated. In the present work, we investigated in vivo the role of various neural pathways potentially implicated in blue-light aversion. Moreover, we studied the light-induced neuroinflammatory processes on the ocular surface and in the trigeminal pathways.

Adult male C57BL/6J mice were exposed either to blue (400-500 nm) or to yellow (530-710 nm) LED light (3 hours, 6 mW/cm^2). Photosensitivity was measured as the time spent in dark or illuminated parts of the cage. Pharmacological treatments were applied: topical instillation of atropine, pilocarpine or oxybuprocaine; intravitreal injection of lidocaine, norepinephrine or "blocker" of the visual photoreceptor transmission; and intraperitoneal injection of a melanopsin antagonist. Clinical evaluations (ocular surface state, corneal mechanical sensitivity and tear quantity) were performed directly after exposure to light and after 3 days of recovery in standard light conditions. Mice were then sacrificed; trigeminal ganglia (TGs), brainstems and retinas were dissected out and conditioned for analyses.

Mice demonstrated strong aversion to blue but not to yellow light. The only drug that significantly decreased the blue light aversion was the intraperitoneally injected melanopsin antagonist. After blue light exposure, dry-eye-related inflammatory signs were observed, notably after 3 days of recovery. We detected the increased immunoreactivity for cFOS and Iba1 in the sensory complex of trigeminal subnucleus, for ATF3 in the TG, and for GFAP, ATF3 and Iba1 in the retina. Moreover, retinal

visual and non-visual light receptors distribution was altered. These data were corroborated by RT-qPCR.

Thus, the wavelength-dependent light aversion was mainly mediated by melanopsin-containing cells, most likely in the retina. Other potential pathways of light reception were also discussed. The phototoxic message was transmitted to the trigeminal system, inducing both inflammation at the ocular surface and stress in the retina. Further investigations of retina-TG connections are needed.

Highlights:

- increased photosensitivity is a function of wavelength
- blue light aversion is accompanied by clinical signs of dry eye
- blue light provokes immuno-activation in trigeminal pathways
- intra-retinal melanopsin is the main mediator of blue light photophobia

1 Introduction

Photophobia is a highly debilitating sensory disturbance provoked by visible light (Wu and Hallett, 2017). In patients exposed to normally non-painful illumination, this syndrome causes discomfort and pain in the eye (K. Digre and K.C. Brennan, 2012). One of the most common neurologic disorders that causes photophobia is migraine; indeed, as much as 80% of migraineurs heavily suffer from increased light sensitivity (Albilali and Dilli, 2018). As a result, many studies have already explored the potential mechanisms underlying the light-induced exacerbation of migraine (Nir et al., 2018; Noseda et al., 2017, 2016, 2010). However, symptoms of photophobia are not limited to headache cases. Photophobia in general and greater sensitivity to blue light in particular are common for many ophthalmological (dry eye, blepharitis, retinal dystrophy), neurological (blepharospasm, traumatic brain injury) and even psychiatric (depression, anxiety) disorders (K. Digre and K.C. Brennan, 2012). Nonetheless, so far, there have been no major randomized control trials for photophobia management (Albilali and Dilli, 2018). The current treatment of this disorder actually remains a challenge for ophthalmologists and relies primarily on optical means such as wearing filtering glasses (Hoggan et al., 2016; Katz and Digre, 2016). Ubiquitous presence of artificial light sources highly emitting in blue spectrum complicates the situation additionally (Lupis, n.d.; Text Request, n.d.).

Several hypotheses about the potential origin of light-aversive behavior have been proposed (K. Digre and K.C. Brennan, 2012; Wu and Hallett, 2017) appealing to the roles of the retina (Dolgonos et al., 2011; Matynia et al., 2015, 2012), trigeminal nerves and neighboring blood vessels (Matynia et al., 2016; Okamoto et al., 2012, 2011, 2009; Rahman et al., 2015). Nonetheless, our understanding of photophobia process is still elusive and much of its neurochemistry remains unknown. In the current work, we used behavior tests and various pharmacological treatments to investigate in vivo which neurological circuits might be implicated in blue-light aversion.

Photophobia is definitely linked to inflammation and pain sensation; however, a pathway for light as a stress-related nociceptive stimulus remains unclear (K. Digre and K.C. Brennan, 2012; Wu and Hallett, 2017). We already demonstrated in vivo the implication of peripheral and central neuro-inflammatory processes in pain-associated ocular damage (Launay et al., 2016). Moreover, we recently reported in vitro the phototoxicity of blue light in epithelial cells of ocular surface (Marek et al., 2018). Both studies were performed within the scope of dry eye disease whose sufferers

frequently complain of higher daily photosensitivity (M. Wade, 2015; Stapleton et al., 2017). Hence, in the present work, we investigated clinically the inflammatory signs induced at the ocular surface by exposure to blue light. We also analyzed the neural phototoxic processes that accompanied the blue-light photophobia.

2 Results

2.1 Blue light aversion is accompanied by inflammation in the lacrimal functional unit

In our preliminary experiments, we put 4 mice in mirrored-wall boxes exposed to light and let them freely move and interact with each other during all the 3 hours of illumination. Mice exposed to blue spectrum exhibited strong aversion to light and permanently hid one behind another. Control yellow-illuminated mice did not demonstrate such kind of behavior (Fig. 1B). To eliminate the inter-animal interactions, mice were then placed in individual compartments and assessed clinically, either directly after the end of 3-hour exposure or after 3 days of recovery in standard lighting conditions, since it was reported that blue-light-induced inflammation was present after a recovery period (Krigel et al., 2016). We set the recovery time to 3 days because Feng et al. observed the peak for various inflammatory biomarkers at this time point (Feng et al., 2017). Blue light provoked a significant increase in corneal mechanical sensitivity (von Frey hair test) compared to baseline (before-illumination value). After the recovery time, this result only deteriorated: the correspondent value was significantly different from the one of yellow-illuminated mice (Fig. 2A). Moreover, blue light-exposed mice demonstrated a significant increase in tear volume either directly after illumination or after the recovery period (Fig. 2B). These signs were not observed in mice exposed to yellow light.

The slit-lamp examination did not reveal any noticeable differences in fluorescein staining i.e. no corneal epithelial damage (data not shown). We then used in vivo confocal microscopy (IVCM) to explore all the layers of the cornea: epithelium, sub-basal plexus, stroma and endothelium. Directly after light exposure, we observed a slight activation of cells in superficial epithelium (hyperreflective nuclei), some dendritic cells in sub-basal plexus and activated keratocytes in stroma. These inflammatory signs were more pronounced after the exposure to blue light as compared to the yellow one (Fig. 3A). After 3 days of recovery, the clinical inflammatory signs decreased or disappeared for the yellow light while they significantly intensified for the blue light (Fig. 3B). The corneal endothelium was not damaged whatever the conditions (data not shown).

2.2 Role of the retina in blue light phototoxicity and aversion

Retina is the most well-known light signal receiver; it may therefore be implicated as the first mediator of phototoxicity. In 3 days after exposure to blue light, we observed the activation of GFAP dendritiform cells, much more pronounced than directly after the end of illumination (Fig. 4A). On the contrary, the ATF3 immunostaining revealed an important fluorescent signal directly after exposure but not after the recovery period (Fig. 4B). The signals were much weaker or absent in yellow-illuminated mice. After 3 days of recovery, Iba1 immunolabeling showed an increased inflammatory reaction for both spectra with a slightly greater staining for the blue one (Fig. 4C). These results were confirmed by the qPCR analysis (Fig. 4D-F).

We then supposed that blue light aversion may depend on the luminous flux that reached the retina. Therefore, we performed behavioral tests in which we compared the blue light aversion between mice instilled (inst) with atropine (atro) for pupil dilatation (to increase retinal illumination), with pilocarpine (pilo) for pupil constriction (to decrease retinal illumination) and with PBS for the

control condition. We also tested the instillation of NaCl as control condition and found no significant difference with PBS instillation (data not shown). Pupil dilatation induced yellow-light aversion that was not observed in our previous experiments. Pupil constriction did not change the behavior under yellow light. It provided with a small trend for a decrease in blue-light aversion; however, this trend appeared to be far from statistically significant ($q = 0.3188$, $p = 0.1902$ after 1 hour of exposure; $q = 0.4670$, $p = 0.2224$ after 3 hours of exposure). Thus, the blue-light aversion was always present and did not exhibit any significant changes due to pupil size alterations (Fig. 5A).

Next, we investigated the role of retinal light receptors. According to our immunohistochemistry study, the rod layer did not exhibit noticeable differences either between 2 spectra or between 2 time points of assessment (before and under recovery) (data not shown). However, for the blue light, we observed numerous “holes” in the cone layer while for the yellow exposure it was almost untouched (Fig. 6A). To evaluate the status of non-visual light receptors, we performed stainings with anti-melanopsin (anti-opn4) and anti-neuropsin (amti-opn5) antibodies. For both illuminations, we observed a new pattern of melanopsin location: after the recovery time, the signal was less present in axons and accumulated more in cell bodies (Fig. 6B). RT-qPCR analysis revealed an increase in melanopsin mRNA expression after recovery for both spectra (Fig. 6D). The neuropsin exhibited no significant changes either in immunohistological or in RT-qPCR studies (Fig. 6C,E).

Taking into account these findings, we further performed the behavioral tests to investigate whether light aversion would change if we disrupted retinal light reception or processing. We verified, by measuring the optokinetic response, that mice in which retinal visual receptors (VR) pathway was blocked (for both rods and cones, see Materials&Methods section for the details) were really blind (data not shown). We found that injection with the correspondent drug (VR blocker) did not alter the behavior of mice at any illumination (Fig. 5B). However, intraperitoneal (ip) injection of melanopsin antagonist (opn4 antago) did significantly decrease the blue light aversion (Fig. 5C).

2.3 Implication of out-retinal melanopsin and trigeminal pathways

Non-retinal tissues that potentially contain melanopsin were then studied. Topical instillation (inst) of local anesthetic (oxybuprocaine - oxybu) on the cornea did not exhibit any impact on behavior under light (Fig. 7A). Intravitreal (ivt) injection of lidocaine (lido), which silenced all the probable trigeminal afferents reaching the choroid and the retina, provided with a trend towards a decrease of blue light aversion; however, it appeared to be non-significant ($q = 0.1983$, $p = 0.1888$ after 1 hour of exposure; $p = 0.0596$, $q = 0.1136$ after 3 hours of exposure; Fig. 7B). Surprisingly, lidocaine ivt injection significantly decreased the time that mice spent under yellow light. Another possibility for light aversion circuit would be to transmit the phototoxic message from the retina to trigeminal afferents situated near blood vessels by dilatation of the latter. However, the ivt injection of norepinephrine (a vasoconstrictor - norip) did not impact mice behavior (Fig. 7C).

To delineate the neuro-inflammatory circuit underlying the phototoxicity, we checked whether any inflammation was induced in trigeminal pathways. In the trigeminal ganglia (TGs) dissected from blue-illuminated mice, we observed an increase in anti-Iba1 staining as compared to the ones from yellow-light-illuminated mice (Fig. 8A,D). This increase was more noticeable directly after light exposure than after the recovery time; the correspondent (though non-significant) trend was detected by means of RT-qPCR (Fig. 8F). For both illuminations after 3 days of recovery, analysis of mRNA expression revealed a significant increase in cFOS rate (Fig. 8E). Moreover, in blue-illuminated mice after recovery, we detected an increase in ATF3 activation by means of both techniques (Fig. 8B,C).

We then studied whether the inflammation observed in the TGs was transmitted to the spinal trigeminal nucleus or sp5 (Vi/Vc and Vc/C1 transition regions). Here, the RT-qPCR analysis

revealed the same cFOS-pattern as the one observed in the TGs (Fig. 9B). This result was confirmed by immunochemistry; in addition, a slightly more important staining in samples from blue-illuminated mice was observed (Fig. 9A). Increase in microglial activation (anti-Iba1 staining and correspondent mRNA expression) was also detected after both exposures (Fig. 9A,C). ATF3 level did not exhibit any significant difference (Fig. 9D).

Finally, we verified by RT-qPCR whether the phototoxicity induced an over-expression of TGFβ2 and TNFα since both cytokines are known to be highly involved in inflammation. In TGs directly after illumination, TGFβ2 rate was significantly decreased in blue-light samples as compared to the yellow-light ones (Fig. S1A). In brainstems for both light conditions, TGFβ2 expression went down after the recovery time when compared to its after-exposure level (Fig. S1C). In TGs, we did not detect any significant changes in TNFα rate (Fig. S1C); however, in brainstems, its level was importantly increased directly after blue light exposure, but then went down after the recovery period (Fig. S1D).

3 Discussion

Photophobia and specific hypersensitivity to blue light are common symptoms of many ocular diseases, foremost among them the dry eye. This issue has been gaining more attention since the spectra of modern light sources contain an important blue part. Nonetheless, the correspondent underlying mechanisms are still debated (Albilali and Dilli, 2018; K. Digre and K.C. Brennan, 2012; Katz and Digre, 2016; Lupis, n.d.; Marshall J., 2014; Matynia and Gorin, 2013; Text Request, n.d.; Wu and Hallett, 2017). Here, we investigated in vivo the origins and effects of spectrum-dependent photophobia by means of behavioral and pharmacological studies in mice exposed to blue or yellow light.

3.1 Blue light aversion is accompanied by clinical signs of dry eye

3-hour-exposure provoked stable light aversion in blue- but not in yellow-illuminated mice thus proving that this photophobic effect was wavelength-dependent and was not simply induced by bright light of random spectrum. As expected, the fluorescein staining test using slit-lamp examination did not reveal any epithelial damage in the cornea. Indeed, even if the average irradiance that we used (6 mW/cm^2) was strong enough to induce light-aversive behavior, it was still within the range of irradiances one may get from daily sun exposure which is not supposed to noticeably injure the ocular surface. In comparison, to induce a significant increase in corneal fluorescent staining, Lee et al. exposed mice to blue light of 29.2 mW/cm^2 irradiance with the entire radiant exposure of 1000 J/cm^2 while in our experiments it was 64.8 J/cm^2 (Lee et al., 2016). The absence of outward signs cannot guarantee the absence of more intrinsic damage though. IVCM imaging revealed the inflammatory signs in epithelium, sub-basal plexus and stroma of mice exposed to blue light. We found that phototoxically induced inflammation accumulated in the cornea after 3 days of recovery, in line with Feng's study (Feng et al., 2017). Exposure to yellow light did not provide with any important clinical signs of damage: IVCM images of yellow-light-illuminated corneas did not exhibit any significant difference with the naïve mice (Fig. S2). Since we were seeking to investigate the blue-spectrum-specific photophobia, we used the yellow illumination as the control lighting condition for our further experiments.

It has already been reported that physical disruption of the corneal surface and increased corneal nociception correlated with increased light aversion (Matynia et al., 2015). Here we showed that exposure to blue light in itself provided with an increase in corneal mechanical sensitivity. In line

with the IVCM data, this result worsened after the recovery time. In addition, blue light provoked an excessive tearing. This might be ascribed to extra-blinking induced by photophobia (K. Digre and K.C. Brennan, 2012) that in turn provided with greater lacrimation. Our result is in line with those of Lei et al. who reported an increased lacrimation in healthy humans exposed to blue light of 470 nm as compared to their baseline values (Lei et al., 2018). Taken together, these data demonstrate clinically that blue light aversion is accompanied by increased inflammation within the cornea as well as by altered lacrimation reflex. Since these clinical signs are the ones frequently observed in dry eye patients (Belmonte et al., 2017; Bron et al., 2017; The National Eye Institute, 2017), our study confirms that blue light exposure may provoke and/or aggravate the dry eye disease, as it has been supposed previously (Ayaki et al., 2015; Lee et al., 2016; Marek et al., 2018; Niwano et al., 2014).

Retinal mediation in the blue-toxic process

Retina is the most well-known center for photic signal reception, processing and transmission to the brain. Numerous studies demonstrated the phototoxic impact of bright blue light on various retinal structures, in vivo (Feng et al., 2017; Jaadane et al., 2015; Krigel et al., 2016; Lee et al., 2016), ex vivo (Roehlecke et al., 2013), and in vitro (Arnault et al., 2013; Godley et al., 2005; Lascaratos et al., 2007; Marie et al., 2013). That is why we first checked whether our light protocol, less aggressive than the one usually reported and therefore closer to daily light conditions, induced any damage in the retina. Expectedly, by means of immunochemistry and of RT-qPCR, we detected increased activation of macro- (GFAP) and micro- (Iba1) glial cells. Phototoxically-induced inflammation accumulated during 3 days thus resulting in more important signal after the recovery time, in line with previous reports (Feng et al., 2017). The GFAP-stain in our experiments was less pronounced than in the work of Krigel et al. (Krigel et al., 2016) and Feng et al. (Feng et al., 2017) since in our illumination protocol, the irradiance and/or exposure time were much less important. One should note that microglial activation was also detected after exposure to yellow light, probably due to greater illuminance of yellow light as compared to the blue one in terms of photometric units (i.e. in lux, as perceived by the human eye). In addition, in retinal ganglion cells (RGCs), we observed the activation of ATF3, a mediator of cellular stress response and a regulator of cellular proliferation. ATF3 is either not expressed or expressed at very low levels in most intact neurons in vivo (Hunt et al., 2012). Since it is an immediate early stress-inducible gene, we expectedly detected it directly after the end of light exposure. Moreover, it has already been reported that light provided with damage in retinal photoreceptors (Contín et al., 2013; Jaadane et al., 2015; Krigel et al., 2016). Indeed, we observed a morphological degradation of the cone layer in retinas of mice exposed to blue but not to yellow light. Taken together, these results confirm that large-spectral blue light, even of smaller radiant exposure, does provoke retinal inflammation and visual receptors damage.

We then tried to modulate the photophobic behavior by altering the luminous flux that entered the eye. Expectedly, pupil dilatation (atropine instillation) provoked the aversion to yellow light that did not take place previously, in line with the results of Matynia (Matynia et al., 2012). Indeed, starting from a certain threshold, light of any spectrum naturally becomes dazzling. As for the time spent under the blue light, atropine instillation did not decrease it significantly since the smaller flux of light (without atropine) was already sufficient to completely turn mice away from light.

Next, we supposed that light aversion might be overcome by disruption of pathways used by retinal visual receptors. Even if mice injected with the correspondent drug (VR blocker) were blind, the induced absence of image-forming vision did not provide with any significant impact on light-aversive behavior. This result is corroborated by the fact that blind patients (Albilali and Dilli, 2018; K. Digre and K.C. Brennan, 2012) as well as mice with ablated rods and cone photoreceptors (Matynia et al., 2012) can still exhibit the photophobic symptoms. Thus, we concluded that the role

of image-forming vision (and therefore of visual receptors) in mediation of spectrum dependent photophobia is not the major one.

We then investigated whether the non-visual light receptors might be responsible for the photophobic behavior. The most well-known light-sensitive and non-visual retinal pigment is melanopsin (opn4). It is present in 2-3% of RGCs (called intrinsically photosensitive RGC – ipRGC) that regulate circadian rhythms, pupillary light reflex (PLR) and other behavioral and physiological responses to environmental illumination (Berson, 2003). Importance of ipRGC in bright light aversion has been extensively reported by the group of Matynia (Matynia et al., 2015, 2012). In our study, we found that mRNA level of melanopsin was decreased directly after the light exposure when compared to its level after the recovery time. This result is in line with those of Hannibal et al. who reported the decrease in melanopsin mRNA level during exposure to constant light (Hannibal et al., 2005). They also found that illumination decreased melanopsin immunostaining in a time-dependent manner, starting from the distal dendrites and going to the proximal dendrites and the soma. We observed the dotted structure in the dendrites of retinas dissected directly after illumination and the disappearance of anti-melanopsin stain in distal dendrites after the recovery period. This is in compliance with Benedetto et al. who exposed rats to constant light for 2-8 days and observed decreased levels of melanopsin retinal immunoreactivity in distal neurites (Benedetto et al., 2017).

Benedetto et al. also reported the increased levels of anti-neuropsin (anti-opn5) immunolabeling in some cells of GCL and INL. This non-visual photoreceptor is gaining today an increasing attention. Its presence and importance for photoentrainment have been discovered in the retina and cornea; however, its precise functions are still not clear (Buhr et al., 2015; Guido et al., 2011). Nonetheless, role of opn5 in photophobia management might be suspected from some recent studies (Hughes et al., 2016; Matynia et al., 2017). We therefore checked the status of neuropsin by immunochemistry and RT-qPCR but did not find any significant differences between the two spectra. This discrepancy could be due to the fact that Benedetto et al. observed increasing levels of neuropsin after 4 days of exposure to light while we illuminated mice only during 3 hours. In addition, the illumination protocol we used was much different from their one (in terms of light spectrum, irradiance and exposure time).

Thus, we hypothesized that melanopsin might be the main blue-light mediator for photophobia. We performed a behavioral test with mice injected with melanopsin antagonist reported to specifically modify melanopsin-dependent light responses including the PLR and light aversion (Jones et al., 2013; Sikka et al., 2014). Indeed, such injection did significantly reduce the blue light aversion. Interestingly, it did not provoke the yellow-light aversion like atropine instillation even if this antagonist is supposed to dilate the pupil. The reason is that the action of antagonist on the PLR is shorter than on the ipRGC activity itself (Jones et al., 2013). Thus, it did not alter significantly the ipRGC-independent behavior of mice under yellow light while reducing the ipRGC-dependent blue-light aversion.

In addition, we measured corneal mechanical sensitivity (von Frey hair test) in mice that were injected with melanopsin antagonist before light exposure. Strikingly, we found that in these mice, corneal sensitivity did not increase as it did in naïve ones (Fig. 10). This result is in compliance with the study of Matynia (Matynia et al., 2015); again, it highlights the crucial role of melanopsin in corneal nociception.

3.2 Implication of out-retinal melanopsin and activation of trigeminal pathways

The retina is not the only mammalian tissue that contains melanopsin. This photopigment was also found in iris (Xue et al., 2012) and in blood vessels (Sikka et al., 2014). The team of Matynia

discovered that melanopsin was expressed in 3% of small TG neurons localized in the ophthalmic branch of the trigeminal nerve, and reported their intrinsic photosensitivity (Matynia et al., 2016). Very recently, Delwig et al. discovered the previously unrecognized localization of this photopigment in nerve fibers within the cornea (Delwig et al., 2018). In our preliminary immunochemistry and electrophoresis experiments, we had detected the presence of melanopsin in the cornea, TGs and brainstem (data not shown).

We were then wondering whether the non-retinal melanopsin-containing tissues might have a role in mediation of blue light photophobia. We performed a behavioral test to assess light aversion in mice instilled with oxybuprocaine. This topical anesthetic numbed the entire surface of the eye thus silencing all the melanopsin-expressing nociceptive neurons it might contain. We did not observe any difference in oxybuprocaine-instilled mice as compared to PBS-instilled ones. According to our clinical practice, oxybuprocaine has a peak in action in 1-15 minutes after the instillation; the correspondent anesthetic effect lasts till 45 minutes. To make sure that we did not miss any short-term effect that oxybuprocaine might have provided with, we checked the results of behavioral test at various time points within the first hour; however, we still did not observe any important difference (Fig. S3A). This result is in accordance with those of Lei et al. who found that topical ocular anesthesia did not alter the psychophysical photophobia thresholds for either blue or red light in humans (Lei et al., 2018b). Moreover, Delwig et al. reported the absence of light responses in the melanopsin-expressing corneal fibers (Delwig et al., 2018). Thus, we may conclude that nerve fibers within the cornea make little contribution, if any, to photophobia.

Next, we investigated the role of photophobic pathways proposed by Okamoto et al. (Okamoto et al., 2012, 2011, 2009; Rahman et al., 2015). According to the authors, light signal, firstly received and processed by the retina, could then activate intraocular TG nerves. This might happen either by transmitters released from parasympathetic postganglionic neurons or, for those fibers apposed to blood vessels, by mechanical deformation of the latter due to changes in blood flow. To check these hypotheses, we injected mice intravitreally either with lidocaine, which blocks the nociceptive trigeminal near-retinal afferents that might be present within the eye, or norepinephrine that constricts potentially dilated blood vessels. None of these pharmacological treatments provided with a significant change in behavior under blue light. According to Okamoto et al., the effect of lidocaine and norepinephrine disappeared in 40-50 minutes after injection, so we checked the behavior at shorter time periods. We still did not observe anything significant (Fig. S3B,C), in disagreement with this group who reported the complete block of light-evoked neural activity. Nevertheless, in our results, one should note the trend for blue-light aversion decrease. Again, we might put down this discrepancy to important differences in experimental protocols, either in illumination (they used 30s white light stimuli of 10^4 lux) or in light impact assessment (electrophysiology). Surprisingly, in our study, lidocaine injection induced yellow light aversion. According to our clinical practice, anesthetic intravitreal lidocaine injection may make patients slightly blind. Indeed, lidocaine blocks the voltage-gated Na channels; in addition to the nociceptive afferents, these channels are present in amacrine cells that participate in the integration of visual signals the retina (Tian et al., 2010). By measuring the optokinetic response, we verified that in mice, lidocaine ivt injection induced significant blindness as compared to control or norepinephrine ivt injection (data not shown). We therefore supposed that lidocaine-injected mice were not able to detect yellow light anymore, thus spending approximately half of illumination time in the dark and another half in the light part of the box.

The group of Okamoto also observed light-induced neuronal activation in trigeminal brainstem of rats (Okamoto et al., 2009). In humans during photophobia periods, Moulton et al. reported fMRI-detected specific activation patterns at the level of the TG, trigeminal nucleus caudalis, and ventroposteromedial thalamus (Moulton et al., 2009). In our team, we already reported an activation

of trigeminal pathways in response to corneal inflammation (Launay et al., 2016). Accordingly, in the current study, we observed important immuno-activation in the TGs and brainstems. For both structures, neuronal inflammation appeared after 3 days of recovery; this latency may mean that neurons of trigeminal pathway were activated indirectly.

3.3 Probable pathways of blue light photophobia

To our knowledge, it is the first in vivo study to report the spectral selectivity of photophobia, in light conditions close to that of the daily living, inferred from behavior assessment supplemented by various pharmacological treatments. Taken together, our results demonstrate that blue light photophobia is mainly mediated by melanopsin-containing cells and does not rely on visual receptors. Although the ocular surface exhibited phototoxically-induced dry eye signs of inflammation and melanopsin-dependent mechanical sensitivity, the intra-corneal trigeminal fibers appear to have a minimal role in intrinsic photosensitivity, if any. Nevertheless, the phototoxic process necessarily implicates the trigeminal nerves since light induced inflammation in the TGs and brainstems. That should mean that the photic signal is received by the ipRGC and then somehow transmitted to the trigeminal pathways, simultaneously inducing the phototoxic stress in the retina. According to our results, this process doesn't implicate the blood flow alterations. Phototoxic message transfer might happen by means of light-induced transmitters released to intraocular TG afferents at the posterior part of the eye; however, this pathway did not appear to be the main one.

There are other possibilities to transmit the phototoxic message from the retina to the trigeminal system. First, the group of Matynia proposed the ipRGC-independent alternative pathway of light avoidance that was unmasked by morphine sensitization (Matynia et al., 2017, 2012); however, the precise operation of this circuit remains to be clarified. Second, Dolgonos et al. suggested an intra-retinal processes, independent on central visual centers, that could produce an enhanced trigeminal response to light (Dolgonos et al., 2011). They proposed that so-called associational retinal ganglion cells, that did not enter the optic nerve, extended into the retinal periphery near the ciliary body. Since this region is richly innervated with trigeminal nociceptors, associational RGC might directly sensitize the neurons of sp5. Third, we cannot exclude the probable role of iris that was reported to contain melanopsin (Xue et al., 2012). Since the iris is innervated by the trigeminal sensory fibers (McDougal and Gamlin, 2015), it would be able to receive and transmit the photic signal in the trigeminal system. In our experiments, these last two pathways were not affected by lidocaine injection since its numbing action might be strongly attenuated while spreading through the vitreous body and the choroid. In addition, although it was initially believed that the retina lacked trigeminal sensory innervation (Albilali and Dilli, 2018), recently Warfinge et al. reported that nerves originating from the TGs did innervate the retina (Warfvinge et al., 2018). Moreover, this group has already detected the presence of CGRP neuropeptide in the rat retina (Blixt et al., 2017). In our experiments, we also observed anti-CGRP immunostaining in GCL and INL (Fig. S4). These findings support the possibility of direct communication between the TGs and ipRGC. Further investigations of retina-TGs connections would allow for better understanding of blue-light aversive behavior mechanisms and consequently for better and targeted treatment for photophobic patients.

4 Materials and methods

4.1 Animals

Adult male C57BL/6 mice (30 g; Janvier Labs, Le Genest Saint Isle, France) were maintained under controlled conditions (22 ± 1 °C, 60 ± 10% relative humidity, 12/12 h light/dark cycle, food and

water ad libitum). All experiments were approved by the Charles Darwin Ethics Committee for Animal Experimentation (Ce5/2011/05) and carried out in accordance with Directive 2010/63/EU of the European Parliament and the Council of 22 September, 2010 and French law (2013/118).

Before the beginning of all the experiments, mice spent 1 week in standard conditions of animal facility; during this period, they were daily handled to be habituated to the experimenter. Animals were weighted before treatment and at the end of the experiments.

4.2 Light protocol (Fig. 1)

Mice were illuminated for 3 hours by custom-mounted commercial LED sources (AVAB Transtechnik France, St. Denis, France) of blue and yellow spectra (Fig. 1A); the corresponding characteristics are summarized in the Table 1. All the experiments were performed either directly after the end of light exposure or in 3 days of recovery in standard lighting conditions of animal facility. For the clinical assessments, RT-qPCR and immunohistochemistry, mice were placed in separate compartments of mirrored-wall cages. For the behavioral tests, mice were placed in separate half-illuminated boxes where they could move freely between illuminated and darkened parts (Fig. 1C). For every experiment, cages and boxes were carefully cleaned. Mice were not able to observe each other or to interact.

4.3 Behavior tests (Fig. 1C)

To acclimatize to the experiment conditions, mice were placed in half-illuminated boxes 10 minutes before the start of exposure. Animals were filmed during all the time of illumination. For every hour, time spent in the illuminated part of the box was calculated for the following representative periods: 0 – 5, 20 – 25, 40 – 45 and 55 – 60 minutes; the values were then summed up.

4.4 Pharmacology

Applied drugs are described in the Table 2. All the instillations and ivt injections were performed bilaterally. Instillation volume corresponded to 1 drop per eye (delivered by a micropipette). For ivt injections, the animal was anesthetized by means of isoflurane (5% then 2%), then the globe was pierced through the sclera posterior to the limbus by a 30 gauge needle, than the drug (2 µl/eye) was delivered from a 33 gauge needle.

To prepare the “visual receptor blocker” (VR blocker) drug, 40 mM of L-AP4 (Tocrys, Biotechne, Lille, France) was mixed with 200 mM of PDA (Abcam, Paris, France). L-AP4 (L-(+)-2-Amino-4-phosphonobutyric acid) is a glutamate receptor agonist and therefore blocks synaptic transmission at the synapse between photoreceptors and ON bipolar cells. PDA (2,3 cis-Piperidine dicarboxylic acid) is an ionotropic receptor antagonist; it suppresses transmission at the synapse between photoreceptors and OFF bipolar cells and horizontal cells (Bush and Sieving, 1994). For each eye, 0.25 ul of this solution was added to 1.75 ul of PBS.

Opn4 antagonist was diluted in DMSO, as proposed by the supplier; applied concentration was 30 mg/kg that resulted in 50-60 µl per animal approximately.

4.5 Clinical assessment

The following clinical assessments were implemented one after another either directly after the end of illumination or after 3 days of recovery in standard lighting conditions.

- Corneal mechanical sensitivity (von Frey hair test)

Mechanical stimulation was performed with calibrated von Frey hairs of increasing force (0.008 – 0.07 g) applied for 1 s to the cornea (de Castro et al., 1998). The response to the stimuli was determined as positive when the mouse presented a complete blink.

- Tear volume (phenol red test)

Tear production was measured with the phenol red thread test (Zone-Quick; Lacrimedics, Eastsound,WA). The threads were placed in the lateral canthus of the conjunctival fornix of the eye for 30 s as previously described (Launay et al., 2016). The thread is initially yellow in color (acidic); when exposed to tears, it changes its color to a red one. After 30 s, the "tear distance" (in millimeters) was determined using a provided scale.

- In vivo confocal microscopy (IVCM)

A laser-scanning in vivo confocal microscope (IVCM, Heidelberg Retina Tomography (HRT)) with II/Rostock CorneaModule (RCM) (Heidelberg Engineering, GmbH, Heidelberg, Germany) was used to examine the entire cornea of anesthetized mice (by ip injection of 150 µL mixture of Ketamine 1000 U (100 mg/kg body weight) and xylazine (10 mg/kg bodyweight) (Virbac, France)) as described previously (Launay et al., 2016). Shown images illustrate the representative state of corneal layers for all the animals.

4.6 RT-qPCR

Mice were deeply anesthetized with 200 µL mixture of Ketamine 1000 U (100 mg/kg body weight) and xylazine (10 mg/kg bodyweight) (Virbac, France) injected intraperitoneally. Animals were then perfused with cold (4ºC) 10 mL 0.9% NaCl solution and the retinas, TGs and brainstems were carefully dissected and placed immediately in liquid nitrogen until the extraction procedure.

RNAs were extracted from TGs, retinas and brainstems using the Macherey-Nagel NucleoSpin RNA extraction kit, according to the manufacturer's protocol. (Macherey-Nagel, Düren, Germany). RNA quality and quantity were assessed using a ND-1000 spectrophotometer (Thermo Scientific, Waltham, Massachusetts, USA). cDNA was further synthesized from equal amounts of RNA using Multiscribe reverse transcriptase (TaqMan Reverse Transcription Reagents, Applied Biosystems, Life Technologies, Carlsbad, CA, USA) according to the manufacturer's protocol. Finally, cDNA were diluted in DNAse/RNAse free water (Gibco) to a final concentration of 5 ng/µL. Real-time quantitative PCR was performed with 25 ng of cDNA added to a 15 µL solution of Applied Biosystems Mastermix (TaqMan Universal PCR Master Mix) and primers to a final volume of 20 µL. All primers and reagents were purchased from Applied Biosystems: GAPDH (Mm99999915.m1), ATF3 (Mm00476032.m1), FOS (Mm00487425.m1), GFAP (Mm01253033.m1), Iba1 (Mm00479862.g1), opn4 (Mm00443523.m1), opn5 (Mm00710998.m1), TNF-α (Mm99999068.m1), and TGFβ2 (Mm00436955.m1). Target cDNA was amplified using the 7300 Real-Time PCR system (Applied Biosystems). Changes in mRNA expression were calculated as $\Delta\Delta Ct = \Delta Ct_{illuminated} - \Delta Ct_{control}$ with $\Delta Ct = Ct_{target\_gene} - Ct_{HK\_gene}$. Ct means cycle threshold and HK_gene means housekeeping gene (GAPDH). Tissues of yellow-illuminated mice dissected directly after light exposure were taken as controls. Since our aim was to investigate the spectral characteristics of photophobia and especially its blue specificity, normalization to the gene expression rates of naïve non-illuminated mice would not provide us with the information relevant to the scope of this study.

4.7 Immunochemistry

Mice were deeply anesthetized with 200 µL mixture of Ketamine 1000 U (100 mg/kg body weight) and xylazine (10 mg/kg bodyweight) (Virbac, France) injected intraperitoneally. Animals were then perfused via the ascending aorta with 5 mL of 0.9% NaCl solution followed by 30 mL of 4%

paraformaldehyde solution. After fixation, brain, trigeminal ganglia, and eyes were carefully dissected out and post-fixed 48 h in the same fixative. Free-floating sections (40 μm) of the trigeminal subnucleus complex were performed by vibratome (Leica, Germany). Retinas were dissected form the eyes. The TGs and retinas were placed sequentially in 10, 20 and 30 % sucrose solution in 1× PBS, overnight for each treatment, immerged in 7.5 % gelatin and 10 % sucrose for TGs and in OCT (Tissue-Tek® O.C.T. Compound, Sakura® Finetek) for retinas and finally frozen in liquid nitrogen. Cryostat sections (Leica, Germany) of 12 μm were then performed and mounted on Superfrost slides; sections were kept at −20 °C until use.

After three washes in 1× PBS, tissues were placed in a blocking buffer (3% normal donkey serum, 0.3% triton) for 2 h, then incubated at 4 °C for 48 h (floating sections) or 24 h (cryostat sections) with the following primary antibodies diluted in blocking buffer: goat anti-Fos (4)-G (Santa Cruz Biotechnology, sc-52-G, 1/500), rabbit anti-ATF3 (Santa Cruz Biotechnology, sc-188, 1/500), chicken anti-GFAP (ThermoFisher Scientific, PA1-10004, 1/1000), rabbit anti-Iba1 (Wako, 019-19742, 1/500), rabbit anti-opn4 (ATS, AB-N39, 1/500), rabbit anti-opn5 (Biorbyt, orb223499, 1/500), rabbit anti-Cone Arrestin (Merck, AB15282, 1/10000). For revelation, cells were incubated with the corresponded Alexa Fluor secondary antibodies (1:500 in PBS, Invitrogen) for 1 hour at RT.

We did not succeed in making work the anti-cFOS staining in TGs (frozen sections) and anti-ATF3 staining in brainstem (floating sections) although we tried various antibodies available on the market.

For all the immunostainings, negative control experiments (without incubation with a primary antibody) were performed, in order to ensure the absence of non-specific fluorescent signal. DAPI coloration is not presented to allow for better visualization of immunostaining of interest.

4.8 Imaging

Samples were imaged with the microscope AXIO Imager.M1 (Zeiss, Germany). Images were recorded via provided ZEN software and then processed with the Fiji (ImageJ version). Identical exposure settings, that minimized oversaturated pixels in the final images, were used for both illumination and recovery (or not) conditions.

4.9 Statistical analysis

All the experiments were performed on minimum 8 animals in every group. Statistical analysis was done using GraphPad (GraphPad Software, La Jolla, CA, USA). Two-way ANOVA analysis with repeated or non-repeated measures followed by False Discovery Rate multiple correction (two-stage step-up method of Benjamini, Krieger and Yekutieli, false discovery rate Q = 0.05) were used. All the data are presented as mean ± SEM. Differences were considered significant when $p < 0.05$ (*/^), $p < 0.01$ (**/^^), $p < 0.001$ (***/^^^) or $p < 0.0001$ (****/^^^^). ^! sign means that the difference was significant according to GraphPad software, although the p-value was slightly above 0.05. Blue and yellow bars correspond to blue and yellow exposures respectively. Red color means increase and blue color decrease in values.

4.10 Tables

	waveband	average irradiance	radiant exposure	average illuminance
blue	400 – 500 nm	6 mW/cm^2	64.8 J/cm^2	400 lux
yellow	530 – 710 nm	6 mW/cm^2	64.8 J/cm^2	3500 lux

Table 1. Spectral and intensity characteristics of customized light source.

drug	reference	time before exposure	method of use	literature
PBS	Life technologies, Carlsbad, CA, USA	directly before	instillation or ivt injection	NA
atropine sulphate 1%	Europhta, Monaco	5 minutes	instillation	(Matynia et al., 2012; Okamoto et al., 2011)
pilocarpine nitrate 1%	Europhta, Monaco	15 minutes	instillation	NA
visual receptors (VR) blocker	see below	5 minutes	ivt injection	(Bush and Sieving, 1994), Gregory Gauvain (personal communication)
opn4 antagonist 30 mg/kg	Merck, St Quentin en Yvelines, France	15 minutes	ip injection	(Jones et al., 2013; Xue et al., 2012)
DMSO HYBRI-MAX	Sigma-Aldrich, St. Louis, MO, USA	15 minutes	ip injection	NA
oxybuprocaine hydrochloride 1.6 mg / 0.4 ml	Thea, Clermont-Ferrand, France	directly before	instillation	NA
lidocaine hydrochloride 2%	Aguettant, Lyon, France	5 minutes	ivt injection	(Okamoto et al., 2011)
DL-norepinephrine hydrochloride 10mM	Sigma-Aldrich, St. Louis, MO, USA	5 minutes	ivt injection	(Okamoto et al., 2011)

Table 2. Name, manufacturer, method and time of application (relative to the beginning of light exposure) and bibliographic reference (if applicable). NA – not applicable

5 Legends to main figures

Figure 1. Custom-mounted illumination system.

A. Illumination system and relative spectra of LED sources.

B. When placed together (and not in separate compartments), mice exposed to blue illumination demonstrated light aversion by hiding behind each other; such behavior did not take place for yellow exposure.

C. Behavior test: mice are placed in half-illuminated boxes and allowed to move freely. As in the previous figure, mice exposed to blue illumination demonstrated a strong light aversion, as compared to the yellow one under which animals prefered to stay.

Figure 2. Clinical assessments

Measurements were made at 3 time points: *before hv* – before the beginning of illumination, *after hv* – directly after 3 hours of illumination, recovery 3d – after 3 days of recovery in standard illumination conditions of animal unit.

A. Measurement of corneal mechanical sensitivity performed by means of von Frey hair test. Greater values mean lower corneal sensitivity. Statistical significance:

- blue illumination group: before hν vs after hν – q = 0.0361, p = 0.1031; before hν vs recovery 3d – q = 0.0003, p = 0.003; after hν vs recovery 3d – q = 0.0136, p = 0.0260;
- recovery 3d group: blue vs yellow – q = 0.0041, p = 0.0020.

B. Measurement of tear quatity performed by means of phenol red thread test placed into the eye for 30 seconds. Greater distances mean more important lacrimation. Statistical significance for the blue illumination group: before hν vs after hν – q = 0.0403 , p = 0.0192; before hν vs recovery 3d – q = 0.0498, p = 0.0475.

Blue and yellow bars correspond to blue and yellow exposures respectively. All the data are presented as mean ± SEM. Differences were considered significant when $p < 0.05$ (*/^), $p < 0.01$ (**/^^), $p < 0.001$ (***/^^^) or $p < 0.0001$ (****/^^^^). Stars correspond to comparisons between values at different time points, within one spectrum. Carets correspond to comparison between blue-illuminated and yellow-illuminated mice, at the same time point. Red color means increase and blue color decrease in values.

Figure 3. IVCM results

Representative images of non-invasive IVCM examination performed directly after exposure to light (A, no recovery) or after 3 days of recovery in standard illumination conditions of animal unit (B, recovery). Alterations were observed in the three following corneal layers: superficial epithelium (cell nuclei in blue-illuminated mice became more hyperreflective), sub-basal plexus (dendritic cells are marked by circles) and stroma (activated keratocytes are marked by arrows).

Figure 4. Light-provided retinal inflammation

A-C. Immunohistochemistry was performed on the retinas of blue- (b) and yellow-exposed (y) mice either immediately after illumination (nRec) or in 3 days of recovery (Rec). Results of anti-GFAP (A), anti-ATF3 (B, immunoactivated cells are marked by arrows) and anti-Iba1 (C, imunoactivated cells are marked by arrows) stainings are presented. Magnification is 10x (A,B) and 20x (C), scale bars correspond to 100 μm.

D-F. Results of RT-qPCR analysis on the retinas: mRNA expression of GFAP (D), ATF3 (E) and Iba1 (F). Statistical significance:

- GFAP: blue no recovery vs recovery – q = 0.0101, p = 0.0096; recovery blue vs yellow – q = 0.0074, p = 0.0070;
- ATF3: blue no recovery vs recovery – q = 0.0230, p = 0.0219; no recovery blue vs yellow – q = 0.0057, p = 0.0054;
- Iba1: blue no recovery vs recovery – q = 0.0118, p = 0.0113; yellow no recovery vs recovery – q = 0.0428, p = 0.0814.

Blue and yellow bars correspond to blue and yellow exposures respectively; clear and hatched bars correspond to the time points of mice dissection, either directly after illumination (no recovery) or in 3 days of recovery (recovery) respectively. All the data are presented as mean ± SEM. Differences were considered significant when $p < 0.05$ (*/^), $p < 0.01$ (**/^^), $p < 0.001$ (***/^^^) or $p < 0.0001$ (****/^^^^). Stars correspond to comparisons between blue-illuminated and yellow-illuminated mice, within one recovery or non-recovery group. Carets correspond to comparison of mice assessed directly after illumination to the ones assessed after 3 days of recovery, within the same spectra. Red color means increase and blue color decrease in values.

Figure 5. Retina-related behavioral tests.

Graphs illustrate the time spent in the illuminated part of the box during the chosen representative periods. For more detail see Materials&Methods section.

A. Pupils were dilated with atropine (atro) or constricted with pilocarpine (pilo). 1 drop per eye was instilled (inst) bilaterally 5 minutes before the start of light exposure (1st hour: PBS blue vs yellow – $q = 0.0004$, $p = 0.0003$; pilo blue vs yellow – $q = 0.0057$, $p = 0.0108$; yellow PBS vs atro – $q < 0.0001$, $p < 0.0001$; 3 hours: PBS blue vs yellow – $q < 0.0001$, $p < 0.0001$; pilo blue vs yellow – $q = 0.0006$, $p = 0.0012$; yellow PBS vs atro – $q < 0.0001$, $p < 0.0001$).

B. Visual receptors' pathway was blocked (VR blocker). 2µl of drug (the composition is described in Materials&Methods section) was injected intravitreally (ivt) bilaterally 5 minutes before the start of light exposure (1st hour: PBS blue vs yellow – $q = 0.0006$, $p = 0.0012$; VR blocker blue vs yellow – $q = 0.0090$, $p = 0.0086$; 3 hours: PBS blue vs yellow – $q < 0.0001$, $p < 0.0001$; VR blocker blue vs yellow – $q = 0.0003$, $p = 0.0002$).

C. Melanopsin antagonist was injected (opn4 antago) intraperitoneally (ip, 30 mg/kg) 15 minutes before the start of light exposure (1st hour: blue DMSO vs opn4 antago – $q = 0.0223$, $p = 0.0212$; DMSO blue vs yellow – $q = 0.0123$, $p = 0.0117$; 3 hours: blue DMSO vs opn4 antago – $q = 0.0155$, $p = 0.0147$; DMSO blue vs yellow – $q = 0.0128$, $p = 0.0122$).

Blue and yellow bars correspond to blue and yellow exposures respectively; clear bars and hatched bars correspond to animals with control (vehicle – PBS or DMSO) or specific drug treatments, respectively. All the data are presented as mean ± SEM. Differences were considered significant when $p < 0.05$ (*/^), $p < 0.01$ (**/^^), $p < 0.001$ (***/^^^) or $p < 0.0001$ (****/^^^^). Stars correspond to comparisons between blue-illuminated and yellow-illuminated mice, treated with the same drug. Carets correspond to comparisons between control and drug-treated animals. Red color means increase and blue color decrease in values. For the results close to be significant, correspondent p and q values are marked on the graph.

Figure 6. Role of retinal light receptors.

A-C. Immunohistochemistry was performed on the retinas of blue- (b) and yellow-exposed (y) mice either immediately after illumination (nRec) or in 3 days of recovery (Rec). Results of anti-Cone Arrestine (A, "holes" in cone layer are marked by arrows), anti-opn4 (B, dotted structure of ipRGC prolongations is pointed by arrows) and anti-opn5 (C, localization of neuropsin-expressing cells is circled) stainings are presented. For A and B, insets with higher zoom are provided. Magnification is 20x (A,C) and 10x (B), scale bars correspond to 100 µm.

D-F. Results of RT-qPCR analysis on the retinas: mRNA expression of opn4 (D; blue no recovery vs recovery – $q = 0.0174$, $p = 0.0166$; yellow no recovery vs recovery – $q = 0.0499$, $p = 0.0951$) and opn5 (E). Blue and yellow bars correspond to blue and yellow exposures respectively; clear and hatched bars correspond to the time points of dissection, either directly after illumination (no recovery) or in 3 days of recovery (recovery) respectively. All data are presented as mean ± SEM. Differences were considered significant when $p < 0.05$ (*/^), $p < 0.01$ (**/^^), $p < 0.001$ (***/^^^) or $p < 0.0001$ (****/^^^^). Carets correspond to comparison of mice assessed directly after illumination to the ones assessed after 3 days of recovery, within the same spectra. Red color means increase and blue color decrease in values.

Figure 7. TGs-related behavioral tests.

Graphs illustrate the time spent in the illuminated part of the box during the chosen representative periods. For more detail see Materials&Methods section.

A. Ocular surface was anesthetized with oxybuprocaine (oxybu). 1 drop per eye was instilled (inst) bilaterally directly before the start of light exposure (1st hour: PBS blue vs yellow – $q = 0.0008$, $p = 0.0008$; oxybu blue vs yellow – $q < 0.0001$, $p < 0.0001$; 3 hours: PBS blue vs yellow – $q < 0.0001$, $p < 0.0001$; oxybu blue vs yellow – $q = 0.0001$, $p = 0.0001$).

B. Intraocular trigeminal afferents were anesthetized with lidocaine (lido). 2µl of drug was injected intravitreally (ivt) bilaterally 5 minutes before the start of light exposure (1st hour: PBS blue vs yellow – $q = 0.0007$, $p = 0.0006$; 3 hours: yellow PBS vs lido – $q = 0.0210$, $p = 0.0200$; PBS blue vs yellow – $q = 0.0004$, $p = 0.0003$).

C. Intraocular blood vessels were constricted with norepinephrine (norip). 2µl of drug was injected intravitreally (ivt) bilaterally 5 minutes before the start of light exposure (1st hour: PBS blue vs yellow – $q = 0.0003$, $p = 0.0003$; norip blue vs yellow – $q < 0.0001$, $p < 0.0001$; 3 hours: PBS blue vs yellow – $q < 0.0001$, $p < 0.0001$; norip blue vs yellow – $q < 0.0001$, $p < 0.0001$).

Blue and yellow bars correspond to blue and yellow exposures respectively; clear bars and hatched bars correspond to animals with control (vehicle – PBS) or specific drug treatments respectively. All the data are presented as mean ± SEM. Differences were considered significant when $p < 0.05$ (*/^), $p < 0.01$ (**/^^), $p < 0.001$ (***/^^^) or $p < 0.0001$ (****/^^^^). Stars correspond to comparisons between blue-illuminated and yellow-illuminated mice, treated with the same drug. Carets correspond to comparisons between control and drug-treated animals. Red color means increase and blue color decrease in values. For the results close to be significant, correspondent p and q values are marked on the graph.

Figure 8. Phototoxicity marks in TGs.

A, B, D. Immunohistochemistry was performed on the TGs of blue- (b) and yellow-exposed (y) mice either immediately after illumination (nRec) or in 3 days of recovery (Rec). Results of anti-Iba1 (A, D; yellow arrows indicate immunoreactive cells; spots of important microglial accumulation are labeled by orange arrows) and anti-ATF3 (B, arrows indicate immunoreactive cells) stainings are presented. Magnifications are 10x (A, B) and 20x (D), scale bars correspond to 100 µm.

C, E, F. Results of RT-qPCR analysis on the TGs: mRNA expression of ATF3 (D), cFOS (E) and Iba1 (F). Statistical significance:

- ATF3: blue no recovery vs recovery – $q = 0.0076$, $p = 0.0072$; recovery blue vs yellow – $q = 0.0243$, $p = 0.0231$;
- cFOS: blue no recovery vs recovery – $q = 0.0129$, $p = 0.0061$; yellow no recovery vs recovery – $q = 0.0339$, $p = 0.0323$.

Blue and yellow bars correspond to blue and yellow exposures respectively; clear and hatched bars correspond to the time points of mice dissection, either directly after illumination (no recovery) or in 3 days of recovery (recovery) respectively. All the data are presented as mean ± SEM. Differences were considered significant when $p < 0.05$ (*/^), $p < 0.01$ (**/^^), $p < 0.001$ (***/^^^) or $p < 0.0001$ (****/^^^^). Stars correspond to comparisons between blue-illuminated and yellow-illuminated mice, treated with the same drug. Carets correspond to comparison of mice assessed directly after illumination to the ones after 3 days of recovery, within the same spectra. Red color means increase and blue color decrease in values.

Figure 9. Phototoxicity marks in brainstem.

A. Immunohistochemistry was performed on the brainstems of blue- (b) and yellow-exposed (y) mice either immediately after illumination (nRec) or in 3 days of recovery (Rec). Results of double anti-Iba1 and anti-cFOS staining are presented. Iba1-immunoreactive cells are indicated by yellow arrows, cFOS-activated neurons are labeled by orange arrows. Scale bar corresponds to 100 μm.

B-D. Results of RT-qPCR analysis on the brainstems: mRNA expression of cFOS (B; blue no recovery vs recovery – $q < 0.0001$, $p < 0.0001$; yellow no recovery vs recovery – $q < 0.0001$, $p < 0.0001$), Iba1 (C) and ATF3 (D).

Blue and yellow bars correspond to blue and yellow exposures respectively; clear and hatched bars correspond to the time points of dissection, either directly after illumination (no recovery) or in 3 days of recovery (recovery) respectively. All the data are presented as mean ± SEM. Differences were considered significant when $p < 0.05$ (*/^), $p < 0.01$ (**/^^), $p < 0.001$ (***/^^^) or $p < 0.0001$ (****/^^^^). Carets correspond to comparison of mice assessed directly after illumination to the ones assessed after 3 days of recovery, within the same spectra. Red color means increase and blue color decrease in values.

Fig. 10. Role of melanopsin in corneal sensitivity.

Measurement of corneal mechanical sensitivity performed by means of von Frey test. Greater values mean lower corneal sensitivity. Test was performed in naïve mice (clear bars, the same results as the ones presented in the Fig. 2) and in mice intraperitoneally (ip, 30 mg/kg) injected with melanopsin antagonist (opn4 antago) 15 minutes before the start of the test. For more detail see Material&Method section.

Statistical significance for the recovery 3d group: blue naïve vs yellow naïve – $q = 0.0010$, $p = 0.0010$, blue naïve vs blue antago opn4 – $q = 0.0008$, $p = 0.0005$, blue naïve vs yellow antago opn4 – $q = 0.0004$, $p = 0.0001$.

Measurements were made at 3 time points: *before hv* – before the beginning of illumination, *after hv* – directly after 3 hours of illumination, recovery 3d – after 3 days of recovery in standard illumination conditions of animal unit. Blue and yellow bars correspond to blue and yellow exposures respectively. All the data are presented as mean ± SEM. Differences were considered significant when $p < 0.05$ (^), $p < 0.01$ (^^), $p < 0.001$ (^^^) or $p < 0.0001$ (^^^^).

6 Abbreviations and conventional signs

antago – antagonist (on the behavioral tests graphs)
atro – atropine (on the behavioral tests graphs)
b – blue – blue-illuminated mice (on immunochemistry images)
GCL – ganglion cell layer
INL – inner nuclear layer
ip – intraperitoneal
ipRGC – intrinsically photosensitive RGC
IVCM – in vivo confocal microscopy
ivt – intravitreal
lido – lidocaine (on the behavioral tests graphs)
norip – norepinephrine (on the behavioral tests graphs)

ONL – outer nuclear layer
oxybu – oxybuprocaine (on the behavioral tests graphs)
pilo – pilocarpine (on the behavioral tests graphs)
PLR – pupillary light reflex
nRec – no recovery – assessment directly after illumination (on the immunochemistry images)
Rec – recovery – assessment after 3 days of recovery (on the immunochemistry images)
RGC – retinal ganglion cells
RPE – retinal pigment epithelium
sp5 – spinal trigeminal nucleus
TG – trigeminal ganglion
VR – visual receptors
y – yellow – yellow-illuminated mice (on the immunochemistry images)

7 Conflict of Interest

Authors VM and TV are employed by company Essilor International. All other authors declare no competing interests.

8 Author Contributions

VM and SMP conceived and designed the work. VM performed the experiments, analyzed and interpreted the results of experiments and wrote the manuscript. ER, JDC, AC, ARLG and SMP were involved in experiments realization. TV, AD and CB were involved in the design of the study. ARLG and SMP reviewed the manuscript.

9 Funding

This work was funded by Essilor International, within the frame of research collaboration with Sorbonne Université / Institut de la Vision.

10 Acknowledgments

We are grateful to Grégory Gauvin for visual receptors blocker preparation and for helpful discussions. We thank Darine Fakih, Sébastien Augustin, Karima Kessal, Hong Liang, Stéphane Fouquet, Quénol Cesar and Manuel Simonutti for technical assistance and Elena Brazhnikova, Coralie Barrau and William Rostène for the insightful comments and advices. We also thank the animal facility and imaging platforms at the Institut de la Vision.

11 Bibliography

Albilali, A., Dilli, E., 2018. Photophobia : When Light Hurts, a Review. Curr. Neurol. Neurosci. Rep. 18, 4–9.

Arnault, E., Barrau, C., Gondouin, P., Bigot, K., Villette, T., Picaud, S., Cohen-tannoudji, D., 2013. Phototoxic Action Spectrum on a Retinal Pigment Epithelium Model of Age-Related Macular Degeneration Exposed to Sunlight Normalized Conditions. PLoS One 8. https://doi.org/10.1371/journal.pone.0071398

Ayaki, M., Niwano, Y., Kanno, T., Tsubota, K., 2015. Blue light induces oxidative damage in human ocular surface cells in culture. ARVO 2015 Annu. Meet. Abstr.

754 Belmonte, C., Nichols, J.J., Cox, S.M., Brock, J.A., Begley, C.G., Bereiter, D.A., Dartt, D.A., Galor,
755 A., Hamrah, P., Ivanusic, J.J., Jacobs, D.S., McNamara, N.A., Rosenblatt, M.I., Stapleton, F.,
756 Wolffsohn, J.S., 2017. TFOS DEWS II pain and sensation report. Ocul. Surf. 15, 404–437.
757 https://doi.org/10.1016/j.jtos.2017.05.002

758 Benedetto, M.M., Guido, M.E., Contin, M.A., 2017. Non-Visual Photopigments Effects of Constant
759 Light-Emitting Diode Light Exposure on the Inner Retina of Wistar Rats. Front. Neurol. | 8, 1–
760 11. https://doi.org/10.3389/fneur.2017.00417

761 Berson, D.M., 2003. Strange vision : ganglion cells as circadian photoreceptors. Trends Neurosci. 26,
762 314–320. https://doi.org/10.1016/S0166-2236(03)00130-9

763 Blixt, F.W., Radziwon-balicka, A., Edvinsson, L., Warfvinge, K., 2017. Distribution of CGRP and its
764 receptor components CLR and RAMP1 in the rat retina. Exp. Eye Res. 161, 124–131.
765 https://doi.org/10.1016/j.exer.2017.06.002

766 Bron, A.J., Paiva, C.S. de, Chauhan, S.K., Bonini, S., Jain, S., Knop, E., Markoulli, M., Ogawa, Y.,
767 Perez, V., Uchino, Y., Yokoi, N., Zoukhri, D., Sullivan, D.A., 2017. TFOS DEWS II
768 pathophysiology report. Ocul. Surf. 15, 511–538. https://doi.org/10.1016/j.jtos.2017.05.004

769 Buhr, E.D., Yue, W.W.S., Ren, X., Jiang, Z., Liao, H.R., Mei, X., Vemaraju, S., 2015. Circadian
770 oscillators in mammalian retina and cornea. PNAS 1–6.
771 https://doi.org/10.1073/pnas.1516259112

772 Bush, R.A., Sieving, P.A., 1994. A proximal retinal component in the primate photopic ERG a-wave.
773 Investig. Ophthalmol. Vis. Sci. 35, 635–645.

774 Contín, M.A., Arietti, M.M., Benedetto, M.M., Bussi, C., Guido, M.E., 2013. Photoreceptor damage
775 induced by low-intensity light : model of retinal degeneration in mammals. Mol. Vis. 2013; 19,
776 1614–1625.

777 de Castro, F., Silos-Santiago, I., de Armentia, M.L., Barbacid, M., Belmonte, C., 1998. Corneal
778 innervation and sensitivity to noxious stimuli in trk A knockout mice. Eur. J. Neurosci. 10, 146–
779 152. https://doi.org/10.1046/j.1460-9568.1998.00037.x

780 Delwig, A., Chaney, S.Y., Bertke, A.S., Verweij, J., Quirce, S., Larsen, D.D., Yang, C., Buhr, E.,
781 Van Gelder, R., Gallar, J., Margolis, T., Copenhagen, D.R., 2018. Melanopsin expression in the
782 cornea. Vis. Neurosci. 35. https://doi.org/10.1017/S0952523817000359

783 Dolgonos, S., Ayyala, H., Evinger, C., 2011. Light-Induced Trigeminal Sensitization without Central
784 Visual Pathways : Another Mechanism for Photophobia. IOVS 52, 7852–7858.
785 https://doi.org/10.1167/iovs.11-7604

786 Feng, C., Wang, X., Liu, T., Zhang, M., Xu, G., Ni, Y., 2017. Expression of CCL2 and its receptor in
787 activation and migration of microglia and monocytes induced by photoreceptor apoptosis. Mol
788 Vis. 765–777.

789 Godley, B.F., Shamsi, F.A., Liang, F.-Q., Jarrett, S.G., Davies, S., Boulton, M., 2005. Blue Light
790 Induces Mitochondrial DNA Damage and Free Radical Production in Epithelial Cells. J. Biol.
791 Chem. 280, 21061–21066. https://doi.org/10.1074/jbc.M502194200

792 Guido, M.E., Nieto, P.S., Valdez, D.J., Acosta-rodrı, V.A., 2011. Expression of Novel Opsins and
793 Intrinsic Light Responses in the Mammalian Retinal Ganglion Cell Line RGC-5 . Presence of
794 OPN5 in the Rat Retina. PLoS One 6. https://doi.org/10.1371/journal.pone.0026417

795 Hannibal, J., Georg, B., Hindersson, P., Fahrenkrug, J., 2005. Light and Darkness Regulate
796 Melanopsin in the Retinal Ganglion Cells of the Albino Wistar Rat. J. Mol. Neurosci. 27.

https://doi.org/10.1385/JMN

Hoggan, R.N., Subhash, A., Blair, S., Digre, K.B., Baggaley, S.K., Gordon, J., Brennan, K.C., Warner, J.E.A., Crum, A. V., Katz, B.J., 2016. Thin-film optical notch filter spectacle coatings for the treatment of migraine and photophobia. J. Clin. Neurosci. 28, 71–76. https://doi.org/10.1016/j.jocn.2015.09.024

Hughes, S., Rodgers, J., Hickey, D., Foster, R.G., Peirson, S.N., Hankins, M.W., 2016. Characterisation of light responses in the retina of mice lacking principle components of rod , cone and melanopsin phototransduction signalling pathways. Nat. Publ. Gr. 1–11. https://doi.org/10.1038/srep28086

Hunt, D., Raivich, G., Anderson, P.N., 2012. Activating Transcription Factor 3 and the Nervous System. Front. Mol. Neurosci. 5, 1–17. https://doi.org/10.3389/fnmol.2012.00007

Jaadane, I., Boulenguez, P., Chahory, S., Carré, S., Savoldelli, M., Jonet, L., Behar-cohen, F., Martinsons, C., Torriglia, A., 2015. Retinal damage induced by commercial Light Emitting Diodes (LED). Free Radic. Biol. Med.

Jones, K.A., Megumi, H., Mure, L.S., Bramley, J.R., Panda, S., 2013. Small molecule antagonists of melanopsin-mediated phototransduction. Nat Chem Biol 9, 630–635. https://doi.org/10.1038/nchembio.1333.Small

K. Digre, K.C. Brennan, 2012. Shedding Light on Photophobia. J Neuroophthalmol. 32, 68–81. https://doi.org/10.1097/WNO.0b013e3182474548.Shedding

Katz, B.J., Digre, K.B., 2016. Diagnosis, pathophysiology, and treatment of photophobia. Surv. Ophthalmol. 61, 466–477. https://doi.org/10.1016/j.survophthal.2016.02.001

Krigel, A., Berdugo, M., Picard, E., Levy-Boukris, R., Jaadane, I., Jonet, L., Dernigoghossian, M., Andrieu-Soler, C., Torriglia, A., Behar-Cohen, F., 2016. Light-induced retinal damage using different light sources, protocols and rat strains reveals LED phototoxicity. Neuroscience 339, 296–307. https://doi.org/10.1016/j.neuroscience.2016.10.015

Lascaratos, G., Ji, D., Wood, J.P.M., Osborne, N.N., 2007. Visible light affects mitochondrial function and induces neuronal death in retinal cell cultures. Vision Res. 47, 1191–1201. https://doi.org/10.1016/j.visres.2006.12.014

Launay, P., Reboussin, E., Liang, H., Kessal, K., Godefroy, D., Rostène, W., Sahel, J.-A., Bauduoin, C., Mélik Parsadaniantz, S., Reaux-Le Goazigo, A., 2016. Neurobiology of Disease Ocular in fl ammation induces trigeminal pain , peripheral and central neuroin fl ammatory mechanisms. Neurobiol. Dis. 88, 16–28. https://doi.org/10.1016/j.nbd.2015.12.017

Lee, H.S., Cui, L., Li, Y., Choi, J.S., Choi, J., Li, Z., Kim, G.E., Choi, W., Yoon, K.C., 2016. Influence of Light Emitting Diode-Derived Blue Light Overexposure on Mouse Ocular Surface. PLoS One. https://doi.org/10.1371/journal.pone.0161041

Lei, S., Goltz, H.C., Chen, X., Zivcevska, M., Wong, A.M.F., 2018a. The Relation Between Light-Induced Lacrimation and the Melanopsin-Driven Postillumination Pupil Response. IOVS 58, 1–3. https://doi.org/10.1167/iovs.16-21285

Lei, S., Zivcevska, M., Goltz, H.C., Chen, X., Wong, A.M., 2018b. The effect of ocular topical anesthesia on photophobia induced by red and blue light stimulus, in: ARVO Annual Meeting.

Lupis, J., n.d. The State of Traditional TV: Updated With Q1 2017 Data [WWW Document]. Mareketing charts. URL http://www.marketingcharts.com/featured-24817 (accessed 11.7.17).

M. Wade, 2015. Symptoms of Dry Eye Disease [WWW Document]. Discov. Eye Found. URL http://discoveryeye.org/symptoms-of-dry-eye-disease/ (accessed 11.6.15).

Marek, V., Mélik-parsadaniantz, S., Villette, T., Montoya, F., Baudouin, C., Brignole-Baudouin, F., Denoyer, A., 2018. Blue light phototoxicity toward human corneal and conjunctival epithelial cells in basal and hyperosmolar conditions. Free Radic. Biol. Med. https://doi.org/10.1016/j.freeradbiomed.2018.07.012

Marie, M., Barrau, C., Gondouin, P., Villette, T., Cohen-tannoudji, D., Sahel, J., Picaud, S., 2013. Blue light decreases oxidative stress defenses in an in vitro model of AMD 968.

Marshall J., 2014. Understanding risks of phototoxicity on the eye [WWW Document]. Point Vue, Int. Rev. Ophthalmic Opt. URL http://www.pointsdevue.com/article/understanding-risks-phototoxicity-eye (accessed 11.7.17).

Matynia, A., Gorin, M., 2013. Unanswered Questions in Headache: So What Is Photophobia, Anyway? Headache 53, 1673–1674. https://doi.org/10.1097/MPG.0b013e3181a15ae8.Screening

Matynia, A., Nguyen, E., Sun, X., Blixt, F.W., Parikh, S., Kessler, J., Pérez, L., Müller, D.S., Habib, S., Kim, P., Wang, Z.Z., Rodriguez, A., Charles, A., Nusinowitz, S., Edvinsson, L., Barnes, S., Brecha, N.C., Gorin, M.B., 2016. Peripheral Sensory Neurons Expressing Melanopsin Respond to. Front. Neurql Circuits 10, 1–15. https://doi.org/10.3389/fncir.2016.00060

Matynia, A., Parikh, S., Chen, B., Kim, P., Mcneill, D.S., Nusinowitz, S., Evans, C., Gorin, M.B., 2012. Intrinsically photosensitive retinal ganglion cells are the primary but not exclusive circuit for light aversion. Exp. Eye Res. 105, 60–69. https://doi.org/10.1016/j.exer.2012.09.012

Matynia, A., Parikh, S., Deot, N., Wong, A., Kim, P., Nusinowitz, S., Gorin, M.B., 2015. Light aversion and corneal mechanical sensitivity are altered by intrinscally photosensitive retinal ganglion cells in a mouse model of corneal surface damage. Exp. Eye Res. 137, 57–62. https://doi.org/10.1016/j.exer.2015.05.025

Matynia, A., Parikh, S., Nusinowitz, S., Gorin, M.B., 2017. Three blind mice, see how they run: Light-dependent behavior in the absence of an optic nerve, in: Nvest. Ophthalmol. Vis. Sci. p. 58(8):4126.

McDougal, D.H., Gamlin, P.D., 2015. Autonomic control of the eye. Compar Physiol 5, 439–473. https://doi.org/10.1002/cphy.c140014.Autonomic

Moulton, E.A., Becerra, L., Borsook, D., 2009. An fMRI case report of photophobia: Activation of the trigeminal nociceptive pathway. Pain 145, 358–363. https://doi.org/10.1016/j.pain.2009.07.018

Nir, R.-R., Noseda, R., Bernstein, C., Buettner, C., Fulton, A.B., Bertisch, S.M., Hovaguimian, A., Buettner, C., Borsook, D., Burstein, R., 2018. Color-Selective Photophobia in Ictal vs . Interictal Migraineurs and in Healthy Controls. Pain. https://doi.org/10.1097/j.pain.0000000000001303

Niwano, Y., Kanno, T., Iwasawa, A., Ayaki, M., Tsubota, K., 2014. Blue light injures corneal epithelial cells in the mitotic phase in vitro. Br. J. Ophthalmol. 98, 990–2. https://doi.org/10.1136/bjophthalmol-2014-305205

Noseda, R., Bernstein, C.A., Nir, R.R., Lee, A.J., Fulton, A.B., Bertisch, S.M., Hovaguimian, A., Cestari, D.M., Saavedra-Walker, R., Borsook, D., Doran, B.L., Buettner, C., Burstein, R., 2016. Migraine photophobia originating in cone-driven retinal pathways. Brain 139, 1971–1986. https://doi.org/10.1093/brain/aww119

Noseda, R., Kainz, V., Jakubowski, M., Gooley, J.J., Clifford, B., Digre, K., Burstein, R., 2010. A

neural mechanism for exacerbation of headache by light. Nat Neurosci 13, 1–17. https://doi.org/10.1038/nn.2475.A

Noseda, R., Lee, A.J., Nir, R.-R., Bernstein, C.A., Kainz, V.M., Bertisch, S.M., Buettner, C., Borsook, D., Burstein, R., 2017. Neural mechanism for hypothalamic-mediated autonomic responses to light during migraine. Proc. Natl. Acad. Sci. 114, E5683–E5692. https://doi.org/10.1073/pnas.1708361114

Okamoto, K., Tashiro, A., Chang, Z., Beriter, D.A., 2011. Bright light activates a trigeminal nociceptive pathway. Pain 149, 235–242. https://doi.org/10.1016/j.pain.2010.02.004.Bright

Okamoto, K., Tashiro, A., Thompson, R., Nishida, Y., Bereiter, D.A., 2012. Trigeminal interpolaris/caudalis transition neurons mediate reflex lacrimation evoked by bright light in the rat. Eur. J. Neurosci. 36, 3492–3499. https://doi.org/10.1111/j.1460-9568.2012.08272.x

Okamoto, K., Thompson, R., Tashiro, A., Chang, Z., D.A., B., 2009. Bright light produces Fos-positive neurons in caudal trigeminal brainstem. Neuroscience 160, 858–864. https://doi.org/10.1016/j.neuroscience.2009.03.003

Rahman, M., Okamoto, K., Thompson, R., Beriter, D.A., 2015. Trigeminal pathways for hypertonic saline and light-evoked corneal reflexes. Neuroscience 26, 716–723. https://doi.org/10.1016/j.neuroscience.2014.07.052.Trigeminal

Roehlecke, C., Schumann, U., Ader, M., Brunssen, C., Bramke, S., Morawietz, H., Funk, R.H.W., 2013. Stress reaction in outer segments of photoreceptors after blue light irradiation. PLoS One 8, e71570. https://doi.org/10.1371/journal.pone.0071570

Sikka, G., Hussmann, G.P., Pandey, D., Cao, S., Hori, D., Taek, J., Steppan, J., 2014. Melanopsin mediates light-dependent relaxation in blood vessels. PNAS 111, 17977–17982. https://doi.org/10.1073/pnas.1420258111

Stapleton, F., Alves, M., Bunya, V.Y., Jalbert, I., Lekhanont, K., Malet, F., Na, K., Schaumberg, D., Uchino, M., Vehof, J., Viso, E., Vitale, S., 2017. The Ocular Surface TFOS DEWS II Epidemiology Report. Ocul. Surf. 15, 334–365. https://doi.org/10.1016/j.jtos.2017.05.003

Text Request, n.d. How Much Time Do People Spend on Their Mobile Phones in 2017? [WWW Document]. Hackernoon. URL https://hackernoon.com/how-much-time-do-people-spend-on-their-mobile-phones-in-2017-e5f90a0b10a6 (accessed 11.7.17).

The National Eye Institute, 2017. Facts About Dry Eye [WWW Document]. URL https://nei.nih.gov/health/dryeye/dryeye (accessed 8.3.18).

Tian, M., Jarsky, T., Murphy, G.J., Rieke, F., Singer, J.H., 2010. Voltage-gated Na channels in AII amacrine cells accelerate scotopic light responses mediated by the rod bipolar cell pathway. J. Neurosci. 30, 4650–4659. https://doi.org/10.1523/JNEUROSCI.4212-09.2010.Voltage-gated

Warfvinge, K., Sörensen, Karin D Edvinsson, L., Fedulov, V., Haanes, K.A., Blixt, F.W., 2018. Expression of the CGRP family peptides and their receptors in the rat retina, in: Nvest. Ophthalmol. Vis. Sci. p. 59(9):5504.

Wu, Y., Hallett, M., 2017. Photophobia in neurologic disorders. Transl. Neurodegener. 6, 26. https://doi.org/10.1186/s40035-017-0095-3

Xue, T., Do, M.T.H., Riccio, A., Jiang, Z., Hsieh, J., Wang, H.C., Merbs, S.L., Welsbie, S., Yoshioka, T., Weissgerber, P., Stolz, S., Flockerzi, V., Freichel, M., Clapham, D.E., 2012. Melanopsin Signaling in Mammalian Iris and Retina. Nature 479, 67–73. https://doi.org/10.1038/nature10567.Melanopsin

Main figures

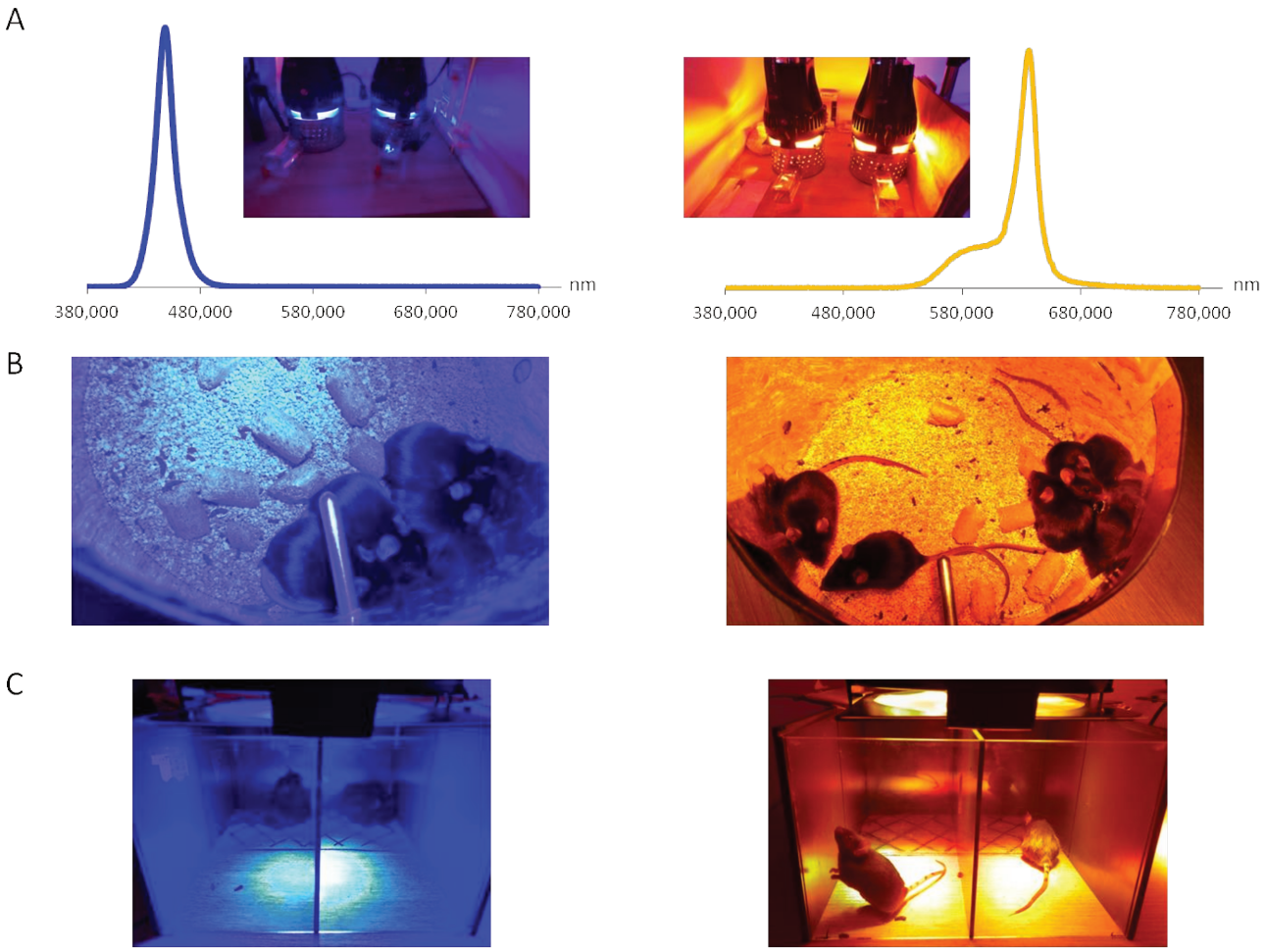

Figure 1. Custom-mounted illumination system.

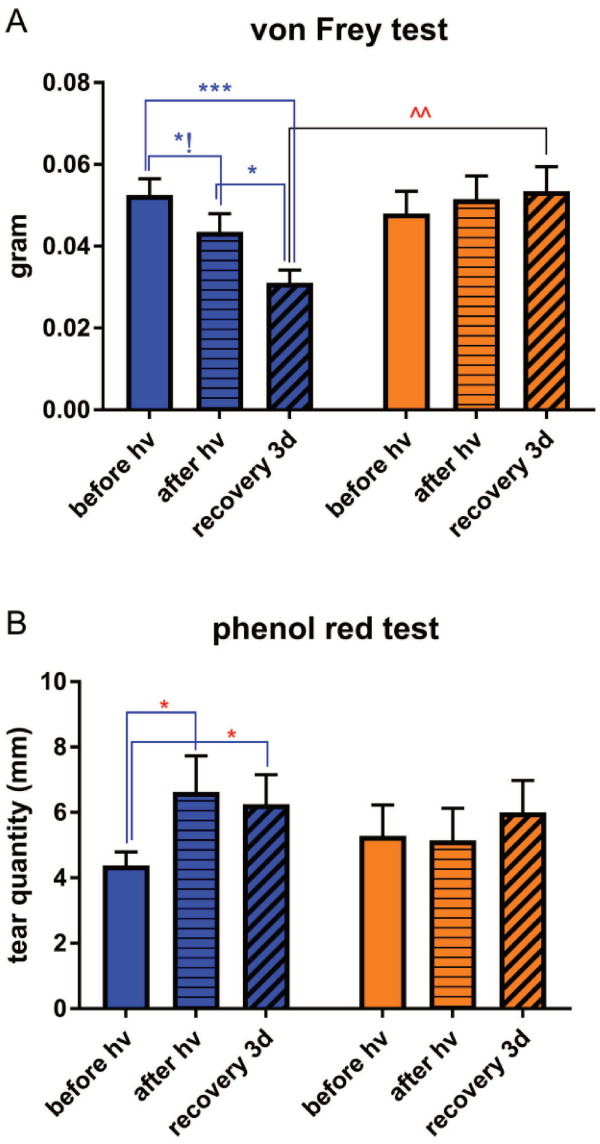

Figure 2. Clinical assessments

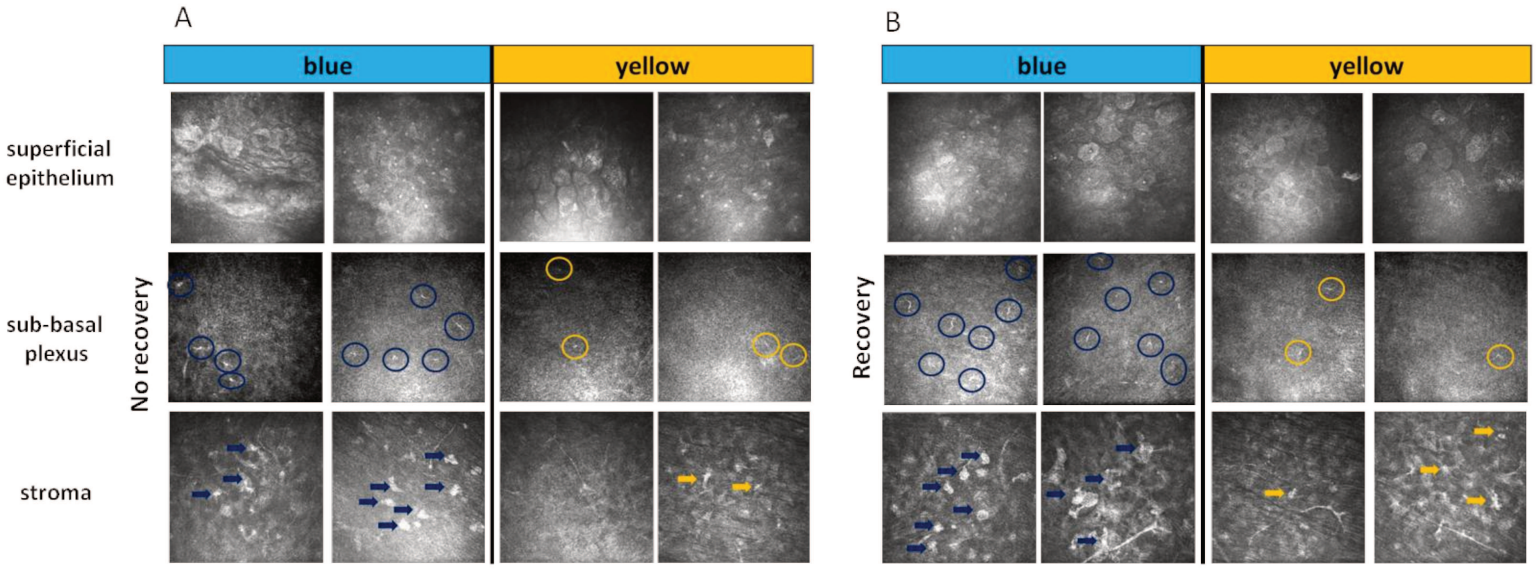

Figure 3. IVCM results

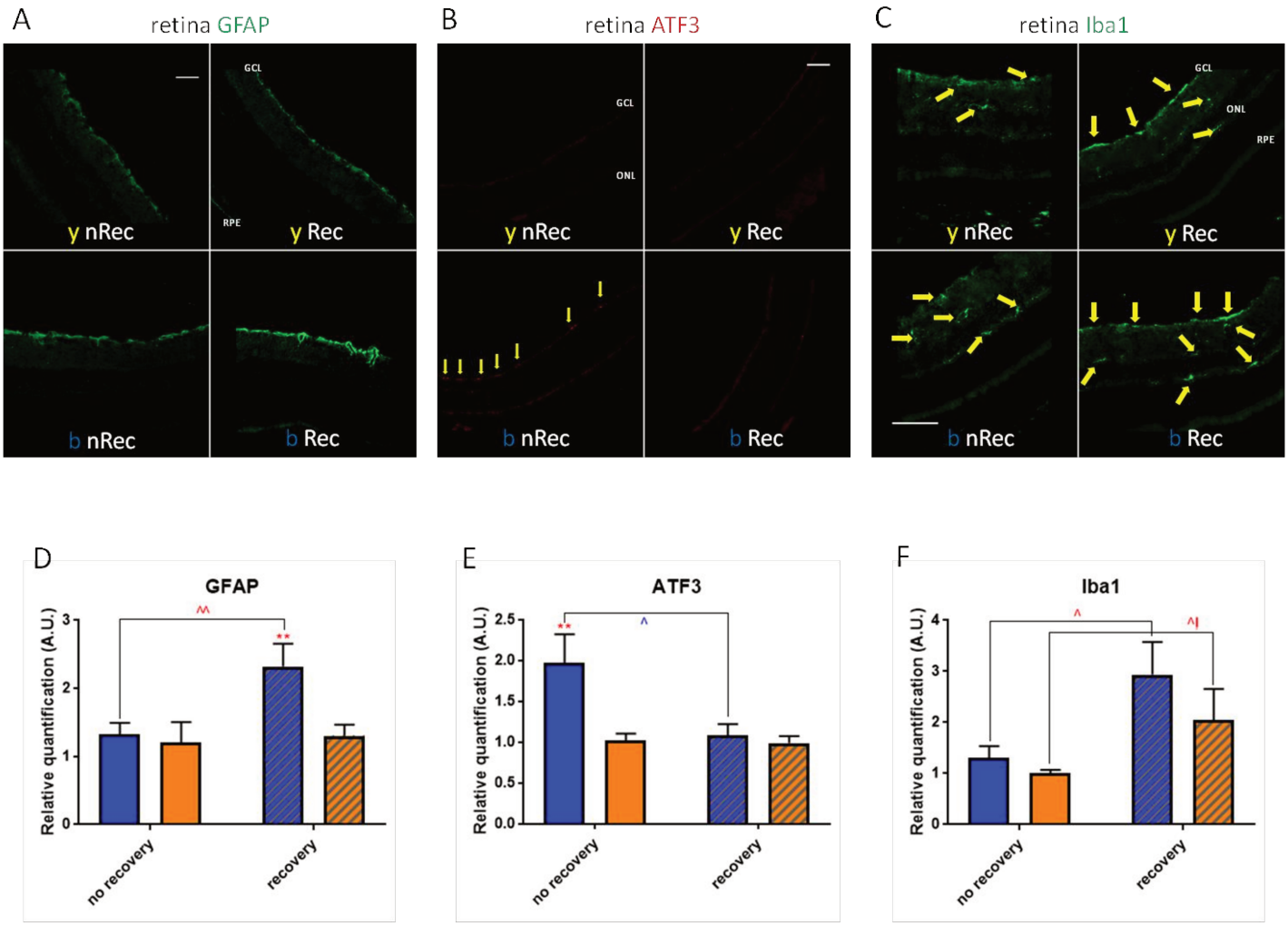

Figure 4. Light-provided retinal inflammation

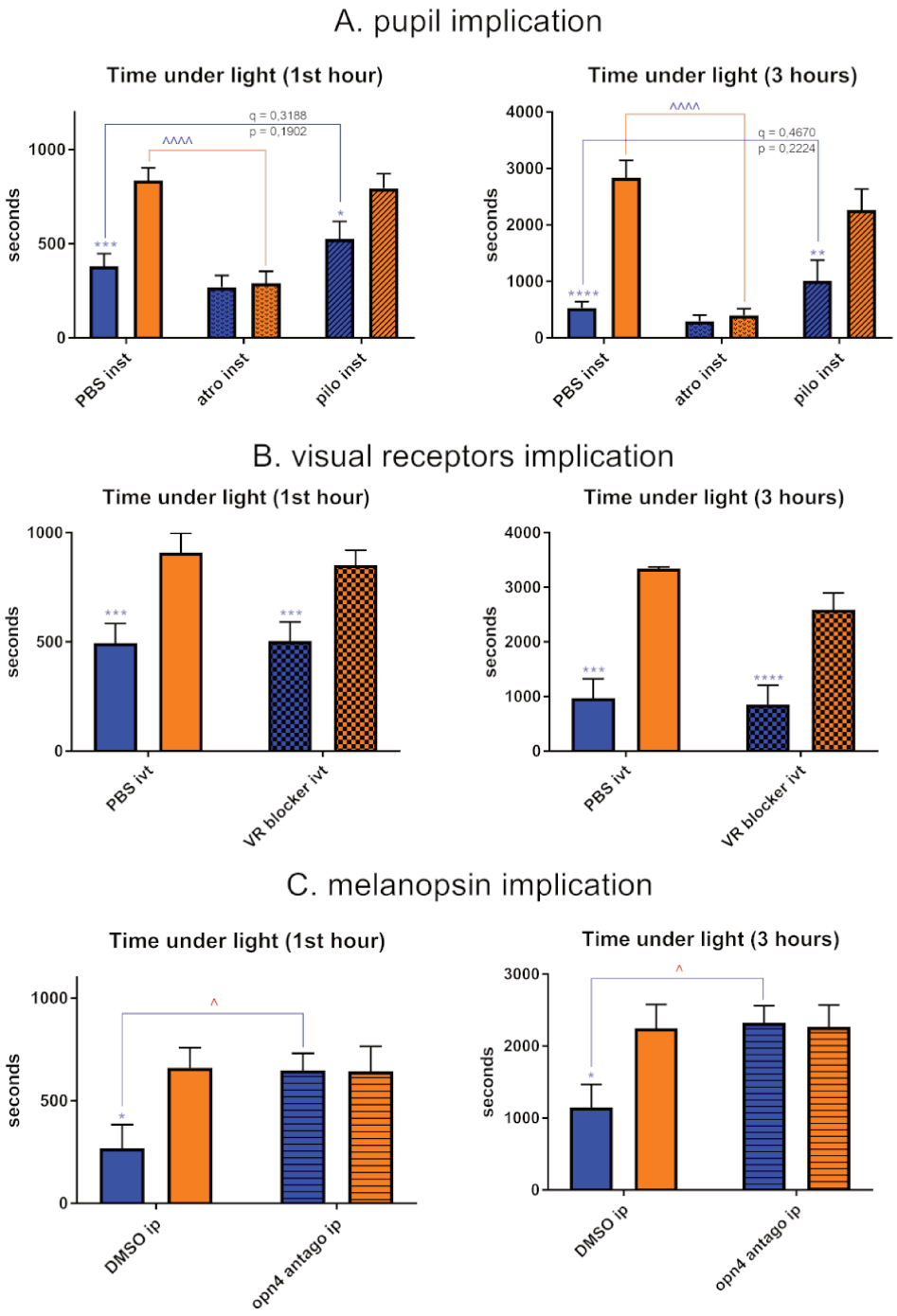

Figure 5. Retina-related behavioral tests.

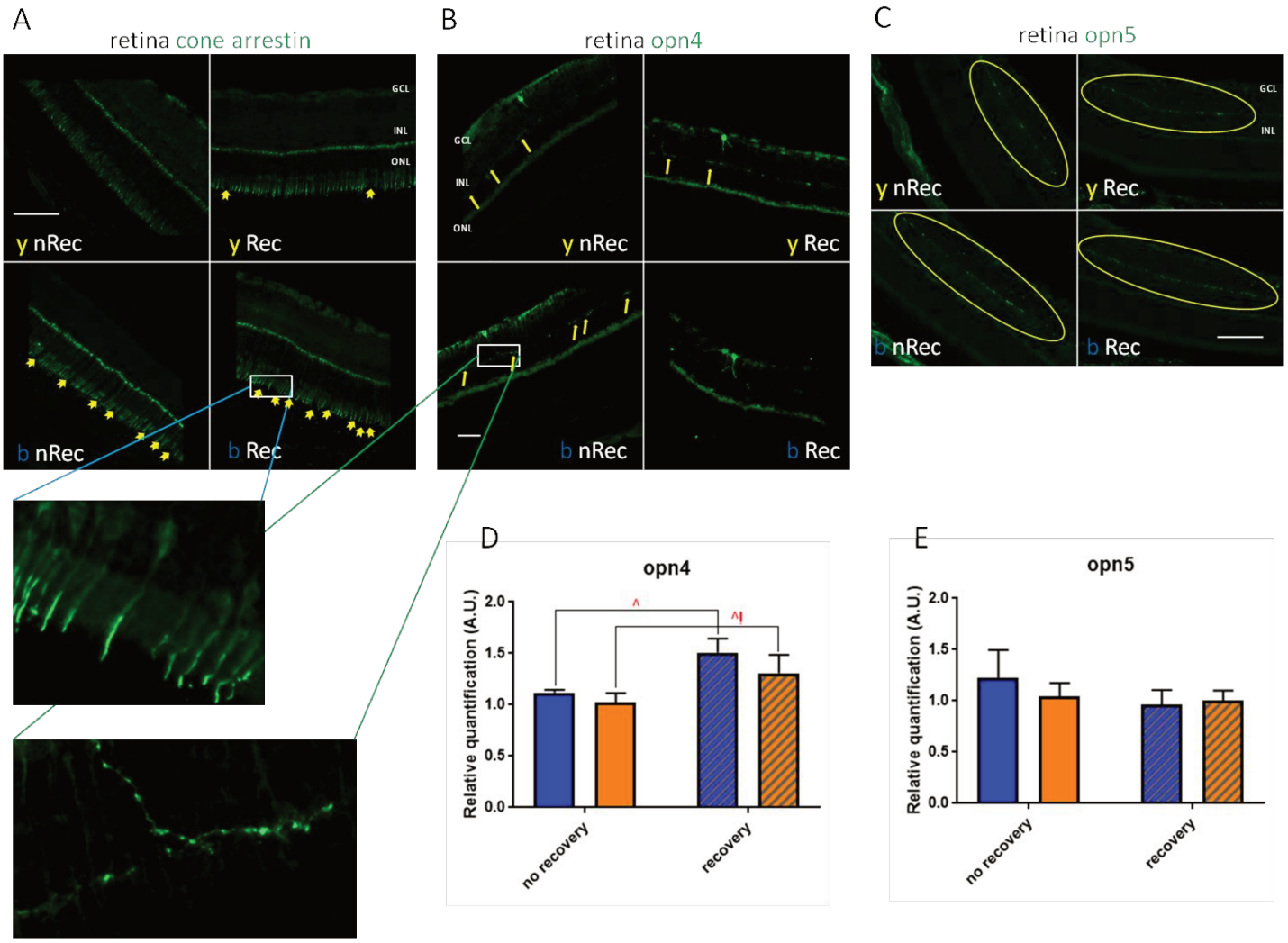

Figure 6. Role of retinal light receptors.

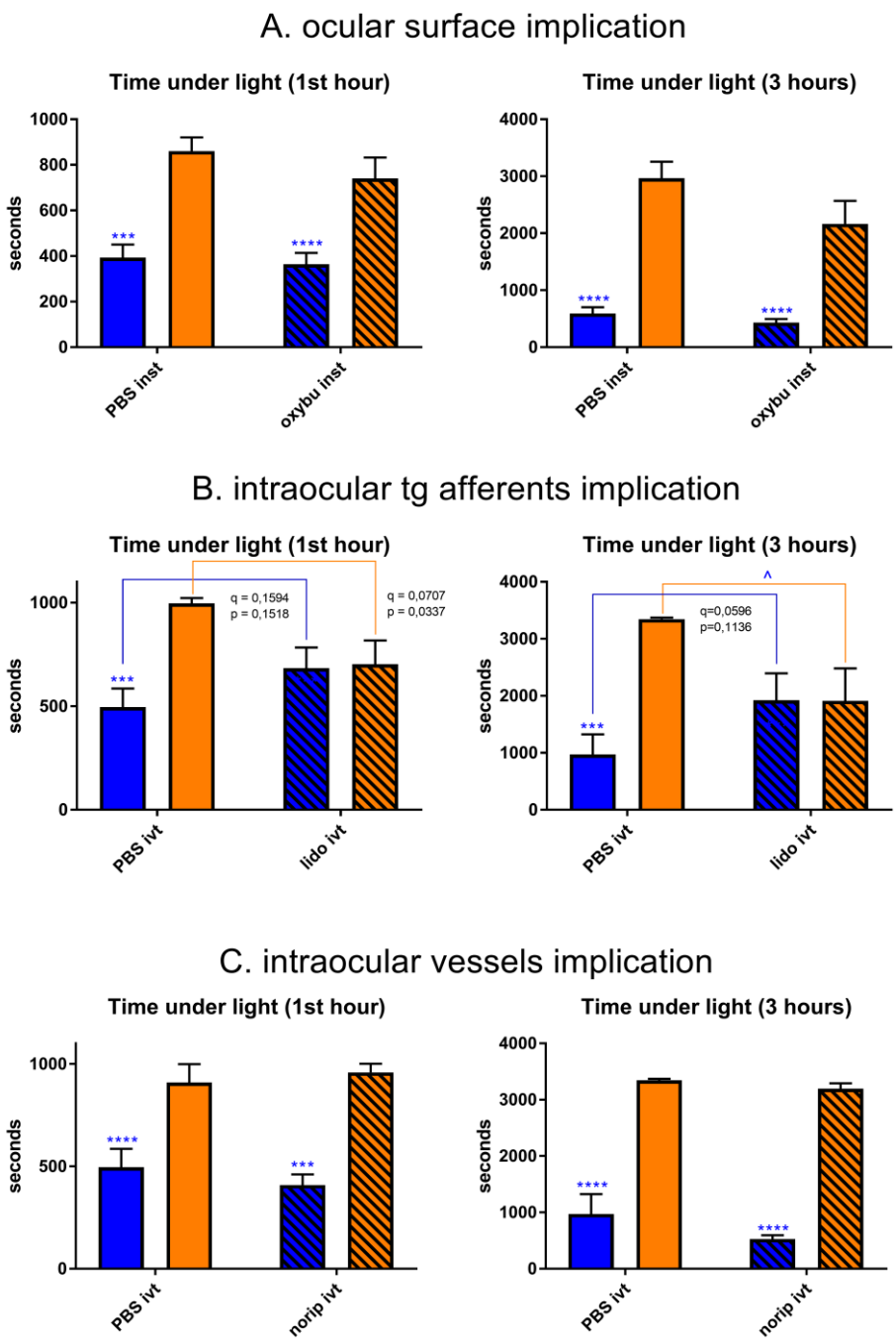

Figure 7. TGs-related behavioral tests.

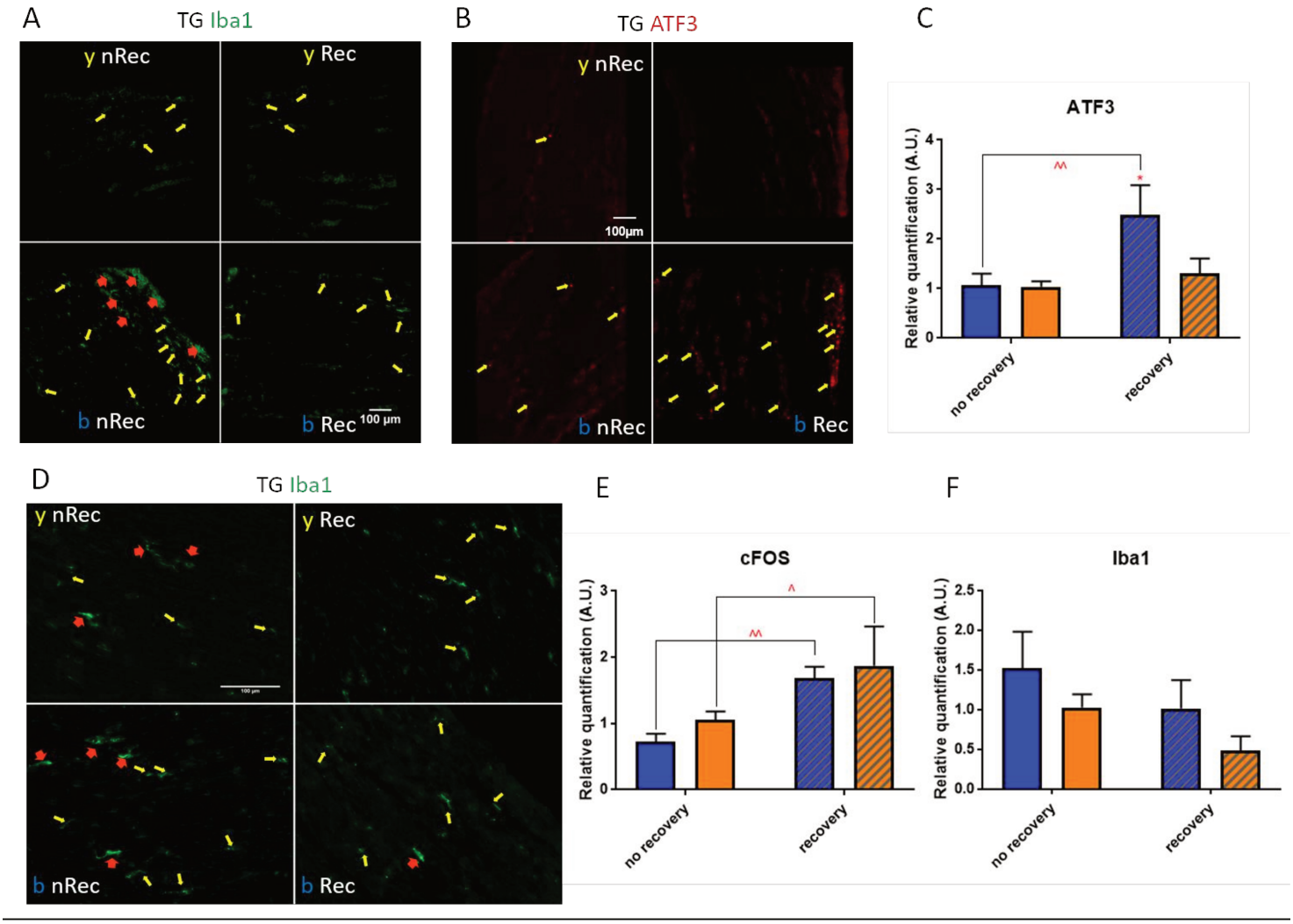

Figure 8. Phototoxicity marks in TGs.

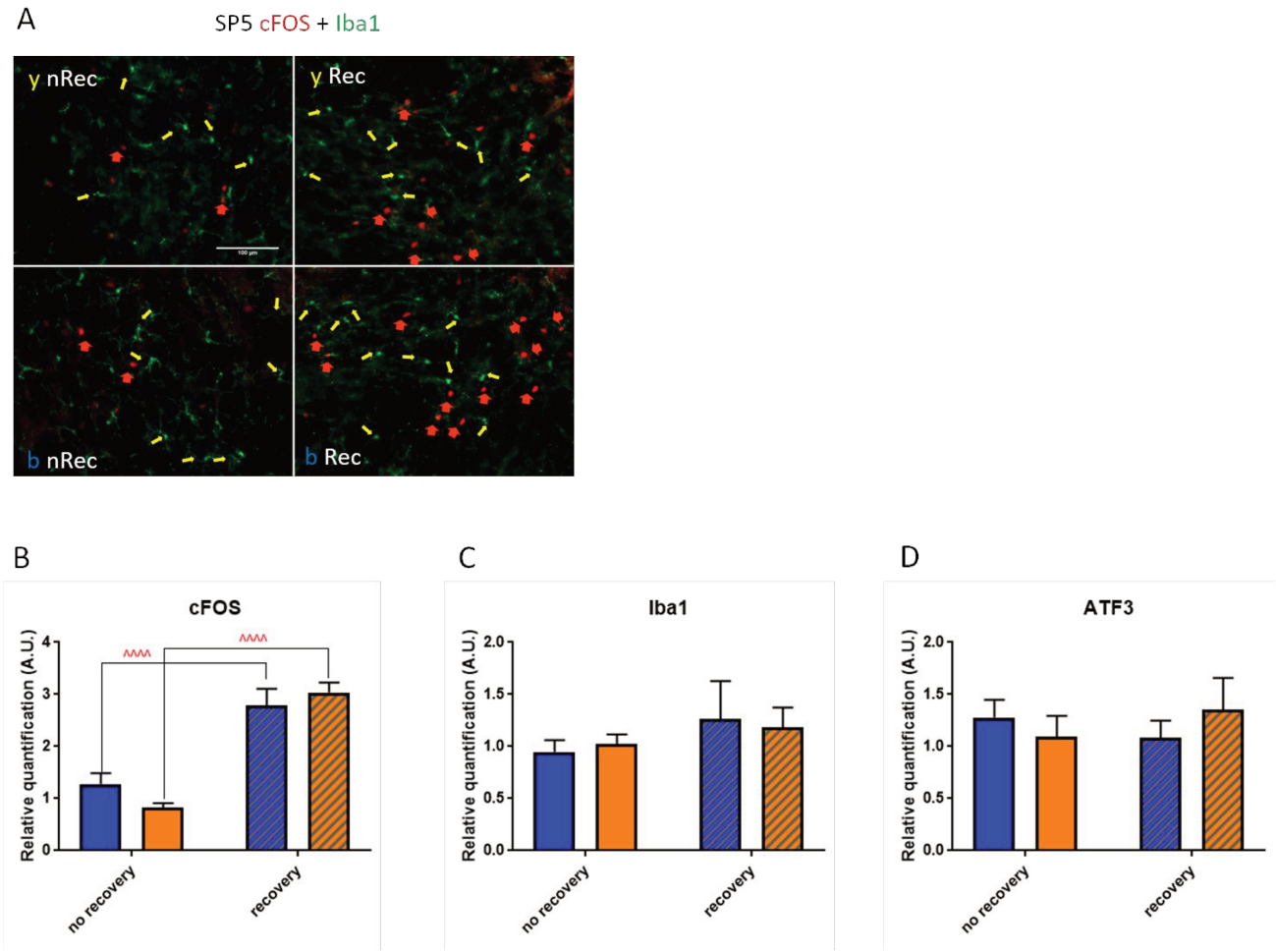

Figure 9. Phototoxicity marks in brainstem.

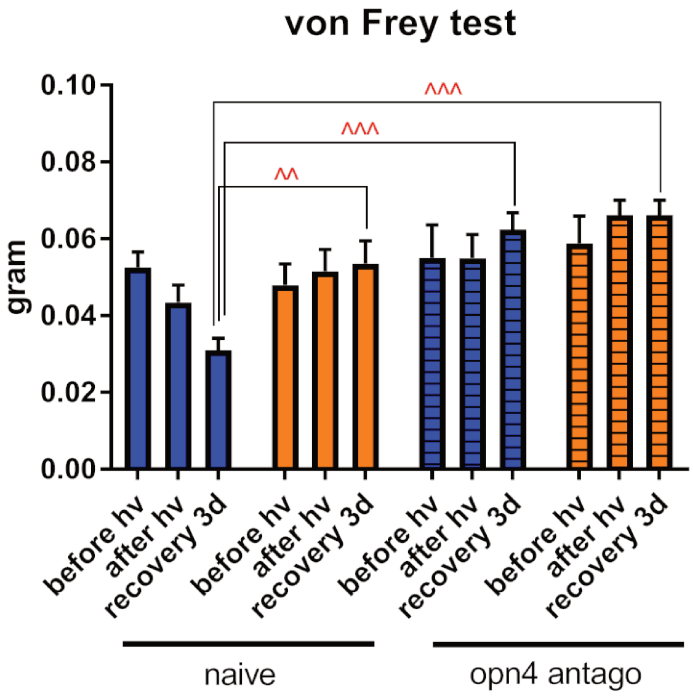

Fig. 10. Role of melanopsin in corneal sensitivity.

Supplementary figures

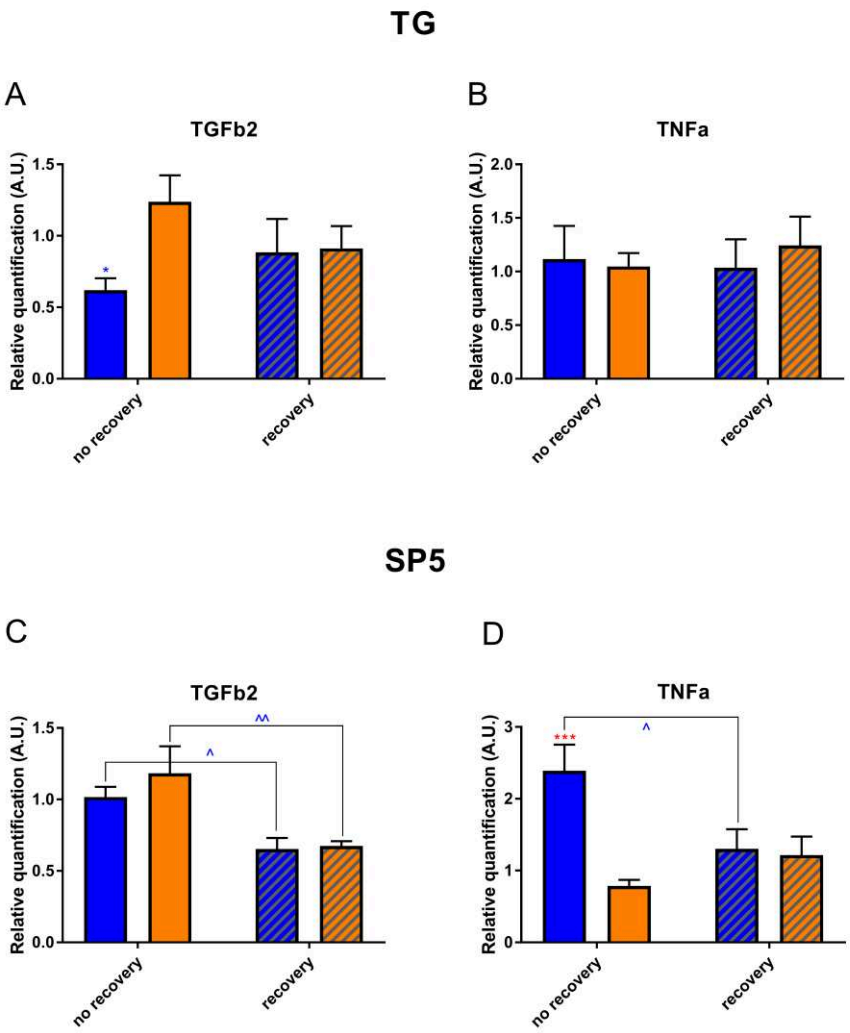

Suppl. figure 1. Cytokine profile in trigeminal pathways.

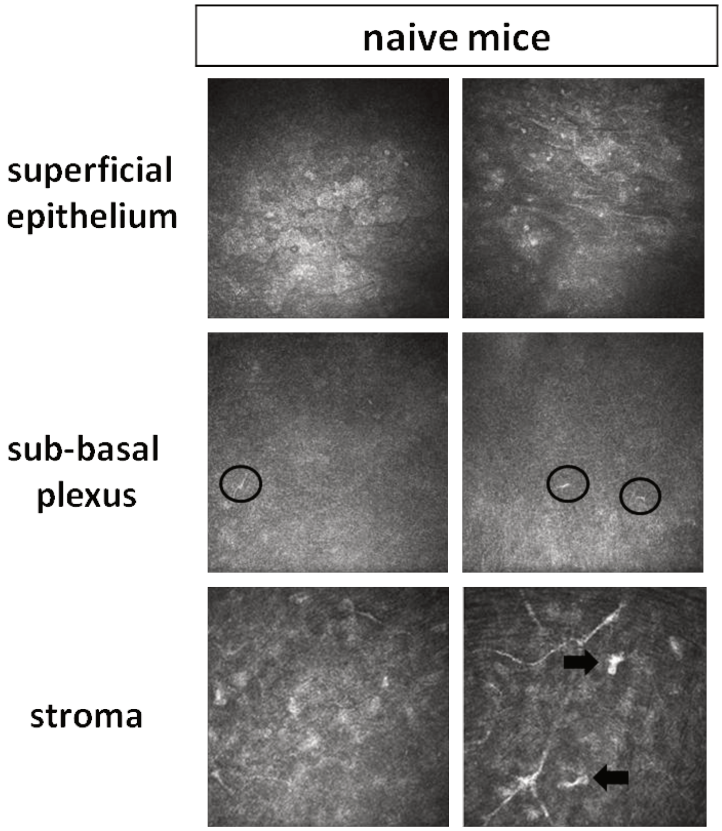

Suppl. figure 2. IVCM results of naïve mice.

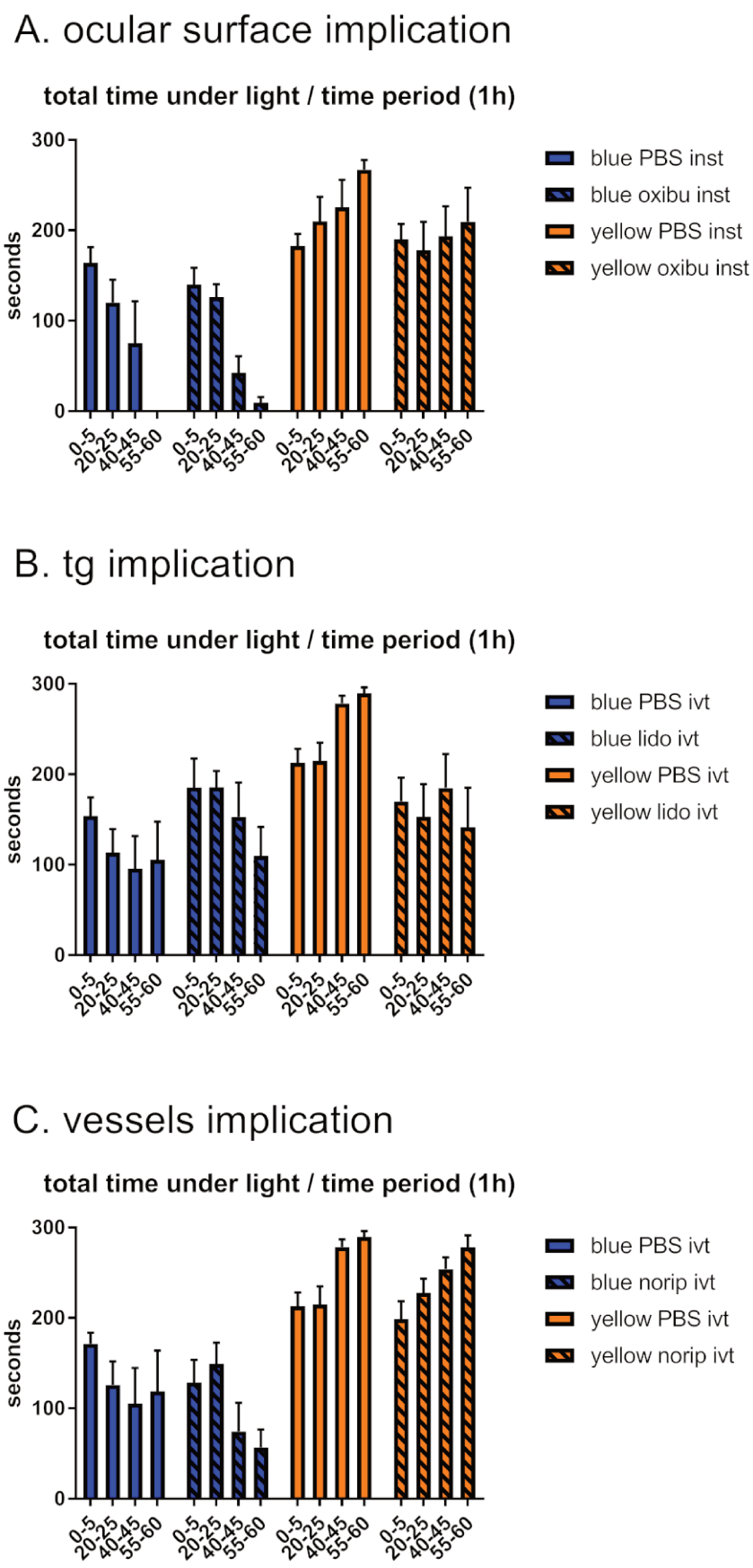

Suppl. figure 3. Shorter periods of behavioral tests.

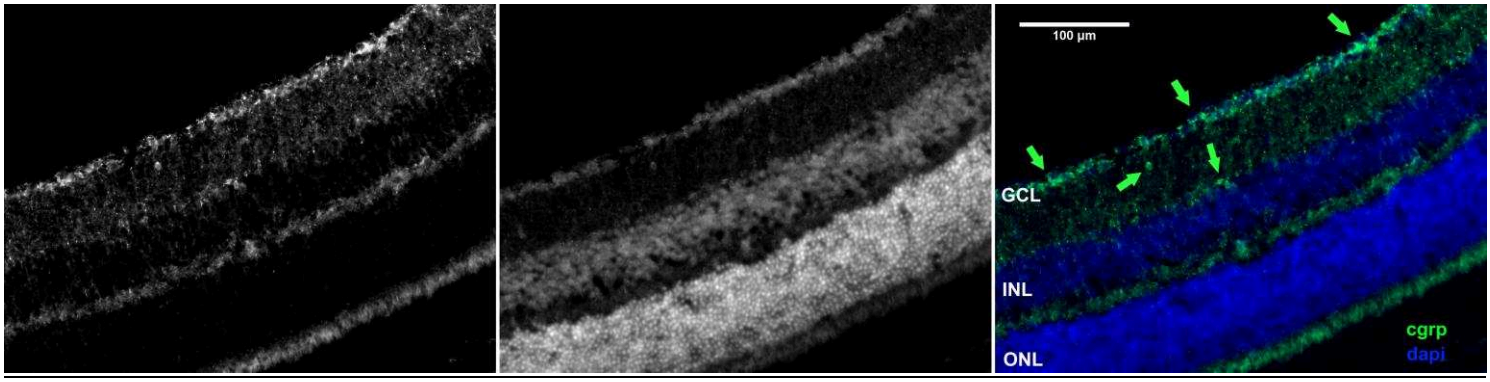

Suppl. figure 4. Potential link between the retina and TG.

Supplementary Material

Implication of melanopsin and trigeminal neural pathways in blue light photosensitivity in vivo

V. Marek*[,1,2], E. Reboussin[2], J. Dégardin-Chicaud[2], A. Charbonnier[2], T. Villette[1], A. Denoyer[2,3,4], C. Baudouin[2,3,5], A. Réaux-Le-Goazigo[2] and S. Mélik Parsadaniantz[2]

*** Correspondence:** Veronika Marek, nika.marek@gmail.com

1 Legends to supplementary figures

Suppl. figure 1. Cytokine profile in trigeminal pathways.

Results of mRNA expression of TGFβ2 and TNFα on the TGs (A, B) and brainstems (C, D). Statistical significance for the TG: TGFβ2 blue no recovery vs recovery – q = 0.0187, p = 0.0178. Statistical significance for the brainstem:

- TGFβ2: blue no recovery vs recovery – q = 0.0169, p = 0.0161; yellow no recovery vs recovery – q = 0.0041, p = 0.0020;
- TNFα: blue no recovery vs recovery – q = 0.0197, p = 0.0188; recovery blue vs yellow – q = 0.0005, p = 0.0005.

Blue and yellow bars correspond to blue and yellow exposures respectively; clear and hatched bars correspond to the time points of dissection, either directly after illumination (no recovery) or in 3 days of recovery (recovery) respectively. All the data are presented as mean ± SEM. Differences were considered significant when $p < 0.05$ (*/^), $p < 0.01$ (**/^^), $p < 0.001$ (***/^^^) or $p < 0.0001$ (****/^^^^). Stars correspond to comparisons between blue-illuminated and yellow-illuminated mice, treated with the same drug. Carets correspond to comparison of mice assessed directly after illumination to the ones assessed after 3 days of recovery, within the same spectra. Red color means increase and blue color decrease in values.

Suppl. figure 2. IVCM results of naïve mice.

Representative images of non-invasive IVCM examination performed in mice kept under standard lighting conditions of animal facility. No significant difference with yellow-illuminated mice (Fig. 3) was observed. The three following corneal layers are represented: superficial epithelium, sub-basal plexus (dendritic cells are marked by circles) and stroma (activated keratocytes are marked by arrows). In these mice, corneal mechanical sensitivity (von Frey hair test) was 0.043 ± 0.03 g.

Suppl. figure 3. Shorter periods of behavioral tests.

Graphs represent how the time spent in the illuminated part of the cage evolved during the 1st hour when oxibuprocaine (A), lidocaine (B) or norepinephrine (C) were applied. Numbers 0 – 5, 20 – 25, 40 – 45 and 55 – 60 (minutes) correspond to time periods within the 1st hour. Blue and yellow bars correspond to blue and yellow exposures respectively; clear bars and hatched bars correspond to

animals with control (vehicle – PBS) or specific drug treatments respectively. All the data are presented as mean ± SEM. Stars correspond to comparisons between blue-illuminated and yellow-illuminated mice, treated with the same drug. Carets correspond to comparisons between control and drug-treated animals. Red color means increase and blue color decrease in values.

Suppl. figure 4. Potential link between the retina and TG.

Immunostaining of the retina with anti-CGRP antibody. On the merged image, CGRP- and DAPI-stainings are shown in green and blue respectively; spots of specific CGRP-staining are indicated by arrows. Magnification is 20x, scale bar corresponds to 100 μm.

Overall conclusions and perspectives

The aim of the current work was to investigate the potential harmful impact of blue light exposure in the context of dry eye disease as well as in relation to ocular pain and photophobia.

In vitro, we demonstrated the phototoxic effect in human epithelial cells of ocular surface as well as on neural and glial cells of mouse trigeminal ganglia. Light impact was spectrum-dependent: greater cytotoxicity was provoked by shorter-wavelength illumination. In HCE, IOBA and TG cells, blue light induced an important decrease in cell viability, major cell death and significant oxidative stress. Alterations in cell morphology and over-production of inflammatory cytokines also took place. Furthermore, we showed the important role of mitochondria for phototoxic signal processing.

In ocular surface cells, blue light provoked a break-down of glutathione- and enzyme-based antioxidant defensive system. We reported a greater photosensitivity of conjunctival cells as compared to the corneal ones. In TG cells culture, we highlighted the significance of endoplasmic reticulum in neuronal transmission of blue-toxic message. We reported that both neurons and glial cells were sensitive to blue light exposure and discussed the potential role of non-visual receptors, melanopsin and neuropsin, in phototoxic process. Taken together, these results corroborated increased photosensitivity frequently observed in clinical practice in patients suffering from dry eye. Indeed, we did show that pre-increased hyperosmolarity, almost indispensable sign of DED, had an impact on the phototoxic effect. In addition, blue-toxicity exhibited by trigeminal neurons might account for light-induced neuropathic pain, present in dry eye as well.

These in vitro experiments may have numerous possible continuations. First, for all the cell types, it is important to analyze cells' secretome. Indeed, the profile of expressed proteins would not only allow for better understanding of underlying phototoxic mechanisms but also for comparison with correspondent clinical data available from tears and conjunctival imprints of dry eye patients. Second, it might be interesting to modify light protocols; for example, we may apply weaker irradiances but for longer time periods thus looking for chronicity. Moreover, an investigation of iterative exposures with recovery time between them would be of worth to study since such light protocol would model our real every-day exposure to light alternating with recovery at night. Third, from the clinical point of view, it would be important to explore the effect of popular symptomatic anti-DED and anti-pain treatments (like artificial tears or cyclosporine (127,128)) in the conditions of exposure to light. Fourth, the inverse experiment should be done: white illumination through the correspondent blue light filters is supposed to provide with no significant phototoxicity.

Within the frame of ocular surface, it would be interesting to verify our results on primary cell cultures as well as on 3-dimensional model of the cornea (129). To better imitate the light impact on real eye surface, phototoxicity in co-cultured corneal and conjunctival cells would be worth to explore. Moreover, special attention should be paid to goblet cells. Indeed, conjunctival goblet cells are the primary source of the ocular mucins that are essential for healthy tear film and for the protection of ocular surface. In patients suffering from dry eye, a decrease in goblet cell number was well-documented (62). Furthermore, mice devoid of

goblet cells exhibited an ocular surface phenotype similar to that in a moderate dry eye (130). Thus, we may partially ascribe the observed higher phototoxicity in conjunctival cells to the absence of goblet cells and may suppose that the latter could mitigate the inflammatory response. However, it was reported that in vitro, IL-6 stimulation may increase the mucin secretion by goblet cells. An excess in mucin production, like in early dry eye and allergic conjunctivitis, is deleterious to the ocular surface (62). Since in our experiments blue light amplified IL-6 mRNA expression, we may also suggest that it could provoke mucin over-production and consequent additional inflammation. In this case, the presence of goblet cells might even amplify the photosensitivity of conjunctival cells. Thus, investigation of blue light phototoxicity in goblet cells, either separately or in co-culture with conjunctival (and corneal) cells, would be an informative study allowing for better understanding of dry eye patients photosensitivity. To our knowledge, so far only one team has proposed a method of human goblet cells culturing (131,132).

As for the trigeminal neurons and glial cells, it is important to confirm the observed phototoxicity in correspondent cell cultures from primate or even human. Phototoxicity in other neural cultures might be worth to explore, in order to confirm (or not) the trigeminal specificity of neural phototoxic response. In addition, following the model of ocular surface cells study, it would be of interest to investigate the operation of antioxidant system as well as to let the cells to recover after light exposure and then follow them up in time. Besides, Matynia et al. reported the intrinsic photosensitivity of TG neurons (99) while Delwig et al. failed to replicate their results (98). Thus, the investigation of probable neural light-evoked activity, by calcium imaging and/or by electrophysiological approach, would be of high scientific significance. This is all the more important given that in our experimental setup, we could study wavelength-dependent neural activity. Further, our understanding of glial cells photosensitivity (that, to our knowledge, has not been reported previously) should be deepened. The pure-glial phototoxic response may be explored in cell lines as well as in primary culture prepared following the examples of (133,134). Finally, the role of non-visual opsins is worth to be explored further. Their role in neural phototoxicity might be confirmed by performing the light experiments on cultured TG neurons from melanopsin or neuropsin (or both) knockout mice. In case of actual importance of non-visual photoreceptors, induced phototoxicity would be significantly decreased as compared to wild type. As for the melanopsin, an application of opn4 antagonist (135) may be also considered. However, one should take into account that this molecule is dissolved in dimethyl sulfoxide that may appear to be initially toxic for the TG cells.

Another next step for the future research would be to explore the blue light phototoxicity in the model of so-called “compartmentalized” trigeminal cell culture, which is currently under development in our team by Michael Vitoux. In this model, a microfluidic device allows for separation of neuron bodies and axons in two fluidically isolated compartments. It could then be possible to apply light exposure only to the axons thus designing a more physiological model of phototoxic nociception.

In vivo, we demonstrated that blue light induced important light aversion in mice without any previously detected pathology. We proved clinically that blue photophobia was accompanied by corneal inflammation as well as by alterations in tearing and corneal sensitivity. Moreover, we observed the light-induced immuno-activation in the retina and in

trigeminal pathways. Performed behavioral and pharmacological experiments highlighted the significance of melanopsin in mediation of photophobic signal. Furthermore, we supposed that visual receptors as well as potentially photosensitive trigeminal afferents had a small role in this process, if any. These results are in line with clinical data reporting the cases of photophobia in blind patients. Moreover, our data corroborate complaints about increased photosensitivity in front of visual displays that are known to highly emit in blue spectra.

These in vivo results need to be deepened. First, it is important to confirm that in our experimental set, the observed inflammatory signs will not appear in melanopsin antagonist-injected mice and the photophobia will not be induced in opn4 knock-out mice. Second, since melanopsin distribution was altered in the retina, one may suppose it to be altered in melanopsin-expressing TG neurons and corneal afferents as well. This might have been proven by immunohistology; however, when used outside the retina, the non-specificity of anti-melanopsin antibodies has been reported (98,99). Therefore, transgenic mice with fluorescent proteins genes driven by the melanopsin promoter might be a solution. Another possibility would be to use a recent RNAscope technique - a novel RNA in situ hybridization (ISH) technology whose probe design strategy provides with simultaneous signal amplification and background suppression. Thus, it would allow for single-molecule visualization while preserving tissue morphology (136,137). Third, the light-receiving role of out-retinal melanopsin-containing tissues should be further explored. Some our preliminary experiments (performed by Fanny Joubert and Darine Fakih) showed that exposure to blue light did not induce any significant alterations in electrophysiological recordings of ciliary nerve activity. Other ways to receive light may implicate direct communication of TG afferents with probably photosensitive iris and ciliary body. This mechanism might be checked by intravitreal lidocaine injection shifted more to the anterior part of the eye. Forth, the role other non-visual photoreceptors is worth to be studied. Experiments on neuropsin knock-out mice would allow for better understating of the probable photophobia-mediating function of this protein. This is all the more important since we detected the neuropsin expression in TG primary cell culture. Moreover, another photopigment – encephalopsin or opn3 – might be involved. Encephalopsin was initially discovered in brain in 1993 (138); its transcripts were later detected in mouse RGCc line (107) and in the retina (139). Further, opn3 was found to be blue-sensitive with an absorption maximum around 465 nm (140); moreover, it was reported that in mice, transcranial light treatment affects opn3 expression in different brain areas (141). Last but not least, Buhr et al. reported that in $Opn3^{-/-}$ mice, the ex vivo retinal rhythm had a lower amplitude as compared to wild type (108). The authors therefore proposed that although encephalopsin was not necessary for local retinal photoentrainment, it nonetheless might have a role in influencing the intrinsic retinal rhythmic activity. To date, the functions of opn3 in mammals remain unknown.

Finally, all the results of this thesis are worth to be verified in a clinical study. Various populations of patients suffering from dry eye, ocular pain and photophobia should be recruited to test the special glasses filtering out or attenuating the irradiance of broad or narrow blue spectra. On the basis of our experimental data, we suppose that such filtering out might significantly alleviate the symptoms of these ocular disorders thus ameliorating the patients' life quality. Moreover, corrections of the spectra of laptop or smartphone displays could aid to decrease the noxious effects of blue light described in this work.

Bibliography

1. Gary Heiting. Ultraviolet (UV) Radiation and Your Eyes [Internet]. All About Vision. 2017. Available from: http://www.allaboutvision.com/sunglasses/spf.htm
2. Heiting G. Blue Light: It's Both Bad And Good For You [Internet]. All About Vision. 2017 [cited 2018 Aug 20]. Available from: https://www.allaboutvision.com/cvs/blue-light.htm
3. Wilts A. Donald Trump stares into solar eclipse without safety glasses, while aides shout "don't look!" [Internet]. The Independent. 2017 [cited 2018 Aug 30]. Available from: https://www.independent.co.uk/news/world/americas/us-politics/trump-solar-eclipse-photo-stares-without-glasses-video-white-house-balcony-dont-look-aides-a7905771.html
4. Sankpill JP. Infrared Radiation : Defending Against the Invisible Workplace Hazard. Prot Updat. 2009;
5. Behar-Cohen F, Baillet G, de Ayguavives T, Garcia PO, Krutmann J, Pena-Garcia P, et al. Ultraviolet damage to the eye revisited: Eye-sun protection factor (E-SPF), a new ultraviolet protection label for eyewear. Clin Ophthalmol. 2014;8(1):87–104.
6. Text Request. How Much Time Do People Spend on Their Mobile Phones in 2017? [Internet]. Hackernoon. [cited 2017 Nov 7]. Available from: https://hackernoon.com/how-much-time-do-people-spend-on-their-mobile-phones-in-2017-e5f90a0b10a6
7. Lupis J. The State of Traditional TV: Updated With Q1 2017 Data [Internet]. Mareketing charts. [cited 2017 Nov 7]. Available from: http://www.marketingcharts.com/featured-24817
8. Van Gelder RN. Vision : Melanopsin and the Pharmacology of Photons. Curr Biol [Internet]. Elsevier Ltd; 2016;26(17):R804–6. Available from: http://dx.doi.org/10.1016/j.cub.2016.07.052
9. Moreau E. Blue Light Filter Applications to Reduce Digital Eye Strain [Internet]. Lifewire. 2018 [cited 2018 Aug 21]. Available from: https://www.lifewire.com/reduce-eye-strain-with-blue-light-filter-apps-4134615
10. Lee HS, Cui L, Li Y, Choi JS, Choi J, Li Z, et al. Influence of Light Emitting Diode-Derived Blue Light Overexposure on Mouse Ocular Surface. PLoS One [Internet]. 2016; Available from: http://dx.doi.org/10.1371/journal.pone.0161041
11. A.P. Cullen. Photokeratitis and Other Phototoxic Effects on the Cornea and Conjunctiva. Int J Toxicol. 2002;(Spring / Primavera):455–64.
12. Voke J. Radiation effects on the eye. Part 3a - Ocular effects of ultraviolet radiation. Optom Today [Internet]. 1999;27–32. Available from: http://www.optometry.co.uk/pages/articles/articles1999.php %5Cn C:%5CLibrary%5CVoke1999.pdf
13. Turner PL, Someren EJW Van, Mainster MA. The role of environmental light in sleep and health : Effects of ocular aging and cataract surgery. Sleep Med Rev [Internet]. Elsevier Ltd; 2010;14(4):269–80. Available from: http://dx.doi.org/10.1016/j.smrv.2009.11.002
14. Voke J. Radiation effects on the eye. Part 3b - Ocular effects of ultraviolet radiation.

Optom Today. 1999;37–41.

15. Roehlecke C, Schumann U, Ader M, Brunssen C, Bramke S, Morawietz H, et al. Stress reaction in outer segments of photoreceptors after blue light irradiation. PLoS One [Internet]. 2013;8(9):e71570. Available from: http://www.pubmedcentral.nih.gov/articlerender.fcgi?artid=3770596&tool=pmcentrez&rendertype=abstract

16. Marie M, Bigot K, Angebault C, Barrau C, Gondouin P, Pagan D, et al. Light action spectrum on oxidative stress and mitochondrial damage in A2E-loaded retinal pigment epithelium cells. Cell Death Dis [Internet]. Springer US; 2018;9(3). Available from: http://dx.doi.org/10.1038/s41419-018-0331-5

17. Kuse Y, Ogawa K, Tsuruma K, Shimazawa M, Hara H. Damage of photoreceptor-derived cells in culture induced by light emitting diode-derived blue light. Sci Rep. 2014;4(5223):1–12.

18. Lascaratos G, Ji D, Wood JPM, Osborne NN. Visible light affects mitochondrial function and induces neuronal death in retinal cell cultures. Vision Res. 2007;47(9):1191–201.

19. Godley BF, Shamsi FA, Liang F-Q, Jarrett SG, Davies S, Boulton M. Blue Light Induces Mitochondrial DNA Damage and Free Radical Production in Epithelial Cells. J Biol Chem [Internet]. 2005;280(22):21061–6. Available from: http://www.jbc.org/lookup/doi/10.1074/jbc.M502194200

20. Arnault E, Barrau C, Gondouin P, Bigot K, Villette T, Picaud S, et al. Phototoxic Action Spectrum on a Retinal Pigment Epithelium Model of Age-Related Macular Degeneration Exposed to Sunlight Normalized Conditions. PLoS One. 2013;8(8).

21. Chang SW, Kim H Il, Kim GH, Park SJ, Kim I-B. Increased Expression of Osteopontin in Retinal Degeneration Induced by Blue Light-Emitting Diode Exposure in Mice. Front Mol Neurosci [Internet]. 2016;9(July):1–12. Available from: http://journal.frontiersin.org/Article/10.3389/fnmol.2016.00058/abstract

22. Jaadane I, Villalpando Rodriguez GE, Boulenguez P, Chahory S, Carré S, Savoldelli M, et al. Effects of white light-emitting diode (LED) exposure on retinal pigment epithelium in vivo. J Cell Mol Med. 2017;21(12):3453–66.

23. Jaadane I, Boulenguez P, Chahory S, Carré S, Savoldelli M, Jonet L, et al. Retinal damage induced by commercial light emitting diodes (LEDs). Free Radic Biol Med. Elsevier B.V.; 2015;84:373–84.

24. Benedetto MM, Guido ME, Contin MA. Non-Visual Photopigments Effects of Constant Light-Emitting Diode Light Exposure on the Inner Retina of Wistar Rats. Front Neurol. 2017;8(August):1–11.

25. Hughes S, Rodgers J, Hickey D, Foster RG, Peirson SN, Hankins MW. Characterisation of light responses in the retina of mice lacking principle components of rod , cone and melanopsin phototransduction signalling pathways. Nat Publ Gr [Internet]. Nature Publishing Group; 2016;(June):1–11. Available from: http://dx.doi.org/10.1038/srep28086

26. Feng C, Wang X, Liu T, Zhang M, Xu G, Ni Y. Expression of CCL2 and its receptor in activation and migration of microglia and monocytes induced by photoreceptor apoptosis. Mol Vis. 2017;(October):765–77.

27. Narimatsu T, Negishi K, Miyake S, Hirasawa M, Osada H, Kurihara T, et al. Blue light-induced inflammatory marker expression in the retinal pigment epithelium-

choroid of mice and the protective effect of a yellow intraocular lens material invivo. Exp Eye Res [Internet]. Elsevier Ltd; 2015;132:48–51. Available from: http://dx.doi.org/10.1016/j.exer.2015.01.003

28. Krigel A, Berdugo M, Picard E, Levy-Boukris R, Jaadane I, Jonet L, et al. Light-induced retinal damage using different light sources, protocols and rat strains reveals LED phototoxicity. Neuroscience [Internet]. IBRO; 2016;339:296–307. Available from: http://dx.doi.org/10.1016/j.neuroscience.2016.10.015

29. Chahory S, Keller N, Martin E, Omri B, Crisanti P, Torriglia A. Neurochemistry International Light induced retinal degeneration activates a caspase-independent pathway involving cathepsin D. Neurochem Int [Internet]. Elsevier Ltd; 2010;57(3):278–87. Available from: http://dx.doi.org/10.1016/j.neuint.2010.06.006

30. Moon JH, Kim KW, Moon NJ. Smartphone use is a risk factor for pediatric dry eye disease according to region and age: A case control study Pediatrics and Strabismus. BMC Ophthalmol [Internet]. BMC Ophthalmology; 2016;16(1):1–7. Available from: http://dx.doi.org/10.1186/s12886-016-0364-4

31. Klamm J, Tarnow KG. Computer Vision Syndrome : A review of literature. CNE Ser. 2015;24(2):89–93.

32. Yazici A, Sari ES, Sahin G, Kilic A, Cakmak H, Ayar O, et al. Change in tear film characteristics in visual display terminal users. EJO. 2015;25(2):85–9.

33. Uchino M, Yokoi N, Uchino Y, Dogru M, Kawashima M, Komuro A, et al. Prevalence of dry eye disease and its risk factors in visual display terminal users: The Osaka study. Am J Ophthalmol [Internet]. Elsevier Inc.; 2013;156(4):759–766.e1. Available from: http://dx.doi.org/10.1016/j.ajo.2013.05.040

34. Kim DJ, Lim C-Y, Gu N, Park CY. Visual Fatigue Induced by Viewing a Tablet Computer with a High-resolution Display. Korean J Ophthalmol [Internet]. 2017;31(5):388. Available from: https://synapse.koreamed.org/DOIx.php?id=10.3341/kjo.2016.0095

35. Ide T, Toda I, Miki E, Tsubota K. Effect of blue light-reducing eye glasses on critical flicker frequency. Asia-Pacific J Ophthalmol. 2015;4(2):80–5.

36. Bogdănici CM, Săndulache DE, Nechita CA. Eyesight quality and Computer Vision Syndrome. Rom J Ophthalmol [Internet]. 2017;61(2):112–6. Available from: http://www.rjo.ro/images/rjo_issue_2_2017/7.bogdanici_camelia_m_final_PR.pdf

37. Sheppard AL, Wolffsohn JS. Digital eye strain: prevalence, measurement and amelioration. BMJ Open Ophthalmol [Internet]. 2018;3(1):e000146. Available from: http://bmjophth.bmj.com/lookup/doi/10.1136/bmjophth-2018-000146

38. E. Porcar, A. Pons, A. Lorente. Visual and ocular effects from the use of flat-panel displays. Int J Ophtalmol. 2014;881–5.

39. Kaido M, Toda I, Oobayashi T, Kawashima M. Reducing Short-Wavelength Blue Light in Dry Eye Patients with Unstable Tear Film Improves Performance on Tests of Visual Acuity. PLoS One [Internet]. 2016;11(4):1–10. Available from: http://dx.doi.org/10.1371/journal.pone.0152936

40. Ribelles A, Galbis-Estrada C, Parras MA, Vivar-Llopis B, Marco-Ramírez C, Diaz-Llopis M. Ocular Surface and Tear Film Changes in Older Women Working with Computers. Biomed Res Int. 2015;2015.

41. Courtin R, Pereira B, Naughton G, Chamoux A, Chiambaretta F, Lanhers C, et al.

Prevalence of dry eye disease in visual display terminal workers : a systematic review and meta-analysis. BMJ. 2016;

42. Knop E, Knop N. Anatomy and Immunology of the Ocular Surface. Chem Immunol Allergy. 2007;92:36–44.

43. Craig JP, Nichols KK, Nichols JJ, Caffery B, Dua HS, Akpek EK, et al. TFOS DEWS II Definition and Classification Report. Ocul Surf [Internet]. 2017;15:276–83. Available from: http://www.theocularsurfacejournal.com/article/S1542-0124(17)30119-2/pdf

44. Bron AJ, Paiva CS de, Chauhan SK, Bonini S, Jain S, Knop E, et al. TFOS DEWS II pathophysiology report. Ocul Surf [Internet]. Elsevier Ltd; 2017;15(3):511–38. Available from: http://www.theocularsurfacejournal.com/article/S1542-0124(17)30104-0/pdf

45. Baudouin C, Pisella P-J, Thanh H-X. Surface oculaire: Rapport SFO 2015. Elsevier Masson; 2015. 714 p.

46. Fingeret M. Classify corneas simply as average, thin or thick [Internet]. Healio: Primary Care Optometry News. 2006 [cited 2018 Aug 20]. Available from: https://www.healio.com/optometry/glaucoma/news/print/primary-care-optometry-news/%7B0c78f021-fde3-4826-a657-f22c13a7e3dd%7D/classify-corneas-simply-as-average-thin-or-thick

47. Tong L, Diebold Y, Calonge M, Gao J, Stern ME, Beuerman RW. Comparison of Gene Expression Profiles of Conjunctival Cell Lines With Primary Cultured Conjunctival Epithelial Cells and Human Conjunctival Tissue. Gene Expr. 2009;14:265–78.

48. Wang S, Ghezzi CE, Gomes R, Pollard RE, Funderburgh JL, Kaplan DL. In vitro 3D corneal tissue model with epithelium, stroma, and innervation. Biomaterials [Internet]. Elsevier Ltd; 2017;112:1–9. Available from: http://dx.doi.org/10.1016/j.biomaterials.2016.09.030

49. Liang H, Baudouin C, Daull P, Garrigue J-S, Brignole-Baudouin F. Ocular safety of cationic emulsion of cyclosporine in an in vitro corneal wound-healing model and an acute in vivo rabbit model. Mol Vis [Internet]. 2012;18(February):2195–204. Available from: http://www.pubmedcentral.nih.gov/articlerender.fcgi?artid=3425577&tool=pmcentrez&rendertype=abstract

50. Lee J, Kim S, Lee S, Kim H, Ahn H, Li Z. Blue Light – Induced Oxidative Stress in Human Corneal Epithelial Cells : Protective Effects of Ethanol Extracts of Various Medicinal Plant Mixtures. Cornea. 2014;55(7):4119–4127.

51. Rönkkö S, Vellonen K, Järvinen K, Toropainen E. Human corneal cell culture models for drug toxicity studies. Drug Deliv Transl Res [Internet]. Drug Delivery and Translational Research; 2016;6:660–75. Available from: http://dx.doi.org/10.1007/s13346-016-0330-y

52. Warcoin E, Baudouin C, Gard C, Brignole-Baudouin F. In Vitro Inhibition of NFAT5-Mediated Induction of CCL2 in Hyperosmotic Conditions by Cyclosporine and Dexamethasone on Human HeLa-Modified. PLoS One [Internet]. 2016;1–19. Available from: http://dx.doi.org/10.1371/journal.pone.0159983

53. Chang RS. Continuous Subcultivation of Epithelial-like Cells from Normal Human Tissues. Exp Biol Med [Internet]. 1954;87(2):440–3. Available from: http://journals.sagepub.com/doi/abs/10.3181/00379727-87-

21406?journalCode=ebma#articleCitationDownloadContainer

54. Diebold Y, Calonge M, de Salamanca AE, Callejo S, Corrales RM, Saez V, et al. Characterization of a Spontaneously Immortalized Cell Line (IOBA-NHC) from Normal Human Conjunctiva AND. IOVS. 2003;44(10).

55. Launay P-S. Etudes de la neuro-inflammation périphérique et centrale dans un modèle pré-clinique de douleur oculaire [Internet]. Université Pierre et Marie Curie - Paris VI; 2015. Available from: https://tel.archives-ouvertes.fr/tel-01627559

56. Muller LJ, Vrensen GFJM, Pels L, Cardozo BN, Willekens B. Architecture of Human Corneal Nerves. IOVS. 1997;38(5):985–94.

57. Belmonte C, Aracil A, Acosta C, Luna C, Gallar J. Nerves and Sensations from the Eye Surface. Ocul Surf. 2004;2(4):248–53.

58. Belmonte C, Nichols JJ, Cox SM, Brock JA, Begley CG, Bereiter DA, et al. TFOS DEWS II pain and sensation report. Ocul Surf [Internet]. Elsevier Ltd; 2017;15(3):404–37. Available from: http://www.theocularsurfacejournal.com/article/S1542-0124(17)30115-5/pdf

59. Réaux-le-Goazigo A, Labbé A, Baudouin C, Melik-Parsadaniantz, Stéphane. La douleur oculaire chronique : mieux la comprendre pour mieux la traiter. Medecine/Science. 2017;33:749–57.

60. Rosenthal P, Borsook D. The corneal pain system. Part I: The missing piece of the dry eye puzzle. Ocul Surf. 2012;10(1):2–14.

61. Stapleton F, Alves M, Bunya VY, Jalbert I, Lekhanont K, Malet F, et al. The Ocular Surface TFOS DEWS II Epidemiology Report. Ocul Surf [Internet]. Elsevier Ltd; 2017;15(3):334–65. Available from: http://dx.doi.org/10.1016/j.jtos.2017.05.003

62. 2007 Report of the International Dry Eye WorkShop (DEWS). Vol. 5, The Ocular Surface. 2007. 65-204 p.

63. Barabino S, Labetoulle M, Rolando M, Messmer EM. Understanding Symptoms and Quality of Life in Patients With Dry Eye Syndrome. Ocul Surf [Internet]. Elsevier Ltd; 2016;14(3):365–76. Available from: http://dx.doi.org/10.1016/j.jtos.2016.04.005

64. Wolffsohn JS, Arita R, Chalmers R, Djalilian A, Dogru M, Dumbleton K, et al. The Ocular Surface TFOS DEWS II Diagnostic Methodology report. Ocul Surf [Internet]. Elsevier Ltd; 2017;15(3):539–74. Available from: http://dx.doi.org/10.1016/j.jtos.2017.05.001

65. Baudouin C, Messmer EM, Aragona P, Geerling G, Akova YA, Benítez-del-castillo J, et al. Revisiting the vicious circle of dry eye disease : a focus on the pathophysiology of meibomian gland dysfunction. BJO. 2016;100:300–6.

66. Jones L, Downie LE, Korb D, Benitez-del-castillo JM, Dana R, Deng SX, et al. The Ocular Surface TFOS DEWS II Management and Therapy Report. Ocul Surf [Internet]. Elsevier Ltd; 2017;15(3):575–628. Available from: http://dx.doi.org/10.1016/j.jtos.2017.05.006

67. K. Digre, K.C. Brennan. Shedding Light on Photophobia. J Neuroophthalmol. 2012;32(1):68–81.

68. Katz BJ, Digre KB. Diagnosis, pathophysiology, and treatment of photophobia. Surv Ophthalmol [Internet]. Elsevier Inc; 2016;61(4):466–77. Available from: http://dx.doi.org/10.1016/j.survophthal.2016.02.001

69. Wu Y, Hallett M. Photophobia in neurologic disorders. Transl Neurodegener [Internet]. Translational Neurodegeneration; 2017;6(1):26. Available from: http://translationalneurodegeneration.biomedcentral.com/articles/10.1186/s40035-017-0095-3

70. Zinflou C, Rochette PJ. Free Radical Biology and Medicine Ultraviolet A-induced oxidation in cornea : Characterization of the early oxidation-related events. Free Radic Biol Med. 2017;108(November 2016):118–28.

71. C. Cejka, J. Platenik, R. Buchard, V. Guryca, J. Sirc, M. Vejerazka, J. Crkovska, T. ARdan, J. Michalek, B. Brunova, J. Cejkova. Effect of Two Different UVA Doses on the Rabbit Cornea and Lens. Photochem Photobiol. 2009;(21):794–800.

72. A. Golu, I. Gheorghisor, A.T. Balasoiu, F. Balta, E. Osiac, L. Mogoanta, A. Bold. The effect of ultraviolet radiation on the cornea – experimental study. RJME. 2013;54(4):1115–20.

73. S.P. Gendron and P.J. Rochette. Modifications in stromal extracellular matrix of aged corneas can be induced by ultraviolet A irradiation. Aging Cell. 2015;433–42.

74. Dadoukis P, Klagas I, Papakonstantinou E. Infrared irradiation alters the expression of matrix metalloproteinases and glycosaminoglycans in the cornea and crystalline lens. Graefes Arch Clin Exp Ophthalmol. 2013;1929–36.

75. M. A. Lemp et al. The Definition & Classification of Dry Eye Disease. In: Guidelines from the 2007 International Dry Eye Workshop. 2008.

76. Hwang H Bin, Kim HS. Phototoxic effects of an operating microscope on the ocular surface and tear film. Cornea [Internet]. 2014;33(1):82–90. Available from: http://www.ncbi.nlm.nih.gov/pubmed/24310622

77. Ipek T, Hanga MP, Hartwig A, Wolffsohn J, O'Donnell C. Dry eye following cataract surgery: The effect of light exposure using an in-vitro model. Contact Lens Anterior Eye [Internet]. 2017;(July):3–6. Available from: http://linkinghub.elsevier.com/retrieve/pii/S1367048417302370

78. Ipek T, Hartwig A, Wolffsohn JS, O'Donnell C. Effect of light exposure on conjunctival fibroblasts using an in-vitro model of dry eye. In: ARVO Annual Meeting Abstract [Internet]. 2018. Available from: https://iovs.arvojournals.org/article.aspx?articleid=2691595

79. Niwano Y, Kanno T, Iwasawa A, Ayaki M, Tsubota K. Blue light injures corneal epithelial cells in the mitotic phase in vitro. Br J Ophthalmol [Internet]. 2014;98(7):990–2. Available from: http://www.ncbi.nlm.nih.gov/pubmed/24682182

80. Ayaki M, Niwano Y, Kanno T, Tsubota K. Blue light induces oxidative damage in human ocular surface cells in culture. ARVO 2015 Annu Meet Abstr. 2015;

81. Deschamps N, Baudouin C. Dry Eye and Biomarkers: Present and Future. Curr Ophthalmol Rep [Internet]. 2013;1(2):65–74. Available from: http://link.springer.com/10.1007/s40135-013-0008-2

82. Choi W, Lian C, Ying L, Kim GE, You IC, Park SH, et al. Expression of Lipid Peroxidation Markers in the Tear Film and Ocular Surface of Patients with Non-Sjogren Syndrome: Potential Biomarkers for Dry Eye Disease. Curr Eye Res. 2016;41(9):1143–9.

83. Rosenthal P, Borsook D. Ocular neuropathic pain. Br J Ophthalmol [Internet]. 2016;100(1):128–34. Available from:

http://bjo.bmj.com/lookup/doi/10.1136/bjophthalmol-2014-306280

84. Galor A, Moein H-R, Lee C, Rodriguez A, Felix ER, Sarantopoulos KD, et al. Neuropathic pain and dry eye. Ocul Surf [Internet]. Elsevier Inc.; 2017; Available from: http://linkinghub.elsevier.com/retrieve/pii/S154201241730068X

85. McMahon SB, Koltwenburg M, Tracey I, Turk DC. Wall and Melzack's textbook of pain. 6th editio. Philadelphia: Elsevier Saunders;

86. Albilali A, Dilli E. Photophobia : When Light Hurts, a Review. Curr Neurol Neurosci Rep. Current Neurology and Neuroscience Reports; 2018;18(62):4–9.

87. Sung CH, Chuang JZ. The cell biology of vision. J Cell Biol. 2010;190(6):953–63.

88. Schmidt TM, Do MTH, Dacey D, Lucas R, Hattar S, Matynia A. Retinal Ganglion Cells : From Form To Function. J Neurosci. 2011;31(45):16094–101.

89. Hatori M, Panda S. The emerging roles of melanopsin in behavioral adaptation to light. Trends Mol Med [Internet]. Elsevier Ltd; 2010;16(10):435–46. Available from: http://dx.doi.org/10.1016/j.molmed.2010.07.005

90. Matynia A. Blurring the Boundaries of Vision: Novel Functions of Intrinsically Photosensitive Retinal Ganglion Cells. J Exp Neurosci [Internet]. 2013;7:JEN.S11267. Available from: http://journals.sagepub.com/doi/10.4137/JEN.S11267

91. Ksendzovsky A, Pomeraniec IJ, Zaghloul KA, Provencio JJ. Clinical implications of the melanopsin-based non–image-forming visual system. Neurology. 2017;88:1–9.

92. Berson DM. Strange vision : ganglion cells as circadian photoreceptors. Trends Neurosci. 2003;26(6):314–20.

93. Legates TA, Fernandez DC, Hattar S. Light as a central modulator of circadian rhythms, sleep and affect. Nat Rev Neurosci. 2014;15(7):443–54.

94. Sexton T, Buhr E, Van Gelder RN. Melanopsin and mechanisms of non-visual ocular photoreception. J Biol Chem. 2012;287(3):1649–56.

95. Detwiler PB. Phototransduction in Retinal Ganglion Cells. Yale J Biol Med [Internet]. 2018;91(1):49–52. Available from: http://www.ncbi.nlm.nih.gov/pubmed/29599657%0Ahttp://www.pubmedcentral.nih.gov/articlerender.fcgi?artid=PMC5872641

96. Matsuyama T, Yamashita T, Imamoto Y, Shichida Y. Photochemical properties of mammalian melanopsin. Biochemistry. 2012;51(27):5454–62.

97. Emanuel AJ, Do MTH. Melanopsin Tristability for Sustained and Broadband Phototransduction. Neuron. 2016;93(4):292–7.

98. Delwig A, Chaney SY, Bertke AS, Verweij J, Quirce S, Larsen DD, et al. Melanopsin expression in the cornea. Vis Neurosci. 2018;35.

99. Matynia A, Nguyen E, Sun X, Blixt FW, Parikh S, Kessler J, et al. Peripheral Sensory Neurons Expressing Melanopsin Respond to. Front Neurql Circuits. 2016;10(August):1–15.

100. Lei S, Zivcevska M, Goltz HC, Chen X, Wong AM. The effect of ocular topical anesthesia on photophobia induced by red and blue light stimulus. In: ARVO Annual Meeting. 2018.

101. Xue T, Do MTH, Riccio A, Jiang Z, Hsieh J, Wang HC, et al. Melanopsin Signaling in Mammalian Iris and Retina. Nature. 2012;479(7371):67–73.

102. Vugler AA, Semo M, Joseph A, Jeffery G. Survival and remodeling of melanopsin cells during retinal dystrophy. Vis Neurosci. 2008;25(2):125–38.

103. Semo M, Gias C, Ahmado A, Vugler A. A role for the ciliary marginal zone in the melanopsin-dependent intrinsic pupillary light reflex. Exp Eye Res [Internet]. Elsevier Ltd; 2014;119:8–18. Available from: http://dx.doi.org/10.1016/j.exer.2013.11.013

104. Rupp A, Schmidt T, Chew K, Yungher B, Park K, Hattar S. ipRGCs mediate ipsilateral pupil constriction. In: ARVO Annual Meeting [Internet]. 2013. Available from: https://iovs.arvojournals.org/article.aspx?articleid=2147859

105. Tarttelin EE, Bellingham J, Hankins MW, Foster RG, Lucas RJ. Neuropsin (Opn5): a novel opsin identified in mammalian neural tissue. FEBS Lett. 2003;554:410–6.

106. Kojima D, Mori S, Torii M, Wada A, Morishita R. UV-Sensitive Photoreceptor Protein OPN5 in Humans and Mice. PLoS One. 2011;6(10).

107. Guido ME, Nieto PS, Valdez DJ, Acosta-rodrı VA. Expression of Novel Opsins and Intrinsic Light Responses in the Mammalian Retinal Ganglion Cell Line RGC-5 . Presence of OPN5 in the Rat Retina. PLoS One. 2011;6(10).

108. Buhr ED, Yue WWS, Ren X, Jiang Z, Liao HR, Mei X, et al. Circadian oscillators in mammalian retina and cornea. PNAS. 2015;(7):1–6.

109. Tsuchiya S, Buhr ED, Higashide T, Sugiyama K, Van Gelder RN. Light entrainment of the murine intraocular pressure circadian rhythm utilizes non-local mechanisms. PLoS One [Internet]. 2017;12(9):1–12. Available from: http://dx.doi.org/10.1371/journal.pone.0184790

110. Hoggan RN, Subhash A, Blair S, Digre KB, Baggaley SK, Gordon J, et al. Thin-film optical notch filter spectacle coatings for the treatment of migraine and photophobia. J Clin Neurosci [Internet]. Elsevier Ltd; 2016;28:71–6. Available from: http://dx.doi.org/10.1016/j.jocn.2015.09.024

111. Amini A, Digre K, Couldwell WT. Photophobia in a blind patient: an alternate visual pathway. J Neurosurg [Internet]. 2006;105(5):765–8. Available from: https://www.ncbi.nlm.nih.gov/pubmed/17121141

112. Matynia A, Parikh S, Chen B, Kim P, Mcneill DS, Nusinowitz S, et al. Intrinsically photosensitive retinal ganglion cells are the primary but not exclusive circuit for light aversion. Exp Eye Res [Internet]. Elsevier Ltd; 2012;105:60–9. Available from: http://dx.doi.org/10.1016/j.exer.2012.09.012

113. Matynia A, Parikh S, Deot N, Wong A, Kim P, Nusinowitz S, et al. Light aversion and corneal mechanical sensitivity are altered by intrinscally photosensitive retinal ganglion cells in a mouse model of corneal surface damage. Exp Eye Res [Internet]. Elsevier Ltd; 2015;137:57–62. Available from: http://dx.doi.org/10.1016/j.exer.2015.05.025

114. Okamoto K, Thompson R, Tashiro A, Chang Z, D.A. B. Bright light produces Fos-positive neurons in caudal trigeminal brainstem. Neuroscience. IBRO; 2009;160(99):858–64.

115. Moulton EA, Becerra L, Borsook D. An fMRI case report of photophobia: Activation of the trigeminal nociceptive pathway. Pain. 2009;145(3):358–63.

116. Okamoto K, Tashiro A, Chang Z, Beriter DA. Bright light activates a trigeminal nociceptive pathway. Pain. 2011;149(2):235–42.

117. Okamoto K, Tashiro A, Thompson R, Nishida Y, Bereiter DA. Trigeminal interpolaris／

caudalis transition neurons mediate reflex lacrimation evoked by bright light in the rat. Eur J Neurosci. 2012;36(July):3492–9.

118. Rahman M, Okamoto K, Thompson R, Beriter DA. Trigeminal pathways for hypertonic saline and light-evoked corneal reflexes. Neuroscience. 2015;26(612):716–23.

119. Dolgonos S, Ayyala H, Evinger C. Light-Induced Trigeminal Sensitization without Central Visual Pathways : Another Mechanism for Photophobia. IOVS. 2011;52(11):7852–8.

120. Matynia A, Parikh S, Nusinowitz S, Gorin MB. Three blind mice, see how they run: Light-dependent behavior in the absence of an optic nerve. In: nvest Ophthalmol Vis Sci [Internet]. 2017. p. 58(8):4126. Available from: https://iovs.arvojournals.org/article.aspx?articleid=2641273&resultClick=1

121. Noseda R, Kainz V, Jakubowski M, Gooley JJ, Clifford B, Digre K, et al. A neural mechanism for exacerbation of headache by light. Nat Neurosci. 2010;13(2):1–17.

122. Noseda R, Bernstein CA, Nir RR, Lee AJ, Fulton AB, Bertisch SM, et al. Migraine photophobia originating in cone-driven retinal pathways. Brain. 2016;139(7):1971–86.

123. Nir R-R, Noseda R, Bernstein C, Buettner C, Fulton AB, Bertisch SM, et al. Color-Selective Photophobia in Ictal vs . Interictal Migraineurs and in Healthy Controls. Pain. 2018;(May).

124. Noseda R, Lee AJ, Nir R-R, Bernstein CA, Kainz VM, Bertisch SM, et al. Neural mechanism for hypothalamic-mediated autonomic responses to light during migraine. Proc Natl Acad Sci [Internet]. 2017;114(28):E5683–92. Available from: http://www.pnas.org/lookup/doi/10.1073/pnas.1708361114

125. Matynia et el. ARVO 2016 Annual Meeting Abstracts. In: Melanopsin expressing neurons are located in the trigeminal ganglia. 2016. p. Poster Board Number D0030.

126. Warfvinge K, Sörensen, Karin D Edvinsson L, Fedulov V, Haanes KA, Blixt FW. Expression of the CGRP family peptides and their receptors in the rat retina. In: nvest Ophthalmol Vis Sci [Internet]. 2018. p. 59(9):5504. Available from: https://iovs.arvojournals.org/article.aspx?articleid=2692859&resultClick=1

127. Meadows M. Dealing with Dry Eye [Internet]. U.S. Food and Drug administration. 2015 [cited 2018 Aug 22]. Available from: https://web.archive.org/web/20090120142920/http://www.fda.gov/fdac/features/2005/305_eye.html

128. Aggarwal S. Ocular Neuropathic Pain [Internet]. EyeWik. 2017 [cited 2018 Aug 22]. Available from: http://eyewiki.aao.org/Ocular_Neuropathic_Pain#TREATMENT

129. Jung K-M, Lee S-H, Ryu Y-H, Jang W-H, Jung H-S, Han J-H, et al. A new 3D reconstituted human corneal epithelium model as an alternative method for the eye irritation test. Toxicol Vitr [Internet]. Elsevier Ltd; 2011;25(1):403–10. Available from: http://linkinghub.elsevier.com/retrieve/pii/S0887233310002778

130. Marko CK, Menon BB, Chen G, Whitsett J a., Clevers H, Gipson IK. Spdef null mice lack conjunctival goblet cells and provide a model of dry eye. Am J Pathol [Internet]. American Society for Investigative Pathology; 2013;183(1):35–48. Available from: http://dx.doi.org/10.1016/j.ajpath.2013.03.017

131. Shatos MA, Ríos JD, Horikawa Y, Hodges RR, Chang EL, Bernardino CR, et al. Isolation and characterization of cultured human conjunctival goblet cells. Investig

Ophthalmol Vis Sci. 2003;44(6):2477–86.

132. Dartt DA, Hodges RR, Li D, Shatos MA, Lashkari K, Serhan CN. Conjunctival goblet cell secretion stimulated by leukotrienes is reduced by resolvins D1 and E1 to promote resolution of inflammation. J Immunol. 2011;186(7):4455–66.

133. Wilkie MB, Lauder DJM. Simple method for the culture of glial cells from embryonic rat brain: Implications for regional heterogeneity and the radial glial lineage. J Neurosci Res [Internet]. 1988;21:220–5. Available from: https://www-ncbi-nlm-nih-gov.gate2.inist.fr/pubmed/?term=Simple+method+for+the+culture+of+glial+cells+from+embryonic+rat+brain%3A+implications+for+regional+heterogeneity+and+the+radial+glial+lineage.

134. Schildge S, Bohrer C, Beck K, Schachtrup C. Isolation and Culture of Mouse Cortical Astrocytes. JoVe. 2013;71(e50079).

135. Jones KA, Megumi H, Mure LS, Bramley JR, Panda S. Small molecule antagonists of melanopsin-mediated phototransduction. Nat Chem Biol. 2013;9(10):630–5.

136. Wang F, Flanagan J, Su N, Wang L, Bui S, Nielson A. RNAscope: A Novel in Situ RNA Analysis Platform for Formalin-Fixed, Paraffin-Embedded Tissues. J Mol Diagnostics. 2012;14(1):22–9.

137. RNAscope® Technology [Internet]. ACD BioTechne brand. 2017. Available from: https://acdbio.com/science/technology-overview

138. Blackshaw S, Snyder SH. Encephalopsin : A Novel Mammalian Extraretinal Opsin Discretely Localized in the Brain. J Neurosci. 1999;19(10):3681–90.

139. Koyanagi M, Takada E, Nagata T, Tsukamoto H, Terakita A. Homologs of vertebrate Opn3 potentially serve as a light sensor in nonphotoreceptive tissue. Proc Natl Acad Sci [Internet]. 2013;110(13):4998–5003. Available from: http://www.pnas.org/cgi/doi/10.1073/pnas.1219416110

140. Sugihara T, Nagata T, Mason B, Koyanagi M, Terakita A. Absorption Characteristics of Vertebrate Non-Visual Opsin, Opn3. PLoS One. 2016;(1158967):1–15.

141. Flyktman A, Mänttäri S, Nissilä J, Timonen M, Saarela S. Transcranial light affects plasma monoamine levels and expression of brain encephalopsin in the mouse. J Exp Biol. 2015;218:1521–6.

Abbreviations and conventional signs

CMZ – ciliary marginal zone
DED – dry eye disease
ERG – electroretinogram
GCL – ganglion cell layer
HCE cell line – Human Corneal Epithelial cell line
IOBA-NHC or IOBA cell line – cell line from Normal Human Conjunctiva
IOP – intraocular pressure
INL – inner nuclear layer
iPLR – intrinsic PLR
ipRGC – intrinsically photosensitive retinal ganglion cells
IR – infrared
IRA – near infrared
IVCM – in vivo confocal microscopy
LED – light emitting diode
LFU – lacrimal functional unit
MGD – meibomian gland dysfunction
μOR – μ opioid receptors
opn4 – melanopsin
opn5 – neuropsin
PLR – pupillary light reflex
RGC – retinal ganglion cells
ROS – reactive oxygen species
TBNC – trigeminal brainstem nuclear complex
TG – trigeminal ganglion
TKO – triple knock-out
UV – ultraviolet
UVA – near ultraviolet

Table of figures